Understanding B Cells in Health and Systemic Lupus Erythematosus

Velounias, Rebekah

Awarding institution:
King's College London

Understanding B Cells in Health and Systemic Lupus Erythematosus

Rebekah Louise Velounias

Supervisors: Professor Jo Spencer and Professor David D'Cruz

A thesis submitted for the Degree of Doctor of Philosophy in Immunobiology at King's College London

2023

This thesis is dedicated in loving memory of my Bapoo.

Declaration

I, Rebekah Louise Velounias, do hereby certify that this Thesis, submitted for the degree of Doctor of Philosophy, has been written by me and is a record of the work carried out by me or in collaboration with others as stated. This work has not been submitted in any previous application for any degree.

Acknowledgements

I am tremendously grateful for many individuals who have supported me throughout this degree. Firstly, I would like to thank my supervisors Professor Jo Spencer and Professor David D'Cruz. It has been an honour to work with Jo; I am very grateful to have learnt so much and discussed so many aspects of B cell immunology and autoimmune disease with her. Jo has also been an incredibly supportive and understanding supervisor throughout my entire journey at King's, and for that I am exceedingly thankful. David has been very insightful and enthusiastic about my project, and I have learnt a great deal about the clinical aspects of SLE from him.

I would also like to thank other members of the Spencer lab, past and present. Dr Thomas Tull has been an excellent mentor to me since we first worked together on my placement year project long before I started this degree. Tom has taught me practical lab skills and protocols as well as being a great source of B cell and lupus knowledge. I am very grateful to have been able to analyse data generated through his single-cell RNA-sequencing experiments as part of this thesis and to work with him on a review paper on B cell subsets. I would also like to thank Dr Michael Pitcher who has guided me through a great deal of the bioinformatics work from this thesis. Mike has been extremely helpful and patient whilst I was navigating through R and learning how to code. I would also like to thank Dr Jacqueline Siu, who has been a great support and friend to me throughout this degree. I am very thankful to her for sharing her extensive scientific and bioinformatic knowledge with me as well as allowing me to work with her on the marginal zone B cell subsets work, that makes up part of this thesis.

I am extremely grateful to all the staff at the Louise Coote Lupus Unit at Guy's Hospital, in particular Louise Nel and Neil Morton for their assistance in getting samples from lupus patients used for this study. I would like to thank all the lupus patients and healthy donors for contributing samples for this project. I would also like to thank the BRC flow core at Guy's Hospital for providing excellent training, as well as assisting with flow and mass cytometry experiments described in this study. I am indebted to Dr Katrina Todd and Cynthia Bishop, who were fundamental in the running and completion of the mass cytometry experiments.

I would like to thank other members of the School of Immunology and Microbial Sciences. My thesis committee, Dr Susan John, Dr Patricia Barral and Dr David Fear, who have provided great support and insight throughout this degree. Professor Stuart Neil and Dr Deena Gibbons, who have both offered invaluable knowledge and great discussions.

On a personal note, I would like to thank my family for their support throughout my whole education. I would especially like to thank my Dad for his endless words of encouragement, and guidance. I would not have been able to achieve any of this without him and I will forever be in debt to him for all that he has done for me. He is my inspiration and the reason I chose to do an immunology-based degree.

I am also hugely thankful to Ben for his love and support throughout the entire journey of this degree. I am so grateful I could count on him to bring me up when I was struggling and that I could share every success with him too.

Finally, I would like to thank my funders, The Oddfellows and The Lupus Trust, for the support and confidence in me, and for making this degree possible.

Abstract

Systemic lupus erythematosus (SLE) is an autoimmune disease characterised by the production of autoantibodies, predominantly to nuclear components, and the loss of B cell tolerance. Changes and imbalances in B cell subsets are a key aspect of lupus pathology, however these alterations are not fully understood.

Transitional B cells are a population of immature B cells that are the first cells to exit the bone marrow and enter the periphery. Transitional B cells emerge in the peripheral blood as transitional 1 (T1) B cells, which then mature into T2 B cells. Two populations of T2 B cells have been characterised and can be distinguished based on their surface expression of IgM. T2 IgMhi B cells have been linked to a gut-homing, integrin β7+ developmental trajectory that leads to the generation of marginal zone B cells, a subset known to be depleted in lupus nephritis. Several changes in the transitional B cell subset in SLE have also been reported, including the expansion of T1 B cells, depletion of T2 IgMhi B cells as well as dysregulated IL-10 signalling and increased survival in the transitional B cell subset. This study used multiple techniques to understand the diversity of the earliest subsets of B cells in the peripheral blood in lupus nephritis and how this compares to what is seen in healthy individuals, with the aim of improving our understanding the makeup of the peripheral B cell compartment in systemic lupus erythematosus (SLE). Transitional B cells are the cells in which all mature B cell subsets develop from and therefore are of particular interest when it comes to investigating altered peripheral B cell development.

Single-cell RNA-sequencing with CITE-seq antibody staining was used to investigate the gene expression patterns and surface marker expression of CD10+ transitional and CD10- naïve B cells from peripheral blood to gain an insight into how these early, antigen-inexperienced B cells differ in lupus nephritis compared to health with the aim of highlighting key features that may underpin differential B cell development seen in lupus nephritis. This analysis firstly highlighted the heterogeneity of transitional B cells in health and emphasised that whilst CD10+ transitional B cells are typically categorised into T1 and T2 subsets, there are distinct transcriptomic differences between cells belonging to the same subset. In addition, this study

identified early, antigen-inexperienced cells with an interferon gene signature, which can be seen in healthy and lupus nephritis bloods.

Following on from the observations made by analysis of single-cell RNA-sequencing data, mass cytometry and flow cytometry were used to explore interferon surface marker expression on blood from healthy donors and lupus nephritis patients. Data generated from these cytometry experiments suggest that transitional B cells express IFITM1 significantly more than all other peripheral B cell subsets in both health and lupus nephritis, and expression of IFITM1 does not differ between health and lupus despite the well-documented interferon signature seen in lupus. IFITM1 expression in transitional B cells correlated with the expression of integrin β7 and IgM, however other interferon markers did not, suggesting a possible link between IFITM1 and the gut-homing B cell developmental trajectory.

Additionally, this study used flow cytometry to compare the proportions of B cell subsets in paired blood samples from lupus nephritis patients at different timepoints during their disease course: when they were flaring, and disease activity was high versus when they were stable and disease activity was lower. This data demonstrated the plasticity of the B cell compartment in peripheral blood. The proportions of subsets were found to be significantly altered in periods of lupus flare compared to health, but in some instances, they returned to levels comparable to health upon disease stability. This data also revealed a reduction in naïve B cells with low IgM expression in lupus nephritis compared to health.

During this study, in a separate project, two subsets of marginal zone B cells were identified by single-cell RNA-sequencing of B cells in tissue from three sites in the gut associated lymphoid tissue. As part of this study, flow cytometry was used to validate the presence of these two marginal zone B cell populations in peripheral blood and investigate the changes in proportions of the two marginal zone subsets in lupus nephritis compared to health. CCR7 and integrin β7 were used to distinguish the marginal zone populations by flow cytometry. Previously it has been established that CD27+IgD+ marginal zone B cells are depleted in lupus nephritis, in this study, it was found that only one of the two novel subsets of marginal zone B cells was depleted in lupus nephritis.

The data presented in this thesis highlight the heterogeneity of transitional B cells in peripheral blood and suggest that early B cells that are naïve to antigen have been influenced by interferon and that this may be key to development of the gut-homing trajectory in both health and lupus nephritis. Additionally, it is evident from the data presented in this study that expression of different interferon inducible protein markers is not all the same and that it may be of use in future studies to explore these proteins individually. Data from paired lupus nephritis samples across different disease activity levels highlighted plasticity in the peripheral blood B cells compartment. Finally, this study has validated the presence of two populations of marginal zone B cells in peripheral blood and has shown that only one of these populations is depleted in lupus nephritis.

Table of Contents

List of Figures

List of Tables

List of Abbreviations

ABCB1	ATP-binding cassette sub family B member 1
AF	Alexa Fluor
AID	Activation induced cytidine deaminase
aNAV	Activated naïve
ANOVA	Analysis of variance
APC	Allophycocyanin
BAFF-R	B cell activating factor receptor
BAX	Bcl-2-associated X protein
BCR	B cell receptor
BLR1	Burkitt lymphoma receptor 1 (CXCR5)
BSA	Bovine serum albumin
BST2	Bone marrow stromal cell antigen 2 (tetherin)
BV	Brilliant violet
BUV	Brilliant ultraviolet
C1q	Complement component 1q
CAS	Cell acquisition solution
CCL19	Chemokine (C-C motif) ligand
CCR7	Chemokine (C-C motif) receptor
CD	Cluster of differentiation
CD40L	CD40 ligand
CD62L	CD62 ligand/L-selectin
CITE-seq	Cellular indexing of transcriptomes and epitopes by sequencing
CLP	Common lymphoid progenitor
CRP	C-reactive protein
CSM	Cell staining medium
CSM	Class-switched memory
CSR	Class-switch recombination
Cy	Cyanine
CyTOF	Cytometry by time-of-flight
CXCR4	Chemokine (CXC motif) receptor
DAPI	4’,6-diamidino-2-phenylindole
DLE	Discoid lupus erythematosus
DMSO	Dimethyl sulfoxide
DN	Double negative
DNA	Deoxyribonucleic acid
dsDNA	Double stranded DNA
EDTA	Ethylenediaminetetraacetic acid
EF	Extrafollicular
ESC	Embryonic stem cell
ESRD	End-stage renal disease
FACS	Fluorescence activated cell sorting
FCγR	Fragment crystalline gamma receptor
FCRL	Fc receptor like
FCS	Foetal calf serum
FSC	Forward scatter

GC	Germinal centre
HCD	Healthy control donor
HD	Healthy donor
HSC	Haematopoietic stem cell
IFITM1	Interferon induced transmembrane protein 1
IFN	Interferon
IFNAR	Interferon-α/β receptor
IFNGR	Interferon-γ receptor
IFNLR	Interferon-λ receptor 1
Ig	Immunoglobulin
IGH	Immunoglobulin heavy chain
IGLL5	Immunoglobulin lambda like polypeptide 5
IL	Interleukin
IL4R	Interleukin 4 receptor
IL10R	Interleukin 10 receptor
IRF	Interferon regulatory factor
Ir	Iridium
ISG	Interferon stimulated gene
JAK	Janus kinase
Leu-13	Leukocyte surface protein 13 (IFITM1)
LN	Lupus nephritis
MAdCAM1	Mucosal adhesion molecule 1
MFI	Mean fluorescence intensity
MHC	Major histocompatibility complex
MX1	MX dynamin like GTPase 1
MZP	Marginal zone precursor
MZB	Marginal zone B cell
NETs	Neutrophil extracellular traps
NF-κB	Nuclear factor kappa B
NOTCH	Neurogenic locus notch homolog protein
OL	Other lupus (non-nephritis)
PB	Plasmablast
PBMC	Peripheral blood mononuclear cells
PBS	Phosphate buffered saline
PCA	Principal component analysis
PFA	Paraformaldehyde
PLD4	Phospholipase D family member 4
PE	Phycoerythrin
PerCP	Peridinin-chlorophyll-protein
P/S	Penicillin-streptomycin
Pre-B	Precursor B cell
Pro-B	Progenitor B cell
RH123	Rhodamine 123
Rag	Recombination activating genes
RNA	Ribonucleic acid
RNP	Ribonucleoprotein
PRR	Pattern recognition receptor

SD	Standard deviation
SELL	Selectin L
SLE	Systemic lupus erythematosus
SLEDAI	SLE disease activity index
Sm	Smith antigen
SOX4	SRY-box transcription factor 4
SPADE	Spanning tree progression analysis of density-normalised events
SS	Sjögren's syndrome
SSC	Side scatter
STAT	Signal transducer and activator of transcription
T1	Transitional 1
T2	Transitional 2
T3	Transitional 3
TACI	Transmembrane activator and CAML interactor
T-bet	T-box expressed in T cells
TCL1A	T cell leukaemia/lymphoma protein 1A
TLR	Toll-like receptor
TS	Transitional B cell
tSNE	t-distributed stochastic neighbour embedding
UMAP	Uniform manifold approximation and projection
VDJ	Variable, diversity, joining
viSNE	Visualisation of stochastic neighbour embedding
VPREB1	V-set pre-b cell surrogate light chain 1
Yaa	Y chromosome-linked autoimmune 18cceleration
ZEB2	Zinc finger E-box binding homebox 2

1 Introduction

B lymphocytes are the cells of the immune system that are responsible for the production of antibodies. In the most part, antibody production benefits the host by protecting against infection using mechanisms including pathogen neutralisation and agglutination, opsonisation, antibody-dependent cellular toxicity, and complement fixation (reviewed by Forthal, 2014). However, antibodies that target self-antigens can also be strong indicators of disease or even cause pathology in autoimmune diseases (Elkon & Casali, 2008; Xiao et al., 2021). Although the reasons that self-antigens become targeted in autoimmune diseases are generally unknown, some of the associated changes in the profiles of B cells present in the blood are well described.

Work in this thesis will describe investigations of subtypes of B cells in human blood in health and in the autoimmune disease systemic lupus erythematosus. Therefore, in this first part of the introduction to this thesis, the development of B cells will be described followed by a description of B cell responses. This will be followed by a practical guide to the identification of B cells subsets in human peripheral blood that is important for many parts of this thesis.

1.1 Human B cell development

1.1.1 Development of transitional B cells from bone marrow precursors

B cell development originates in the bone marrow, where haematopoietic stem cells first give rise to common lymphoid progenitors. These common lymphoid progenitors then develop into CD34+ progenitor (pro)-B cells (Galy et al., 1995). Pro-B cells undergo rearrangement of their immunoglobulin variable (V), diversity (D) and joining (J) genes on the heavy chain gene locus to produce the heavy chain of the immunoglobulin, although these pro-B cells do not express immunoglobulins on the cell surface (Tonegawa, 1983). Pro-B cells give rise to precursor (pre)-B cells. First large pre-B cells develop from pro-B cells, which then develop into a smaller pre-B cell, both of which do not express a fully formed surface IgM (Gathings et al., 1977). Instead, pre-B cells express the immunoglobulin heavy chain together with a pseudo light chain in a complex termed the pre-B cell receptor (Kerr et al., 1989; Nishimoto et al., 1991).

The pre-B cells undergo rearrangement of light chain gene loci, most often at the κ (kappa) locus, if not at the λ (lambda) locus (Korsmeyer et al., 1982). After light chain rearrangement, cells develop into immature B cells that express both heavy and light chains of the B cell receptor. These immature B cells are known to express CD19 and CD20, much like peripheral blood B cells; additionally, immature B cells have been characterised by their CD10+CD21-CD23-CD24+++CD38+++IgM+ surface phenotype (Sims et al., 2005).

A central checkpoint within the bone marrow exists to prevent immature B cells with an autoreactive B cell receptor from exiting the bone marrow and entering the peripheral blood (Nemazee, 2017). After passing through the tolerance checkpoint and upon surface expression of IgD, cells are classed as transitional B cells. Transitional B cells have a CD19+CD10+CD21+CD24+++CD38+++IgM+IgD+ surface phenotype, similar to that of their immature bone marrow-resident precursors, with the exception of IgD expression. Transitional B cells, specifically transitional 1 (T1) B cells, are the first subset of B cells to emerge in the peripheral blood from the bone marrow (Palanichamy et al., 2009; Sims et al., 2005). Studies of B cell repopulation after haematopoietic stem cell transplantation and B cell depletion therapy with rituximab have demonstrated how T1 B cells are the first subset to reconstitute the B cell pool in the peripheral blood (Marie-Cardine et al., 2008; Palanichamy et al., 2009). The stages development of transitional B cells from a haematopoietic stem cell precursor is demonstrated in Figure 1.1.

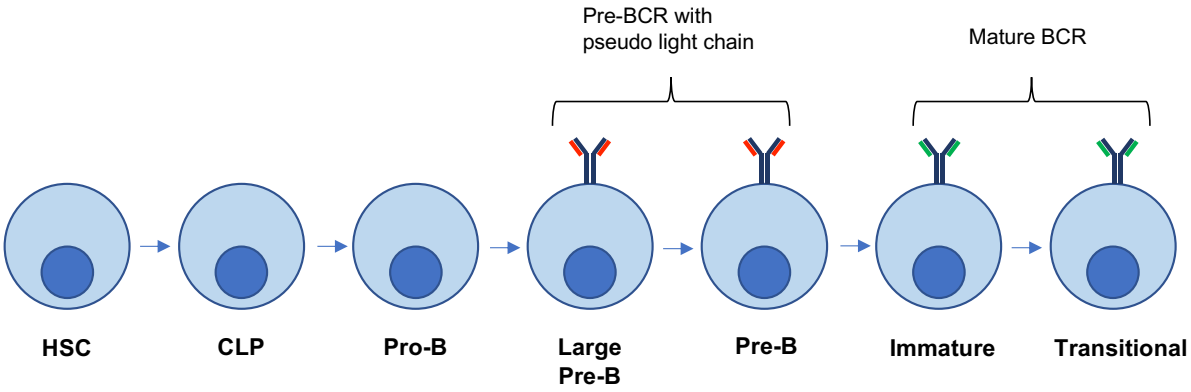

Figure 1.1: Development of transitional B cells from haematopoietic stem cells in the bone marrow. Schematic diagram demonstrating the stages of B cell development in the bone marrow starting from a haematopoietic stem cell (HSC) through to the transitional B cells, which are the first subset of B cells to exit the bone marrow and emerge in the peripheral blood. CLP, common lymphoid progenitor; BCR, B cell receptor.

1.1.2 Development of marginal zone B cells from transitional B cell precursors

T1 B cells in the peripheral blood develop into transitional 2 (T2) B cells, this development is characterised by the downregulation of CD24 and CD38 expression and the upregulation of CD21 (Suryani et al., 2010). Recently, Tull et al. (2021) identified a bifurcation in peripheral blood B cell development at the T1 to T2 stage. It was established that two populations of T2 B cells, defined by the level of expression of surface IgM, develop from T1 B cells (Tull et al., 2021). These subsets were termed T2 IgMhi and T2 IgMlo. T2 B cells, specifically T2 IgMhi cells, are known to express the gut homing receptor α4β7 integrin and have been found to be present and selectively recruited into the gut associated lymphoid tissue (Tull et al., 2021; Vossenkämper et al., 2013). T2 IgMhi cells have been found to express markers of activation CD69 and CD80 upon entering the gut associated lymphoid tissue (Tull et al., 2021).

The maturation of the earliest transitional B cells into late-stage transitional T3 B cells and subsequently mature naïve B cells is typified by downregulation of CD10, CD24 and CD38 expression and upregulation of CD21 (Cuss et al., 2006; Sims et al., 2005; Suryani et al., 2010). Both T3 and naïve B cell subsets have IgMhi and IgMlo subpopulations much like the T2 subset. Through pseudo time gene expression analysis using Slingshot, it is understood that the peripheral blood IgMhi B cell populations belong to a gut-homing trajectory that leads to the development of naïve marginal zone precursors and eventually marginal zone B cells (Tull et al., 2021), shown schematically in Figure 1.2. The naïve precursors to marginal zone B cells, known as MZP, express high levels of surface IgM and CD45RB and undergo NOTCH ligation and maturation into marginal zone B cells (Descatoire et al., 2014). MZP also have a similar transcriptomic profile to marginal zone B cells (Descatoire et al., 2014). It has been hypothesised that TLR9 stimulation drives transitional B cells towards marginal zone B cell differentiation by upregulating surface expression of IgM and NOTCH2 (Guerrier et al., 2012). In addition, the Slingshot analysis by Tull et al. (2021) identified a group of B cells beyond marginal zone cells on the trajectory that had features of DN2 B cells, including expression of *ZEB2* and *MX1*, however there are currently no known links between marginal zone B cells and DN2 cells (Jenks et al., 2018). DN2 B cells are known to be derived from a separate developmental branch,

the extrafollicular pathway, shown in Figure 1.2, whereby mature naïve cells become activated via TLR7 and IFNγ stimulation and eventually form DN2 cells then antibody secreting cells (Jenks et al., 2018; Tipton et al., 2015).

Marginal zone B cells are called as such due to their shared surface phenotype with B cells in the marginal zone of the spleen (Weller et al., 2004). Blood and splenic marginal zone B cells also have similar gene expression profiles and are known to be closely related (Weller et al., 2004). Although marginal zone B cells are CD27+ much like classical class-switched memory B cells, there is evidence to support the notion that they are a distinct subset of B cells, as described below.

Firstly, marginal zone B are phenotypically related to CD27-CD45RB+ precursors in a separate developmental IgMhi branch from memory B cells (Tull et al., 2021; Y. Zhao et al., 2018). It is not known whether the IgMlo developmental branch is linked to the development of class-switched memory cells, however it is evident that class-switched memory cells do not develop from the IgMhi branch, thus evidencing that marginal zone and memory B cells are distinct subsets. Secondly, marginal zone B cells and class-switched memory B cells are functionally different. Marginal zone B cells are innate-like and are important for immunity against encapsulated bacteria (Cerutti et al., 2013; Weller et al., 2004), whereas class-switched memory B cells function as long-term responders upon re-exposure to antigen (Akkaya et al., 2020).

When naïve B cells encounter antigen in the periphery, and receive help from preactivated cognate T cells, they may contribute to the germinal centre response in secondary lymphoid organs (Lanzavecchia, 1985; Rock et al., 1984). The enzyme activation induced cytidine deaminase (AID) catalyses two processes in association with the germinal centre response: class-switch recombination and somatic hypermutation (Muramatsu et al., 1999, 2000). Class-switch recombination is the process of changing the constant region of the immunoglobulin heavy chain to switch from IgM and IgD expression to expression of different immunoglobulin isotypes, namely IgG, IgA or IgE (Dunnick et al., 1993). Somatic hypermutation is the first part of the process of affinity maturation. As B cells divide as centroblasts in the dark zone

of the germinal centre, variable regions of the B cell receptor gene become targets of the AID enzyme, which converts cytidines into uracil (Chaudhuri et al., 2003; Dickerson et al., 2003; Muramatsu et al., 1999, 2000; Lodwig et al., 2003). The error prone mechanisms that repair the mutation result in diversification of the variable region sequence primarily through the introduction of point mutations (Rada et al., 2004). The B cells with mutated variable region genes then mature into less proliferative centrocytes and migrate to the light zone of the germinal centre (Casamayor-Palleja et al., 1996). B cells are then tested for their specificity by competition for antigen retained by follicular dendritic cells (Suzuki et al., 2009; Tew et al., 1990). The B cells that successfully compete for antigen present antigen peptides to T follicular helper cells that reside within the germinal centre and thus acquire the help they need to survive (Okada et al., 2005). Thus, only the B cells with the highest specificity for antigen mature to become either memory B cells or antibody producing cells (Anderson et al., 2009; Takahashi et al., 1998).

Human marginal zone B cells may not undergo class-switch recombination, but they do have somatic hypermutations in their immunoglobulin variable genes, albeit at a lower level than class-switched memory B cells (Klein et al., 1998; Weller et al., 2001). The mechanisms by which marginal zone B cells acquire somatic hypermutations is not entirely clear (Zhao et al., 2018). The very presence of these mutations suggests that marginal zone B cells acquire mutations in the germinal centre like class-switched memory B cells do (Weller et al., 2004). However, it has been observed that marginal zone B cells with somatic hypermutations exist in individuals with a CD40L deficiency and it has been proposed that these mutations could be acquired outside the germinal centre via a different mechanism to classical memory B cells (Weller et al., 2001). However, clones of marginal zone B cells with members in blood and the germinal centres of gut associated lymphoid tissue have been described (Zhao et al., 2018). It is possible that patients with mutations in CD40L have small germinal centres in the gut and mutations may have been acquired here (Facchetti et al., 1995).

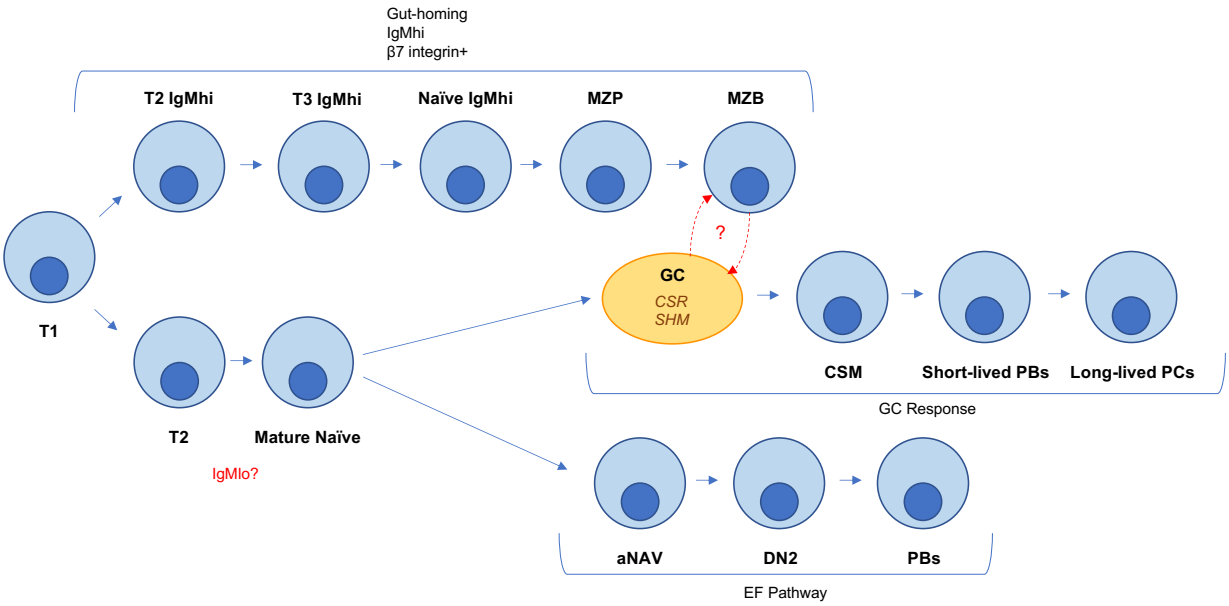

Figure 1.2: Model of B cell developmental pathways in the periphery. Schematic diagram demonstrating B cell development pathways post-exit from the bone marrow. Peripheral B cell development begins at the transitional B cell stage with transitional 1 (T1) B cells, which develop into transitional 2 (T2) and eventually transitional 3 (T3) B cells. The IgMhi gut-homing developmental trajectory characterised by work from Tull et al. (2021) and Vossenkämper et al. (2013) involves the sequential maturation of peripheral B cell subsets all of which have high surface expression of IgM and integrin β7. Subsets of B cells along this trajectory result in the development of marginal zone precursors (MZP) and then marginal zone B cells (MZB). The development of class-switched memory (CSM) B cells involves mature naïve B cells undergoing a germinal centre (GC) response, where somatic hypermutation (SHM) and class-switch recombination (CSR) take place, which leads to the production of class-switched memory (CSM) B cells and antibody secreting cells, namely plasmablasts (PBs) and plasma cells (PCs). The extrafollicular (EF) pathway stems from activated naïve (aNAV) cells responding to TLR7 stimulation and subsequently maturing into double negative (DN2) B cells (Jenks et al., 2018, 2019; Tipton et al., 2015).

Several surface protein markers are used to classify peripheral B cells into subsets; these markers enable the tracking of development from the earliest peripheral B cell subsets, the transitional subsets, to the terminally differentiated subsets, such as marginal zone and class-switched memory B cells. Many of these protein markers also have functional relevance to B cells as well as other immune cells. A summary of the

functions of the proteins used to classify peripheral B cells in this study is presented in Table 1.

Table 1.1: Functional relevance of surface protein markers used to classify peripheral B cell subsets.

Protein Marker	Function
CD1c	Lipid antigen presentation to T cells. CD1c expression is reduced upon B cell activation, lowering its lipid antigen-presenting function (Allan et al., 2011)
CD10	Endopeptidase that functions to inactivate signalling peptides by cleaving peptide bonds. Functional relevance has primarily been characterised in leukaemia. (Mishra et al., 2016)
CD11c	Forms complexes with other integrins to act as a cell adhesion receptor to facilitate cell migration, survival, and proliferation (Golinski et al 2020)
CD19	Functions as part of the B cell co-receptor complex with CD21 and CD81. Involved in lowering B cell receptor (BCR) signalling threshold and facilitating downstream BCR signalling (Otero et al., 2003; Fearon and Carter, 1995)
CD21	Functions as part of the B cell co-receptor complex with CD19 and CD81. Involved in lowering B cell receptor (BCR) signalling threshold (Fearon and Carter, 1995). Complement receptor (CR2) that binds opsonised antigens upon BCR-antigen binding to enhance B cell antigen response (Hannan, 2016; Cherukuri et al., 2001).
CD22	Inhibitory co-receptor of the B cell receptor (BCR) (Sieger et al., 2013; Poe et al., 2000).
CD23	Low affinity receptor for IgE that binds IgE/antigen complexes for presentation to T cells, enhancing the antibody response (Hjelm et al., 2006).
CD24	Induces apoptosis in B cells and promotes maturation of B cells from early developmental stages (Christian, 2022; Suzuki et al., 2001). Functional relevance predominantly characterised in B cells in the bone marrow.
CD27	Function in B cells is not well reported. Thought that ligation of CD27 allows for B cells to enter developmental pathway that leads to terminally differentiated plasma cells (Agematsu et al., 2000).
CD38	Functions as both receptor to CD31 and an enzyme to enable cell adhesion and metabolism, respectively (Piedra-Quintero et al., 2020).
CD40	Binds CD40L on T helper cells for facilitation of the T-dependent pathway, GC formation, isotype switching and somatic hypermutation (Elgueta et al., 2009).
CD45RB	CD45 functions as a regulator of Src kinases, therefore, regulates B cell receptor (BCR) signalling (Zikherman et al., 2012). CD45RB is a glycosylated form of CD45, distinctive functions of this form in B cells are not well understood.
CD62L	Mediates leukocyte tethering to the endothelium to facilitate B cell migration to lymph nodes (Lafouresse et al., 2015)
CCR7	Involved in trafficking B cells to and within secondary lymphoid tissues (Alrumaihi 2022).
CXCR5	Together with its ligand, CXCL13, directs B cells into follicles of secondary lymphoid organs (Förster et al., 1996).
Integrin β7	Involved in trafficking and retention of B cells in gut-associated lymphoid tissues (GALT) (Gorfu et al., 2009).

1.1.3 B cell homing and trafficking

B cell homing and trafficking are essential components of B cell development. These processes ensure B cells are kept in the appropriate microanatomical niche for relevant developmental changes. For instance, the interaction between the chemokine receptor CXCR4 and its ligand CXCL12 is important for retaining haematopoietic stem cells and B cell progenitors in their bone marrow niches so they can develop fully into immature B cells before exiting the bone marrow (Ma et al., 1999). In CXCR4-deficient mice, pro- and pre-B cells are absent from the bone marrow and are present at abnormally high levels in the blood, which consequently leading to a reduction in mature B cells In the blood (Ma et al., 1999) and in secondary lymphoid tissues (Nie et al., 2004) as cells have not fully developed in their bone marrow niches before entering the periphery.

Homing receptors also play a key role in the development of B cells post-bone marrow exodus. The receptor ligand pairs described below are those relevant to the work in this thesis.

As previously described in 1.2.2, marginal zone B cells and their IgMhi precursor subsets express the gut homing receptor integrin α4β7 (Tull et al., 2021; Vossenkämper et al., 2013). The integrin α4β7 is known to bind to mucosal adhesion molecule 1 (MAdCAM1), which is expressed on high endothelial venules of gut associated lymphoid tissues, to facilitate migration of B cells to the gut (Kraal et al., 1995). Expression of integrin β7, used as a surrogate for α4β7, on T2 IgMhi B cells selectively recruits this subset of cells to the gut associated lymphoid tissue that subsequently leads to cell activation (Tull et al., 2021; Vossenkämper et al., 2013). As it is known that marginal zone B cells develop from T2 IgMhi progenitors (Tull et al., 2021), it can be proposed that the early expression of integrin α4β7 homing receptor by progenitors is key to the development of the marginal zone B cell compartment.

Another chemokine receptor important for B cell trafficking is CXCR5. It is known that CXCR5, also known as BLR1, is expressed abundantly on the surface of the majority of mature circulating B cells (Förster et al., 1994). CXCR5 is the primary chemokine

receptor, along with its ligand CXCL13, responsible for the migration of B cells towards the B cell zone in secondary lymphoid organs, once they exit from the peripheral blood (Förster et al., 1996; Henneken et al., 2005). The importance of CXCR5 for lymphocyte homing was initially observed in mice whereby B cells from CXCR5 double knockout (*blr-/-*) mice fail to migrate to the B cell follicles of secondary lymphoid organs, namely the spleen and Peyer's patches, of *blr+/+* host mice (Förster et al., 1996), thus preventing these cells from undergoing relevant developmental changes in the follicle.

The chemokine receptor CCR7 is a further example of a key receptor important for homing B cells in the peripheral blood to secondary lymphoid organs. CCR7 has two ligands, CCL19 and CCL21 (Förster et al., 2008) and is primarily expressed on B cell subsets in the peripheral blood, however it has been reported that CCR7 is weakly expressed on pro- and pre-B cells in the bone marrow (Honczarenko et al., 2006). In addition to its homing function, CCR7 has been found to play a role in B cell activation (Förster et al., 1999).

L-selectin, also known as CD62L, is a cell adhesion molecule important for homing to secondary lymphoid organs (Gallatin et al., 1983). L-selectin is expressed on the surface of most circulating lymphocytes and has been found to be highly expressed on cells in the bone marrow that are destined for either the lymphoid or myeloid lineages (Kohn et al., 2012). L-selectin expressed on the surface of lymphocytes functions by facilitating binding to high endothelial venule walls, which allows for trafficking to lymph nodes (Lafouresse et al., 2015). The gene that codes for L-selectin, *SELL*, is known to be expressed at a higher level on IgMlo T2 B cells in comparison with their IgMhi counterparts (Tull et al., 2021). It has been observed that in patients with SLE levels of soluble serum L-selectin are significantly greater than that of healthy donor controls and that the level of L-selectin in serum correlates with disease activity and double-stranded DNA antibody titres (Font et al., 2002).

1.2 Systemic lupus erythematosus (SLE)

1.2.1 SLE overview and pathogenesis

Systemic lupus erythematosus (SLE) is an autoimmune disease that involves multiple facets of the immune system. SLE can affect several organs including the skin, joints, the kidneys, and the central nervous system; the involvement of these organs manifests in many forms such as malar rashes, hair loss, arthritis, glomerulonephritis and in some cases seizures and psychosis (Kaul et al., 2016). SLE is nine times more prevalent in women compared to men and is more common in individuals from African or Caribbean ethnic groups (D'Cruz et al., 2007; Izmirly et al., 2021; Kumar et al., 2009).

SLE, like many other autoimmune diseases, is characterised by periods of flare in which the patient's symptoms and clinical features are worsened. SLE disease activity index (SLEDAI) is a scoring system used to assess disease activity and health status of patients with SLE (Bombardier et al., 1992; Gladman et al., 2002). SLEDAI considers several disease manifestations across multiple organ systems to determine how the severity of disease activity. This scoring system can be used as an indicator for periods of disease flare and will evoke the appropriate clinical management.

The process of humoral autoimmunity causing the production of autoantibodies is a hallmark of SLE. Autoantibodies produced in SLE are predominantly anti-nuclear antibodies. The most common autoantibodies found in patient sera include anti-double-stranded DNA (dsDNA), anti-Smith antigen (Sm), anti-ribonucleoproteins (RNP) and anti-Sjögren's-syndrome-related antigen A and B (SSA/Ro, and SSB/La, respectively) (Ceppellini et al., 1957; Provost et al., 1991; Tan & Kunkel, 1966). Although there have been numerous other autoantibodies detected in patients with SLE including those against complement system component C1q (Yaniv et al., 2015). The presence of autoantibodies is often detectable before the disease presents clinically (Arbuckle et al., 2003). Autoantibodies contribute to the build-up of immune complexes, which can lead to inflammation and damage to organs when these immune complexes are deposited (Levinsky et al., 1977).

In addition, the failure to clear apoptotic debris has been proposed as a key aspect of lupus pathogenesis (reviewed by Mũoz et al., 2010); the defects in clearance of apoptotic debris can promote inflammation and a breakdown of self-tolerance. Furthermore, the formation of neutrophil extracellular traps (NETs), via a process known as NETosis, is another key aspect of SLE pathogenesis. NETs are extracellular structures composed of decondensed chromatin, produced by neutrophils (Brinkmann and Zychlinsky, 2007). Typically, in health, NETs are important in trapping and neutralising pathogens; however, when dysregulated NETosis can contribute to the breakdown of self-tolerance in SLE. NETs comprising of SLE autoantigens have been found to induce autoantibody production and the formation of immune complexes, which then contributes to the formation of more NETs and leads to a cycle of autoantibody immune complex formation (Garcia-Romo et al., 2011; Lande et al., 2011).

Lupus nephritis is the most severe manifestation of SLE that occurs in approximately 40% of individuals with SLE (Maria & Davidson, 2020) and often occurs within the first five years of SLE diagnosis (Cervera et al., 2003; Hanly et al., 2015). Of the cohort of SLE patients with lupus nephritis, between 10-30% of them develop end-stage renal disease (ESRD) (Maroz & Segal, 2013). Glomerular damage in the kidney is caused by the deposition of immune complexes, leukocyte recruitment, complement activation and the formation of NETs (Flores-Mendoza et al., 2018). The proportions of several B cell subsets in the peripheral blood are altered in lupus nephritis specifically, not in other forms of lupus where nephritis is not present, thus highlighting the importance of investigating B cells in this cohort of SLE patients.

Numerous alleles, in which the proteins that they encode are involved in several aspects of the immune system, have been identified in association with an increased risk of SLE. A few of these include in risk alleles in *FCGR2A* and *FCGR3B*, which bind the Fc portion of immunoglobulins (Harley et al., 2008; Morris et al., 2010), *IL10*, an anti-inflammatory cytokine (Gateva et al., 2009), *PTPN22*, a negative regulator of T cell receptor signalling (Gateva et al., 2009; Kyogoku et al., 2004), transcription factor

STAT4 (Han et al., 2009; Harley et al., 2008) and inflammatory marker *CRP* (Edberg et al., 2008).

Multiple genome wide association studies have highlighted common polymorphisms in or near the (toll-like receptor 7) *TLR7* gene (dos Santos et al., 2012; Shen et al., 2010; Wang et al., 2014). The TLR7 protein is central in the pathogenesis of SLE as it drives the production of DN2 B cells and autoantibody secreting cells (Jenks et al., 2018). In mouse models of SLE, overexpression of *Tlr7* due to expression of the Yaa (Y chromosome-linked autoimmune acceleration) locus results in increased TLR7 signalling and expansion of CD11c+CXCR5- double negative B cells (Deane et al., 2007; Ricker et al., 2021; Subramanian et al., 2006). The Yaa locus is comprised of the Y chromosome with an additional translocated cluster of X-linked genes, which confers a lupus-like syndrome in mice (Fairhurst et al., 2008; Izui et al., 1994; Pisitkun et al., 2006; Subramanian et al., 2006). In male mice with the Yaa locus, transcription of many of the translocated X-chromosome genes is increased 2-fold, one of which is TLR7, which is thought to be the major causation of the autoimmune phenotypes seen in mice expressing the Yaa locus (Fairhurst et al., 2008; Ricker et al., 2021).

Genetic variations in TLR7 in humans have not been as extensively reported, however, recently Brown et al. (2022) identified three *TLR7* gain-of-function variants in patients with SLE: Y264H, F507L and R28G. Interestingly, in the patient with the $TLR7^{F507L}$ variant, it was noted that the patient's mother, who also had SLE, carried the same $TLR7^{F507L}$ variant (Brown et al., 2022). The $TLR7^{Y264H}$ variant was introduced into mice (termed kika mice), and it was found that this variant was associated with aberrant B cell survival, extrafollicular B cell proliferation and glomerulonephritis (Brown et al., 2022). The kika mice also produced antibodies to Sm and RNP proteins (Brown et al., 2022). These findings highlighted the first gain-of-function variants of *TLR7* in humans with SLE, which can be directly linked to characteristic pathogenic disease features.

Typically, SLE is treated with immunosuppressants, such as mycophenolate mofetil (MMF) and azathioprine. Both MMF and azathioprine have proven effective in the long-term treatment of lupus nephritis (Houssiau et al., 2010). The anti-malarial,

hydroxychloroquine, is also frequently used in SLE treatment. Hydroxychloroquine can pass through the cell membrane due to its lipophilicity, where it then disrupts cellular function (Dima et al., 2022). It has been identified that hydroxychloroquine has been shown to inhibit the action of TLR7 and TLR9 (Kužnik et al., 2011; Lamphier et al., 2014), inhibit cyclic GMP-AMP synthase (cGAS) activity in mouse models (An et al., 2018), and decrease NET formation *in vitro* (Smith and Kaplan, 2015). Thus, it is thought that hydroxychloroquine can disrupt several pathogenic processes in SLE.

In recent years, B cells have specifically been the target of lupus therapies. Most used biologic therapies include belimumab, a fully humanised monoclonal antibody against the BAFF and rituximab, a chimeric anti-CD20 monoclonal antibody. Belimumab was the first targeted biological treatment for SLE (Navarra et al., 2011), it's mechanism of action involves binding soluble BAFF to prevent interaction with BAFF-R to decrease B cell survival (Baker et al., 2003). Rituximab targets CD20 on the surface of all B cells, thus allows for complete B cell depletion. Studies have shown that the occurrence of flares is less frequent in SLE patients after they have undergone rituximab-induced B cell depletion (Gracia-Tello et al., 2017). Given that these biologics significantly reduce the B cell pool, it has been established that these therapies pose an additional risk of infection to SLE patients, whom are already at an increased risk of infection compared to healthy individuals (Rodziewicz et al., 2023). However, in patients with moderate-to-severe SLE, both rituximab and belimumab are proven effective therapies despite this increased infection risk (Rodziewicz et al., 2023).

1.2.2 Loss of B cell tolerance in SLE

Throughout B cell development, B cells go through tolerance checkpoints in order to eliminate autoreactive B cells. In healthy humans two checkpoints exist, the first being in the bone marrow and the second in the periphery. In the bone marrow, autoreactive B cells are removed in a series of processes collectively known as central tolerance. The mechanisms underpinning central tolerance include clonal deletion, receptor editing and anergy (Brink et al., 1992; Gay et al., 1993; Nemazee & Bürki, 1989). At the pre-B cell stage, after the expression of a surface B cell receptor, autoreactive B cells may undergo clonal deletion whereby these autoreactive cells are "deleted" from the bone marrow by apoptosis (Nemazee & Buerki, 1989). If autoreactive B cells are not removed by clonal deletion, the self-reactive B cell receptors on immature B cells in the bone marrow interact with self-antigens and signal the upregulation and activation of recombinase-activating genes (Rag), which in turn promote receptor editing (Gay et al., 1993; Hertz & Nemazee, 1997; Nemazee & Bürki, 1989; Tiegs et al., 1993). Receptor editing involves rearrangement of the immunoglobulin light chain locus, which results in a change in the specificity of the B cell receptor on immature B cells in the bone marrow (Gay et al., 1993). Immature B cells that escape the other central tolerance mechanisms may undergo the process of anergy, which results in cells becoming functionally silent and unresponsive to antigen.

After B cells exit the bone marrow and enter the periphery, they go through a second checkpoint, known as peripheral tolerance, in order to remove any autoreactive B cells that were not removed via central tolerance mechanisms in the bone marrow. However, the exact mechanisms by which this occurs are not fully understood. In health, it has been reported that approximately 40% of newly emerged transitional B cells and 20% of mature naïve B cells in the periphery express B cell receptors with auto-reactivity (Wardemann et al., 2003). In SLE, it has been observed that whilst there is no significant difference in the percentage of transitional B cells with auto-reactivity compared to health, there is a loss of peripheral tolerance and failure to remove autoreactive B cells before development into mature naïve B cells (Yurasov et al., 2005). Yurasov et al. (2005) reported between 40-50% of mature naïve B cells in

SLE have a B cell receptor with self-specificity compared to 20% in healthy donors. The loss of peripheral tolerance in SLE contributes to the elevated production of autoreactive, pathogenic B cells.

1.2.3 Altered B cell subset frequencies and function in SLE

There are several known alterations in the proportions of certain B cell subsets, especially in lupus nephritis, as demonstrated in the altered model of peripheral B cell development in Figure 1.3. SLE is characterised by the expansion of CD27-IgD- double negative B cells, specifically the DN2 subset (Wei et al., 2007). It has been reported that DN2 B cells are derived from aNAV cells and both subsets are hyperresponsive to TLR7 stimulation, (Jenks et al., 2018; Tipton et al., 2015). Jenks et al. (2018) identified that TLR7 and IL-21, in conjunction with interferon-γ (IFNγ), drive B cell differentiation from aNAV B cells into DN2 B cells then into antibody secreting cells as part of the extrafollicular response pathway. In health, the DN2 population comprises less than 5% of the total peripheral blood B cell pool, however in SLE the frequency of DN2 B cells is over double that of health at approximately 10-15% of all B cells (Jenks et al., 2018; Morbach et al., 2010). The increase in DN2 B cells in SLE leads to increased production of antibody secreting cells which produce autoreactive antibodies, a hallmark of SLE pathogenesis (Tipton et al., 2015).

Expansion of the CD27-IgD- B cell compartment seen in SLE is not evident across other similar autoimmune conditions, such as Sjögren's Syndrome. In contrast to SLE, it has been found that patients with Sjögren's have less CD27-IgD- B cells than healthy controls (Martin-Gutierrez et al., 2021), but interestingly the expansion of DN2 B cells and an enhanced extrafollicular response has been observed in cases of severe acute respiratory syndrome coronavirus 2 (SARS-CoV-2) infections (Woodruff et al., 2020). It has previously been shown that upon activation of the extrafollicular pathway in SLE, the increase in the abundance of DN2 B cells coincides with a decrease in the number of DN1 B cells (Jenks et al., 2018; Tipton et al., 2015). Woodruff et al. (2020) identified that the DN1:DN2 ratios were significantly higher in patients with severe SARS-CoV2 infections and active SLE compared to healthy controls, however this ratio was not different between the two disease cohorts.

Reduced proportions of marginal zone B cells in the peripheral blood of lupus nephritis patients have previously been identified (Tull et al., 2021; Zhu et al., 2018). In peripheral blood of healthy donors, marginal zone B cells account for 10-15% of all

CD19+ B cells, whereas in lupus nephritis marginal zone B cells account for less than 5% of the peripheral B cell population (Morbach et al., 2010; Tull et al., 2021; Zhu et al., 2018). Tull et al. (2021) also noted that the precursor population of marginal zone B cells, MZP, are also significantly reduced in lupus nephritis patients compared to healthy donors. The functional implications of the loss of marginal zone B cells and their precursors are not well understood. However, there have been reports of increased susceptibility to and severity of bacterial infections in patients with SLE (Battaglia & Garrett-Sinha, 2021; Danza & Ruiz-Irastorza, 2013) and as marginal zone B cells are known to play a role in immunity against encapsulated bacteria (Cerutti et al., 2013; Weller et al., 2004), the loss of these cells in the most severe manifestation of SLE may be linked to increased and worse bacterial infections.

In addition, regarding the transitional subset, it has been previously reported that there is a relative increase in the proportion of CD24hiCD38hi transitional B cells in lupus nephritis compared to health (Simon et al., 2016), however further sub-dividing of the transitional B cell population has revealed more differences in the abundance of transitional B cells in SLE. B cells belonging to the T1 subset from SLE patients have been found to produce significantly less IL-10 than T1 B cells from healthy donors and therefore lack the usual immunosuppressive function these cells possess in health, thus contributing to the hyperimmune responses typical of autoimmune diseases (Blair et al., 2010). Additionally, it has been found that there is also a decrease in the proportion of T2 IgMhi and T3 CD45RBhi/IgMhi cells in lupus nephritis compared to health (Tull et al., 2021). The reduction in frequency of T2 IgMhi and T3 CD45Rbhi cells is a feature of the peripheral B cell compartment in lupus nephritis patients only; the frequencies of these transitional subsets is of a similar level to that of health in lupus patients with no nephritis (Tull et al., 2021).

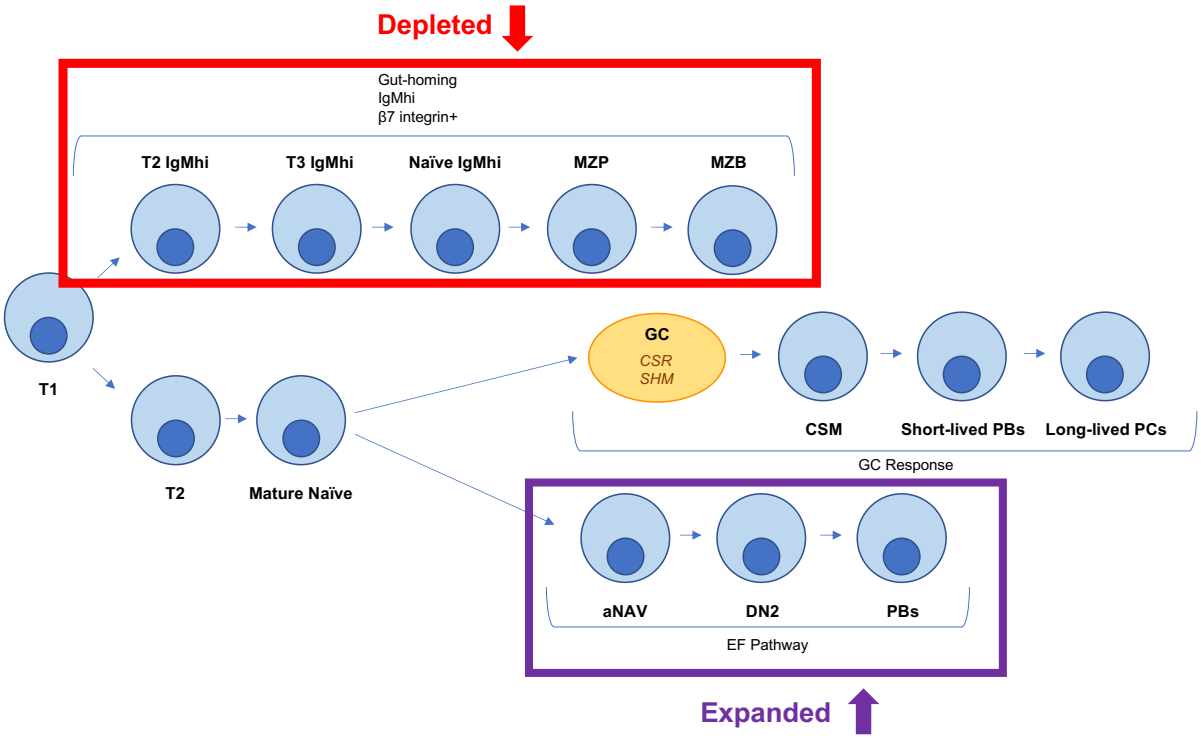

Figure 1.3: Altered model of B cell development pathways in the periphery in lupus nephritis. Schematic diagram showing observed changes in the B cell development pathways post-exit from the bone marrow in lupus nephritis in comparison to peripheral blood B cell development in healthy individuals (shown in Figure 1.2). The IgMhi gut-homing developmental trajectory, characterised by Tull et al. (2021) and Vossenkämper et al. (2013), that leads to the development of marginal zone B cells (MZB) has been found to be depleted in lupus nephritis (Tull et al., 2021; Zhu et al., 2018). The extrafollicular (EF) pathway involving the development of double negative (DN2) B cells and subsequently plasmablasts (PBs) from activated naïve (aNAV) precursors after TLR7 stimulation is expanded in SLE (Jenks et al., 2018, 2019; Tipton et al., 2015). T1, transitional 1; T2, transitional 2; T3, transitional 3; GC, germinal centre; CSR, class-switch recombination; SHM, somatic hypermutation; CSM, class-switched memory; PCs, plasma cells.

1.2.4 Interferon in SLE

Interferons (IFN) have been long associated with anti-viral response (Isaacs & Lindenmann, 1957; Katze et al., 2002); however, they are known to have prominent role in SLE pathogenesis (Bennett et al., 2003; Psarras et al., 2017; Rönnblom & Alm, 2001). There are three types of interferon (type I, type II, type III). Type I interferons encompass 13 subtypes of IFNα, IFNβ, IFNω, IFNε and IFNκ (Pestka et al., 2004; Psarras et al., 2017). Type I interferons signal via the interferon-α/β receptor (IFNAR1), which is comprised of two subunits IFNAR1 and IFNAR2 (Novick et al., 1994). IFNAR1 is associated with the tyrosine kinase JAK1, which is key for type I interferon signal transduction (Shemesh et al., 2021). The type II interferon family comprises only one member, IFNγ, which binds the interferon-γ receptor (IFNGR) and signals via the JAK/STAT pathway, similar to type I interferons (Darnell et al., 1994). Type III interferons are termed IFNλ1-4 and are known to signal through the interferon-λ receptor 1 (IFNLR1) and the IL10R to promote an anti-viral response (Kotenko et al., 2003).

It was previously thought that plasmacytoid dendritic cells were the main cell type responsible for the production of type I interferons (Siegal et al., 1999). However, more recent studies have revealed that plasmacytoid dendritic cells do not co-localise with interferon in renal tissue but instead, highest levels of interferon is found in the glomeruli area, suggesting an alternate source of interferon within the tissue is more prevalent (Iwamoto et al., 2022). In a typical immune response, interferon production is triggered in response to stimulation of pattern recognition receptors (PRRs) by microbial antigens (reviewed by McNab et al., 2015). In SLE, immune complexes comprising immunoglobulin bound to nucleic acid are key drivers of interferon production by plasmacytoid dendritic cells. Immune complexes bind the receptor FCγRIIa on plasmacytoid dendritic cells, which results in the activation of toll-like receptors (TLR7 or TLR9) and the subsequent production of IFNα (Båve et al., 2003). Additionally, increased presence of apoptotic cells in SLE present another source of nucleic material, which can promote the production of IFNα by plasmacytoid dendritic cells (Båve et al., 2003). Type I interferons have been found to enhance the survival of transitional B cells from patients with SLE through activation of the NF-κB pathway

and the reduced expression of the pro-apoptotic molecule BAX (Liu et al., 2019). Additionally, Liu et al. (2019) observed the promotion of pro-inflammatory properties, namely the production of IL-6, in transitional B cells from SLE patients due to an overactivated type I interferon signalling pathway.

Elevated serum IFNα has been observed in SLE patients and there is a positive correlation between the level of IFNα in serum and disease severity (Rönnblom & Alm, 2001). The prevalence of severe lupus nephritis is associated with an increase in serum interferon (Iwamoto et al., 2022). In kidney biopsy samples from SLE patients with the most severe form of lupus nephritis, mRNA encoding IFNα has been found to be most highly expressed in the tubular epithelial cells, suggesting possible autocrine production of IFNα in the kidneys of lupus nephritis patients (Castellano et al., 2015).

In a recent study by Zheng et al. (2022), single-cell RNA-sequencing was used to identify plasmablasts with an interferon gene signature in the dermis and epidermis of the skin from patients with the skin-only manifestation of lupus, discoid lupus erythematosus (DLE), as well as in the skin of SLE patients. It was found that B cells in the epidermal layer in healthy controls were predominantly associated with RNA catabolic processes whereas B cells in the same epidermal layer in patients with DLE and SLE were involved in type I interferon signalling and response to interferon gamma, suggesting enhanced interferon activity at the sites of skin lesions in lupus (Zheng et al., 2022).

An interferon gene signature characterised by the upregulation of interferon stimulated genes (ISG) is typical of immune cells in individuals with SLE (Nehar-Belaid et al., 2020). ISG expression occurs after a cell is exposed to interferon and the subsequent signalling cascade is triggered (Der et al., 1998; Schoggins and Rice, 2011). Peripheral blood cells from patients with active SLE have been found to have a >2-fold change in expression of 286 interferon inducible genes compared to that of healthy donors (Baechler et al., 2003). ISG expression has been identified in B cells from patients with SLE (Bennett et al., 2003; El-Sherbiny et al., 2018). Assessing the level

of ISG expression can be used as a predictor for disease progression and severity (Mai et al., 2021).

Genetic susceptibility to SLE is complicated, with numerous loci being identified as risk alleles, some of which are directly related to interferon. One example being the interferon regulatory factors (IRFs), first identified over 30 years ago (Miyamoto et al., 1988), that are a family of transcription factors crucial for negatively regulating the expression of interferon inducible genes (Honda & Taniguchi, 2006; Taniguchi et al., 2001). The IRF family consists of nine members, some of which have been identified as possible SLE risk alleles, for instance *IRF5* alleles (rs2004640T and rs10488631) have been associated with increased exon splicing and increased transcript and protein levels of IRF5 isoforms in SLE (Feng et al., 2010; Graham et al., 2006). In addition, single nucleotide polymorphisms in another IRF family member, IRF7, have been linked to genetic susceptibility to SLE (Fu et al., 2011; Harley et al., 2008). IRF7 is plays an important role in the regulation of IFNα production. Fu et al. (2011) identified a single nucleotide polymorphism in IRF7 (Q412R) in Asian, European, and African American SLE patients, which resulted in a 2-fold increase in interferon-stimulated transcriptional activity and elevated IRF7 activity.

Whilst type I interferons are known to have many associations with SLE, type II interferon, IFNγ, also has been linked to SLE pathogenesis. In mice, IFNγ, along with IL-4 and IL-21, is known to increase expression of T-bet and CD11c in TLR-activated antibody-secreting cells (Naradikian et al., 2016). In humans, TLR7 stimulation in the presence of IFNγ and IL-21 causes the development of DN2 and plasmablasts from aNAV B cells in SLE (Jenks et al., 2018), thus demonstrating the role of IFNγ in the extrafollicular response and the production of pathogenic antibody secreting cells in SLE.

1.3 Methodologies applied to investigate B cells in peripheral blood in this study

This study has used several methodologies with the aim of investigating subsets of B cells from peripheral blood at a greater resolution and in greater depth. Single-cell RNA-sequencing with CITE-seq antibody labelling allowed for the integration of protein and transcriptome data at a single-cell level (Stoeckius et al., 2017). A type of mass cytometry measured by time-of-flight (CyTOF) was used in this study to investigate expression of a wide range of proteins given the large panel size compatible with this method. Flow cytometry is a frequently used for immunophenotyping and has been used in this study to make comparisons between B cells subsets from peripheral blood in health versus lupus nephritis as well as being used to validate findings observed by other methodologies.

1.3.1 10X single-cell RNA-sequencing with CITE-seq antibody staining

The single-cell RNA-sequencing dataset analysed in this study was generated prior to the start of this project. Cell samples are stained with oligonucleotide-labelled CITE-seq (Cellular Indexing of Transcriptomes and Epitopes by sequencing) antibodies prior to sequencing. The 10X Chromium system uses droplet-based encapsulation whereby a single cell is encased in a gel bead in what is known as a gel bead in emulsion (GEM); each gel bead is labelled with oligonucleotides that includes a unique barcode so data outputs can be traced back to a single cell (See et al., 2018). Downstream processing includes reverse transcription, cDNA amplification and library construction followed by sequencing and data acquisition. Data outputs available for analysis include single-cell gene expression profiles, cell surface marker expression via CITE-seq antibody staining and B cell receptor VDJ sequences. Analysis of this data is performed using the R package known as Seurat (Stuart et al., 2019). Seurat uses top differentially expressed genes to generate clusters of cells with similar gene expression patterns. Average log2 fold change in expression of genes of interest can then be compared between clusters of cells. The inclusion of CITE-seq antibody staining adds value to the data as it can be used to aid identification of cell subsets as well as providing surface

protein data expression. The data analysis pipeline used for the analysis of single-cell RNA-sequencing data is described in 2.3 in Materials and Methods.

1.3.2 Mass cytometry (CyTOF)

Mass cytometry is used for phenotypic and functional analysis of cells. Unlike flow cytometry, mass cytometry does not use fluorescence, instead antibodies are conjugated to metal isotopes (Kay et al., 2016). The type of mass cytometry used in this study is known as CyTOF (cytometry by time-of-flight), which allows for the detection and quantification of multiple extracellular and intracellular markers simultaneously. CyTOF can be used to detect small subsets of cells (Yao et al., 2014), thus making it useful for characterising some of the smaller peripheral blood B cells subsets previously described such as the transitional populations. Mass cytometry also allows for approximately 35 markers to be included on one panel, which can be useful when defining multiple subsets of B cells as well as investigating expression of experimental markers. The protocol used for mass cytometry experiments is outlined in 2.4 in Materials and Methods.

1.4 Aim and Hypotheses

The aim of this study was to investigate the differences, in terms of abundance, gene expression and, protein marker expression between subsets of B cells from peripheral blood in healthy donors compared to that of lupus nephritis patients. This aim was established because lupus nephritis remains the most severe manifestation of SLE and there are known changes to the peripheral B cell compartment in this disease. The aim of this study was to explore some of these changes in greater depth.

To investigate this study aim, the following hypotheses were tested:

Chapter 3:

- T1 B cells from lupus nephritis patients express lower levels of IgMhi-associated genes compared to T1 B cells from healthy donors
- T1 B cells from lupus nephritis patients express genes associated with proliferation and activation at a lower level than T1 B cells from healthy donors
- T2 IgMhi B cells are less abundant in lupus nephritis compared to health

Chapter 4:

- B cells from lupus nephritis patients have greater expression of proteins of ISGs compared to B cells from healthy donors
- Transitional B cells express IFITM1, IRF7, MX1 and BST2 at the protein level in both health and lupus nephritis
- B cells that expression proteins of ISGs also express chemokine CXCR4 and activation markers CD69 and CD83 at a higher level than other B cells

Chapter 5:

- B cells that are known to be depleted in lupus nephritis, such as MZB, are reduced more during lupus flares compared to when disease is more stable
- B cell subsets that are depleted in lupus nephritis, such as MZB and MZP, can return to levels like that of health upon disease stability
- DN2 B cells are expanded in lupus nephritis flares compared to health more so than during stable disease

Chapter 6:

- MZB subset of B cells comprises two populations, MZB1 and MZB2, that can be differentiated based on expression of integrin β7 and CCR7
- MZB1 B cells are depleted in lupus nephritis
- MZB subsets differ in terms of activation

2 Materials and Methods

For this study, data generated from the following techniques were included: single-cell RNA-sequencing, mass cytometry and flow cytometry. Prior to the start of this study, the single-cell RNA-sequencing dataset had been generated by another member of the lab group. For this study, I used computational methods to analyse this RNA-sequencing dataset for the first time. In addition, I conducted both the mass cytometry and flow cytometry wet lab experiments and computational analyses included in this thesis.

2.1 List of Reagents

All reagents used for wet lab experiments included in this study are listed below in Table 2.1.

Table 2.1: Reagents used for experiments in this study

Reagent	Supplier	Product Code
Reagents for buffers and media		
Foetal calf serum	ThermoFisher Scientific–- Gibco	10270-106
RPMI medium (1X) + L-Glutamine	ThermoFisher Scientific–- Gibco	21875-034
Penicillin-streptomycin	Sigma Aldrich	P0781
Dulbecco's Phosphate Buffered Saline (DPBS 1X)	ThermoFisher Scientific–- Gibco	14190144
Phosphate Buffered Saline (PBS 1X)	ThermoFisher Scientific–- Gibco	10010023
dNase I Grade II from bovine pancreas	Sigma Aldrich	10104159001
eBioscience™ Foxp3/ Transcription Factor Staining Buffer Set	ThermoFisher Scientific–- Invitrogen	00-5323-00
0.5M EDTA, pH8	ThermoFisher Scientific–- Invitrogen	15575020
Bovine serum albumin	Sigma Aldrich	A3294
Mass cytometry antibodies and other reagents		
Anti-CD10 158Gd clone HI10A	Fluidigm (now Standard BioTools)	3158011B
Anti-CD1c 173Yb clone L161	Biolegend	331502
Anti-CD11c 147Sm clone Bu15	Fluidigm (now Standard BioTools)	3147008B
Anti-CD124 (IL4R) 149Sm clone G077F6	Biolegend	355002
Anti-CD184 (CXCR4) 156Gd clone 12G5	Fluidigm (now Standard BioTools)	3156029B
Anti-CD185 (CXCR5) 171Yb clone RF8B2	Fluidigm (now Standard BioTools)	3171014B

Anti-CD19 14^{2N}d clone HIB19	Fluidigm (now Standard BioTools)	3165025B
Anti-CD197 (CCR7) 175Lu clone G043H7	Biolegend	353237
Anti-CD21 152Sm clone BL13	Fluidigm (now Standard BioTools)	3152010B
Anti-CD22 159Tb clone HIB22	Fluidigm (now Standard BioTools)	3159005B
Anti-CD23 164Dy clone EBVCS-5	Fluidigm (now Standard BioTools)	3164018B
Anti-CD24 169Tm clone ML5	Fluidigm (now Standard BioTools)	3169004B
Anti-CD267 (TACI) 168Er clone 1A1	Biolegend	311902
Anti-CD268 (BAFF-R) 155Gd clone 11C1	Fluidigm (now Standard BioTools)	3155005B
Anti-CD27 167Er clone 323	Fluidigm (now Standard BioTools)	3167002B
Anti-CD38 154Sm clone HIT2	Biolegend	303535
Anti-CD40 165Ho clone 5C3	Fluidigm (now Standard BioTools)	3165005B
Anti-CD45 89Y clone H130	Fluidigm (now Standard BioTools)	3089003B
Anti-CD45RB 145Nd clone MEM-55	Fluidigm (now Standard BioTools)	3145009B
Anti-CD62L (L-selectin) 153Eu clone DREG-56	Fluidigm (now Standard BioTools)	3153004B
Anti-CD69 144Nd clone FN50	Fluidigm (now Standard BioTools)	3144018B
Anti-CD74 166Er clone LN2	Fluidigm (now Standard BioTools)	3166018B
Anti-CD83 143Nd clone HB15e	Biolegend	305302
Anti-CD86 150Nd clone IT2.2	Fluidigm (now Standard BioTools)	3150020B
Anti-CD99 170Er clone HCD99	Fluidigm (now Standard BioTools)	3170012B
Anti-BST2 174Yb clone RS38E	Biolegend	348402
Anti-IFITM1 163Dy clone EPR22620-12	Abcam	ab25573
Anti-IgA 148Nd clone polyclonal	Fluidigm (now Standard BioTools)	3148007B
Anti-IgD 146Nd clone IA6-2	Fluidigm (now Standard BioTools)	3146005B
Anti-IgM 172Yb clone MHM-88	Fluidigm (now Standard BioTools)	3172004B
Anti-Ig kappa 160Gd clone MHK-49	Fluidigm (now Standard BioTools)	3160005B
Anti-Ig lambda 151Eu clone MHL-38	Fluidigm (now Standard BioTools)	3151004B
Anti-integrin β7 162Dy clone FIB504	Fluidigm (now Standard BioTools)	3162026B
Anit-IRF7 141Pr clone 12G9A36	Biolegend	656002
Anti-MX1 176Yb clone EPR19967	Abcam	ab222492
Cell-ID Intercalator-Ir 125uM	Fluidigm (now Standard BioTools)	201192A
Cis-Diamineplatinum(II) dichloride (cisplatin)	Sigma Aldrich	479306

Paraformaldehyde solution, 4% in PBS	Thermo Scientific	15670799
Flow cytometry antibodies and other reagents		
Anti-CD1c PE clone L161	Biolegend	331506
Anti-CD1c BV510 clone L161	Biolegend	331534
Anti-CD10 BV421 clone HI10a	Biolegend	312217
Anti-CD19 PerCP-Cy5.5 clone HIB19	Biolegend	302230
Anti-CD21 BUV737 clone B-ly4	BD Biosciences	612788
Anti-CD24 BV605 clone ML5	Biolegend	311124
Anti-CD27 APC clone M-T271	Biolegend	356410
Anti-CD38 BUV395 clone HB7	BD Biosciences	563811
Anti-CD45RB AF594 clone MEM-55	Biolegend	310208
Anti-IgD APC-Cy7 clone IA6-2	Biolegend	348218
Anti-IgM BV711 clone MHM-88	Biolegend	314540
Anti-IFITM1 clone EPR22620-12	Abcam	ab233545
Anti-integrin β7 FITC clone FIB504	Biolegend	321212
Anti-BST2 PE-Cy7 clone RS38E	Biolegend	348416
Anti-CCR7 BV605 clone G043H7	Biolegend	353224
Donkey anti-rabbit IgG PE clone Poly4064	Biolegend	406421
APC mouse IgG1k isotype control clone MOPC-21	Biolegend	400120
APC-Cy7 mouse IgG2a,κ isotype control clone MOPC-173	Biolegend	400230
BV711 mouse IgG1κ isotype control clone MOPC-21	Biolegend	400168
BV605 mouse IgG2a,κ isotype control clone MOPC-173	Biolegend	400270
BV421 mouse IgG1κ isotype control clone MOPC-21	Biolegend	400158
PE-Cy7 mouse IgG1κ isotype control clone MOPC-21	Biolegend	981816
DAPI (4',6-Diamidino-2-phenylinodole, dihydrochloride)	ThermoFisher Scientific–- Invitrogen	D1306
Rhodamine 123, 25mg	ThermoFisher Scientific–- Invitrogen	R302
BD™ CompBeads Anti-Mouse Ig,κ/Negative Control Compensation Particles Set	BD Biosciences	552843
BD™ CompBeads Anti-Rat Ig,κ/Negative Control Compensation Particles Set	BD Biosciences	552844
UltraComp eBeads™ Compensation Beads	ThermoFisher Scientific–- Invitrogen	01-2222-42
Other reagents		

Human TruStain FcX™ (Fc receptor blocking solution)	Biolegend	422302
Trypan Blue solution, 0.4%	ThermoFisher Scientific–- Gibco	15250061
Ficoll	ThermoFisher Scientific	11778538
DMSO	Sigma Aldrich	472301

2.2 Sample Collection and Processing

2.2.1 Sample collection and ethical approval

Blood samples from SLE patients and healthy donors were obtained from consenting individuals with research ethics committee approval (REC reference 11/LO/1433: Immune regulation in autoimmune rheumatic disease, London – City Road & Hampstead Research Ethics Committee). SLE samples were collected from patients in the Louise Coote Lupus Unit, Guy's Hospital, London. Experimental work was also approved by REC reference 11/LO/1274: Immunology the intestine: features associated with autoimmunity, London – Camberwell St Giles Research Ethics Committee.

2.2.2 Selection criteria of healthy donors and lupus patients

Healthy control donors selected were adults with no known health conditions. Lupus nephritis patient donors were recruited providing nephritis had been confirmed via a renal biopsy and patients had not received biologics, rituximab or belimumab, or immunosuppressive drug azathioprine. Non-nephritis lupus patients were recruited providing they had not received any biologics or immunosuppressive drugs.

2.2.3 Isolation of peripheral blood mononuclear cells

Samples were processed on the same day in which the blood samples had been taken, with the aim to isolate PBMCs and cryopreserve them within 3 hours. Fresh whole blood was diluted 1:1 in RPMI medium, then the diluted blood was layered onto Ficoll-Hypaque solution, at a ratio of 2:1 blood to Ficoll, to separate the blood components based on density. Next, the blood on Ficoll was centrifuged at 400 x g for 25 minutes with no break and acceleration at room temperature. After the first spin cycle, the buffy coat was extracted and added to RPMI with 10% foetal calf serum (FCS) and 1% penicillin-streptomycin (P/S), then washed at 400 x g for 7 minutes with high break and acceleration at room temperature. The cell pellet was resuspended in RPMI (+ 10% FCS and 1% P/S) to prepare cells for counting.

2.2.4 Cell counting

Cells we counted using a haemocytometer and the Countess FL II automated cell counter (ThermoFisher) according to the manufacturer's instructions. Equal volumes of PBMC cell suspension and trypan blue vital stain were mixed and approximately 5uL of the trypan blue-stained cells were loaded into the haemocytometer underneath an affixed coverslip. The haemocytometer was loaded into a cassette and placed into the cell counter. Readouts from the cell counter included number of cells per millilitre and the percentage of live and dead cells within the loaded sample.

2.2.5 Cryopreservation of peripheral blood mononuclear cells

Freezing medium was prepared by thawing heat-inactivated FCS and adding 10% DMSO; aliquots of freezing medium were stored at -20°C. To prepare cells for cryopreservation, freshly isolated PBMCs in suspension in RPMI (+10% FCS and 1% P/S) were centrifuged at 400 x g for 5 minutes at room temperature then resuspended in an appropriate volume of freezing medium so the suspension contained between 3-10x10^6 cells/ml. Approximately a millilitre of cell suspension was aliquoted into cryovials and froze slowly at -80°C. Cryopreserved cells were transferred on dry ice to a vapour phase liquid nitrogen tank within 24 hours of the initial freezing at -80°C.

2.2.6 Thawing cryopreserved peripheral blood mononuclear cells

Cryopreserved cells were thawed in a water bath at 37°C then added to RPMI (+ 10% FCS and 1% P/S) and centrifuged at 400 x g for 5 minutes at 37°C. Next, cells were resuspended in RPMI with 0.1mg/ml dNase and rested for at least 45 minutes at 37°C. Cells were rested for longer than 45 minutes depending on the downstream experiments.

2.3 Single-cell RNA-sequencing data analysis

2.3.1 Quality control

The R package, Seurat (version 3), and the standard workflow described by Stuart et al. (2019) was used for single-cell RNA-sequencing analysis of B cells from healthy donors (n=3) and lupus nephritis patients (n=3). The workflow was run on data from sorted CD10+ B cells and total CD19+ B cells, respectively, which was generated prior to the start of this project. These two datasets were distinguished using hashing. Prior to data acquisition and analysis, hashtag oligonucleotide-conjugated antibodies were used to uniquely tag the sorted CD10+ B cells and total CD19+ B cells. Total CD19+ B cells were tagged with a hashtag antibody known as HTO-AHH1-TotalSeqC and sorted CD10+ B cells were labelled with a hashtag antibody known as HTO-AHH2-TotalSeqC. The process of hashing allowed for the two groups of cells to be combined for the sequencing run but then separated for data analysis.

Raw data files were uploaded and read in Seurat using the "Read10X" function. The raw data files contained barcodes, which were codes unique to each cell and features, which included gene expression data and antibody capture data. The antibody capture data was the expression of surface markers CD5, CD10, CD21, CD24, CD27, CD38, IgD, IgM, IL4R, integrin β_7 and CXCR5, all of which were TotalSeqC antibodies. Data files from each of the six samples were initially put through the quality control pipeline individually and then were integrated when it was relevant to do so for the purpose of comparative analysis.

The first step in the quality control workflow was to remove immunoglobulin variable genes so they were not identified as the top differentially expressed genes. Immunoglobulin genes are variable in every individual, irrelevant of disease state, therefore, the presence of these genes in the dataset did not allow for gene expression variability to be clearly identified. Then the dataset was filtered based on RNA count, RNA transcript levels and percentage of mitochondrial gene reads. Removing cells with an abnormally high RNA count, most likely to be doublets, ensured analysis was only conducted on single cells. Low-quality cells with very few genes have low RNA

transcript levels and so these were removed to guarantee analysis was carried out on high quality cells, representative of B cells in the blood. Furthermore, cells with a high percentage of mitochondrial reads were removed because these cells were likely to be dying. The same filtering process was used for all health donor and lupus nephritis patient samples separately.

2.3.2 Data normalisation, integration, and clustering

After filtering, data were normalised, and the 2000 most variable features were identified. The Satija Laboratory Integration and Label Transfer protocol was followed, and 200 integration anchor features were used to integrate data from multiple samples together into one dataset (Stuart et al., 2019). The data were scaled, and a principal component analysis (PCA) was run. The standard deviation of each principal component was plotted and used to select the number of dimensions (principal components) to use for clustering. Neighbours and clusters were found using the FindNeighbours and FindClusters Seurat functions, respectively. A UMAP displaying clusters of B cells was generated. The resolution used to generate the UMAP determines how small the clusters will be. Resolution is an arbitrary measurement and so several resolutions were tested to generate a large enough number of clusters so that variation between cells was apparent but not so many clusters that they contained very few cells.

2.3.3 Analysis of B cell clusters

Feature plots, violin plots and dot plots were generated using the FeaturePlot, VlnPlot and DotPlot Seurat functions, respectively. Heatmaps were produced using the DoHeatmap function in Seurat and the Complex Heatmap library in R. Conserved markers were found using the FindConservedMarkers function. The AverageExpression function was used to establish the average surface marker expression between clusters. IgMhi and IgMlo transitional B cells were identified by cross-referencing conserved marker gene lists with a list of genes that distinguish these two groups of cells previously published by Tull et al. (2021), shown in Table 2.2.

Table 2.2: Top differentially expressed genes in IgMhi and IgMlo transitional (TS) B cells identified by Tull et al. (2021) from single-cell RNA-sequencing analysis of n=5 healthy donors.

TS IgMhi	TS IgMlo
PLD4	*ADAM28*
ITM2C	*IL4R*
NEIL1	*PIK3IP1*
ACTG1	*CCR7*
RGS2	*PLPP5*
CCDC191	*SELL*
MZB1	*FCER2*
TNFRSF18	*CD83*
RP11-164H13.1	*TXNIP*
FCRLA	*NFKBIA*
UCP2	*STAG3*
GADD45B	*CTSH*
SOX4	*CD69*
FAM129C	*MEF2C*
ALOX5	*TMEM2*
PTMA	*DNAJB1*
PPP1R14A	*KLF6*
CD9	*EMP3*
HERPUD1	*CD44*
PIM1	*FLF2*
NR4A1	*SCPEP1*
CD1C	*AKAP2*
AHNAK	*BTG1*
CXXC5	*SESN1*
GPR183	*KLF9*

2.4 Mass cytometry

2.4.1 Preparation of cryopreserved PBMCs for use in mass cytometry

Cryopreserved PBMCs from healthy donors (n=9) and lupus nephritis patients (n=9) were thawed at 37°C in a water bath then washed in RPMI (+10% FCS and 1% P/S) with 0.1mg/ml dNase at 400 x g for 5 minutes at 37°C. After washing, cells were resuspended in RPMI with dNase at 37°C for 2 hours.

2.4.2 Viability and surface antibody staining

Approximately $8x10^6$ cells per sample were viability stained with 1ml 25µM cisplatin in 1X PBS for 3 minutes. Cells were then washed in cell staining medium (CSM), which was made up of 1X PBS with 0.5% BSA and 2mM EDTA. After washing, cells were resuspended in TruStain Fc block at a 1:50 dilution for 10 minutes on ice. Fc block was washed off in CSM at 1000 x g for 1 minute. Cells stained with a master mix of metal-tagged surface antibodies, shown in Table 2.3, for 15 minutes on ice in the dark. Excess, un-bound antibody was washed off after incubation by adding CSM to cells and spinning at 1000 x g for 1 minute.

Table 2.3: Mass cytometry panel used for investigation of protein marker expression in peripheral blood B cell subsets.

**Intracellular markers*

Marker Group	Marker	Metal Tag
Lymphocyte	**CD45**	89Y
B Cell Lineage	**CD19**	14^{2N}d
	CD27	167Er
	IgD	146Nd
	IgM	172Yb
	IgA	148Nd
	CD10	158Gd
	CD38	154Sm
	CD21	152Sm
	CD24	169Tm
	CD45RB	145Nd
	CD40	165Ho
	CD22	159Tb
	CD23	164Dy
	CD1c	173Yb
Interferon	**MX1***	176Yb
	IFITM1	163Dy
	BST2	174Yb
	IRF7*	141Pr
Activation	**CD69**	144Nd
	CD86	150Nd
	CD83	143Nd
Chemokine Receptor	**CCR7 (CD197)**	175Lu
	CXCR4 (CD184)	156Gd
	CXCR5 (CD185)	171Yb
Cytokine Receptor	**IL4R (CD124)**	149Sm
Homing Receptor	**CD62L**	153Eu
B Cell Light Chain	**Ig lambda**	151Eu
	Ig kappa	160Gd
Integrin	**Integrin β7**	162Dy
	CD11c	147Sm
TNF Superfamily	**TACI**	168Er
	BAFF-R	155Gd
Adhesion/Migration	**CD99**	170Er
MHC	**CD74**	166Er

2.4.3 Fixation, permeabilisation and intracellular antibody staining

The eBioscience™ Foxp3 fixation/intracellular staining kit was used to fix and permeabilise cells prior to intracellular antibody surface staining. The intracellular proteins included in this panel were MX1 and IRF7, as shown in Table 2.2. Fixation and permeabilisation buffers were prepared according to the manufacturer's instructions. Cells were resuspended in fixation buffer for 25 minutes in the dark at room temperature. After fixation, cells were washed in permeabilisation buffer at 800 x g for 5 minutes and resuspended in intracellular antibodies in permeabilisation buffer and incubated for 20 minutes. After intracellular staining, cells were washed in CSM at 1000 x g for 1 minute.

2.4.4 Iridium/paraformaldehyde staining

Stock paraformaldehyde was diluted in 1X PBS to give a 2% paraformaldehyde solution. Iridium (Ir-intercalator 500X) was added to the 2% paraformaldehyde. Cells were resuspended in the iridium paraformaldehyde solution and incubated at 4°C overnight.

2.4.5 Preparation prior to data acquisition

After overnight incubation, cells were washed twice in CSM and most of the CSM was aspirated off, leaving the cell pellet intact covered by a small volume of supernatant. Samples were transported to the Biomedical Research Centre at Guy's Hospital where cells were washed in CAS solution and EQ beads were spiked into samples. Cell concentration was adjusted so the acquisition rate was steady. Data was acquired on a Helios™ Mass Cytometer.

2.4.6 Mass cytometry data analysis

Raw data files were obtained from the mass cytometer in the .fcs format. The .fcs files were uploaded to the premessa package (https://github.com/ParkerICI/premessa) in R. Data points were visualised and EQ™ calibration beads were selected in all n=18 data files then normalisation was run. Any data files that needed to be concatenated were done so using the premessa concatenation tool. After normalisation, the bead

data that was used to normalise the .fcs files were removed. Beads were filtered out of the dataset by determining a bead distance threshold, whereby datapoints closest to a true bead value (those with a small bead distance) were removed.

Normalised data files with beads removed were uploaded into Cytobank software (https://mrc.cytobank.org/cytobank). In the gating editor on Cytobank, data were cleaned up by removing any "residual", "centre", "offset" and "length" outlier data points. After clean-up steps, live CD19+ B cells were gated. To begin classifying CD19+ cells into B cell subsets, a viSNE was generated. viSNE is a high-dimensionality visualisation tool that facilitates the visualisation of data in 2D whilst keeping differences within the data identifiable (Amir et al., 2013). To generate the viSNE, an equal number of CD19+ events (n=5,555) from each of the health and lupus samples (n=18) were sampled and the following lineage markers were used: CD27, IgD, IgA, CD10, CD38, CD24, CD21, IgM and CD45RB. Once the viSNE had been generated, the viSNE coordinates were used to generate SPADE trees. The SPADE trees were made up of 200 nodes, with each node comprising groups of similar cells. Expression of various B cell lineage markers was overlaid on the SPADE tree and was used to classify B cell subsets according to the surface phenotypes shown in Table 2.4 (Chapter 2.6). Median expression of markers of interest and cell count data were exported from the Cytobank software and plotted in GraphPad Prism (v9).

2.5 Flow cytometry

2.5.1 Preparation of cryopreserved PBMCs for use in flow cytometry

Cryopreserved PBMCs were thawed at 37°C in a water bath then suspended in RPMI (+10% FCS and 1% P/S) with 0.1mg/ml dNase and washed at 400 x g for 5 minutes at 37°C. Cells were resuspended in RPMI with dNase for 45 minutes at 37°C for flow cytometry protocols that did not use rhodamine dye extrusion; for protocols that included dye extrusion the protocol in 2.4.2 was followed. Each cell sample was counted using the cell counting protocol outlined in 2.2.4.

2.5.2 Rhodamine dye extrusion

Rhodamine at a stock concentration of 50mM was diluted to a concentration of 1mM in 100% CH_3OH then added to the cell suspension and incubated for 10 minutes at 37°C. Excess rhodamine was washed off twice by centrifuging cells in RPMI at 400 x g for 5 minutes. After washing, cells were resuspended in RPMI with dNase and incubated for 3 hours at 37°C. Alongside healthy donor and lupus patient samples, approximately $2x10^6$ buffy coat cells from leukocyte cones were stained with rhodamine in the same manner for use as a compensation control.

2.5.3 Compensation bead and antibody master mix preparation

Equal volumes of positive and negative compensation beads were mixed and aliquoted into the appropriate number of tubes, depending on how many markers were in the panel. Beads were stained with marker antibodies for approximately 10 minutes in the dark, then washed at 400 x g for 5 minutes at 4°C and resuspended in 1X PBS. Antibodies were titrated prior to use in experimental protocols. Antibody master mixes were prepared by aliquoting the appropriate volume of each antibody, dependent on the concentration chosen after titration, into the working volume of FACS buffer (1X PBS with 2mM EDTA and 10% FCS). When it was applicable, an isotype control master mix was also prepared in FACS buffer. The volume of isotype control used was dependent on the concentration of the respective fluorochrome-conjugated antibody, as they were used at the same concentration.

2.5.4 Antibody, isotype, and live/dead staining

After cells were rested, approximately $2x10^5$ cells were aliquoted for use as unstained and live/dead controls. Around $2x10^6$ cells were stained per sample. Firstly, cells were incubated on ice for 10 minutes with TruStain Fc block and after incubation, unbound Fc block was washed off cells in FACS buffer at 1000 x g for 1 minute at room temperature. Cells were resuspended in either antibody master mix or isotype master mix and incubated on ice for 15 minutes. After cells were stained with the antibody master mix, they were washed in FACS buffer and spun at 1000 x g for 1 minute. Cells were then resuspended in FACS buffer and transferred to FACS tubes prior to data acquisition on a BD Fortessa™. The live/dead stain DAPI was prepared by diluting the 0.1ug/ml stock 1:1000. DAPI was added to live/dead control cells and all sample cells just before samples were run on the BD Fortessa™.

2.5.5 Flow cytometry data analysis

Data files were generated from BD FACSDiva™ software in the .fcs file format. These .fcs files were loaded into FlowJo software, which was used for all flow cytometry data analysis. B cell subsets were gated using the gating strategy outlined in Figure 2.1. Lymphocytes were selected from all events and live, single, CD19+ cells were gated. T1 cells were gated as CD27-IgD+CD10+CD38+++CD24+++CD21lo. T2 cells were gated as CD27-IgD+CD10+CD38++CD24++CD21hi then gated further based on IgM expression; IgMhi cells were those in the top 30% of the positive IgM signal and IgMlo were those in the bottom 30%. T3 cells were gated as CD27-IgD+CD10-CD38+CD24++RH123+ and CD45RB high or low for the relevant subset. Naïve cells were gated as CD27-IgD+CD10-CD45RB-RH123- and as IgM high or low using the same method as was used for T2 cells. MZP were gated as CD27-IgD+CD10-CD45RB+RH123- and MZB were gated as CD27+IgD+IgM+CD1c+. Two populations of MZB (MZB1 and MZB2) were gated for based on CCR7 expression (see Chapter 6). aNAV were gated as CD27-IgD+CD10-CD24loCD38loCD45RB-RH123+. DN2 were gated as CD27-IgD-CD24-CD21-. CSM were gated as CD27+IgD-IgM-. IgM-only were gated as CD27+IgD-IgM+. The same gating strategies were implemented for the relevant isotype controls. A

detailed explanation on the identification of peripheral B cell subsets in blood is provided in Chapter 2.6.

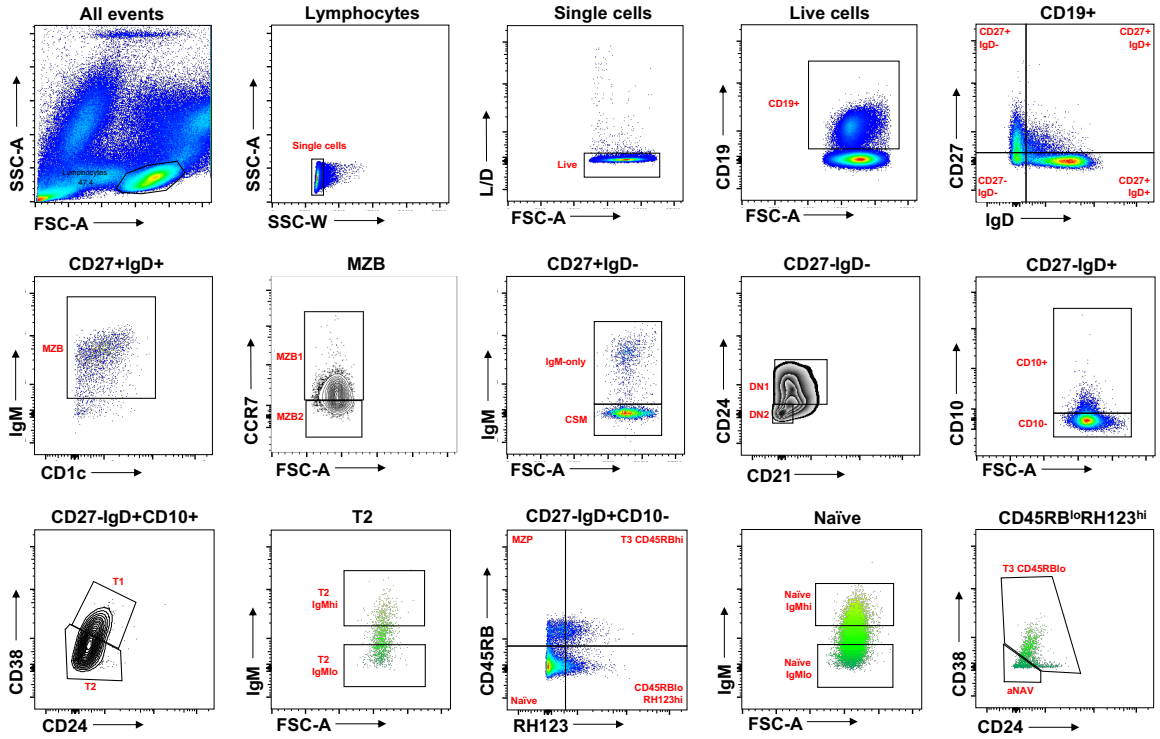

Figure 2.1: Flow cytometry gating strategy of peripheral blood B cell subsets. Flow cytometry plots are from a representative healthy donor. Gating strategy shown was applied to all flow cytometry analysis in this study.

2.6 Identifying human B cell subsets in peripheral blood

The antigens on the surfaces of lymphocytes, whilst having important functional relevance, can also be used as markers to divide B cells into subsets. Both CD19 and CD20 are expressed on the surface of most B cells in the peripheral blood (Bendall et al., 2014; Wang et al., 2012), though CD20 expression is lost upon B cell differentiation into plasmablasts (Sanz et al., 2019). When identifying B cell subsets in peripheral blood through cytometry methods, such as flow or mass cytometry, plasmablasts can be separated from the rest of the peripheral blood B cell pool by gating for CD27+++CD38+++CD24- plasmablasts within the CD19+ population, as shown in the flow cytometry gating strategy in Figure 2.2.

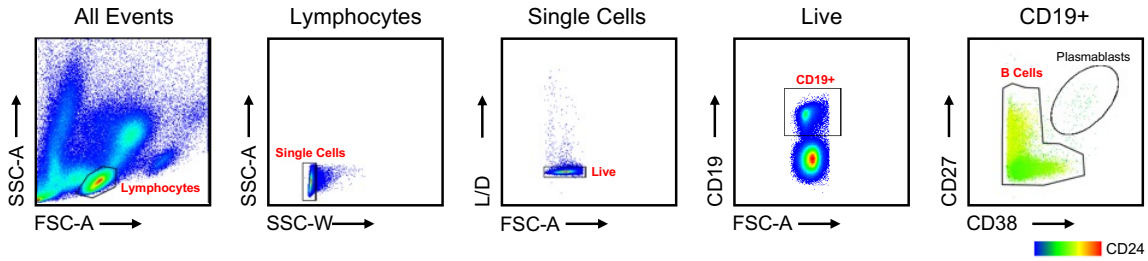

Figure 2.2: Identification of CD19+ B cells and plasmablasts in peripheral blood. Flow cytometry gating strategy plots to identify live, single cell, CD19+ B cells. Plasmablasts are distinguishable from the rest of the CD19+ population as cells that are CD27+++CD38+++CD24-. Plots are from a representative healthy donor.

Peripheral blood B cell subsets can be broadly categorised into CD27- cells that are mostly antigen inexperienced and CD27+ B cells that are mostly memory cells. CD27+ B cells are often described as memory B cells (Agematsu et al., 2000), however, there are a group of unconventional memory B cells belonging to the so-called double negative (DN) B cell subset that are CD27- , but unlike most CD27- B cells they are also IgD- (Wei et al., 2007). Likewise marginal zone B cells express CD27, but many groups consider that these are not memory B cells. In general, CD27 is used in combination with several other lineage markers can be used to define multiple B cell subsets in peripheral blood, as shown in Table 2.4.

Table 2.4: Surface protein markers of peripheral blood B cell subsets.

Subset	Key Lineage Markers	Additional Markers and Sub-Populations
T1	CD27- IgD+ IgMhi CD10+ CD21lo CD24+++ CD38+++	CD62Llo
T2	CD27- IgD+ IgM+ CD10+ CD21hi CD24++ CD38++	CD62L+ **T2 IgMhi:** IgMhi CCR7hi β7hi **T2 IgMlo:** IgMlo CCR7lo β7lo
Ie	CD27- IgD+ IgM+ CD10- CD24+ CD38+ ABCB1+ CD45RBlo	**IgMhi Naïve:** **IgMlo Naïve:** IgMlo
Activated Naïve	CD27- IgD+ CD10- CD21lo CD24lo CD38lo	CXCR5-
Marginal Zone Precursors	CD27- IgD+ IgMhi CD10- CD24+ CD38+ ABCB1+ CD45RB+	CD1c+
Marginal Zone B	CD27+ IgD+ IgM+	CD45RB+ CD1c+ β7+
IgM-Only	CD27+ IgD- IgM+	CD45RB+
Class-Switched Memory	CD27+ IgD- IgM-	CD45RB+ IgG+, IgA+ or IgE+
Double Negative	CD27- IgD-	**DN1:** CD21+ CXCR5+ **DN2:** CD21- CXCR5- CD11c+ **DN3:** CD21- CXCR5- CD11c- **DN4:** CD21+ CD11c+

2.6.1 Transitional B cells

Transitional B cells are an immature subset of B cells and are the first population of B cells to emerge from the bone marrow in the peripheral blood (Palanichamy et al., 2009; Sims et al., 2005). As shown in Table 2.4, there are three distinct subsets of transitional B cells, T1, T2 and T3, all of which are CD27-IgD+. Both T1 and T2 B cell subsets express CD10 much like the immature B cells in the bone marrow, however CD10 expression is lost upon development into T3 B cells (Bemark, 2015; Agrawal et al., 2013; Cuss et al., 2006; Palanichamy et al., 2009). Transitional B cells emerge from the bone marrow as T1 cells and have been found to develop into T2 B cells then eventually T3 B cells. CD10+ transitional B cells (T1 and T2) account for approximately 4-10% of CD19+ B cells in the peripheral blood of healthy adults (Dieudonné et al., 2019; Marie-Cardine et al., 2008; Sims et al., 2005). CD10- T3 B cells make up approximately 10% of CD19+ B cells in healthy adult blood (Palanichamy et al., 2009; Tull et al., 2021). The development from T1 to T2 is characterised by downregulation of CD24 and CD38 and upregulation of CD21 (Suryani et al., 2010). CD24, CD38 and CD21 can be used to identify T1 and T2 subsets using the flow cytometry gating strategy displayed in Figure. 2.3. T1 and T2 B cells can be further distinguished based on expression of CD62L (L-selectin), whereby T1 cells express far lower levels of CD26L, which is likely associated with the lack of homing abilities of T1 cells (Tull et al., 2021; Allman et al., 2001).

All transitional B cells express relatively high levels of surface IgM in comparison to naïve B cells; the literature suggests that expression of IgM is highest on T1 B cells and is downregulated through the T2 and T3 stages (Bemark, 2015). A recent study by Tull et al. (2021) has identified two populations of T2 B cells, that can be distinguished based on surface expression of IgM, termed T2 IgMhi and T2 IgMlo, as shown in Figure 2.3. The T2 IgMhi subset of T2 B cells has been found to express higher levels of integrin β7 and CCR7 and are enriched in gut-associated lymphoid tissue (Tull et al., 2021). Additionally, IgMhi and IgMlo transitional B cells have distinct gene expression profiles. IgMhi transitional B cells have been found to express genes associated with marginal zone B cells such as *MZB1* and *CD1c* and T2 IgMhi cells have been identified

as progenitors of marginal zone precursors and terminally differentiated marginal zone B cells (Tull et al., 2021).

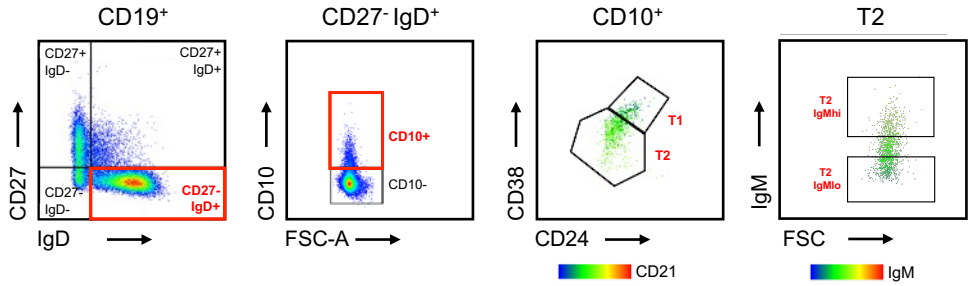

Figure 2.3: Identification of CD10+ transitional B cell populations in peripheral blood. Flow cytometry gating strategy used to identify T1 and T2 B cell subsets using the following markers: CD27, IgD, CD10, CD38, CD24 and CD21. T2 B cells can be further subdivided in to T2 IgMhi and T2 IgMlo by assessing IgM expression. Plots are from a representative healthy donor.

T3 B cells are late-stage transitional B cells that been proposed as an intermediate population between T2 and naïve B cells in peripheral blood B cell development (Allman et al., 2001). T3 B cells can be distinguished from naïve B cells due to a lack of expression of the ABCB1 transporter and resultant inability to extrude rhodamine or mitotracker green dyes (Wirths & Lanzavecchia, 2005). Due to this inability to extrude rhodamine (RH123), T3 B cells retain rhodamine and therefore are RH123hi when distinguishing T3 B cells from naïve B cells by flow cytometry, as shown in Figure 2.4A. When using flow cytometry, the level of rhodamine staining is often across a spectrum and so it can be challenging to recognise the threshold for positive staining. Thus, it is useful to first generate a biaxial gate using CD27 and RH123 within the total CD19+ B cell population, as shown in Figure 2.4A, as the threshold for positive rhodamine staining will line up with the CD27+ population as both memory and marginal zone B cells do not express the ABCB1 transporter, therefore do not extrude rhodamine and are RH123+. This gate can then be applied to the CD10- population and will place an accurate gate between T3 and naïve B cell populations, as demonstrated in Figure 2.4A.

Similar to T2 B cells, T3 B cells can be sub-divided into two populations. CD45RBhi and CD45RBlo variants of T3 B cells have been characterised in peripheral blood; CD45RBhi T3 cells express higher IgM and CD1c than CD45RBlo T3 cells, as shown in Figure 2.4B, thus linking the CD45RBhi T3 population to a marginal zone B cell trajectory (Tull et al., 2021).

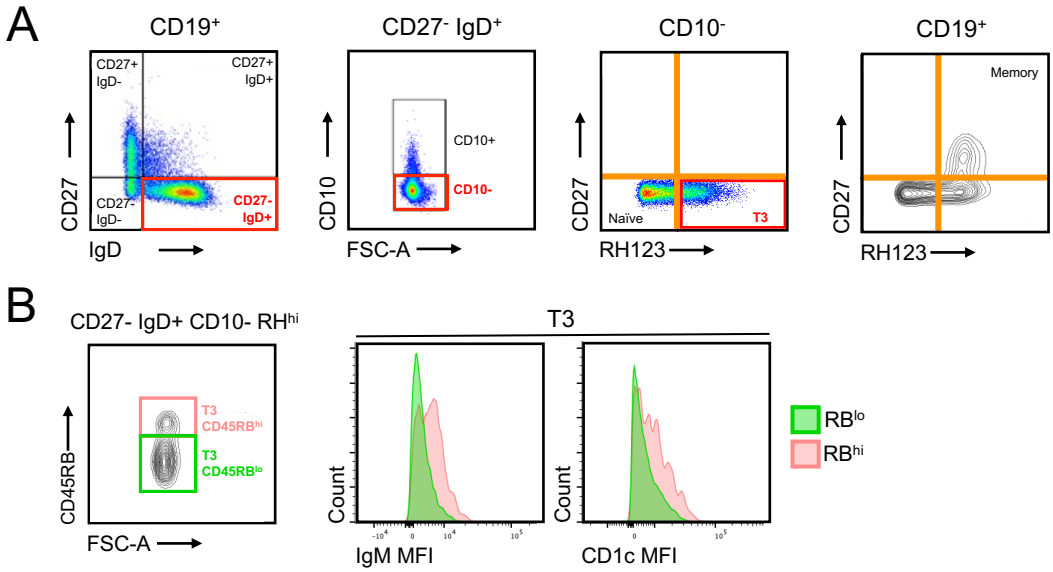

Figure 2.4: Identification of T3 B cell subsets in peripheral blood. (A) Flow cytometry gating strategy used to gate for T3 B cells as CD27-IgD+CD10-RH123+. RH123 (rhodamine dye) staining is used to infer the expression of the ABCB1 transporter. T3 RH123+ cells do not extrude the dye therefore do not express the ABCB1 transporter. RH123+ threshold can be determined using a CD27/RH123 biaxial gate generated on CD19+ B cells, shown in orange. **(B)** Gating strategy to identify sub-populations of T3 B cells based on CD45RB expression. Histograms show comparisons in IgM and CD1c mean fluorescence intensity (MFI) between T3 CD45RBhi (pink) and T3 CD45RBlo (green). Plots are from a representative healthy donor.

2.6.2 Naïve B cells

Naïve B cells comprise between 40-60% of all CD19+ B cells in the peripheral blood (Morbach et al., 2010; Palanichamy et al., 2009), making it the largest subset of B cells in the peripheral blood of healthy adults. Naïve B cells are the population of B cells that are antigen inexperienced. As shown in Table 2.4, naïve B cells are CD27-IgD+CD10- and express CD24 and CD38 albeit at lower levels than transitional B cells (Sanz et al., 2019). As previously described in 2.6.1, naïve B cells can only be distinguished from T3 B cells by their ability to extrude rhodamine or mitotracker green dyes. Naïve B cells express the ABCB1 transporter thus can extrude these dyes (Wirths & Lanzavecchia, 2005). Naïve B cells can be identified and distinguished from other CD27-IgD+CD10- subsets using flow cytometry as RH123-CD45RBlo, as shown in Figure 2.5A.

Naïve B cells have been found to express IgM at varying levels. Tull et al. (2021) noted that the naïve B cell subset can be divided into IgMhi and IgMlo naïve populations. Through principal component analysis of markers expressed by IgMhi and IgMlo transitional and naïve B cells, Tull et al. (2021) also found that the naïve IgMhi and naïve IgMlo subsets were more closely related to the respective IgMhi and IgMlo transitional subsets in terms of surface protein expression than to each other. There is some suggestion that naïve B cells with the lowest expression of IgM have anergic properties, evidenced by significantly reduced upregulation of the early activation marker, CD69, after *in vitro* B cell receptor stimulation compared to the rest of the naïve B cell population (Quách et al., 2011). This group of anergic B cells is thought to represent only 2.5% of the total peripheral blood B cell population (Duty et al., 2009).

Marginal zone precursors (MZP) are a subset of naïve B cells with a CD27-IgD+IgM+CD45RB+CD1c+ABCB1- cell surface phenotype, which make up 1-5% of total CD19+ B cells in the peripheral blood in healthy adults (Descatoire et al., 2014; Tull et al., 2021). When gating for MZP in flow cytometry, they can be separated from the rest of the naïve population using CD45RB, as shown in Figure 2.5A, and gating can be confirmed by checking for greater expression of marginal zone markers IgM and CD1c, as shown in Figure 2.5B.

Activated naïve B cells (aNAV) are a subset of CD27-IgD+CD10- naïve B cells that can be distinguished from the rest of the naïve subset based on the lower expression of CD21, CD24 and CD38 and expression of CD11c and FCRL5 (Jenks et al., 2018; Tipton et al., 2015). aNAV B cells do not express the ABCB1 transporter unlike the rest of the naïve B cell population (Jenks et al., 2019). aNAV in peripheral blood can be identified using flow cytometry by gating for CD38-CD24-CD21- cells within the T3 CD45RBlo gate, as shown in Figure 2.5C. The aNAV B cell subset is clonally related to antibody-secreting B cell populations and cells belonging to this B cell subset are hyperresponsive to TLR7 stimulation (Jenks et al., 2018; Tipton et al., 2015).

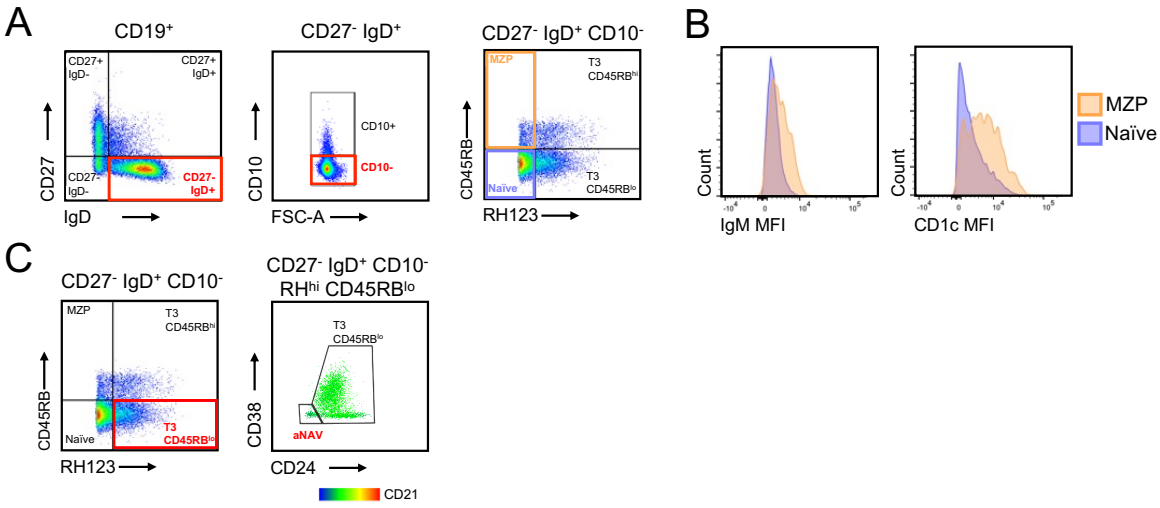

Figure 2.5: Identification of CD10- naïve subsets in peripheral blood. (A) Flow cytometry gating strategy to identify naïve B cells as CD27-IgD+CD10-RH123-CD45RBlo and marginal zone precursors (MZP) as CD27-IgD+CD10-RH123-CD45RB+. **(B)** Histograms comparing IgM and CD1c mean fluorescence intensity (MFI) between naïve and MZP B cell subsets. **(C)** Flow cytometry gating strategy to identify activated naïve (aNAV) B cells. aNAV B cells are gated as CD38-CD24-CD21- within the CD27-IgD+CD10-CD45RBloRH123+ T3 gate. Plots are from a representative healthy donor.

2.6.3 Marginal zone B cells

CD27+IgD+IgM+ B cells in the peripheral blood are termed marginal zone B cells due to their shared surface phenotype with a group of B cells that are present within the marginal zone of the spleen (Weller et al., 2004). The precursors to marginal zone B cells, MZP, have been found to undergo differentiation into CD27+IgD+ marginal zone B cells following NOTCH ligation (Descatoire et al., 2014). Much like their precursors, marginal zone B cells express CD1c and CD45RB (Descatoire et al., 2014; Weller et al., 2004), as shown in Figure 2.6. Marginal zone B cells comprise approximately 10-15% of all CD19+ B cells in the peripheral blood in healthy adults (Zhu et al., 2018). Tull et al. (2021) have identified a B cell developmental trajectory in peripheral blood characterised by high expression of IgM and the gut-homing molecule integrin β7, whereby marginal zone B cells are derived from T2 IgMhi B cells. Marginal zone B cells are innate-like lymphocytes and function in an T cell-independent manner; they are important for immunity against encapsulated bacteria (Cerutti et al., 2013; Weller et al., 2004).

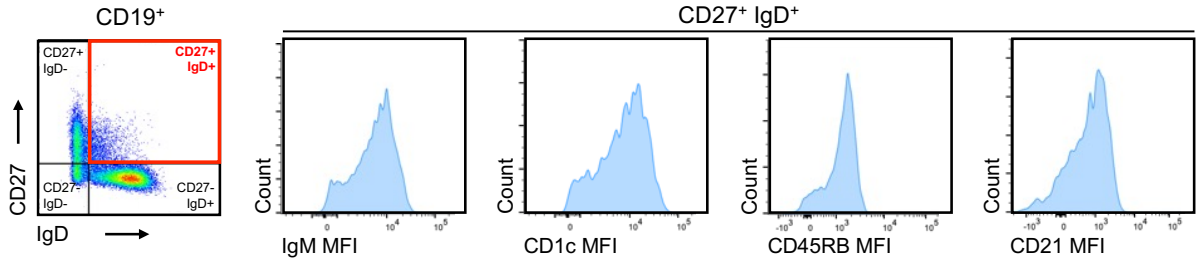

Figure 2.6: Identification of marginal zone B cells in peripheral blood. Flow cytometry gating strategy to identify CD27+IgD+ marginal zone B cells. Histograms demonstrate high expression of IgM, CD1c, CD45RB and CD21 inferred by mean fluorescence intensity (MFI). Plots are from a representative healthy donor.

2.6.4 Class-switched memory and IgM-only B cells

Memory B cells develop from mature naïve B cells after an antigen encounter and a T follicular helper cell-dependent immune response and maturation in the germinal centre (Garside et al., 1998; Paus et al., 2006). Memory B cells are distinguishable from naïve B cells by their gain of CD27 expression and loss of expression of IgD and are vital for immunity against re-encountered antigens (Klein et al., 1998; Sanz et al., 2008). This subset of B cells accounts for 10-20% of all CD19+ B cells in the peripheral blood in healthy adults (Morbach et al., 2010). This subset of B cells undergoes class-switch recombination by altering the constant region of the immunoglobulin heavy chain to allow for the expression of different immunoglobulin isotypes, IgG, IgA or IgE, instead of IgM and IgD, which their naïve B cell precursors express (Dunnick et al., 1993). Most class-switched memory B cells in the peripheral blood are either IgG+ or IgA+, as shown in Figure 2.7, IgE+ memory B cells are incredibly rare in the peripheral blood (Geha et al., 2003; Saunders et al., 2019).

However, there is a small subset of CD27+IgD- memory B cells that have not undergone class-switch recombination and therefore still express IgM, this subset of cells is known as IgM-only memory cells (Klein et al., 1997) and can be gated for by following the flow cytometry gating strategy shown in Figure 2.7. IgM-only memory B cells account for approximately 10% of all B cells in the peripheral blood of healthy adults (Klein et al., 1998). The function of this subset of is not fully understood, but it has been proposed that IgM-only memory cells represent a population of pre-switched memory B cells in an intermediate state that have not yet undergone class-switching (Berkowska et al., 2011).

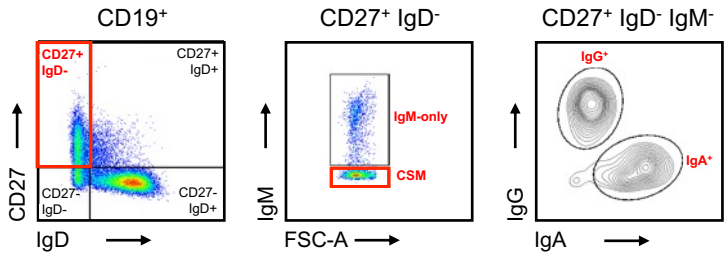

Figure 2.7: Identification of class-switched memory and IgM-only B cells in peripheral blood. Flow cytometry gating strategy for the identification of CD27+IgD- memory B cells. Class-

switched memory (CSM) B cells are IgM- and can be further subdivided based on the immunoglobulin isotype they express (IgG or IgA). IgE+ memory B cells are extremely rare in the peripheral blood, therefore are not shown in this gating strategy. IgM-only memory cells are classified as CD27+IgD-IgM+. Plots are from a representative healthy donor.

2.6.5 Double negative B cells

Double negative B cells are a distinct subset of CD27- memory B cells, often called non-classical memory B cells. They are termed “double negative” due to their lack of expression of both CD27 and IgD (Wei et al., 2007). The predominant subsets of double negative B cells present in the peripheral blood, termed DN1 and DN2, account for 5-10% of all CD19+ B cells in healthy adult peripheral blood (Jenks et al., 2018). DN1 B cells are characterised by expression of CD21, CXCR5 and CD24 and lack of CD11c expression, whereas DN2 B cells have a CD21-CXCR5-CD24-CD11c+ phenotype (Jenks et al., 2018). DN2 B cells are thought to be derived from aNAV B cells; both aNAV and DN2 are also hyperresponsive to TLR7 stimulation and are associated to the extrafollicular response (Jenks et al., 2018; Tipton et al., 2015).

More recently, two other less abundant subsets of double negative B cells, termed DN3 and DN4, have been identified, making up less than 5% of all B cells in the peripheral blood of healthy adults (Sosa-Hernández et al., 2020). DN3 B cells are CD21-CXCR5-CD11c- and DN4 B cells are CD21+CD11c+ (Sosa-Hernández et al., 2020; Woodruff et al., 2020). Their role in the peripheral blood is not currently fully understood.

To identify double negative B cells in peripheral blood using flow cytometry, a CD27/IgD biaxial gate allows for the gating of CD27-IgD- B cells, as shown in Figure 2.8A. Double negative B cells can be further subdivided using various markers including CD21 and CD24, as demonstrated in Figure 2.8A. CXCR5 and CD11c can also be used in flow cytometry gating strategies, however given the panel size constraints it is not possible to include all these markers when designing a panel to identify all the peripheral blood B cell subsets discussed in this chapter (2.6). For this reason, and their relatively low abundance in peripheral blood, it can be challenging to gate for DN3 and DN4 subsets. Nevertheless, the four double negative subsets can be gated for using mass cytometry. This form of cytometry, in comparison with flow cytometry, allows for a much larger panel of markers and so more of the relevant markers can be included in the panel. As shown in the SPADE tree Figure 2.8B, the double negative subsets can be classified based on the expression of CD21, CD11c and CXCR5. The

methodology used to generate the SPADE tree and the mass cytometry gating strategy is discussed in 2.4.6 in section 2.4 of Materials and Methods.

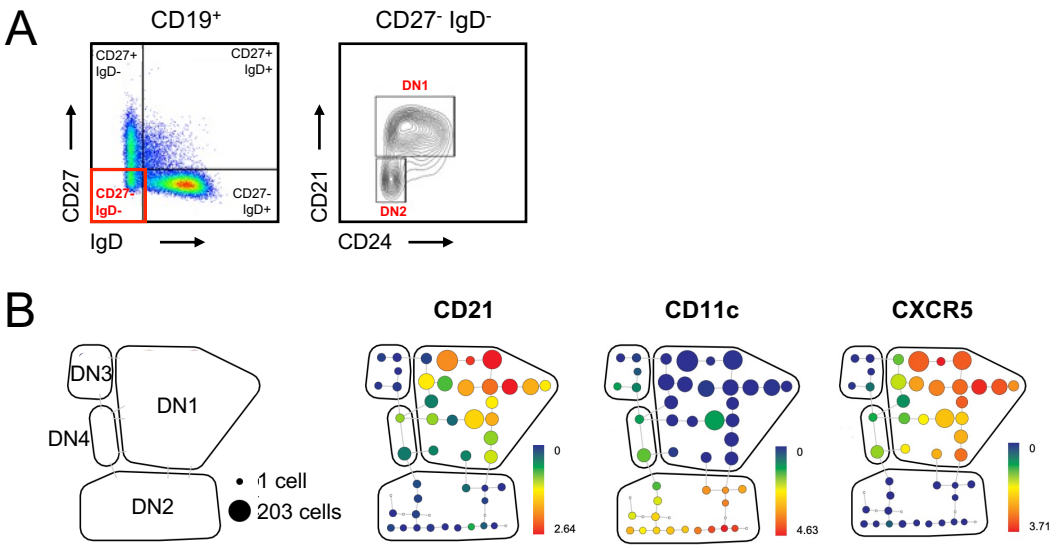

Figure 2.8: Identification of doubled negative B cell subsets in peripheral blood. (A) Flow cytometry gating strategy to identify double negative CD27-IgD- B cells and sub-divide this subset of cells into DN1 and DN2 using CD21 and CD24. Plots are from a representative healthy donor. **(B)** SPADE trees generated from mass cytometry. Nodes indicate groups of cells with a similar surface phenotype. The larger the node, the greater the cell count. Nodes are classified into DN1, DN2, DN3 and DN4 B cell subsets. DN1 B cells are classed as CD21+CD11c-CXCR5+. DN2 cells are classed as CD21-CD11c+CXCR5-. DN3 B cells are classed as CD21-CD11c-CXCR5-. DN4 B cells are classed as CD21+CD11c+CXCR5+. The colour scale indicates level of marker expression with red being the highest expression and blue being the lowest. SPADE trees are from a representative healthy donor.

2.7 Demographics and clinical information of study participants

Tables 2.5-2.9 display the demographics and clinical information of study participants for all experiments in this study. Information on age, sex and ethnicity is shown. In addition, lupus patients' autoantibody profile and medication are presented. In some instances, information was not disclosed and has been indicated in the tables accordingly. Table 2.8 shows the clinical information, such as SLEDAI score, urine protein, dsDNA titres and complement level for paired lupus nephritis samples; prior to sample collection, experienced personnel in the lupus clinic used this information to deem whether a sample was included in the 'flare' or 'stable' cohort.

Table 2.5: Demographics and clinical information of study participants for single-cell RNA-sequencing experiment (Chapter 3)

Cohort	Age	Sex	Ethnicity	Autoantibody Profile	Medication
Health	34	F	Caucasian	--	--
	43	F	Caucasian	--	--
	42	F	African Caribbean	--	--
Lupus Nephritis	31	F	African Caribbean	ANA, dsDNA, Sm, RNP, C1Q	HCQ, MMF
	48	F	Caucasian	ANA, DNA, RNP	HCQ
	30	F	African Caribbean	ANA, Sm, RNP, La, C1Q	HCQ, MMF, PRED

Table 2.6: Demographics and clinical information of study participants for mass cytometry experiments (Chapters 4 and 6)

Cohort	Age	Sex	Ethnicity	Autoantibody Profile	Medication
Health	35	F	South American	--	--
	41	F	Caucasian	--	--
	31	F	SE Asian	--	--
	32	F	Caucasian	--	--
	42	F	Black Caribbean	--	--
	Not disclosed	F	Black Caribbean	--	--
	36	F	Caucasian	--	--
	42	F	Caucasian	--	--
	28	F	Black Caribbean	--	--
Lupus Nephritis	27	F	Caucasian	ANA, DNA	PRED, HCQ, MMF
	47	F	Caucasian	ANA, DNA	PRED, HCQ
	39	F	Caucasian	APL+++	PRED, MMF
	47	F	Not disclosed	ANA	HCQ, MMF
	37	F	Black African	ANA, DNA, Sm, RNP, Ro	
	64	F	Black African	ANA, DNA, Sm, RNP, Ro	HCQ, MMF
	43	F	Black African	ANA, DNA, Sm, RNP	PRED, HCQ, MMF
	24	F	Black African	Ro, La	PRED, HCQ
	49	F	Black African	ANA, DNA, Ro	PRED, HCQ, MMF

Table 2.7: Demographics and clinical information of study participants for flow cytometry experiments to investigate the expression of IFITM1 in B cell subsets (Chapter 4)

Cohort	Age	Sex	Autoantibody Profile	Medication
Health	25	F	--	--
	Not disclosed	F	--	--
	36	F	--	--
	Not disclosed	F	--	--
	26	F	--	--
	26	F	--	--
	29	F	--	--
	30	F	--	--
	Not disclosed	F	--	--
	29	F	--	--
Lupus Nephritis	37	F	Not disclosed	Not disclosed
	19	F	DNA	PRED HCQ
	46	F	ANA Sm RNP	HCQ MMF
	27	F	ANA DNA	PRED HCQ MMF
	20	F	ANA DNA Ro Sm RNP La	PRED HCQ MMF
	49	F	ANA DNA	PRED HCQ MMF
	68	F	ANA DNA Sm	PRED HCQ
	36	F	ANA DNA Ro	PRED HCQ MMF
	43	F	ANA DNA Sm RNP	PRED HCQ MMF
	24	F	ANA DNA Sm	MMF
Other Lupus	29	F	ANA DNA	PRED HCQ
	36	F	ANA Ro Sm RNP	
	38	F	ANA DNA	
	21	F	ANA DNA Ro	PRED
	49	F	ANA DNA Ro Sm RNP C1Q	PRED
	30	F	ANA RNP	HCQ
	53	F	ANA Ro RNP	HCQ
	52	F	ANA	HCQ
	52	F	DNA Ro	

Table 2.8: Clinical information of study participants for paired lupus flow cytometry experiments (Chapter 5)

Pair ID	Sex	SLEDAI	Urine Protein (mg/L protein: mmol creatinine)	dsDNA (IU/mL)	Complement Level	Medication
1	F	13	179	>400	Low	PRED, HCQ
		4	8	134	Low	PRED, HCQ, MMF
2	F	13	169	307	Low	-
		11	59	50	Normal	PRED, HCQ, MMF
3	F	13	165	>400	Low	PRED, HCQ
		2	15	24	Normal	-
4	M	-	308	100	Low	PRED
		-	73	20	Normal	PRED, MMF
5	F	13	-	-	-	PRED, HCQ, MMF
		5	-	-	-	PRED, HCQ, MMF
6	F	13	-	-	-	PRED, HCQ, MMF
		5	-	-	-	PRED, HCQ, MMF
7	F	13	123	237	Low	HCQ
		3	-	-	-	PRED, HCQ, MMF

Table 2.9: Demographics and clinical information of study participants for flow cytometry experiments to investigate subsets of marginal zone B cells (Chapter 6)

Cohort	Age	Sex	Autoantibody Profile	Medication
Health	33	F	--	--
	34	F	--	--
	30	F	--	--
	26	F	--	--
	29	F	--	--
	35	F	--	--
	32	F	--	--
	36	F	--	--
	42	F	--	--
	28	F	--	--
Lupus Nephritis	35	F	ANA, Sm, RNP	HCQ, PRED
	68	F	ANA, DNA, Sm	HCQ, PRED
	46	F	ANA, Sm, RNP	HCQ, MMF
	47	F	ANA, DNA	HCQ, PRED
	54	F	ANA, DNA, Ro	PRED
	36	F	ANA, DNA, Ro	HCQ, MMF, PRED
	43	F	ANA, DNA, Sm, RNP	HCQ, MMF, PRED
	49	F	ANA, DNA, Ro, C1Q	HCQ, MMF, PRED
	65	F	ANA, DNA, Ro, Sm, RNP, La	HCQ, PRED
	24	F	ANA, DNA, Sm	MMF, PRED

2.8 Statistical and data analysis methods

2.8.1 Data analysis software

A summary of the statistical and data analysis packages used in this study is presented in Table 2.10.

Table 2.10: Summary of software and data analysis packages used for this study

Software/Data Analysis Packages Used	Description
Seurat v3	R package used for the analysis of single-cell RNA-sequencing data including quality control, dataset merging and, normalisation. Data visualisation through UMAPs, dot plots and violin plots were conducted using the Seurat package.
ComplexHeatmap	R package used for the generation of heatmaps included in Chapter 3 of this study. Package allows for .csv files to be visualised as scaled and unscaled heatmaps.
Premessa	R package used to concatenate and normalise mass cytometry .fcs files. Premessa was also used to remove beads from .fcs data files prior to downstream analysis in Cytobank.
Cytobank	Online software used for the analysis of mass cytometry (CyTOF) data. Cytobank was used to identify live, single, CD19+ B cells and for data clean-up. viSNE and SPADE plots were generated using this software.
BD FACSDIVA™	Software used for flow cytometer application setup and data acquisition. This software was used in conjunction with the BD Fortessa™ flow cytometer.
FlowJo	Software used for analysing flow cytometry data (.fcs files). Data filtering and gating to identify populations of interest was performed using this software. Information on B cell subsets as a proportion of the total B cell pool were generated using FlowJo.
PRISM - GraphPad	Application used for statistical analysis and graph production. Statistical analyses such as Student's t-tests and ANOVAs were conducted using the 'Analyse' function.

2.8.2 Statistical analysis methods

The R package Seurat was used for the statistical analyses conducted on gene expression from the single-cell RNA-sequencing experiment described in Chapter 3. The average log2 fold change and statistical significance was conducted upon the running of code to identify the top gene markers between specified groups of cells. The statistical analysis of all other datasets was conducted using PRISM – GraphPad (version 9) software. For normally distributed data, parametric student's t-tests were used to compare the means between groups and determine statistical significance. This statistical test was used for flow cytometry and mass cytometry data where mean fluorescence intensity or percentage of subset were being compared. Most t-tests

were unpaired, except the t-tests that were ran to compare the means of data from the paired lupus nephritis samples, presented in Chapter 5. To compare the expression of protein markers of interest between health and lupus nephritis cohorts as well as within each cohort respectively, a 2-way ANOVA with Tukey's multiple comparisons test was used. This allowed for multiple means to be compared between multiple variables. For all statistical analyses, significance was deemed as $p<0.05$.

2.8.3 Rationale for the number of patients included in analyses

In the data presented in Chapter 3, a total of n=6 patients, healthy donors (n=3) and lupus nephritis patients (n=3), were included in the single-cell RNA-sequencing dataset. This dataset includes a small sample size because it was an initial pilot experiment whereby the 10X protocol and CITE-seq antibody panel was tested for the first time, by Tull et al., prior to the start of this study.

The number of samples used for the mass cytometry analyses, presented in Chapter 4, was a total of 18 (n=9 health and n=9 lupus nephritis). This number of samples was chosen to meet the minimum sample number requirements for downstream analysis in Cytobank for methods such as SPADE.

The data presented In Chapter 5 included a total of n=14 lupus nephritis paired samples from n=7 patients and n=8 samples from healthy donors. Paired lupus samples were challenging to collect given the inconsistent frequency in which lupus patients visited the Louise Coote Lupus Clinic at Guy's Hospital, London and more so the COVID-19 pandemic which resulted in the suspension of all lupus blood sample collections. Therefore, the sample size for the data presented in Chapter 5 is smaller than intended but provides some interesting observations that can be explored further in future studies. The healthy donor samples were run alongside lupus nephritis samples to balance this dataset.

The data in Chapter 6 includes analysis from both flow cytometry and mass cytometry experiments. A total of n=10 samples from lupus nephritis patients and n=10 from

healthy donors were used in the flow cytometry experiment. The 20 samples included were deemed sufficient for this experiment as it was used as a confirmation of previous findings from a pilot experiment by Siu et al. (2022). The mass cytometry data presented in Chapter 6 comprises the same dataset used in Chapter 4, thus the same reasoning for sample size applies.

3 Identifying a group of early B cells with an interferon signature

3.1 Introduction

Transitional B cells are the first population of B cells to enter the peripheral blood from the bone marrow. They give rise to mature B cell subsets (Palanichamy et al., 2009; Sims et al., 2005). It is well established that peripheral B cell development in lupus nephritis is altered in numerous ways, so understanding the heterogeneity in health and differences between the transitional cells in health versus lupus nephritis is important.

There are several known differences in transitional B cells in lupus nephritis compared to health including relative increase in CD38hiCD24hi cells (Simon et al., 2016), a lack of T2 IgMhi cells (Tull et al., 2021) and dysregulated production of IL-10 (Blair et al., 2010). Therefore, it is important to study the make-up of the transitional population that begins the B cell developmental trajectory after emigration from bone marrow to blood in greater detail to understand the changes observed in B cells in SLE.

Prior to the start of this project, a single-cell RNA-sequencing dataset was generated from B cells from age- and sex-matched healthy control donors (n=3) and lupus nephritis patients (n=3). Total CD19+ B cells and transitional B cells, defined as CD19+CD27-IgD+CD10+, were sorted separately by fluorescent-activated cell sorting. Cells were then stained with a cocktail of CITE-seq antibodies, made up of oligonucleotide-conjugated antibodies against B cell markers, which included IgD, IgM, CD5, CD10, CD21, CD24, CD27, CD38, IL4R and integrin β_7. The use of CITE-seq antibodies enables surface protein phenotyping in conjunction with RNA-sequencing. This is particularly important for the identification of IgMhi cells because the level of expression of IgM on the cell surface that can define cell subsets is not necessarily reflected in the amount of RNA present. Additionally, two distinct hashtag oligonucleotide-conjugated antibodies were used to separately tag the total CD19+ B cells and the sorted transitional B cells in a process known as hashing. Total CD19+ B cells were labelled with the hashtag antibody termed HTO-AHH1-TotalSeqC and sorted transitional B cells were labelled with the antibody termed HTO-AHH2-TotalSeqC. Hashing allowed for the two cell groups to be pooled together in the same

lane on the 10X controller and for the sequencing run but then separated for the purpose of data analysis. Gene expression libraries were made using the 5' gene expression workflow from 10X Genomics.

The analysis for this thesis began post-sequencing whereby data were pre-processed and analysed using the R package known as Seurat. This study investigates the diversity of transitional B cells because building on the current understanding of transitional B cells in health is key to deciphering alterations of these cells that are seen in the most severe manifestation of SLE, lupus nephritis.

3.2 Aims

- To investigate the diversity of transitional B cells and investigate gene expression patterns between transitional subsets in cells from healthy donors

  To compare gene expression patterns of transitional B cells from healthy donors and lupus nephritis patients

3.3 Results

3.3.1 Filtering data to select for sorted transitional B cells

Single-cell data RNA-sequencing data from healthy donors (n=3) were analysed using the R package, Seurat V3 (Stuart et al., 2019). Pre-processing quality control steps were performed on each healthy donor sample individually.

Firstly, sorted transitional B cells were separated from total CD19+ cells. These two datasets could be separated by selecting appropriate hashtag thresholds, as shown in Figure 1A. The aim was to select cells that were only positive for one of the hashtag antibodies and therefore only belonged to one of the datasets. CD19+ cells were tagged with HTO-AHH1-TotalSeqC (hash 1) and sorted transitional B cells were tagged with HTO-AAH2-TotalSeqC (hash 2). As demonstrated in Figure 1A, total CD19+ were selected as cells with a signal greater than the hash 1 threshold and lower than the hash 2 threshold. Transitional B cells, tagged with hash 2, were cells with a signal greater than the hash 2 threshold but less than the hash 1 threshold (Figure 3.1A).

Cells from the transitional B cells dataset were then filtered to remove doublets and cells with low transcript levels using RNA count and Feature RNA. Cells with a high percentage of mitochondrial gene reads were also filtered out as this was indicative of cells that were dying. Thresholds for RNA count, RNA transcript levels (feature RNA) and percentage of mitochondrial genes were determined using histograms shown in Figure 3.1B. The transcript levels and RNA count were plotted against each other to check appropriate data were being kept in the dataset, as demonstrated in Figure 3.1C. After filtering was complete, all three samples were integrated ready for clustering.

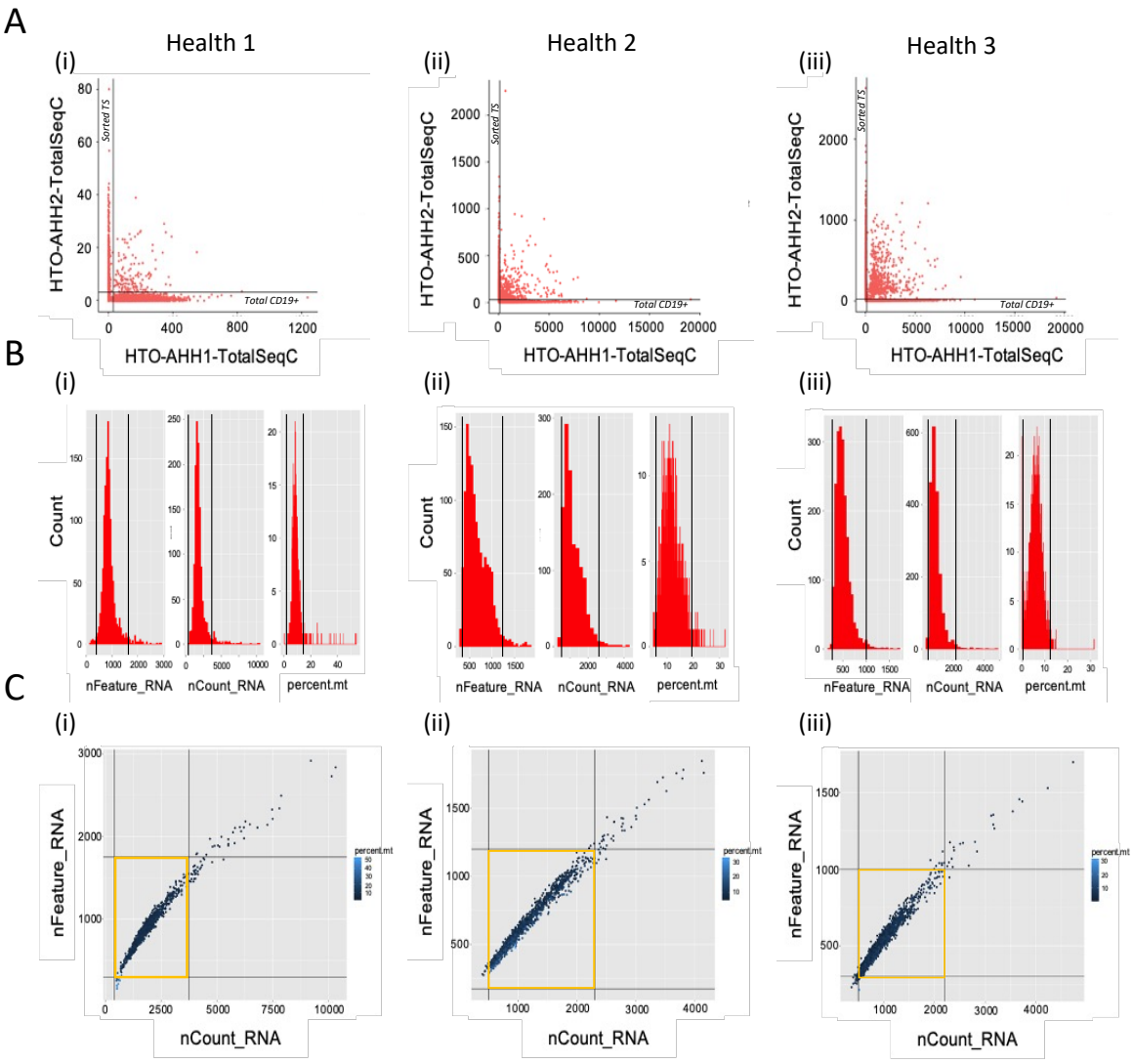

Figure 3.1: Filtering single-cell RNA-sequencing data from healthy donor samples. (A) Scatterplot used to visualise thresholds for hashtag oligonucleotide-conjugated antibodies. Sorted transitional B cells were tagged with the HTO-AHH2-TotalSeqC antibody on the y-axis and total CD19+ B cells were tagged with the HTO-AHH1-TotalSeqC antibody on the x-axis. Sorted transitional cells were those that were greater than the HTO-AHH2-TotalSeqC threshold and less than or equal to the HTO-AHH1-TotalSeqC threshold. CD19+ B cells were cells that were greater than the HTO-AHH1-TotalSeqC threshold and less than or equal to the HTO-AHH2-TotalSeqC threshold. Black lines indicate thresholds. **(B)** Histograms displaying three parameters used for filtering data: nFeature, nCount and percentage of mitochondrial genes. Black lines indicate thresholds. **(C)** Scatterplot displaying nFeature versus nCount and the threshold values (indicated by black lines) that were selected to filter single cells. Percentage of mitochondrial gene reads is indicated by colour scale; high mitochondrial gene

reads was indicative of dying cells. Points within the orange square show the data selected for downstream analysis. Panels (i) display data from Health 1, (ii) are from Health 2 and (iii) are Health 3.

3.3.2 Quality control to remove non-transitional cells

Once pre-processing was complete, the first aim was to classify clusters of transitional cells prior to downstream, in-depth gene expression pattern analysis. Firstly, cells were clustered based on the top 2000 differentially expressed genes into four separate clusters. The more similar the gene expression profile of two cells, the more likely they were to be placed in the same cluster. Clusters were visualised using the dimension reduction algorithm UMAP (uniform manifold approximation and projection) (Becht et al., 2019) (Figure 3.2A). It was confirmed that cells from all three samples clustered together by overlaying clusters from each sample onto a single UMAP, shown in Figure 3.2B, and that each sample had cells belonging to all four clusters, shown in Figure 3.2C.

Clusters separated into two distinct islands on the UMAP, which indicated the need for an additional quality control step to ensure all cells were in fact transitional B cells. To investigate this, a feature plot was made, displayed in Figure 3.2D, whereby the UMAP was overlaid with surface protein marker expression, generated by CITE-Seq antibody staining. When investigating surface protein expression, it was evident that the cells on the smaller island comprising cluster 2 were CD27+IgD-, which is the typical phenotype of memory B cells as opposed to transitional cells which are CD27-IgD+.

Furthermore, the average log2 fold change of gene expression for the suspected memory cluster was calculated. The fold change was calculated in comparison to the other three clusters in the dataset shown in Figure 3.2A, and all fold changes had a p-value of <0.0001. As demonstrated in Figure 3.2E, it was found that cluster 2 had positive average log2 fold changes for memory-markers *IGHA2*, *COCH*, *CD27* and *IGHA1* and negative log2 fold changes for markers associated with transitional cells such as *TCL1A*, *IGHD* and *IGHM*, thus confirming this cluster as non-transitional. It was likely these cells were not gated out upon sorting for CD10+ cells. Cluster 2 was removed from the dataset. The other three clusters, 0, 1 and 3, all were identified as CD27-IgD+CD10+, evidenced in Figure 3.2D, and so the cells were re-clustered for downstream analysis.

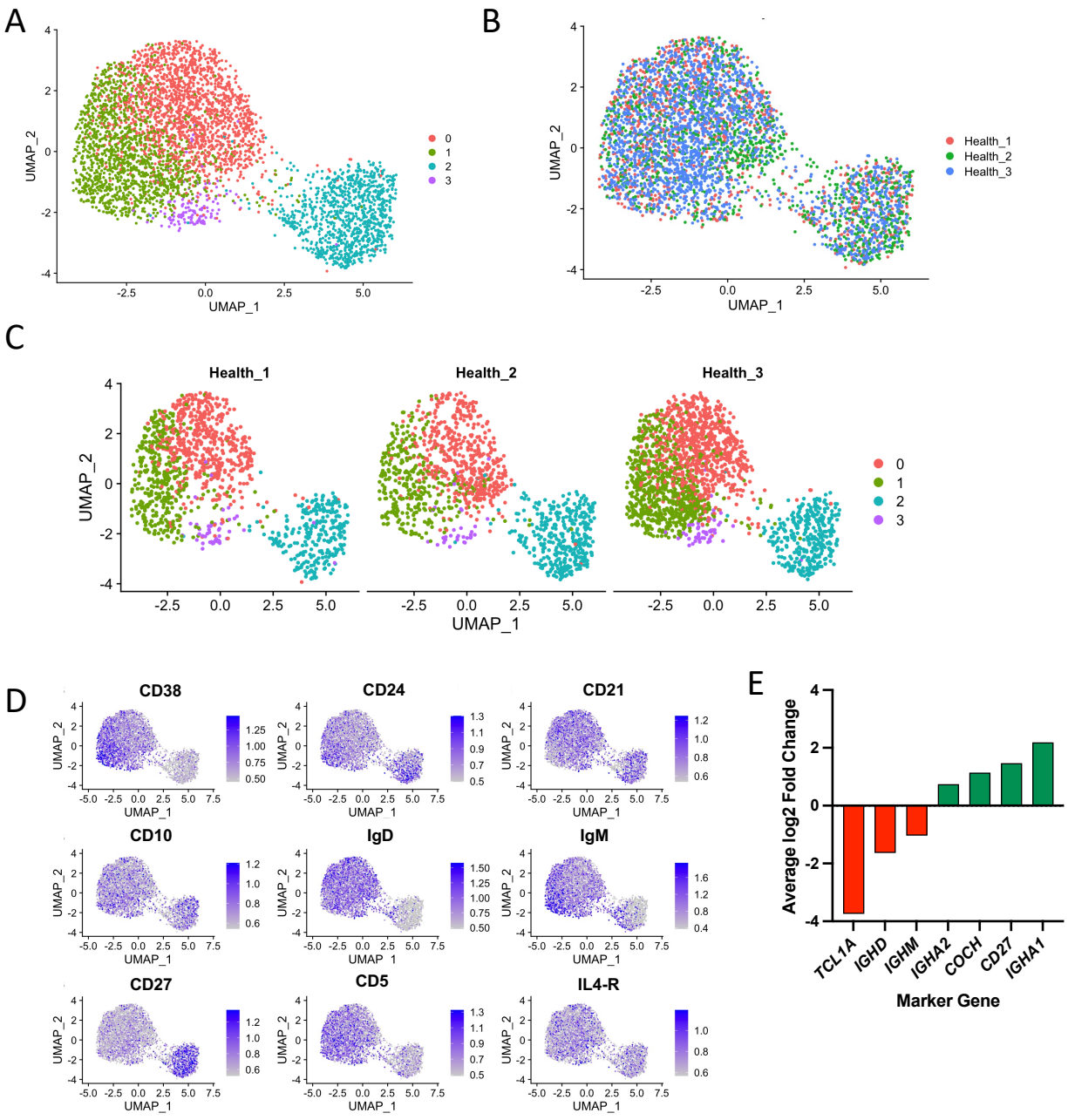

Figure 3.2: Quality control to remove of non-transitional cells from dataset. (A) UMAP plot showing four clusters of B cells from n=3 healthy donors, generated from 2000 differentially expressed genes. **(B)** UMAP plot from panel A coloured by healthy donor. **(C)** UMAP plot from panel A showing four clusters of B cells, separated by donor. **(D)** Feature plots displaying surface protein expression, generated by CITE-seq antibody staining, overlaid on UMAP plot. Scale indicates level of expression, with the greatest expression in dark purple and lowest expression in grey. **(E)** Bar graph displaying gene expression average log2 fold change of cluster 2. Positive and negative log2 fold change shown in green and red, respectively.

3.3.3 Investigating transitional B cell heterogeneity

The cells, now confirmed as transitional B cells, from the three healthy donors were grouped into six clusters, shown in Figure 3.3A, based on differential gene expression patterns. Before proceeding with further analysis, all three samples were overlaid on a single UMAP to check clusters from each donor were aligned (Figure 3.3B). The "Health 3" sample had the greatest total number of cells (1576 cells) compared to "Health 1" which had 924 cells and "Health 2" which has 837. However, all six clusters were present in each of the three samples, no cluster was from one sample only, shown in the UMAPs in Figure 3.3C. Furthermore, each cluster made up approximately the same proportion of the total transitional cells across all three samples, except for cluster 3 from "Health 3", which was double the size of that of the other two healthy samples (Figure 3.3D).

To begin classifying the clusters, surface marker expression was projected onto the UMAP, presented in Figure 3.3E, whereby the greater expression was identified by darker purple dots, and conserved gene markers for each cluster were determined. Conserved gene markers are genes that are markers for a particular cluster across all three samples. It was noted that the area of the UMAP with the highest CD38, CD24 and IgM surface protein expression, highlighted by red arrows in Figure 3E, also had the lowest CD21 expression. This area of the UMAP correlated with cluster 2, suggesting that this cluster was made up of T1 B cells due to this population of B cells having a $CD38^{+++}CD24^{+++}IgM^{+++}CD21^{lo/-}$ surface phenotype. Furthermore, cluster 2 had positive expression of T1 markers including *PPP1R14A*, which had an average log2 fold change of +1.6, shown in Figure 3.3F, indicating cluster 2 had three times the level of expression of this gene compared to the other transitional clusters. Furthermore, cluster 2 had other T1-associated positive gene markers including *ACTG1*, *GNG3*, *SOX4* and *MZB1*, and negative expression of markers associated with T2 populations such as *SELL*, *CD69* and *IL4R* (Figure 3.3F).

The remaining clusters were found to have a surface phenotype resembling that of T2 B cells ($CD38^{++}CD24^{++}CD21^{+++}$), with lower expression of CD38 and CD24, and higher expression of CD21 in comparison to T1 cells, as shown in the heatmap in Figure 3.3G.

Clusters 1 and 3 were classified as T2 IgMlo cells due to having the lowest expression of surface IgM, as seen in Figure 3.3G, and notable higher expression of T2 IgMlo markers such as *IL4R* and *SELL* compared to the other T2 clusters, shown in Figure 3.3H. Clusters 0 and 4 were identified as T2 IgMhi as they had higher average surface IgM expression and were able to be distinguished from the IgMlo cells based on positive expression of genes such as *PLD4*, *ITM2C*, *CD1C* and *MZB1*, as presented in the heatmap in Figure 3.3H.

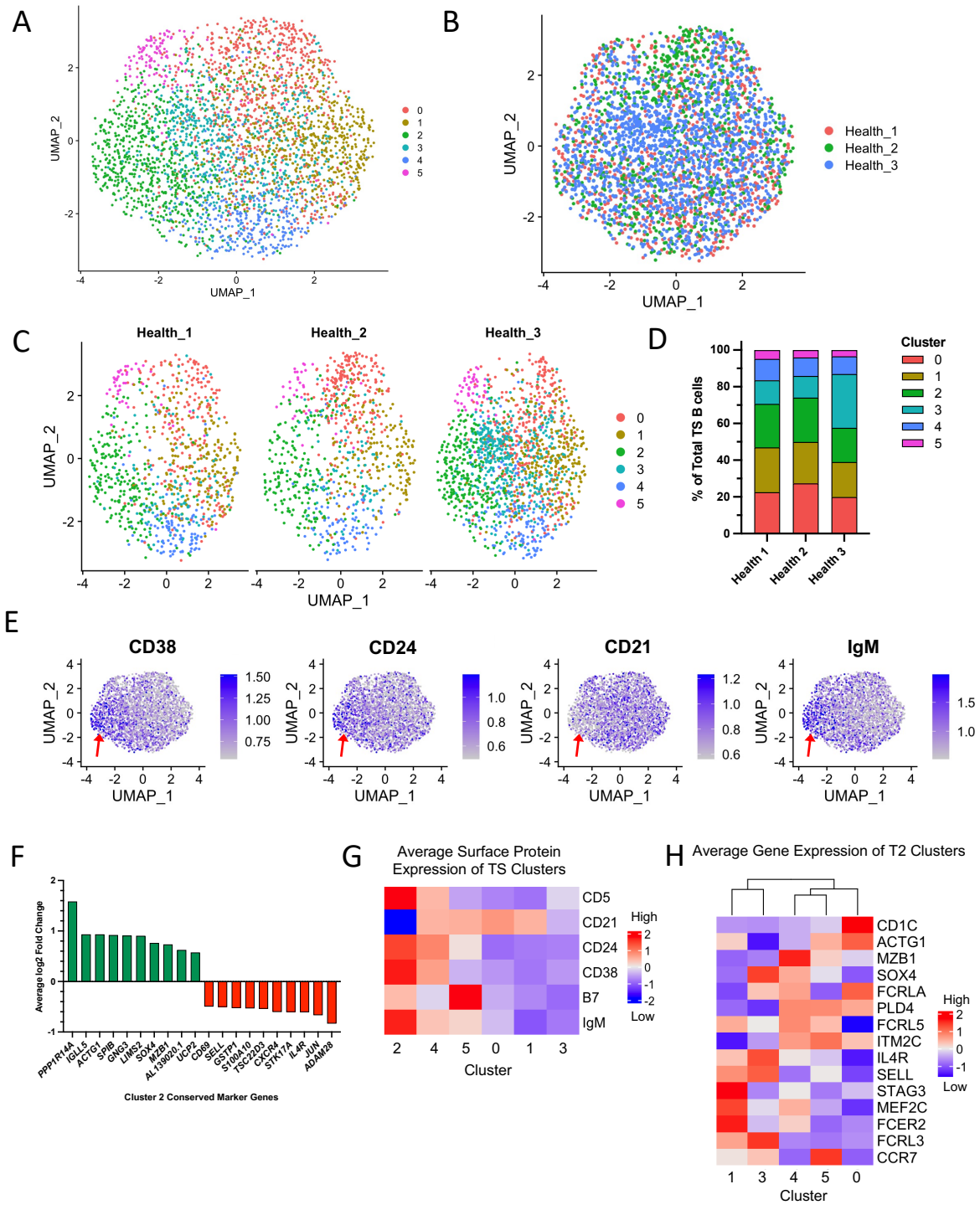

Figure 3.3: Classification of transitional B cells in healthy donors. (A) Seven clusters on a UMAP plot generated from the top 2000 differentially expressed genes of transitional B cells from healthy donors (n=3). **(B)** UMAP plot from panel A coloured by donor. **(C)** UMAP from panel A separated by donor. **(D)** Bar chart showing size of each cluster as a proportion of total transitional B cells in each of the n=3 healthy donors. **(E)** UMAP plot from panel A overlaid with surface protein expression. Colour scale indicates expression level whereby the darker

purple dots represent higher expression level. Red arrows indicate region where cells have a T1 surface phenotype. **(F)** Bar graph showing average log2 fold change of cluster 2 (T1) conserved gene markers. Green and red bars indicate positive and negative log2 fold change, respectively. **(G)** Heatmap comparing average surface marker expression, from CITE-seq antibody staining, of CD5, CD21, CD24, CD38, integrin β_7 (B7) and IgM, across all six transitional cell clusters. Colour scale indicates level of expression, with red being the highest expression and blue being the lowest. **(H)** Heatmap comparing expression of typical transitional cell marker genes in T2 clusters (clusters 0, 1, 3, 4 and 5). Colour scale indicates level of expression, with red being the highest expression and blue being the lowest.

The gene markers that aided classification of IgMhi and IgMlo transitional B cells clusters in this thesis were generated in a previous study by Tull et al (2021) using pooled IgMhi and IgMlo transitional cells sorted from total CD10 expressing transitional B cells, shown in Table 2.1 in Materials and Methods. The data analysed here included more transitional B cells and thus the increased cell numbers allowed for removal of T1 cells, in addition to subclassification of T2 cells. This enabled the identification of additional genes that can distinguish IgMhi and IgMlo T2 transitional cells. For example, as shown in Table 3.1, when comparing the average log2 fold change of gene expression in T2 IgMhi cells with that of T2 IgMlo cells, *FOS* and *JUN* are expressed more highly in T2 IgMhi cells, indicated by a positive log2 fold change. Additionally, the ISG IFITM1 was also found to be expressed at a greater level in IgMhi T2 cells compared to IgMlo T2 cells with an average log2 fold change of 0.43.

Table 3.1: Differentially expressed genes between T2 IgMhi cells versus T2 IgMlo cells.

DEG	Positive Average log2FC T2 IgMhi vs T2 IgMlo	p-value	DEG	Negative Average log2FC T2 IgMhi vs T2 IgMlo	p-value
AL138963.3	0.99	2.18E-22	*RAC1*	-0.30	3.44E-02
FOS	0.77	4.71E-16	*SCIMP*	-0.30	9.40E-03
MT-ND6	0.72	8.55E-19	*TRIR*	-0.31	5.36E-04
COBLL1	0.71	1.22E-11	*SNW1*	-0.31	3.52E-03
CD69	0.63	1.94E-17	*MRPS26*	-0.32	3.73E-02
COTL1	0.61	4.14E-12	*C12orf57*	-0.32	2.12E-06
*PLD4**	0.56	1.48E-09	*LSM10*	-0.32	8.69E-03
JUNB	0.56	1.08E-09	*S100A6*	-0.33	2.77E-03
JUN	0.54	7.48E-16	*ID3*	-0.34	9.39E-04
MYC	0.54	3.51E-09	*DEK*	-0.34	9.15E-03
*ACTG1**	0.53	1.61E-13	*DNAJC15*	-0.35	5.24E-03
DUSP1	0.51	1.67E-09	*SNHG7*	-0.35	9.08E-04
PCDH9	0.50	1.26E-10	*LY6E*	-0.35	4.01E-04
HSPA8	0.48	4.85E-08	*LIMS2*	-0.35	1.84E-02
MTRNR2L12	0.48	1.34E-10	*RWDD1*	-0.36	6.57E-03
IFITM1	0.43	2.55E-10	*PIN4*	-0.36	4.33E-03
*ITM2C**	0.43	1.44E-07	*S100A10*	-0.38	2.68E-03
CXCR4	0.40	1.38E-10	*PTPRCAP*	-0.39	3.51E-08
NBPF14	0.40	2.66E-07	*PLPP5**	-0.39	8.30E-10
ACTB	0.38	1.65E-14	*MEF2C**	-0.41	5.16E-13
PIM2	0.37	1.70E-06	*STAG3**	-0.43	3.81E-03
*MZB1**	0.37	2.32E-07	*IL4R**	-0.50	4.06E-08
EEF1A1	0.35	1.13E-14	*LHPP*	-0.51	1.71E-06
MT-ATP6	0.35	3.02E-16	*LINC01857*	-0.52	1.08E-06
FAM107B	0.35	2.08E-06	*PPP1R14A**	-0.53	6.15E-04
SH3BP5	0.35	1.43E-05	*SOX4**	-0.54	3.57E-04
*ALOX5**	0.35	8.29E-05	*SKAP1*	-0.72	1.28E-11
PUF60	0.35	3.65E-05	*FCRL3*	-0.72	1.19E-11
PGK1	0.35	2.44E-05	*TARSL2*	-0.73	9.06E-11

**Genes that have also been identified by Tull et al (2021) and used in reference gene list*

It was evident that there was heterogeneity amongst the T2 cells given that both the T2 IgMhi and T2 IgMlo populations were each made up of two separate clusters. Differentially expressed genes between T2 IgMhi clusters (cluster 0 versus cluster 4) were determined in order to investigate the heterogeneity within the T2 IgMhi population. As shown in Figure 3.4A, cluster 0 had greater expression of interferon-associated genes *IFITM1* and *IRF1* than cluster 4 and lower expression of genes associated with immaturity such as *IGLL5* and *VPREB1*. The same differential gene

expression patterns were analysed within the T2 IgMlo clusters (cluster 1 versus cluster 0), shown in Figure 2.4B and it was found that cluster 1 had 2-times lower expression of genes associated with the earliest immature peripheral B cells, *PPP1R141A*, *VPREB1* and *SOX4*, than cluster 3. This data highlights differences within the T2 sub-populations of B cells, thus further demonstrating the complexity of the transitional B cell pool.

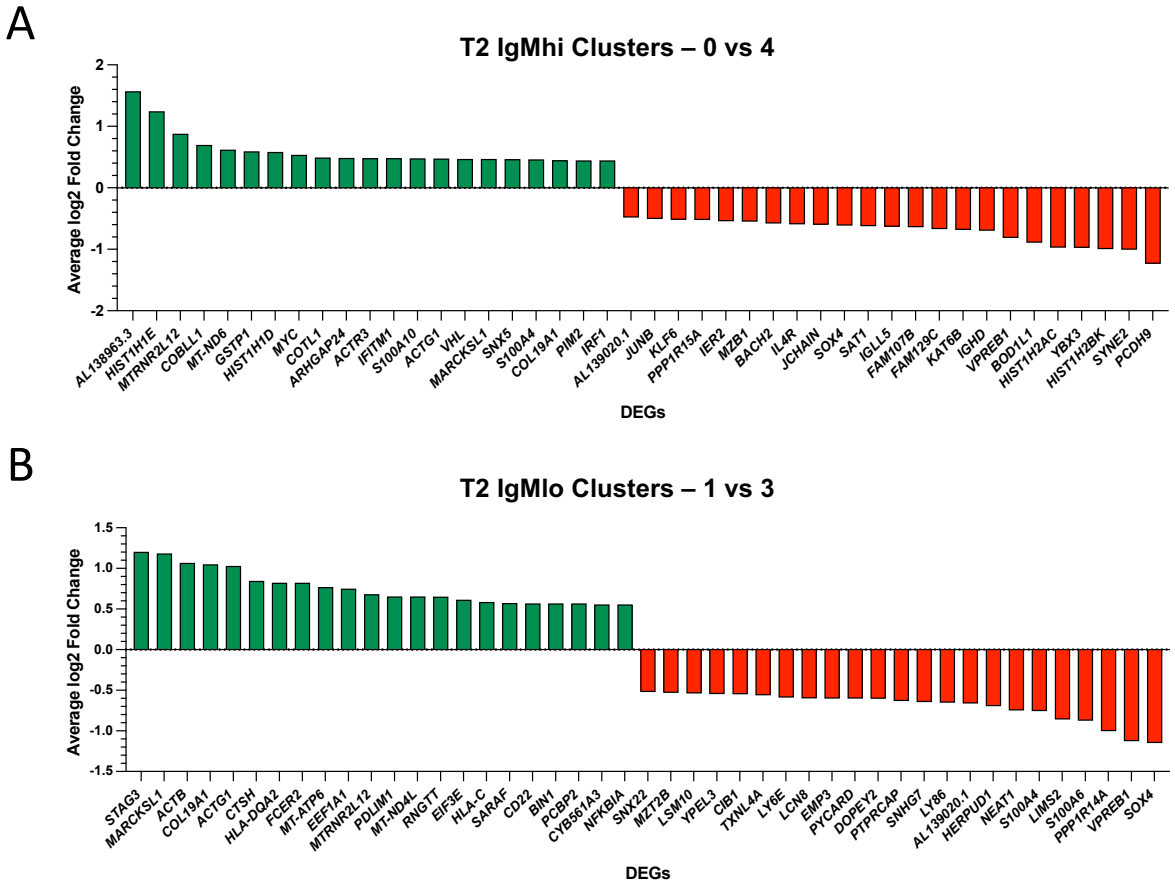

Figure 3.4: Differentially expressed genes amongst sub-populations of T2 B cells. (A) Bar graph showing average log2 fold change gene expression of T2 IgMhi clusters, generated by comparing differential gene expression of cluster 0 to cluster 4. Green and red bars indicate positive and negative log2 fold change, respectively. **(B)** Bar graph showing average log2 fold change gene expression of T2 IgMlo clusters, generated by comparing differential gene expression of cluster 1 to cluster 3. Green and red bars indicate positive and negative log2 fold change, respectively. DEGs; differentially expressed genes.

Post-classification, it was evident that cluster 5 could not be classed as one of the known transitional B cell populations as it did not have any clear transitional gene expression patterns. When determining the expression of typical transitional genes, shown in Figure 3.3H, cluster 5 was found to express both T2 IgMhi and T2 IgMlo markers. For instance, expression of *PLD4*, *MZB1* and *ITM2C*, associated with T2 IgMhi, as well as *CCR7* and *SELL*, which are known to be expressed by the T2 IgMlo cells. Despite cluster 5 making up only approximately 2-4% of the total transitional cell pool, the conflicting gene expression patterns were of interest, and it was deemed important to understand the characteristics of the cells that made up cluster 5. The conserved marker genes of cluster 5 indicated that the cells in this cluster expressed numerous ISGs, such as *IFI44L*, *IFITM1* and *MX1*, shown in Figure 3.5A. The cells in cluster 5 had a T2-like surface phenotype (Figure 3.3G) and expressed higher surface IgM and integrin β_7, reminiscent of T2 IgMhi cells, however no characteristic transitional genes were conserved markers of this cluster (Figure 3.5B). It was concluded that the cells belonging to this cluster were a unique group of cells within the transitional pool of healthy individuals.

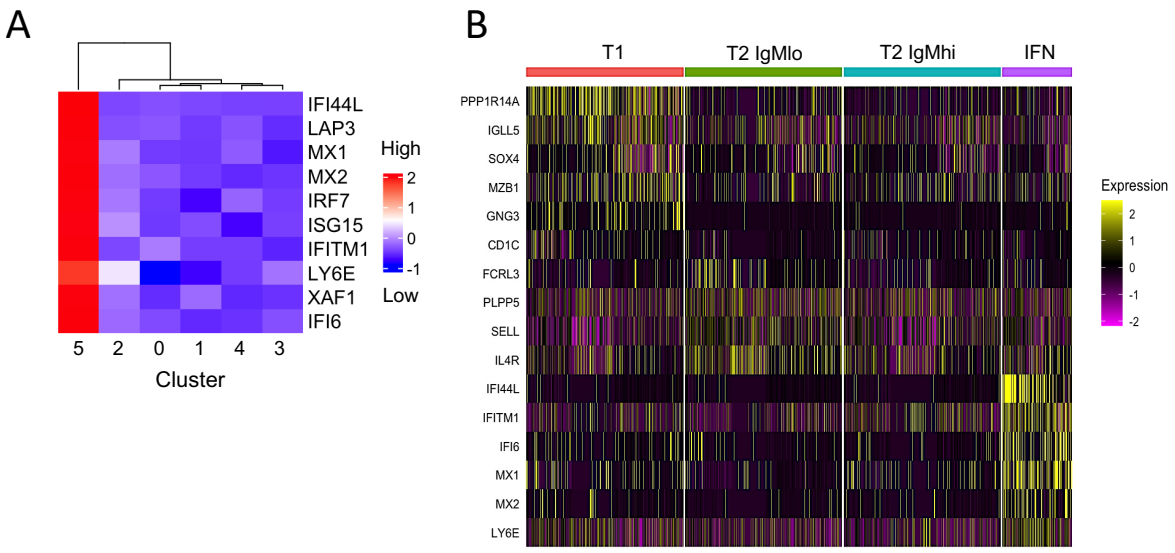

Figure 3.5: Group of transitional B cells with an interferon gene signature. (A) Heatmap comparing expression ISGs, taken from the of top 10 marker genes of interferon-associated cluster 5, in cells from six transitional B cell clusters from n=3 healthy donors. Highest expression shown in red and lowest expression in blue. **(B)** Heatmap comparing expression of typical transitional B cell genes and ISGs in cells from transitional B cell populations from n=3

healthy donors. Colour scale indicates expression level. Yellow and pink denote highest and lowest expression, respectively.

3.3.4 Identification of a group of naïve B cells with an interferon gene signature in health

Much like transitional cells, it is known that there are respective naïve IgMhi and IgMlo populations in the B cell pool of healthy individuals (Tull et al., 2021). As naïve cells are also an early B cell subset, the next aim was to investigate whether a group of naïve B cells had an interferon gene signature like that of the transitional B cells in this study.

The same single-cell RNA sequencing dataset from three healthy donors used in this project for transitional B cell analysis was used for naïve B cell analysis, however the total CD19+ data was used as opposed to the sorted transitional cell data. The total CD19+ B cell dataset, tagged with the HTO-AHH1-TotalSeqC (hash 1) antibody, was separated from the transitional dataset, and pre-processed using the same pipeline outlined in 3.3.1. CD19+ B cells were clustered based on the top 2000 differentially expressed genes into twenty-one clusters, shown in Figure 3.6A.

Firstly, the naïve clusters were identified by expression of *TCL1A*, a known marker of early B cells – the transitional and naïve subsets (Brinas et al., 2021), shown in purple on the UMAP in Figure 3.6B. However, as transitional cells are included in the *TCL1A*+ group of cells, surface protein expression was used to confirm which clusters were naïve. As shown in Figure 3.6C, the *TCL1A*+ cells were CD27+IgD+, consistent with a transitional and naïve surface phenotype. CD10 expression was localised to x=4 y=3 on the UMAP, displayed in Figure 3.6C, suggesting that cells in this region were transitional cells; the rest of the *TCL1A*+ cells on the UMAP were CD10-, thus clusters in this region were classed as naïve B cells. Nine clusters of naïve cells were identified, highlighted in orange in Figure 3.6D. Conserved marker genes were determined for each naïve cluster, and it was found that cluster 13, highlighted in blue in Figure 3.6E, had a strong interferon gene signature.

A total of forty-one positive and two negative conserved gene markers were found for cluster 13, as shown in Figure 3.6F and it was noted that ISGs, including *IFITM1*, *MX1*,

ISG15, *IFI15*, *IF44L* and *BST2*, made up the majority of the positive gene markers for cluster 13. Average log2 fold changes comparing gene expression between cluster 13 and all other naïve clusters were generated. The top marker gene, *IFITM1*, had an average log2 fold change of over +2, indicating that the expression of *IFITM1* was four-times greater in the interferon-associated naïve cells compared to the rest of the naïve clusters. It was noted that similar groups of genes were present in both the transitional and naïve interferon populations; these included *IFITM1*, *MX1*, *IFI6* and *IFI44L*. Generally, this group of naïve B cells accounted for a very small percentage of the total B cell pool, approximately 2%, but accounted for between 3-5% of the naïve B cell population.

The data presented in 3.3.4 show that a group of naïve B cells express interferon-associated genes, like that found in the transitional B cell pool. It is well-established that interferon plays a role in lupus nephritis pathology so next it was important to investigate these interferon-associated early B cells in cells from lupus nephritis patients.

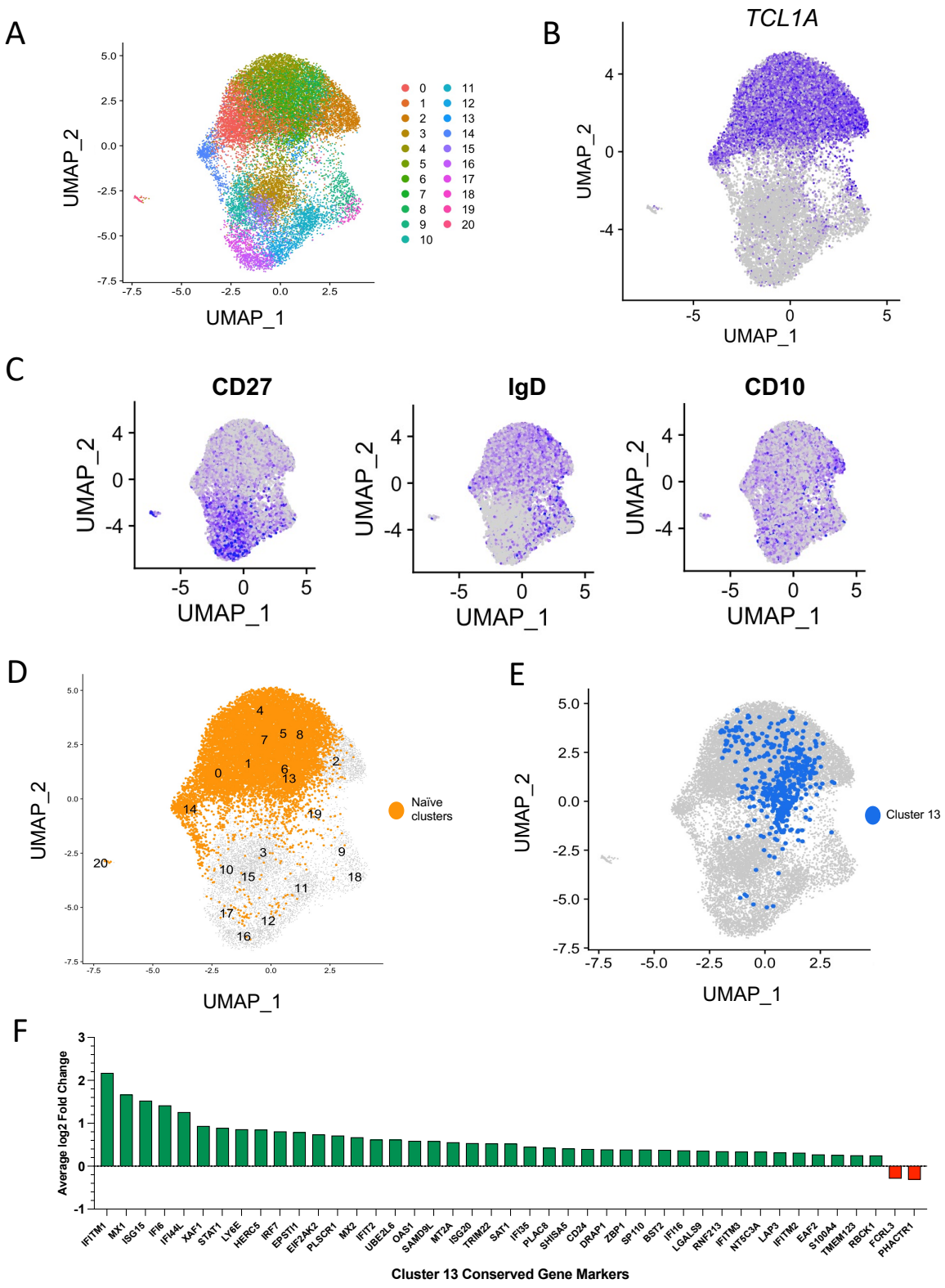

Figure 3.6: Group of naïve B cells with an interferon gene signature. (A) UMAP plot of twenty-one CD19+ B cell clusters generated using the top 2000 differentially expressed genes. UMAP is comprised of n=3 healthy donor samples integrated. **(B)** UMAP plot from panel A displaying *TCL1A* expression. Purple dots indicate positive expression and grey dots indicate

negative expression. The darker the purple dots the higher the expression. **(C)** UMAPs from panel A showing expression of surface proteins CD27, IgD and CD10. Purple dots indicate positive expression and grey dots indicate negative expression. The darker the purple dots the higher the expression. **(D)** UMAP from panel A highlighting naïve B cell clusters (clusters 0, 1, 4, 5, 6, 7, 8, 13 and 14) (shown in orange). **(E)** UMAP from panel A highlighting naïve cluster 13, found to have an interferon gene signature. **(F)** Bar graph showing gene expression average log2 fold change between cluster 13 and all eight other naïve clusters. Positive and negative fold changes are represented by green and red bars, respectively.

3.3.5 Filtering data and quality control to merge health and lupus nephritis datasets

Once it was established that groups of both transitional and naïve B cells from healthy individuals expressed an interferon gene signature it was key to investigate these early B cell populations in lupus nephritis. The aim of this analysis was to compare gene expression patterns of B cells from patients with lupus nephritis with that of healthy donors.

Firstly, the sorted transitional B cell single-cell RNA-sequencing dataset from three healthy donors was pre-processed using the same quality control pipeline displayed in Figure 3.1. The pipeline was then run for three lupus nephritis patient samples. Just the same as the healthy donor samples, both sorted transitional cells and total CD19+ cells from lupus nephritis patients had been tagged with hashtag oligonucleotide-conjugated antibodies. So, transitional cells were separated from total CD19+ cells by selecting for cells with the transitional hashtag antibody (HTO-AHH2-TotalSeqC), as shown in Figure 3.7A. Cells were then filtered based on RNA count and feature RNA, to eliminate doublets and any cells with negligible transcript levels, and percentage of mitochondrial genes to remove dying cells; threshold values were chosen using histograms shown in Figure 3.7B. Filtering parameters were plotted against each other to check suitable data were kept in the dataset, shown in Figure 3.7C.

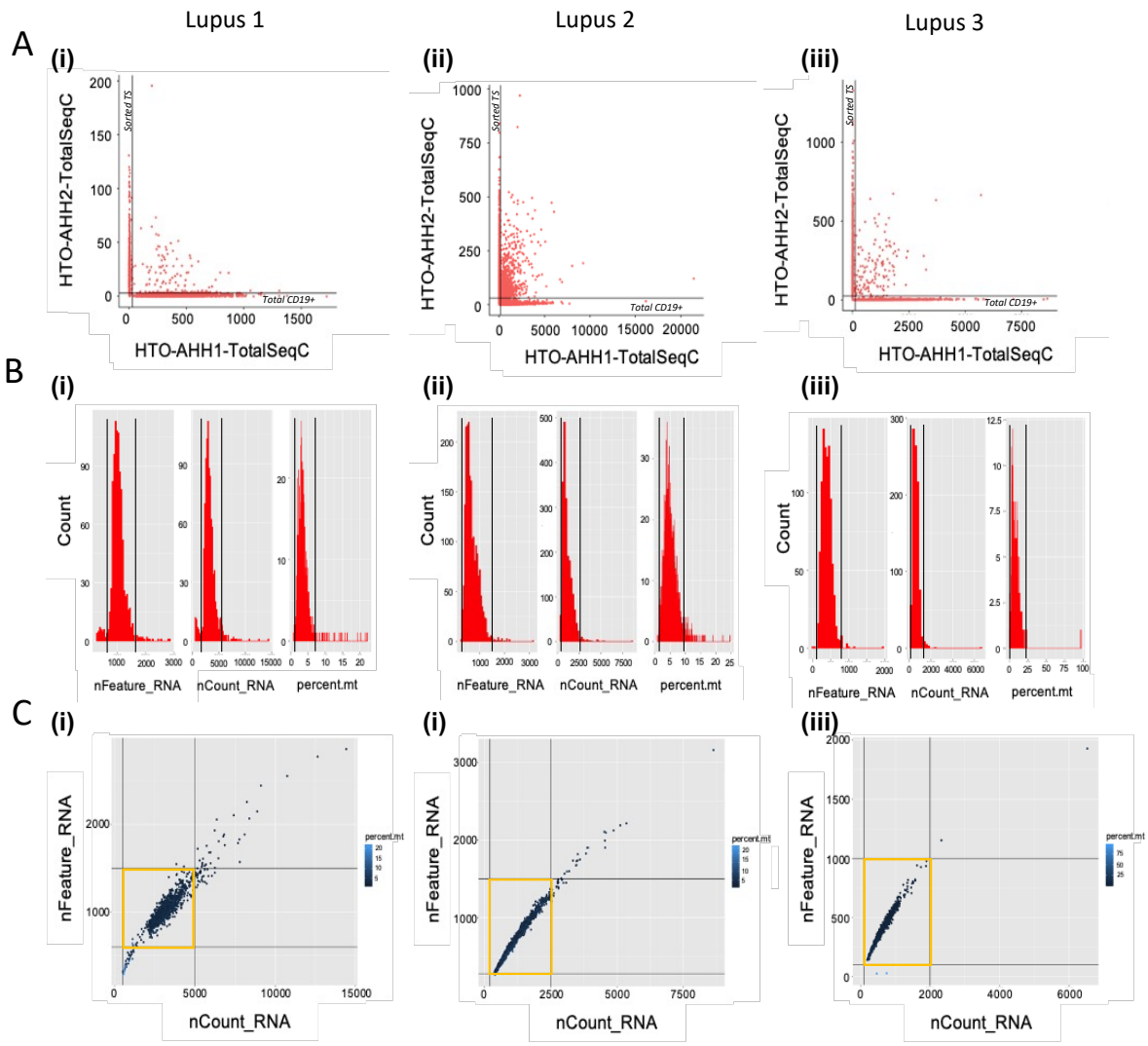

Figure 3.7: Filtering single-cell RNA-sequencing data from lupus nephritis patient samples. **(A)** Scatterplot used to visualise thresholds for hashtag oligonucleotide-conjugated antibodies. Sorted transitional B cells were tagged with the HTO-AHH2-TotalSeqC antibody on the y-axis and total CD19+ B cells were tagged with the HTO-AHH1-TotalSeqC antibody on the x-axis. Sorted transitional cells were those that were greater than the HTO-AHH2-TotalSeqC threshold and less than or equal to the HTO-AHH1-TotalSeqC threshold. CD19+ B cells were cells that were greater than the HTO-AHH1-TotalSeqC threshold and less than or equal to the HTO-AHH2-TotalSeqC threshold. Black lines indicate thresholds. **(B)** Histograms displaying three parameters used for filtering data: nFeature, nCount and percentage of mitochondrial genes. Black lines indicate thresholds. **(C)** Scatterplot displaying nFeature versus nCount and the threshold values (indicated by black lines) that were selected to filter single cells. Percentage of mitochondrial gene reads is indicated by colour scale; high

mitochondrial gene reads was indicative of dying cells. Points within the orange square show the data selected for downstream analysis. Panels (i) display data from Lupus 1, (ii) are from Lupus 2 and (iii) are Lupus 3.

The health and lupus datasets were then integrated to give a total of six samples. Cells were grouped based on differential gene expression into seven clusters, shown in the UMAP plot in Figure 3.8A. Some clustering differences between the health and lupus samples was expected and so clusters from each cohort were superimposed on a single UMAP to ensure the clusters generated were comparable (Figure 3.8B). CITE-seq antibody staining signal, representative of surface marker expression, was overlaid on the UMAP as a means of quality control to ensure all clusters were transitional. It was evident that clusters 3 and 6 were CD27+, as seen in Figure 3.8C, and so they were removed.

The data were re-clustered into eight new clusters, shown in Figure 3.8D, and gene markers were found. Cluster 7 had numerous memory B cell gene markers including *IGHG3*, *IGHA1*, *CD27* and *HOPX*, as well as four-times lower expression of early B cell marker *TCL1A* compared to all other cells (Figure 3.8E), therefore it was also removed from the dataset. As seen in Figure 3.8F, a second re-clustering resulted in a new eight clusters, one of which, cluster 6, was also found to have positive memory-associated gene markers (Figure 3.8G) and so this cluster was removed. The remaining seven clusters, confirmed to be transitional cells, were re-clustered for a final time in preparation for subsequent gene expression analysis.

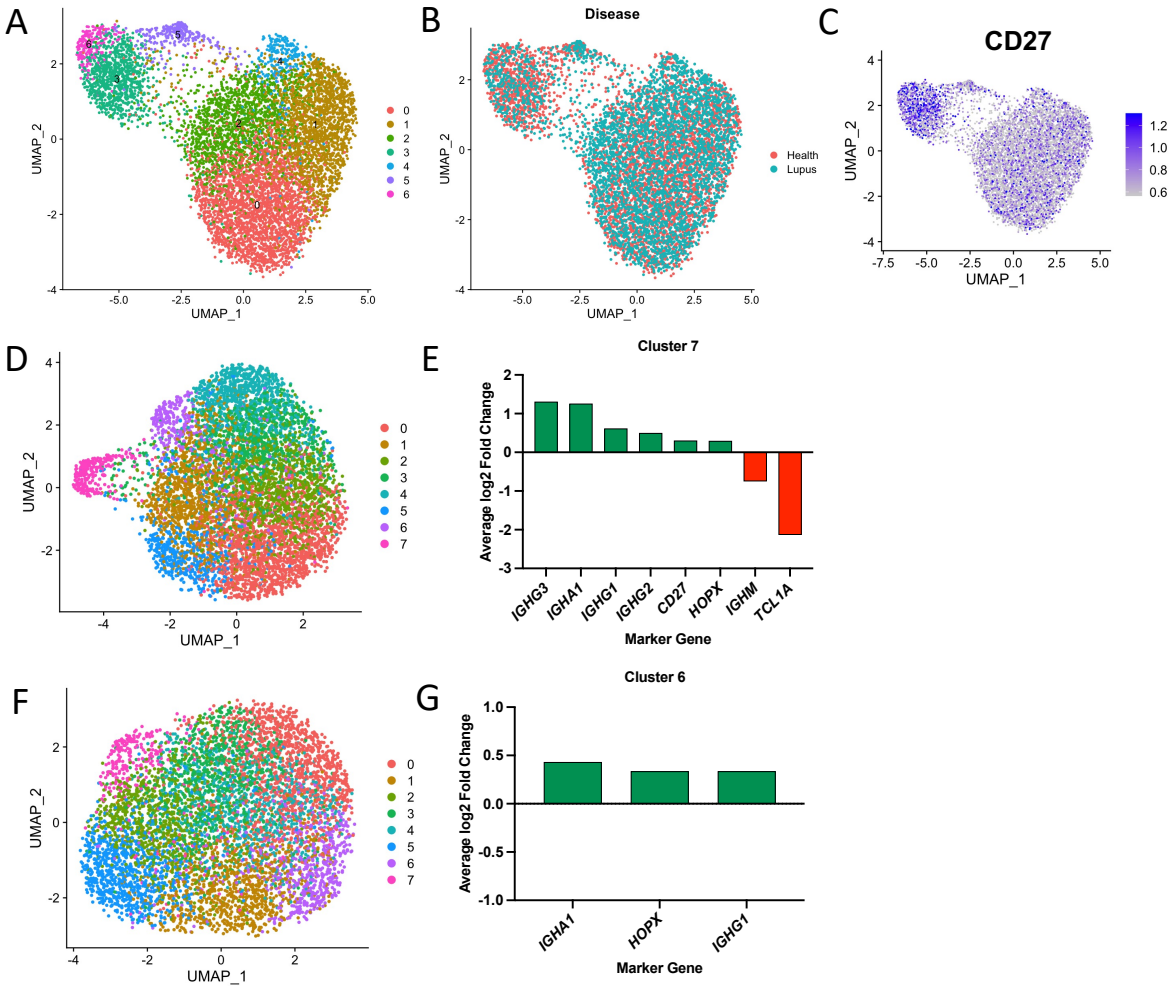

Figure 3.8: Identification and removal of non-transitional B cells. (A) UMAP plot showing seven clusters of sorted CD10+ transitional B cells from n=3 healthy donors and n=3 lupus nephritis patients, integrated. UMAP generated from 2000 differentially expressed genes. **(B)** UMAP plot from panel A coloured by disease status. **(C)** Feature plot displaying CD27 surface protein expression overlaid on UMAP plot. Scale indicates level of expression, with the greatest expression in dark purple and lowest expression in grey. **(D)** UMAP plot showing re-clustered sorted CD10+ transitional B cells from panel A. **(E)** Bar graph displaying gene expression average log2 fold change of cluster 7 from the UMAP in panel D. Positive and negative log2 fold change signified by green and red bars, respectively. **(F)** UMAP plot showing re-clustered sorted CD10+ transitional B cells from panel D. **(G)** Bar graph displaying gene expression average log2 fold change of cluster 6 from the UMAP in panel F. Positive log2 fold change represented by green bars.

3.3.6 Comparing transitional B cells in health versus lupus nephritis

The top 2000 differentially expressed genes were used to generate seven clusters of transitional cells, shown in Figure 3.9A, upon re-clustering after quality control steps. It was confirmed that the health and lupus nephritis samples had been clustered comparably as cells from both sample cohorts superimposed onto the UMAP plot, shown in Figure 3.9B. Additionally, clustering between individual samples was checked to ensure clusters were representative of all samples; it was deemed suitable for downstream analysis as samples overlaid on the UMAP uniformly (Figure 3.9C). All seven clusters were present in all healthy and all lupus nephritis samples, as shown in Figure 3.9D. To classify each cluster, surface protein expression and gene expression levels of typical transitional markers were assessed. For the purposes of classifying, health and lupus nephritis samples were kept pooled together.

Surface protein marker expression, from CITE-seq antibody staining, was displayed on a UMAP feature plot, shown in Figure 3.9E. It was noted that the cells in the region of the UMAP at 3.5,1, indicated by the red arrows in Figure 3.9E, had the highest expression of CD38, CD24 and IgM, whilst also having the lowest expression of CD21, which is the surface phenotype characteristic of T1 B cells. These cells corresponded with cluster 5 and it was evident that this cluster expressed T1-associated gene markers, demonstrated in Figure 3.9F, such as *PPP1R14A*, *PLD4* and *SOX4*.

The remaining clusters were identified as T2 cells as they had lower expression levels of CD38 and C21, and higher levels of CD21 in comparison to T1 cells, as demonstrated in the plots shown in Figure 3.9D. Sub-populations of T2 cells, IgMhi and IgMlo cells, were identified by assessing differences in surface IgM expression. As shown in Figure 3.9G, cells in the region of the UMAP highlighted by a yellow arrow had higher average IgM expression in comparison to the region highlighted by the blue arrow. The cells with higher IgM corresponded to clusters 0, 2 and 4, as demonstrated in Figure 3.9G; these clusters had positive conserved gene markers which were typical for T2 IgMhi cells, such as *CD1C*, *PLD4*, *MZB1*, *ITM2C* and *SOX4*, shown in Figure 3.9F. The cells with lowest IgM expression were found to be in clusters 1 and 3, evidenced in Figure 3.9G,

and T2 IgMlo-associated genes such as *IL4R*, *CCR7*, *SELL* and *FCRL3* were found as marker genes for these clusters (Figure 3.9F).

Cluster 6 did not appear to align with either T2 sub-populations; the cells in this cluster expressed a combination of T2 IgMhi (*CD1C*, *SOX4*) and IgMlo markers (*CCR7*, *SELL*), as shown in the heatmap in Figure 3.9F. As previously mentioned in section 3.3.3, transitional cells from healthy donors only had a group of cells that did not clearly belong to a known transitional population, which was subsequently identified as an interferon-associated cluster. Analysis of healthy donor and lupus nephritis samples combined had also outlined an atypical group of transitional cells (cluster 6), which was then found to have an interferon gene signature. Conserved gene markers of cluster 6, which were the top positive differentially expressed genes in both health and lupus samples compared to all other clusters, were predominantly ISGs, as shown in Figure 3.6H. *IFITM1* was expressed most abundantly across more than 75% of the cells in cluster 6.

Classification of transitional cells was done with health and lupus nephritis samples combined. It was evident that an interferon-associated cluster was present in both sample cohorts, but given the association of interferon with lupus, it was important to compare this interferon population in lupus versus health. Firstly, it was noted that cluster 6 accounted for a greater percentage of transitional cells in lupus nephritis compared to health, as depicted in Figure 3.9I. Overall, this interferon-associated cluster was small in comparison to the other transitional sub-populations; it made up approximately 3.4% of the transitional B cell pool in health but made up significantly more, over twice the as much, in lupus nephritis at approximately 7.3% (Table 3.2) ($p=0.049$).

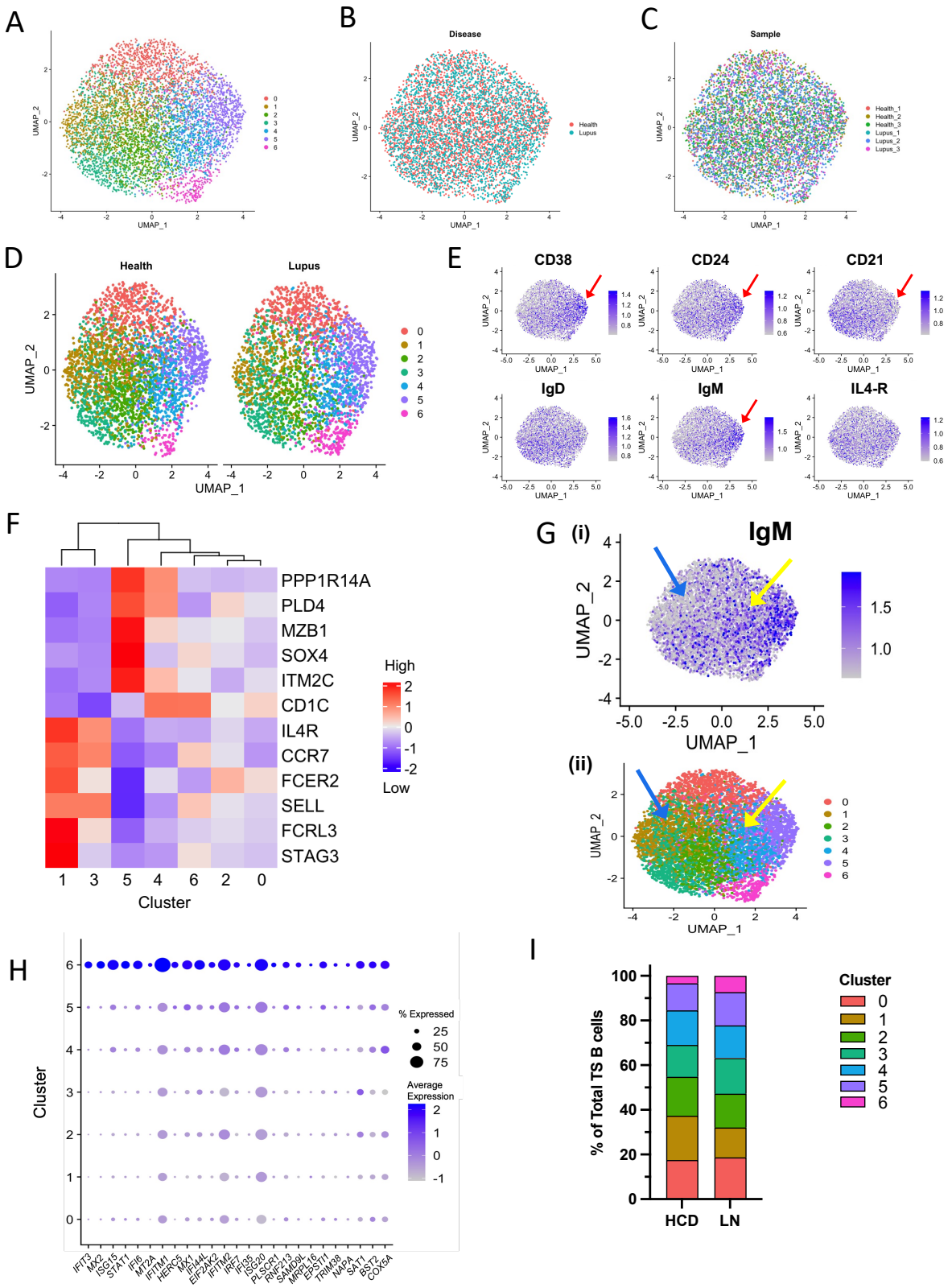

Figure 3.9: Classification of transitional B cells from healthy donors and lupus nephritis patients. (A) Seven clusters visualised on a UMAP plot generated from differentially expressed genes of transitional B cells from n=3 healthy control donors and n=3 lupus nephritis patients. **(B)** UMAP plot from panel A coloured by sample cohort. Cells from healthy

donors are in red and cells from lupus nephritis patients are in blue. **(C)** UMAP from panel A coloured by sample. **(D)** UMAP from panel A separated by sample cohort. **(E)** UMAP plot from panel A overlaid with surface protein expression of CD38, CD24, CD21, IgD, IgM and IL4-R. Colour scale indicates expression level whereby the darker purple dots represent higher expression level. Red arrows indicate region where cells have a T1 surface phenotype. **(F)** Heatmap comparing expression of typical transitional cell marker genes in transitional cell clusters outlined in UMAP from panel A. Colour scale indicates level of expression, with red being the highest expression and blue being the lowest. **(G) (i)** UMAP from panel A overlaid with average expression levels of surface IgM, from CITE-seq antibody staining. Blue arrow indicates region of UMAP where IgM expression is lowest and yellow arrow indicates region of higher IgM expression. **(ii)** UMAP displaying seven clusters of transitional cells from n=3 healthy donors and n=3 lupus nephritis patients. Blue arrow highlights cells from clusters 1 and 3 where IgM expression is lowest, and yellow arrow highlights cells from clusters 0, 2 and 4 where IgM expression is relatively higher. **(H)** Dot plot displaying average expression and percentage of expression of the top 25 positive conserved markers of cluster 6 across all seven transitional B cell clusters. Size of the dots represent percentage of cells within the cluster expressing a particular gene. The larger the dot, the greater the percentage of cells expressing the gene. Colour scale indicates level of average expression; dark blue represents highest average expression and light grey represents lowest average expression. **(I)** Bar chart showing size of each cluster as an average proportion of total transitional B cells in healthy control donors (HCD) compared to lupus nephritis patients (LN).

Table 3.2: Proportion of interferon-associated transitional B cells from healthy donors and lupus nephritis patients. Students t-test used to calculate statistical significance.

Sample	Number of Cells		% Of all TS B cells	Average %	p-value
	TS interferon cluster	Total TS cells			
Health 1	26	919	2.8292	3.3943	0.0490
Health 2	31	835	3.7126		
Health 3	54	1483	3.6413		
Lupus 1	30	795	3.7736	7.3031	
Lupus 2	142	1472	9.6467		
Lupus 3	50	589	8.4890		

To investigate the differences between the interferon-associated transitional cell populations module scoring was implemented. The module score function scores cells based on the gene expression of a group of defined gene markers. The greater the module score, the greater the expression of the gene "module" signature. An interferon module score was generated using the marker genes common to both the transitional naive blood interferon-associated cells from healthy donors. For a cell to score positive for this interferon module score, cells must express all genes together. The interferon score module was comprised of the following genes: *IFIMT1*, *IFITM2*, *IFITM3*, *MX1*, *IFI44L*, *ISG15*, *ISG20*, *IFI6*, *IFI35*, *IFIT2*, *BST2*, *HERC5*, *DRAP1*, *EIF2AK2*, *EPSTI1*, *STAT1*, *UBE2L6* and *XAF1*. The interferon score was overlaid onto a UMAP, as depicted in Figure 3.10A, where the greater the module score, the darker purple the dots on the UMAP. In both health and lupus nephritis, expectedly cluster 6 scored most highly for the interferon score across all samples (Figure 3.10B). However, it was evident that all transitional cells in lupus nephritis had a higher interferon score compared to the same transitional populations in health, as displaying in the violin plot in Figure 3.10C.

Despite the marked increase in expression of ISGs in the transitional cells from lupus nephritis compared to health, there is a clear group of interferon-associated transitional cells in health. To explore the differences between these interferon-associated transitional cells, the top differentially expressed genes between the B cells with an interferon signature in health and lupus populations were determined. As displayed in the heatmap in Figure 3.11, many of the top differentially expressed genes were ISGs, as expected due to the overall increase in ISG expression in lupus compared to health.

Overall, analysis of gene expression in transitional cells revealed an overall increase in ISG expression across all transitional cells in lupus nephritis patients compared to health. In addition to this, it was found that interferon-associated transitional cells from lupus nephritis patients have other non-ISG differentially expressed genes compared to the same group of cells found in healthy donors; for example, *CXCR4* and *PLD4*, that were increased in the subset of transitional B cells with an interferon

signature in lupus nephritis compared to health were of interest, as shown in Figure 3.11.

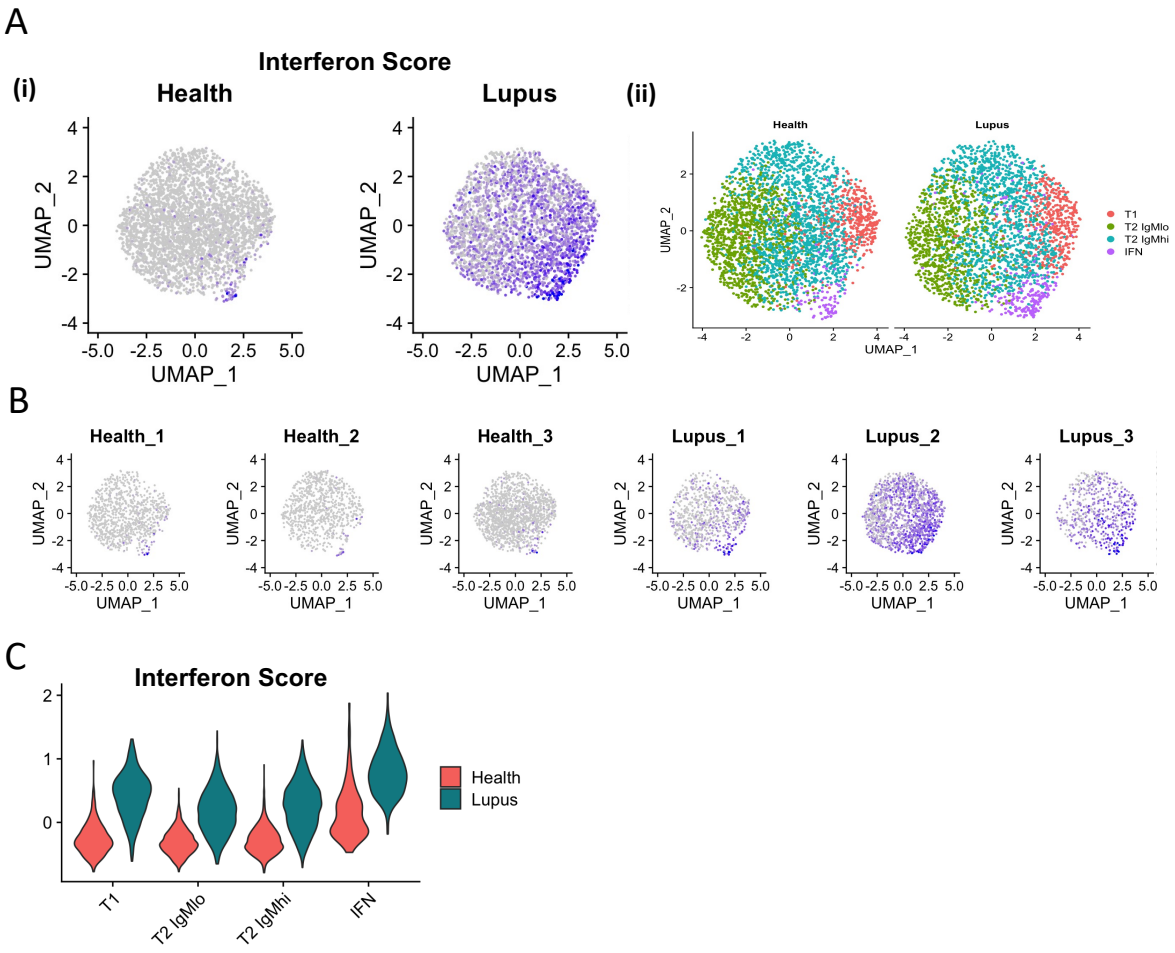

Figure 3.10: Interferon module scoring in transitional B cells from healthy donors and lupus nephritis patients. (A) (i) UMAP plot of clusters of transitional B cells from n=3 healthy donors and n=3 lupus nephritis patients overlaid with module score, termed interferon score. Score is based on the collective expression of the following genes: *IFIMT1*, *IFITM2*, *IFITM3*, *MX1*, *IFI44L*, *ISG15*, *ISG20*, *IFI6*, *IFI35*, *IFIT2*, *BST2*, *HERC5*, *DRAP1*, *EIF2AK2*, *EPSTI1*, *STAT1*, *UBE2L6* and *XAF1*. The higher the module score, the higher the expression of the module score genes. Highest interferon score is represented by dark purple dots, lowest expression is represented by light great dots. **(ii)** UMAP plots of classified transitional B cell clusters in from n=3 healthy donors and n=3 lupus nephritis patients. Purple cluster, termed IFN, aligns with highest module score in (i). **(B)** UMAPs displaying module score in panel A, separated by sample. **(C)** Violin plot comparing interferon module score between transitional B cell subsets: T1, T2 IgMlo, T2 IgMhi and the group of cells with an interferon gene signature (IFN). Scores from

n=3 healthy donors are shown in red and scores from n=3 lupus nephritis patients are shown in teal. Purple dotted line shows threshold for positive and negative module score.

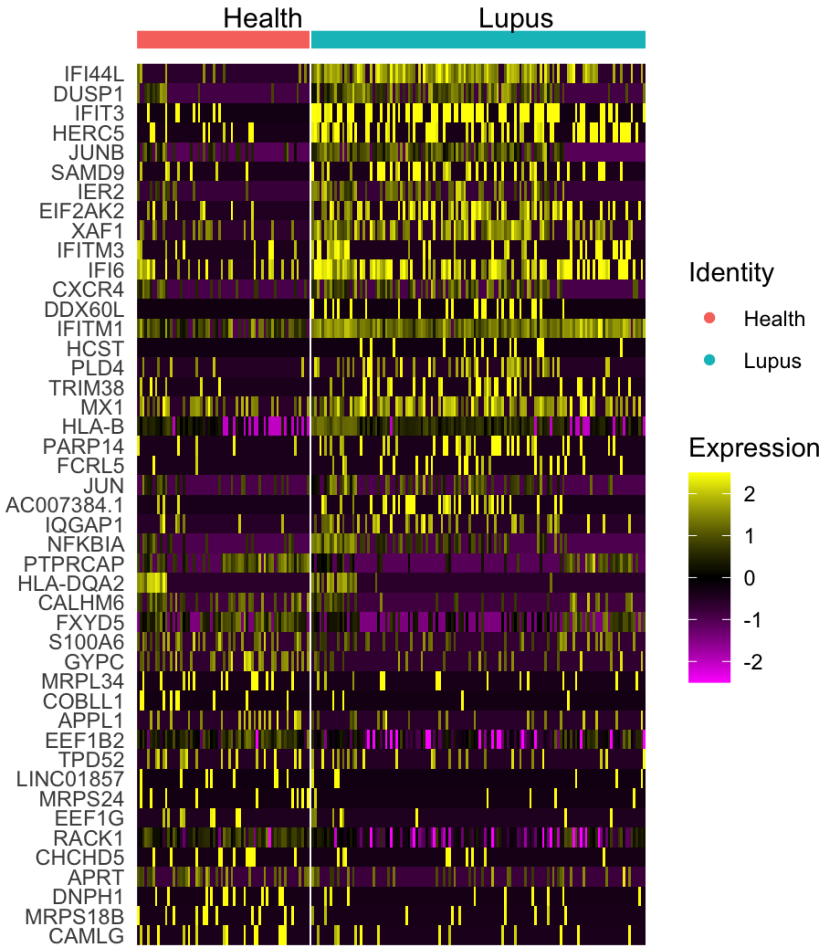

Figure 3.11: Differential gene expression in interferon-associated transitional B cells in lupus nephritis compared to health. Heatmap comparing 45 differentially expressed genes between transitional B cells with an interferon gene signature in health versus lupus nephritis. Expression levels are indicated by colour scale. Yellow denotes highest expression and pink denotes lowest expression.

3.3.7 ISGs expressed in all B cells in lupus nephritis

After identifying ISG patterns and differences in the transitional subset, naïve cells that are the other early B cell subset with an interferon-associated population in health were studied. The single-cell RNA-sequencing dataset from total CD19+ B cells from n=3 healthy donors and n=3 lupus nephritis patients was filtered according to the pipeline outlined in Figures 3.1 and 3.7. CD19+ B cells were tagged with HTO-AHH1-TotalSeqC hashtag antibody and so cells above the threshold for this antibody were selected, then filtered to remove doublets and dying cells. The same clustering shown in three healthy donors (Figure 3.5A) was replicated with the addition of three lupus nephritis samples. The module score function was used to generate an interferon score and compare the expression of marker ISGs; the same ISGs used to generate an interferon score in the transitional dataset analysis were used for total CD19+ dataset.

Module scoring for ISGs demonstrated a widespread increase in ISGs across all B cells in lupus nephritis compared to health, as shown in Figure 3.12A. The increase in expression of ISGs was seen in all lupus samples (Figure 3.12B). In comparison, in healthy samples, only the interferon-associated naïve cells, previously identified as cluster 13 in 3.3.4, scored positively for the interferon score, shown in Figures 3.12A and 3.12B. Cluster 13 on the lupus samples (shown in Figure 3.12C) scored the highest interferon module score compared to the other lupus B cells, demonstrating the strong interferon gene signature seen within the naïve pool. As with the transitional cells, the group of naïve interferon cells was relatively small in comparison to the whole B cell pool; in lupus nephritis, this group of cells represented approximately 5% of all B cells, in comparison to health in which is represented approximately 2% (Table 3.3).

Comparisons between the interferon-associated naïve populations between health and lupus patients were made by finding differentially expressed gene markers, shown in the heatmap in Figure 3.12D. Naïve interferon cells from lupus patients expressed higher levels of ISGs compared to health, as expected, but also expressed higher levels of *CXCR4*, as observed in transitional B cells, as well as *CD69*, *JUN*, and *CD83*.

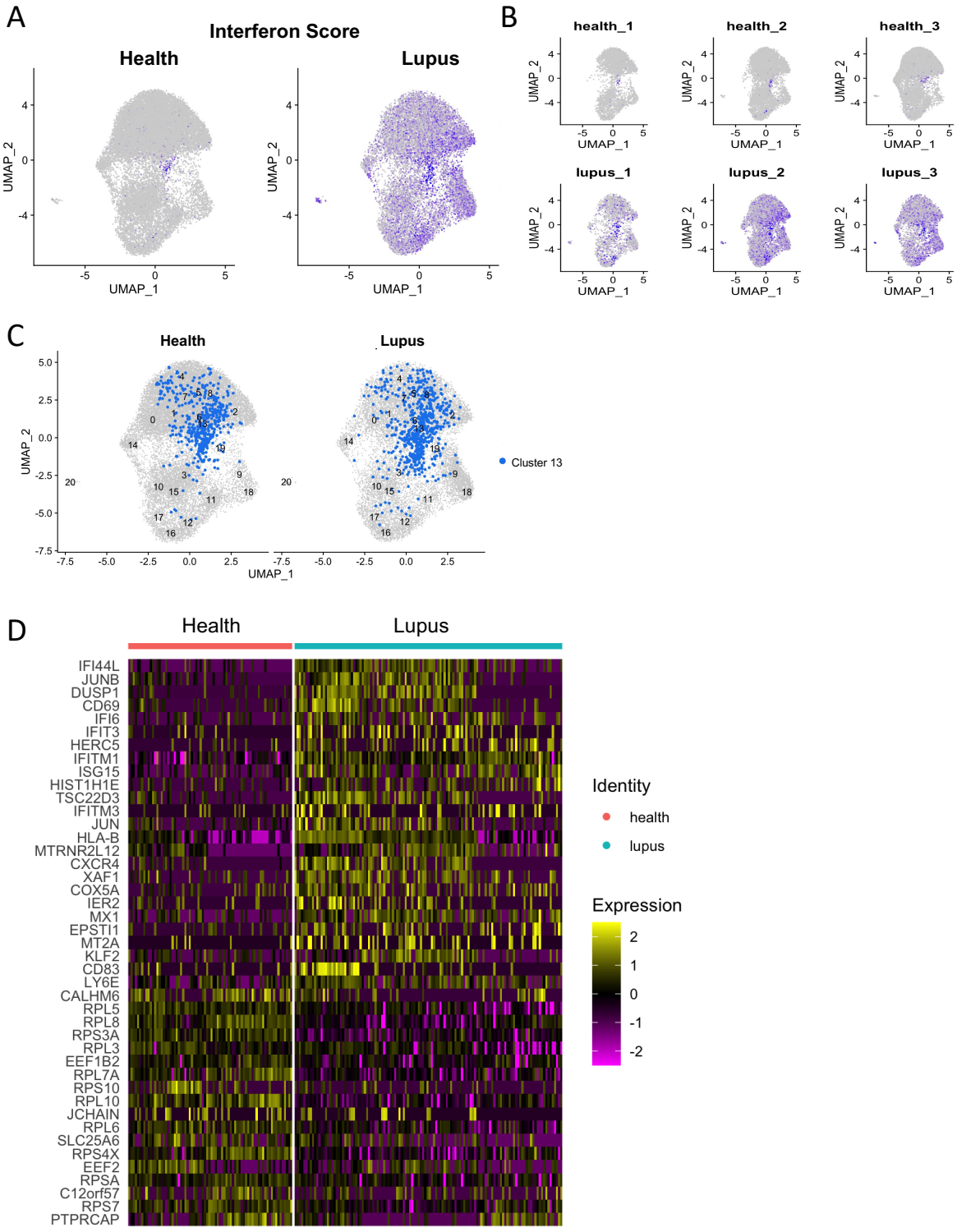

Figure 3.12: Interferon-associated naïve cells in lupus nephritis. (A) UMAP plots displaying module score on CD19+ B cells from n=3 healthy donors and n=3 lupus nephritis patients, respectively. Module score is based on the collective expression of the following genes: *IFIMT1*, *IFITM2*, *IFITM3*, *MX1*, *IFI44L*, *ISG15*, *ISG20*, *IFI6*, *IFI35*, *IFIT2*, *BST2*, *HERC5*, *DRAP1*, *EIF2AK2*, *EPSTI1*, *STAT1*, *UBE2L6* and *XAF1*. The higher the module score, the higher the

expression of the module score genes. Highest interferon score is represented by dark purple dots, lowest expression is represented by light great dots. **(B)** UMAP plots displaying module score from panel A, separated by sample. **(C)** UMAP plots of CD19+ B cells highlighting naïve cluster 13 in health and lupus nephritis, respectively. **(D)** Heatmap comparing differentially expressed genItween naive B cells with an interferon gene signature in health versus lupus nephritis. Expression levels are indicated by colour scale. Yellow denotes highest expression and pink denotes lowest expression.

Table 3.3: Proportion of interferon-associated naïve B cells from healthy donors and lupus nephritis patients. Students t-test used to calculate statistical significance.

Sample	Number of Cells		% of all CD19+ B cells	Average %	p-value
	Naïve interferon cluster	Total CD19+ cells			
Health 1	107	3850	2.7792	2.2954	0.002
Health 2	147	6678	2.2012		
Health 3	210	11019	1.9058		
Lupus 1	126	2486	5.0684	4.6598	
Lupus 2	302	6717	4.4961		
Lupus 3	209	4734	4.4149		

3.4 Chapter 3 Summary

A summary of the key findings from this chapter is presented in Figure 3.13. The results presented in this chapter have demonstrated the expression of an interferon gene signature in antigen-inexperienced B cells in peripheral blood (Figure 3.13A). Whilst the expression of these genes is greater in B cells from lupus nephritis patients, the gene signature is present in B cells from healthy donors (Figure 3.13B).

A

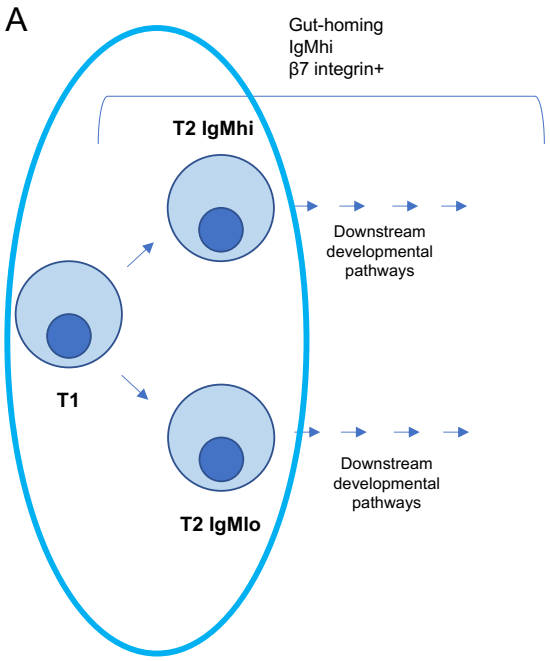

B

Gene	Average log2FC (Lupus Nephritis n=3)	Adjusted p-value (Lupus Nephritis n=3)	Average log2FC (Health n=3)	Adjusted p-value (Health n=3)
IFIT3	1.8540	0.0000	1.1767	0.0000
MX2	1.5434	0.0000	1.8960	0.0000
IFITM1	1.1947	0.0000	2.3949	0.0000
STAT1	1.4539	0.0000	1.6534	0.0000
ISG15	1.4629	0.0000	1.9119	0.0000
IFI6	1.2934	0.0000	1.6971	0.0000
MX1	0.7966	0.0000	1.6100	0.0000
HERC5	1.1018	0.0000	1.0282	0.0000
IFI44L	0.7953	0.0000	1.3344	0.0000
MT2A	1.2007	0.0000	0.9707	0.0000
EPSTI1	0.4995	0.0431	1.1134	0.0000
IFITM2	0.6020	0.0000	0.5036	1.0000
TAGLN2	-0.6129	0.0002	-0.6849	0.4974
ISG20	0.5520	0.0003	0.4333	1.0000
SAT1	0.4837	1.0000	0.8596	0.0003
PLSCR1	0.5493	1.0000	1.0513	0.0009
NFKBIA	-0.6400	0.0011	-0.6585	1.0000
XAF1	0.4589	0.3649	0.9230	0.0028
EIF2AK2	0.6132	0.0589	0.6756	1.0000
MYC	-0.8656	0.1475	-0.2537	1.0000
JUN	-0.5456	0.1612	-0.7607	1.0000
MAP3K8	-0.7354	0.4120	-0.2730	1.0000
LY6E	0.3719	1.0000	0.7180	0.6024
SAMD9L	0.5366	0.7992	0.6324	1.0000
COX5A	0.4672	0.9160	0.2659	1.0000
UCP2	-0.4238	1.0000	-0.3257	1.0000
IRF7	0.5718	1.0000	0.7856	1.0000
BST2	0.4770	1.0000	0.2657	1.0000
IFI35	0.5670	1.0000	0.7244	1.0000
EEF1A1	-0.2667	1.0000	-0.2930	1.0000

Figure 3.13: Summary of Chapter 3. (A) Schematic diagram highlighting the earliest subsets of B cells in the peripheral blood (transitional B cells) where an interferon gene signature was identified through analysis of single-cell RNA-sequencing data. **(B)** Table of the top 30 gene markers of the transitional B cells with an interferon gene signature common to both lupus nephritis patients and healthy donors.

3.5 Discussion

This study has demonstrated the heterogeneity of peripheral blood transitional B cells and has highlighted the presence of early B cells with an interferon gene signature in healthy donors and lupus nephritis patients through analysis of single-cell RNA-sequencing data. The induction of ISG expression has been long associated with an anti-viral response (Katze et al., 2002) and autoimmune diseases (Bennett et al., 2003), however ISGs in immature transitional B cells in healthy human blood are not well described. As ISG expression occurs upon interferon exposure and subsequent signalling (Der et al., 1998; Schoggins and Rice, 2011), it was interesting to find ISG expression in early B cells which have recently emerged from the bone marrow.

As demonstrated in 3.3.1, 3.3.2 and 3.3.5, pre-processing and quality control steps are key to generating good quality datasets for successful downstream analysis. The number of clusters to be analysed is set by the experimenter and can be considered somewhat arbitrary. To ensure only CD10+ transitional B cells were used for differential gene expression analysis, the initial clustering of all CD10+ B cells, stained with HTO-AAH2-TotalSeqC (hash 2), were clustered using a resolution of 0.75. This resolution allowed for enough clusters to be made so that any prominent differences between cells could be seen clearly. For example, as shown in Figure 3.2A, two distinct islands of cells were generated. As transitional cells are a single subset of B cells with a similar genetic profile in comparison to other B cell subsets, it is expected that transitional cells would cluster very closely together. A lower resolution would have resulted in few clusters and poorer separation of cells when projected on the UMAP and so any differences would have been more difficult to identify. A higher resolution would have resulted in a good separation but a much higher number of clusters which would have made the quality control protocol far less streamlined.

It is well-established that transitional B cells progress from the T1 stage to a T2 stage and this can be tracked through the gradual loss of surface CD38 and CD24 (Palanichamy et al., 2009; Sims et al., 2005) and the increase in CD21 expression (Suryani et al., 2010). More recently, the T2 population has been further sub-

categorised based on surface expression of IgM into T2 IgMhi and T2 IgMlo and it was noted that IgMhi and IgMlo transitional B cells have several differentially expressed genes, shown in Table 2.1 in Materials and Methods (Tull et al., 2021). In this study, additional differentially expressed genes between T2 IgMhi and T2 IgMlo cells were identified, shown in Table 3.1. It was noted that T2 IgMhi cells expressed genes belonging to the FOS-JUN family more than 1.5-times that of T2 IgMlo cells. Furthermore, T2 IgMhi cells could be distinguished from T2 IgMlo cells based on greater expression of chemokine *CXCR4* and ISG *IFITM1* and lower expression of Fc receptor-like gene *FCRL3*. FCRL3 expression in B cells has been found to enhance TLR9-mediated B cell proliferation and activation (Li et al., 2013). This suggests that the IgMlo B cells may be those that are activated through FCRL3-TLR9 interactions more so than IgMhi cells.

Whilst classifying clusters into known transitional populations two clusters with distinct gene signatures were observed that made up each of the IgMhi and IgMlo T2 sub-populations. Clusters 0 and 4 were the IgMhi clusters. Differential gene expression analysis of T2 IgMhi clusters showed that cluster 0 expressed genes associated with interferon stimulation (*IFITM1*) and regulation (*IRF1*) as well as oncogene *MYC* at a level 1.4-times greater than that of cluster 4 suggesting that cells in cluster 0 may have encountered an interferon rich microenvironment and/or have been activated. In contrast, cells belonging to cluster 0 had far lower expression of genes associated with early, immature B cells such as *IGLL5* and *VPREB1*, suggesting that cluster 4 is more immature since they retain genes encoding pre-B cell receptor that is expressed during B cell development (Nishimoto et al., 1991). Clusters 1 and 3 were the T2 IgMlo clusters. Cluster 1 has significantly lower expression of *VPREB1*, *PPP1R14A* and *SOX4* compared to cluster 3 suggesting that cluster 3 is more immature. In future studies, it would be interesting to explore concepts of early B cell development through gene trajectory analysis, whereby the changes in gene expression can be mapped across clusters to show how one cluster of cells leads to another, using packages such as Slingshot or Monocle (van den Berge et al., 2020).

Whilst to our knowledge subsets of transitional and naïve B cells with a signature of interferon regulated genes has not been described in blood before. Siu et al (2022) reported a population of 'activated' B cells that they termed AcB4, from the appendix, mesenteric lymph node and spleen of three healthy cadaver donors with an interferon gene signature. This group of cells was identified through analysis of single-cell RNA-sequencing data and was found to express ISGs such as *MX1*. Whilst the genes reported to identify this cluster did not include those associated with naïve or transitional B cells, they did tend to occupy and area of the UMAP that was CD27-IgD+, suggesting that they could be naïve. This suggests that the interferon-associated CD27-IgD+ B cells from peripheral blood described in this study could be present in secondary lymphoid tissues.

ISGs are known to be expressed in B cells from patients with SLE (Bennett et al., 2003; El-Sherbiny et al., 2018) and type I IFNs have been found to promote the survival of transitional B cells from lupus patients (Liu et al., 2019). IFITM genes were some of the first anti-viral ISGs to be described (Friedman et al., 1984) and IFITM1, also known as Leu-13, has been associated with B cell receptor signalling, specifically with the CD19/CD21/CD81(TAPA-1) complex (Matsumoto et al., 1991). The significance of *IFITM1* expression in transitional and naïve B cells is yet to be fully understood. It is possible that it could provide some resistance of early B cells to infection (Wu et al., 2018).

Interferon has often been identified as a distinguishing feature of not only transitional B cells, but on B cells generally in SLE. For instance, using ISG scoring generated by factor analysis, both naïve and memory B cells from SLE patients have been found to express a group of ISGs, which include *MX1*, *BST2*, *IFI16*, *STAT1* and *TRIM38*, at a significantly greater level ($p<0.05$) than the same populations in healthy donors (El-Sherbiny et al., 2018). Data from this study also identified the presence of ISGs in a group of naïve B cells in the lupus nephritis cohort, which accounted for 5% of all B cells.

Whilst the interferon-associated tItional and naive B cells in health and lupus nephritis samples expressed similar interferon-stimulated marker genes, some interesting significant differential gene expression patterns were observed when the clusters with interferon signatures in health were compared to those observed in lupus nephritis. For example, *CXCR4* and *PLD4*, a known lupus risk allele (Terao et al., 2013), were found to be expressed at a higher level in interferon-associated transitional cells from lupus nephritis patients compared to those of healthy donors. Both *CXCR4* and *PLD4* have been established as markers of IgMhi transitional cells in this study and by Tull et al. (2021), respectively. This suggests that possibly the group of transitional cells with an interferon gene signature may be more IgMhi-like in lupus nephritis compared to health. CXCR4, in conjunction with its ligand CXCL12, plays a role in maintaining cells within the bone marrow (Nie et al., 2008) and facilitates organisation of the dark zone of germinal centres (Allen et al., 2004). Additionally, CXCR4 overexpression in all B cells has been found to correlate with SLE disease severity and the likelihood of renal involvement (Zhao et al., 2017). This suggests that the higher expression of CXCR4 seen in the transitional and naïve cells with an interferon signature in the lupus samples in this study may be a feature of nephritis as opposed to being a feature of the interferon-associated cells. Therefore, this warrants further investigation into the expression of CXCR4 in all B cell subsets in a larger cohort of lupus nephritis patients.

Naïve cells with an interferon gene signature in lupus nephritis expressed higher levels of activation markers *CD69* and *CD83,* compared to naïve B cells with an interferon signature in health. The higher expression of activation markers and stronger interferon gene signature suggests that this group of cells are more activated in lupus nephritis compared to the equivalent group of cells in health. Additionally, there was marked low expression of ribosomal genes and eukaryotic elongation factor genes in lupus nephritis compared to health. This may suggest that these interferon-associated naïve cells in lupus nephritis may have altered protein synthesis functions.

To conclude, this analysis of single-cell RNA-sequencing data from transitional and naïve B cells has shown heterogeneity within the earliest peripheral blood B cell subset in health and has identified groups of early B cells with interferon gene signatures.

Similar groups of transitional and naïve cells with an interferon gene signature were also identified in the peripheral blood of lupus nephritis patients at approximately twice the abundance of that in health. Whilst these cells can be characterised by the expression of genes such as *IFITM1*, *MX1* and *IFI44L*, there are notable gene expression differences between these populations in lupus compared to health.

4 Investigation of B cell subsets expressing interferon markers

4.1 Introduction

As outlined in Chapter 3, clusters of transitional and naïve B cells in a dataset derived from single-cell RNA-sequencing were found to have a strong interferon gene signature. These cells were identified in a small cohort of healthy donor samples (n=3) lupus nephritis patient samples (n=3). Therefore, it was important to increase the cohort size to firstly see if these cells are present in a greater number of individuals and secondly, to use a larger panel of surface protein markers to subdivide peripheral blood B cells into subsets. Here, mass cytometry was used to explore the expression of some proteins whose genes were identified as features of early, interferon-associated B cells in healthy donors and lupus nephritis patients.

Markers included in the mass cytometry panel for this study because they were identified as conserved gene markers for the group of transitional and naïve cells that had an interferon gene signature and these markers included IFITM1, MX1, BST2 and IRF7. In chapter 3, IFITM1 was consistently in the top ten conserved marker genes for transitional and naive cells with an interferon signature, thus it was of interest at the protein level. IFITM1 has been linked to B cell receptor signalling, specifically with the CD19/CD21/CD81(TAPA-1) complex (Matsumoto et al., 1991) and has also been found to be expressed in human embryonic stem cells (ESCs) and may be part of an intrinsic anti-viral programme in stem cells (Wu et al., 2018). As this study is focused on the earliest peripheral B cells, which have newly emerged from the bone marrow, the potential role of IFITM1 in their stem cell precursors makes this marker a protein of interest.

Another conserved marker gene of early B cells with an interferon gene signature was the anti-viral MX1, which has previously been associated with multiple cell types in SLE. Becker et al. (2013) found that expression of MX1 in B cells increases with increasing SLE severity and correlates with SLEDAI score. Lupus nephritis is the most severe manifestation of SLE and so MX1 expression in this cohort of patients was investigated in this study.

BST2, also known as tetherin, was first described in the context of HIV and its ability to inhibit retroviral release from cells (Neil et al., 2008), but it has since been associated with SLE. It was found that expression of BST2 on memory B cells measured by flow cytometry had a strong relationship with SLE disease activity and has the potential for use as a SLE biomarker (El-Sherbiny et al., 2020). Additionally, El-Sherbiny et al. (2020) have also described the expression of BST2 on naïve cells and therefore it would be of interest to explore BST2 expression in our smaller sub-populations of transitional B cells at the protein level.

IRF7 is an interferon-regulatory protein first identified as being associated with Epstein-Barr Virus latency (Zhang & Pagano, 1997) and is now known to regulate type I interferon responses, which are known to have a role in SLE pathogenesis (Au et al., 1998; Honda et al., 2005). Additionally, several single nucleotide polymorphisms in the IRF7 gene have been associated with SLE (Xu et al., 2012). Thus, investigation of IRF7 expression across B cell subsets in health and lupus nephritis may give an indication as to which subsets undergo the greatest interferon regulation.

Additionally, CXCR4, CD83 and CD69 expression was also investigated in this study as these markers were previously found to be top differentially expressed genes when comparing gene expression in B cells with an interferon gene signature between lupus nephritis and healthy donor cohorts. CXCR4 expression in B cells has previously been found to correlate with SLEDAI scoring and kidney involvement in SLE (Zhao et al., 2017). Therefore, it would be of interest to determine which subset of B cells expression of CXCR4 is greatest in and whether this differs between health and lupus nephritis. Furthermore, CD83 and CD69 are markers of B cell activation and so investigating the expression of these markers at the protein level would provide some insight as to whether any B cell subsets in lupus nephritis are differentially activated compared to the same subsets in health.

4.2 Aims

- To use a larger panel of surface markers to subdivide B cells into peripheral B cell subsets and explore features of interferon-associated genes expressed by early B cells
- To explore further markers that discriminated between early B cells with an interferon gene signature in health compared to lupus nephritis

4.3 Results

4.3.1 Pre-processing mass cytometry data

Mass cytometry was used to investigate surface protein marker expression of peripheral blood B cells from healthy donors (n=9) and lupus nephritis patients (n=9). PBMC were stained with a panel of 35 markers (outlined in Table 2.2 in Chapter 2, Materials and Methods). PBMC were used as opposed to sorted or enriched CD19+ B cells as this allowed for a larger cell pellet that enhanced cell viability throughout all stages of the staining protocol. Stained PBMC were run on a Helios™ mass cytometer.

The premessa package (https://github.com/ParkerICI/premessa) was run in R and used for bead selection, data normalisation, concatenation, and bead removal. Firstly, the EQ™ calibration beads used to set up the mass cytometer had to be identified to allow for normalisation of .fcs data files. The beads were selected by plotting iridium (Ir193Di), which was used as a cell identification marker due to its DNA intercalating properties, against each of the different calibration beads. As shown by the red gates in Figure 4.1A, beads were selected as data points that were positive for bead metals (between 6-8 along the x-axis) and had low iridium (4 or less on the y-axis). Low iridium indicates a lack of DNA intercalation, thus those datapoints are unlikely to be cellular. This gating process was repeated for all health and lupus nephritis samples then normalisation was run. Normalisation was essential for comparisons between samples to be made, as samples were run on multiple days. As shown in Figure 4.1B, bead intensities were within a smaller range across all data files after normalisation compared to before normalisation. Data files from one sample were concatenated using the premessa concatenation tool as the data was saved onto two .fcs files.

After beads were used to normalise all samples and prior to uploading data into Cytobank, bead data points were removed from the .fcs files to ensure that all data to be analysed were only cells. Using the premessa package, data were visualised on scatterplots generated by plotting bead metals against each other and were colour-coded according to "bead distance", shown in Figure 4.1C. Bead distance indicates how far away a data point is plotted from a representative data point that is known to be a true bead; therefore, the smaller the bead distance the closer that data point is to a true bead value. A bead distance threshold cut-off value was determined by identifying the bead distance value in which all beads were below the threshold, and all cells were above it. For example, as indicated by the red arrows in Figure 4.1C, bead distance thresholds between 13-15 were set to allow all beads, shown in red boxes, to be removed from the dataset and all cells to be kept.

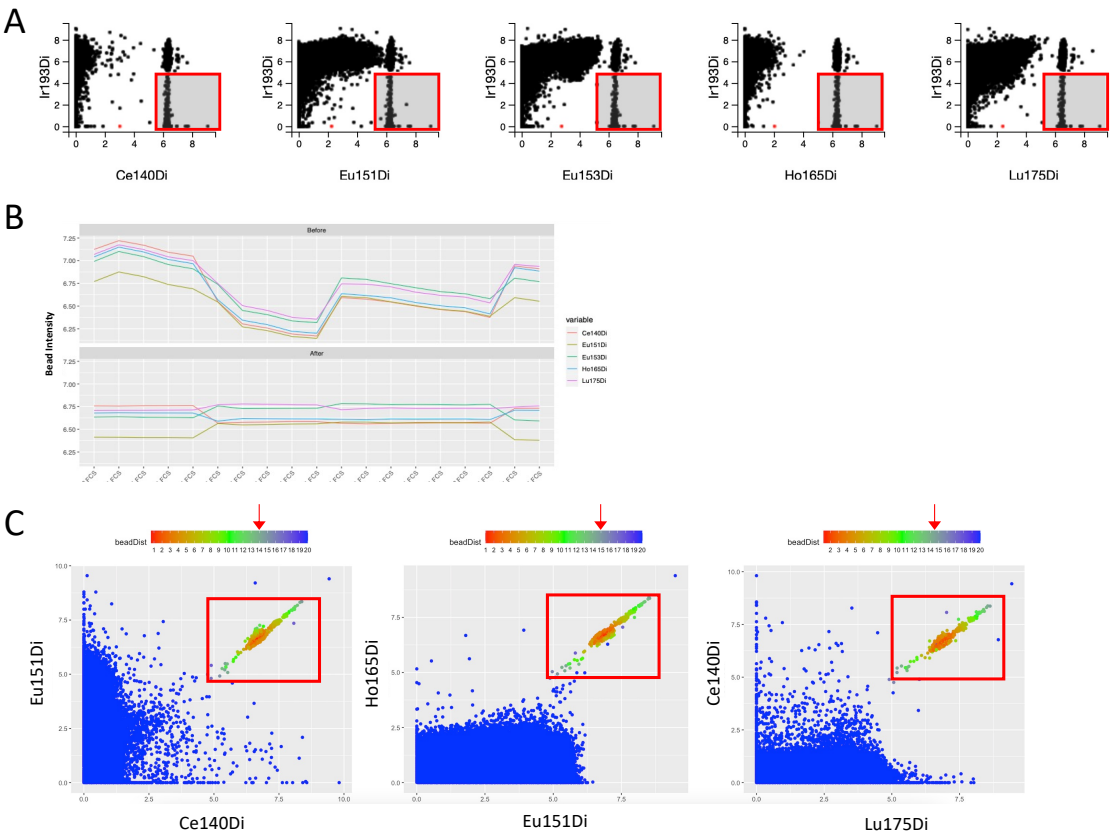

Figure 4.1: Pre-processing and gating B cells from mass cytometry data. (A) Scatterplots displaying pre-normalised events (cells and beads) generated by mass cytometry of PBMCs from healthy donors (n=9) and lupus nephritis patients (n=9). Each scatterplot shows calibration beads (Ce140Di, Eu151Di, Eu153Di, Ho165Di and Lu175Di) plotted against cell identification maker, iridium (Ir193Di). Red boxes indicate bead selection gates used prior to

data normalisation. **(B)** Plot displaying bead intensities before and after bead-based normalisation across all .fcs files**. (C)** Scatterplots displaying normalised events generated by mass cytometry of PBMCs from healthy donors and lupus nephritis patients. Axes are beads embedded with metals. Dots are colour-coded according to bead distance (beadDist). The smaller the beast distance the closer the event is to a true bead. True beads are double positive for bead metals. Bead distance is indicated by a colour scale with red being the smallest bead distance and blue being the largest. Bead distance thresholds (indicated by red arrows) were set to filter out beads from the rest of the events (cells). Bead events that were removed are highlighted in red boxes. Panels **A-C** are from a representative healthy donor.

Normalised data files containing data from only cells were uploaded to Cytobank and then live, in-tact CD19+ B cells were gated for using the gating strategy shown in Figure 4.2. First, in-tact cells were selected as the events that were appropriate length and were positive for iridium, as shown in Figure 4.2(i). Second, live cells were gated by selecting events that were low for cisplatin viability stain, demonstrated in Figure 4.2(ii). Cisplatin was used as a viability stain due to its ability to preferentially bind non-viable cells (Fienberg et al., 2012). Next, additional "clean-up" gates were used to ensure any outlier events were removed, as depicted in Figures 4.2(iv)-(vi). Finally, as shown in Figure 4.2(vii), CD19+ B cells were gated. The same gating strategy was repeated for all health and lupus nephritis samples. The data were then used in downstream analysis.

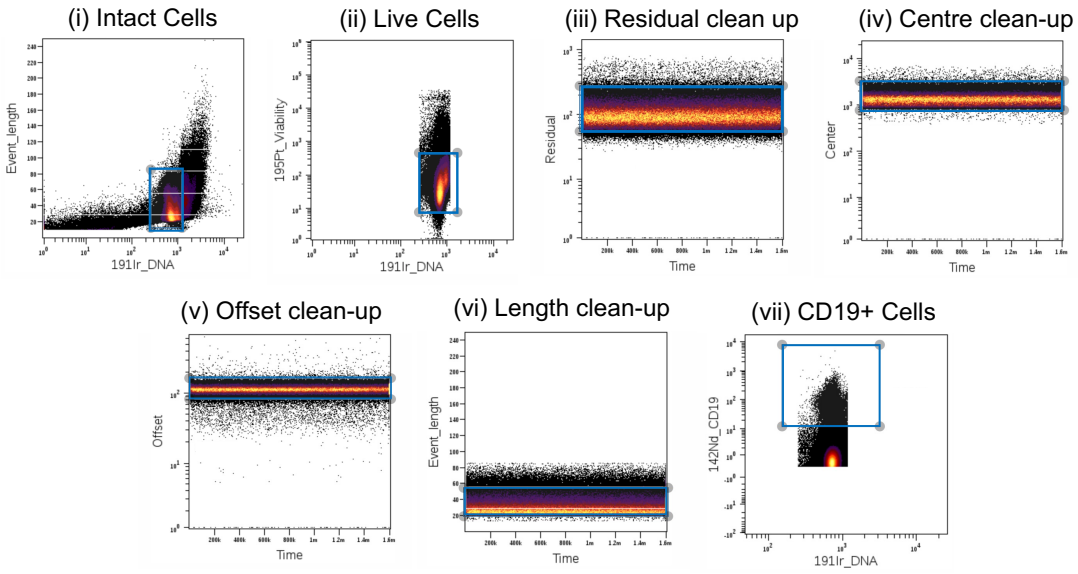

Figure 4.2: Gating strategy to identify viable CD19+ B cells from normalised mass cytometry data. Scatterplots showing gating strategy used to select CD19+ B cells from normalised mass cytometry data. Gating was performed using a gating editor in Cytobank software. (i) Gating for intact cells using event length and iridium (191Ir_DNA). (ii) Gating live cells using cisplatin (195Pt_Viability) and iridium. (iii) Gating to remove residual outliers. (iv) Gating to remove centre outliers. (v) gating to remove offset outliers. (vi) Gating to remove event length outliers. (vii) Gating to select CD19+ B cells.

4.3.2 Classification of peripheral B cell subsets using viSNE and SPADE

To begin the process of classifying CD19+ cells into peripheral blood B cell subsets, a high-dimensionality visualisation tool known as viSNE was used. viSNE uses the t-Distributed Stochastic Neighbour Embedding (t-SNE) algorithm and allows for the 2D visualisation of data at a single-cell resolution whilst keeping local and global differences within the data recognisable (Amir et al., 2013). Equal sampling of CD19+ events (n=5,555) from all health and lupus nephritis samples (n=18) were used to run the viSNE. The following nine B cell lineage markers were used to generate the viSNE map: CD27, IgD, IgA, CD10, CD38, CD24, CD21, IgM and CD45RB. These markers were selected so data events were placed based on only these known subset markers. The rest of the markers included in the panel therefore would remain undirected and would not influence the distribution of cells on the viSNE. The viSNE maps were visualised for each sample separately, as shown in Figures 4.3A (representative healthy donor) and 4.3B (representative lupus nephritis patient). Once the viSNE had been run, the viSNE coordinates, tSNE1 and tSNE2, were used to generate SPADE trees.

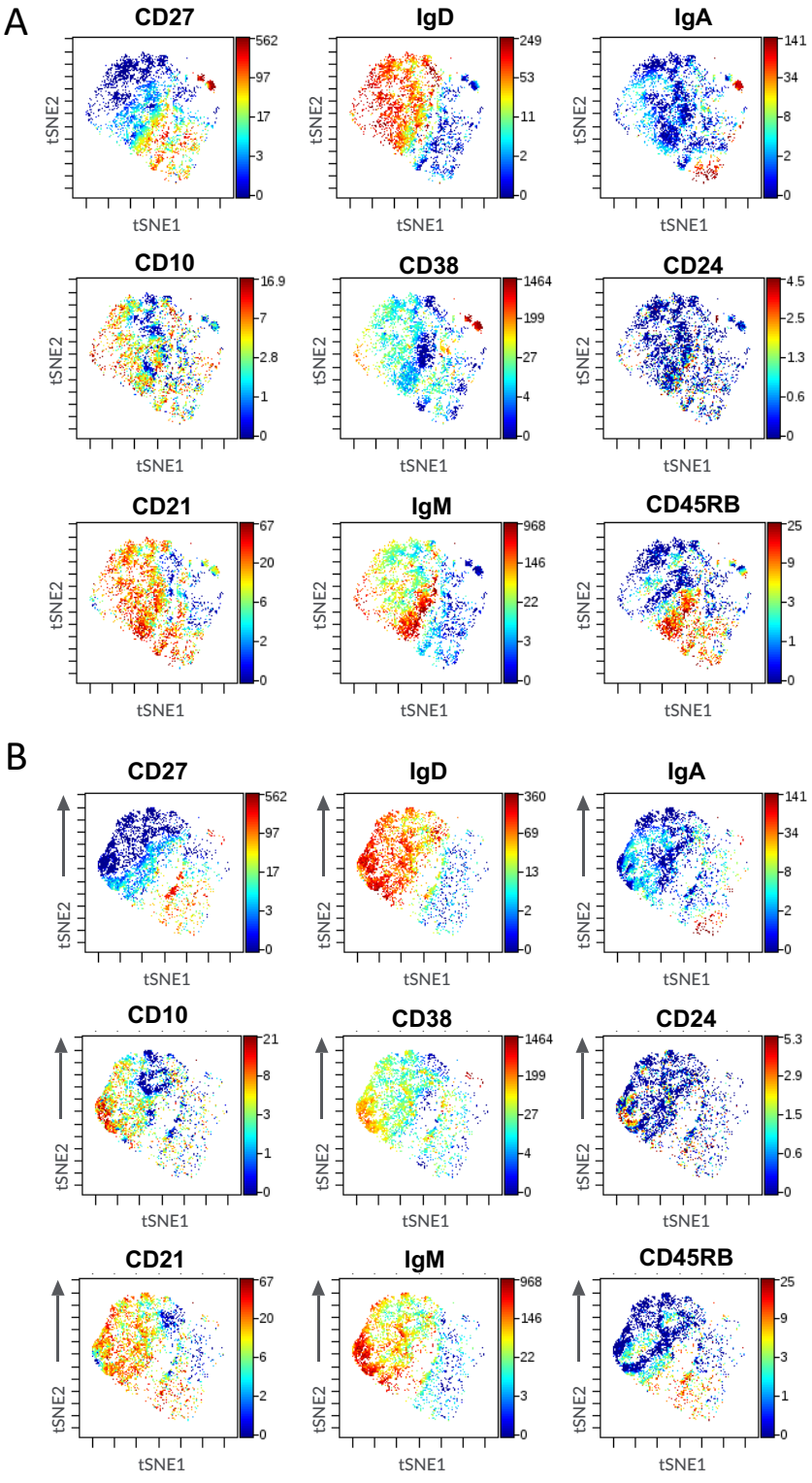

Figure 4.3: viSNE maps of B cell lineage markers in health and lupus nephritis. viSNE maps of CD19+ B cells generated from mass cytometry data using B cell lineage markers CD27, igD, IgA, CD10, CD38, CD24, CD21, IgM and CD45RB. Each viSNE is overlaid with a respective lineage marker expression. Colour scale indicates level of expression with red being the

highest and blue being the lowest. viSNE maps from **(A)** are from a representative healthy donor and viSNE maps from **(B)** are from a representative lupus nephritis patient.

To subdivide CD19+ B cells into subsets, viSNE coordinates were used to generate SPADE trees. SPADE is a computational method used to enable the exploration of cellular heterogeneity, identification of cell types and the comparison of marker expression (Qiu et al., 2011). SPADE trees are made up of a web of connected nodes, which comprise groups of similar cells. Nodes vary in size according to how many cells are present within the node. Additionally, nodes can be colour-coded according to marker expression.

Healthy donor samples were used to group nodes into "bubbles", which represented B cell subsets. Nodes were grouped following the same gating strategy principle used in flow cytometry, shown in Figure 4.4. Plasmablasts were gated as CD27+++CD38+++, then CD27 and IgD were used to broadly categorise nodes into: CD27-IgD+ cells, comprising transitional, naïve, aNAV, and marginal zone precursor subsets, CD27-IgD- double negative B cells, CD27+ IgD+ marginal zone cells and CD27+IgD- memory cells. Further subdivision of these four subsets was achieved by following the step-by-step process outlined in Figure 4.5A and resulted in classifications of twelve peripheral blood B cell subsets, shown in Figure 4.5B. Representative SPADE plots from a healthy donor overlaid with expression levels of key B cell markers is shown in Figure 4.6.

Due to the larger panel used for mass cytometry, additional markers, such as IgA, CD11c, CXCR5, CD1c, CCR7 and integrin β7 were able to be used to classify additional groups of cells and aid gating of subsets. For example, IgA was used to identify a sub-population of memory B cells that had undergone class-switching to become IgA+ memory cells. The distribution of the rest of these markers were of particular interest because they were note used in the viSNE clustering and so their distribution is not directed. CD11c and CXCR5 were used classify aNAV and DN2 subsets, which are CD11c+CXCR5-. Positive CD1c expression was used to confirm classification of marginal zone cells and their precursors. The marginal zone subset was sub-divided

into MZB1 and MZB2 based on differing expression levels of CCR7 and integrin β_7 (see Chapter 6).

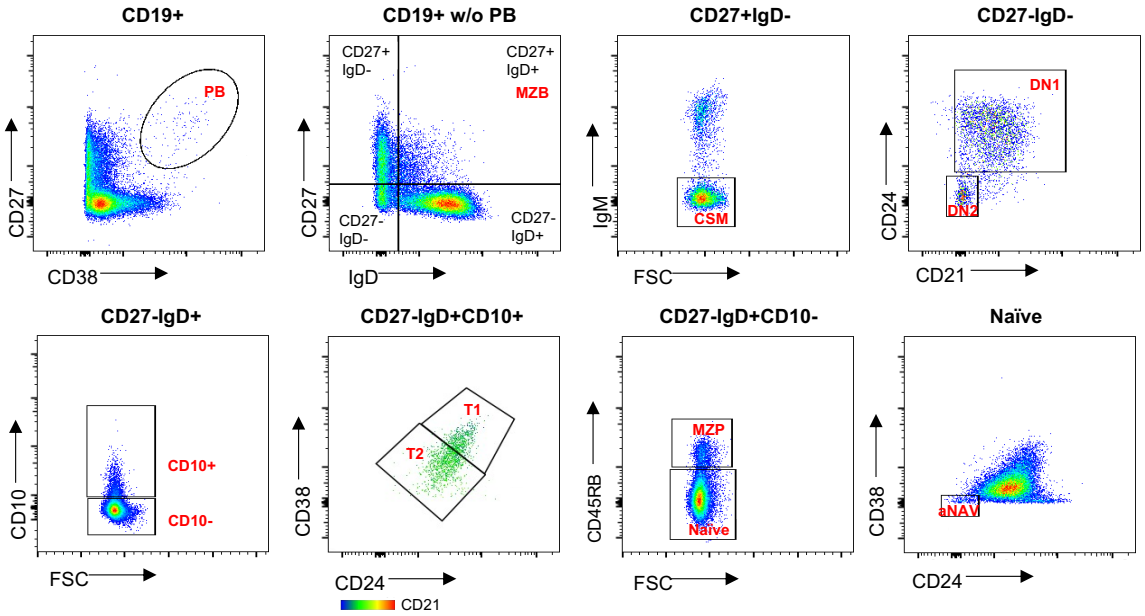

Figure 4.4: Gating strategy to identify B cell subsets from peripheral blood. Dot plots generated from flow cytometry of peripheral blood CD19+ B cells from a representative healthy donor. Plasmablasts (PB) are classified as CD27+++CD38+++. Marginal zone cells (MZB) are classed as CD27+IgD+. Class-switched memory B cells (CSM) are classed as CD27+IgD-IgM-. Double negative B cells are classified as CD27-IgD- and further divided into DN1 and DN2 based on CD21 and CD24. Transitional cells are CD27-IgD+CD10+; T1 are distinguished from T2 based on higher expression of CD38 and CD24, and lower expression of CD21. Naïve cells are CD27-IgD+CD10-CD45RB-CD38+CD24+ and marginal zone precursors are CD27-IgD+CD10-CD45RB+. Within the naïve gate, activated naïve (aNAV) can be identified based on low expression of CD38 and CD24.

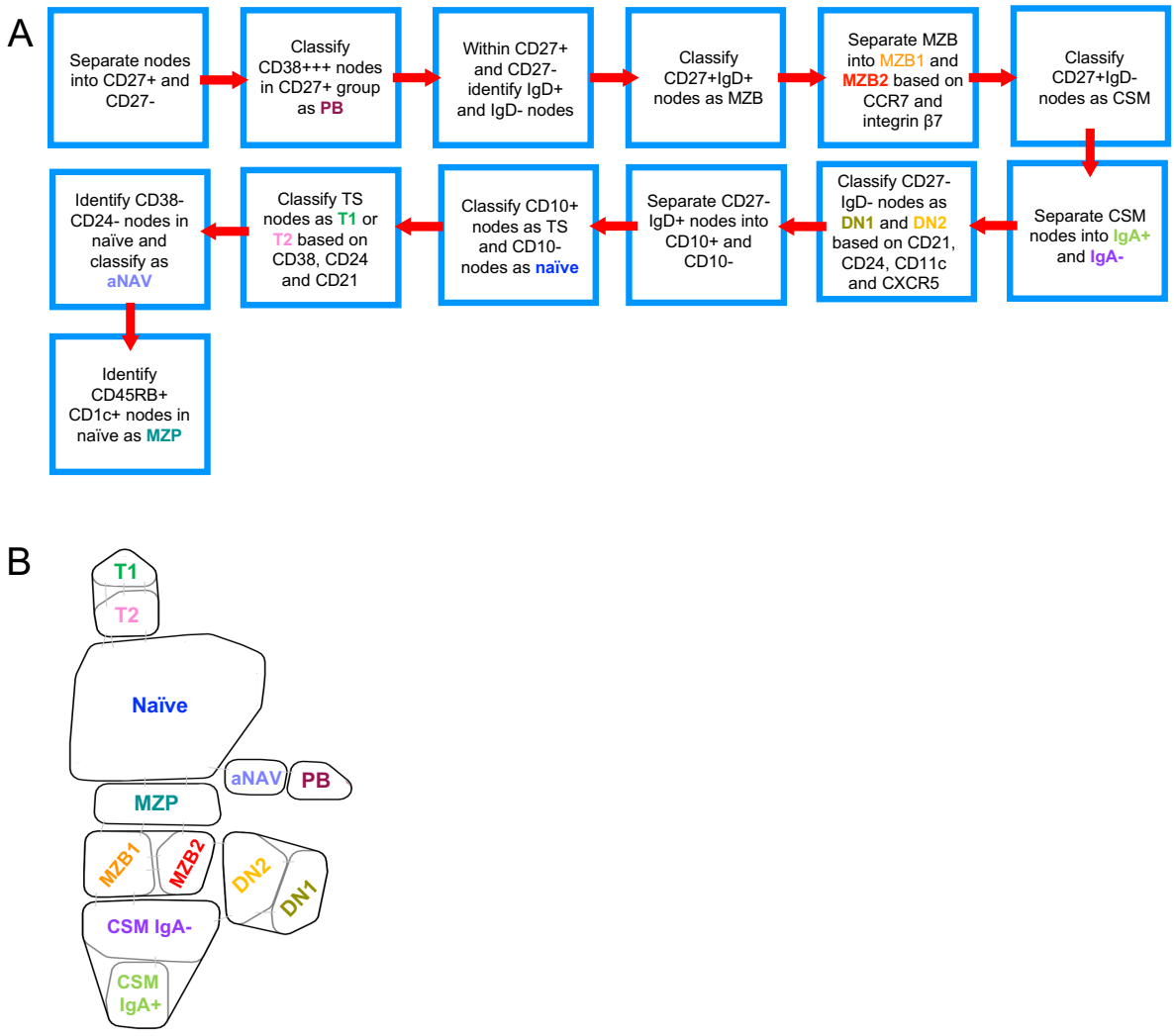

Figure 4.5: Step-by-step process used to classify SPADE nodes into B cell subsets. (A) Flowchart of steps taken to classify SPADE nodes into B cell subsets. Nodes were manually gated. After each step in the gating process, placement of gates was cross-referenced across all samples. **(B)** Schematic SPADE diagram showing final B cell subset classifications. B cell subset labels are colour-coded to correspond with flowchart steps.

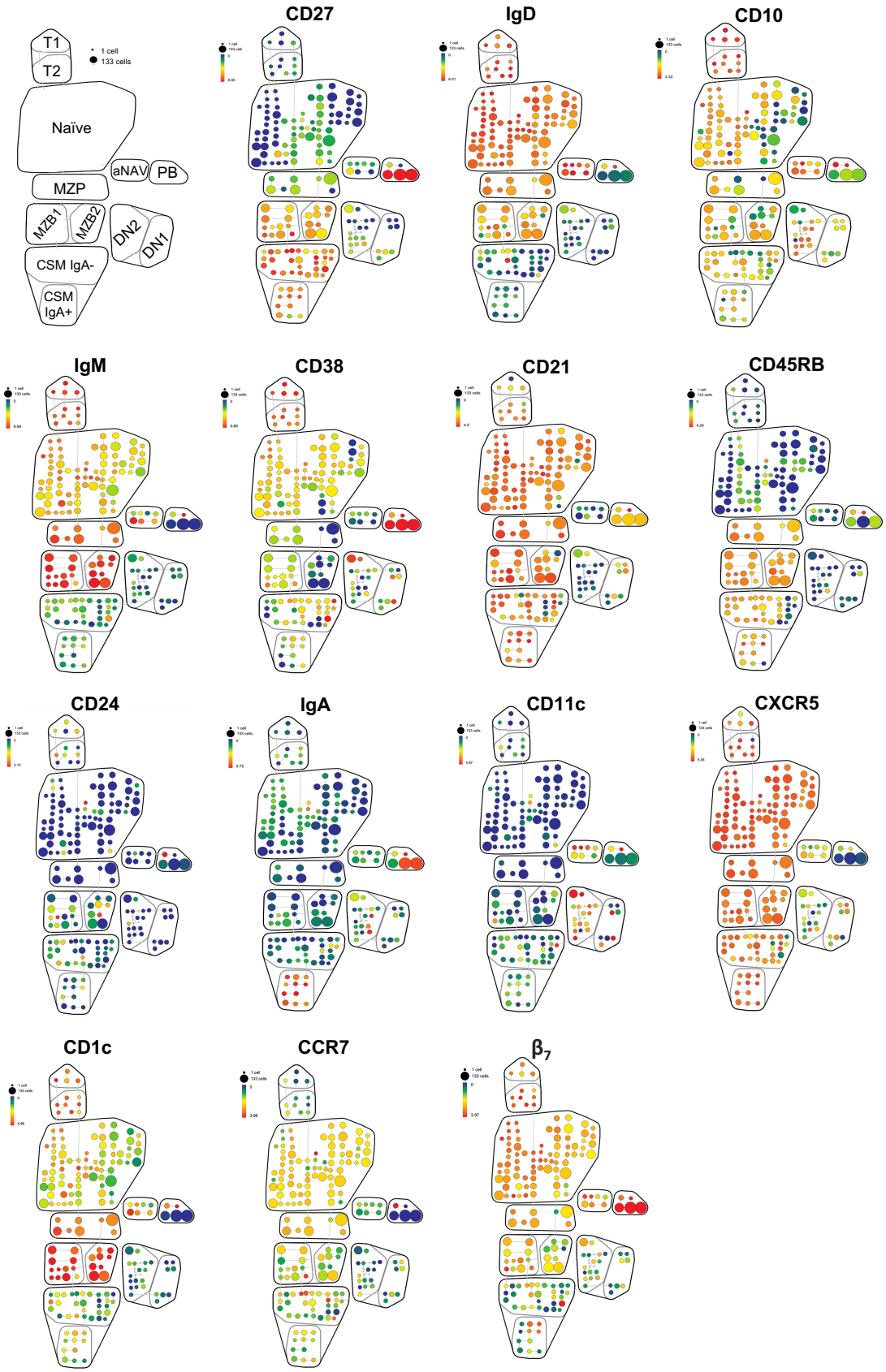

Figure 4.6: B cell lineage marker expression and subset classification. SPADE trees generated from viSNE coordinates from mass cytometry of CD19+ B cells. CD27, IgD, CD10, IgM, CD38,

CD21, CD45RB, CD24 and IgA were all used to generate viSNE. CD11c, CXCR5, CD1c, CCR7 and integrin β_7 were not used for viSNE, therefore have not influenced viSNE coordinates or SPADE tree nodes. Schematic tree indicates subset classifications. Size of nodes indicates number of cells. The larger the node the greater the number of cells. SPADE trees are colour-coded according to various B cell marker expression levels. Red nodes denote highest expression and blue nodes denote lowest. T1/2; transitional, aNAV; activated naïve, MZP; marginal zone precursor, MZB1/2; marginal zone B cells, CSM; class-switched memory, DN1/2; double-negative, PB; plasmablasts. SPADE trees are from a representative healthy donor.

After node classification, it was evident that the size of nodes, indicative of cell count, from the same subset differed between health and lupus nephritis samples, as shown by representative SPADE trees in Figure 4.7A. As shown in Figure 4.7B, in agreement with what has previously been reported in the literature, it was noted that significantly more aNAV and DN2 cells were present in lupus nephritis samples compared to health (Tipton et al., 2015; Wei et al., 2007). Furthermore, it was found that marginal zone precursors and a subset of marginal zone cells, MZB1, were significantly reduced in lupus nephritis compared to health, as demonstrated in Figure 4.7B. This observation was also consistent with what has previously been described in the literature (Siu et al., 2022; Tull et al., 2021; Zhu et al., 2018).

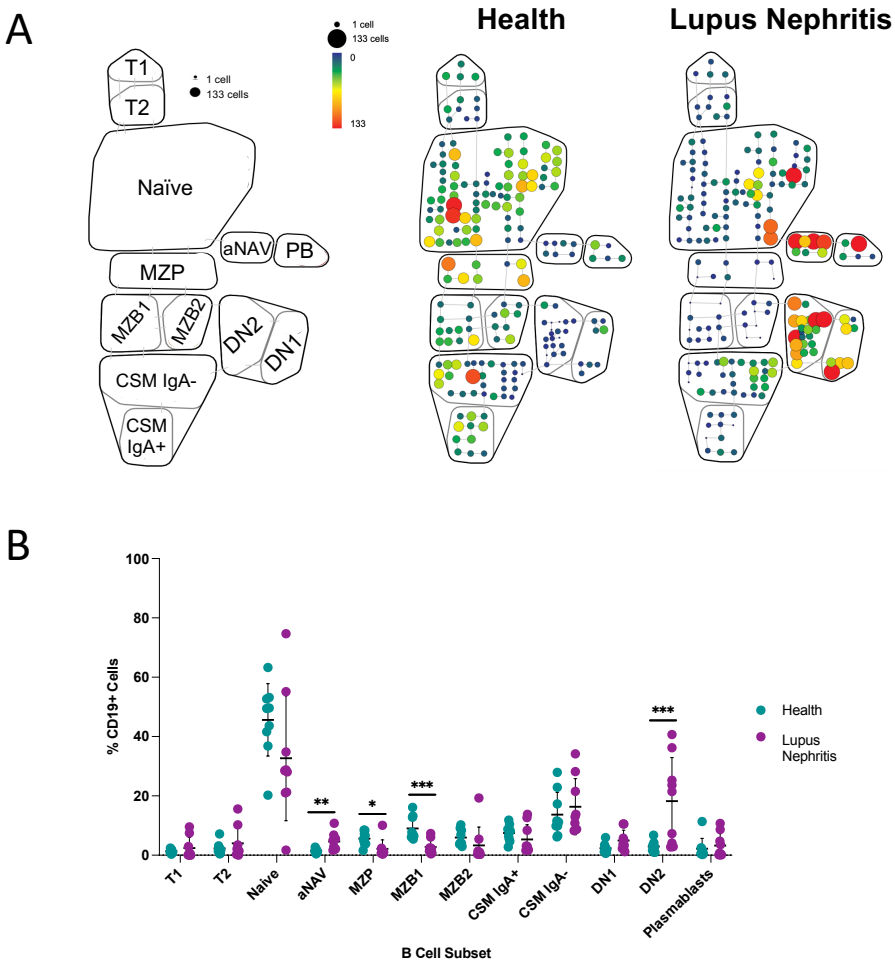

Figure 4.7: Changes in B cell subset proportions in lupus nephritis compared to health. (A) Representative SPADE trees from a healthy donor and a lupus nephritis patient showing B cell subset proportions. Schematic tree indicates subset classifications. Size of nodes indicates number of cells. The larger the node the greater the number of cells. SPADE trees are colour-coded according to cell count. The highest number of cells is represented by red nodes and the lowest is represented by blue nodes. **(B)** Comparison of peripheral blood B cell subsets as a percentage of total CD19+ cells in healthy donors (n=9) versus lupus nephritis patients (n=9). Statistical significance was determined by a student's t-test and was deemed as $p<0.05$.

4.3.3 Exploration of surface marker expression of interferon stimulated proteins

Previous gene expression data analysis outlined in Chapter 3 demonstrated the expression of ISGs in groups of cells within early B cell subsets (transitional and naïve) in health and lupus nephritis. Additionally, within all peripheral B cells in lupus nephritis samples higher expression of ISGs was observed. This analysis of mass cytometry data was performed to investigate the features identified in these early B cells in a larger cohort of patient samples and across peripheral blood B cell subsets defined using a more complex set of surface markers. The mass cytometry panel included proteins of ISGs *IFITM1*, *MX1* and *BST2* and interferon-regulatory gene *IRF7*, all of which were identified as conserved marker genes of the groups of transitional and naïve cells with an interferon gene signature.

The median expression of IFITM1, MX1, BST2 and IRF7 from each of the B cell subsets, shown in the SPADE tree maps in Figure 4.8, was extracted from the Cytobank software for all health (n=9) and lupus nephritis (n=9) samples. Plasmablasts were not included in this analysis because of their known expression of interferon (Nehar-Belaid et al., 2020). Firstly, a 2-way ANOVA with Tukey's multiple comparisons test was run to determine if there were significant differences in expression of IFITM1, MX1, BST2 and IRF7 between B cell subsets from healthy donors and lupus nephritis patients. The results of the 2-way ANOVA, shown in Table 4.1, showed that expression of all markers between subsets was found to be significantly different ($p<0.0001$), so this was investigated further by analysing the multiple comparisons data.

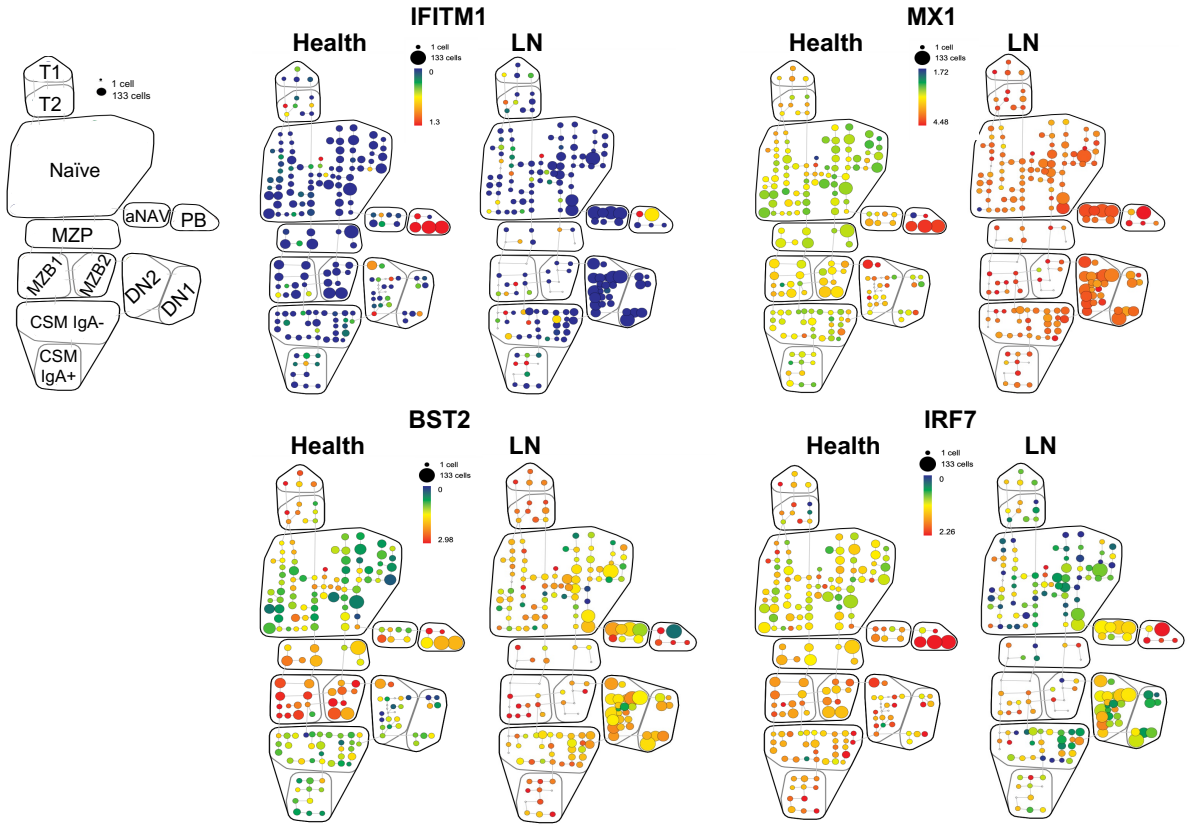

Figure 4.8: Expression of protein markers identified as features of interferon-associated early B cells. SPADE trees of CD19+ B cells from mass cytometry of PBMCs from healthy donors (n=9) and lupus nephritis (LN) patients (n=9). SPADE trees are from respective healthy donor and lupus nephritis patient representatives. Schematic tree indicates subset classifications. Size of nodes indicates number of cells. SPADE trees are colour-coded according to protein marker expression levels. Red nodes denote highest expression and blue nodes denote lowest. T1/2; transitional, aNAV; activated naïve, MZP; marginal zone precursor, MZB1/2; marginal zone B cells, CSM; class-switched memory, DN1/2; double-negative, PB; plasmablasts.

Initially, median BST2 appeared to be highly expressed in transitional and marginal zone subsets in both health and lupus nephritis samples, as shown in Figure 4.9A. As both transitional and marginal zone cells are known to express high levels of IgM and are associated with a gut-homing B cell developmental trajectory (Tull et al., 2021), the relationship between IgM and BST2 was investigated as it was important to investigate whether expression of BST2 could potentially be another defining marker of the IgMhi gut-homing developmental branch. BST2 expression mapped very closely onto IgM, as shown in Figure 4.9B. When the relationship between BST2 median expression and IgM median expression across all B cells was assessed, shown in scatterplots in Figure 4.9C, a marked association between these two markers was observed.

After assessing the panel used to generate this mass cytometry data it was realised that IgM and BST2 channels were relatively close in terms of the metals the antibodies were tagged to (172Yb and 174Yb, respectively). A spill over matrix (from Standard BioTools) indicated that spill over between these channels was minor: 0.5 from 172Yb (IgM) into 174Yb (BST2). These two channels have been used together in the past with no problem (Zhao et al., 2018). However, it was not possible to rule out that spill over was causing this striking association. Therefore, to validate this finding, flow cytometry of n=8 healthy donor PBMCs was used to investigate and the expression of BST2 and IgM in CD19+ B cells. Flow cytometry analysis did not reveal the same association between BST2 and IgM; there was no significant relationship between these two markers, as shown in Figure 4.9D. Whilst spill over between these two channels is usually minor, the lack of validation of this finding through flow cytometry meant that BST2 expression was not analysed any further in this dataset.

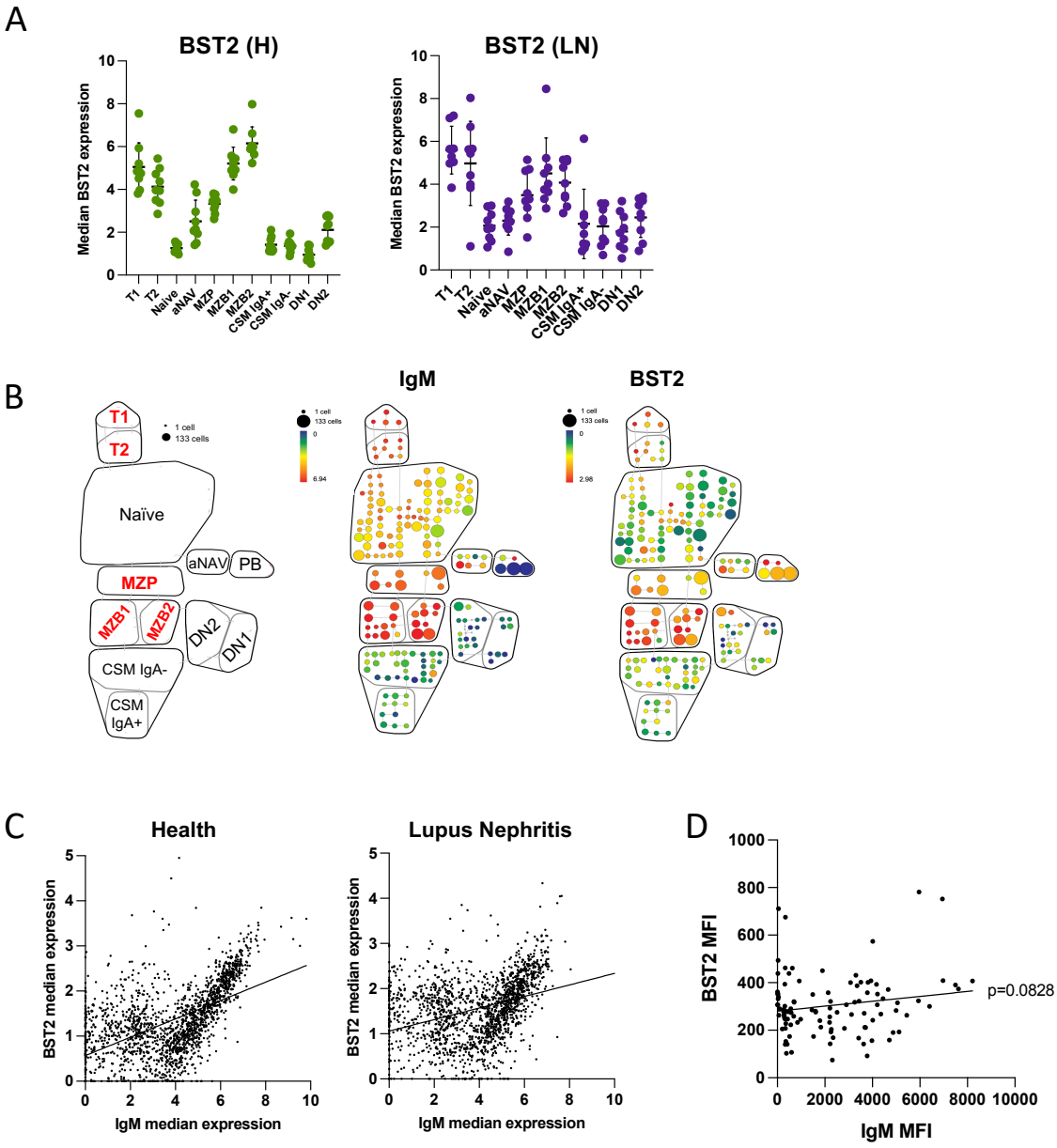

Figure 4.9: Investigation of potential artefact in mass cytometry data. (A) Median expression of BST2 across peripheral blood CD19+ B cell subsets in healthy donors (H) (n=9) and lupus nephritis patients (LN) (n=9) generated from mass cytometry. **(B)** SPADE trees showing surface IgM and BST2 expression on peripheral blood CD19+ B cell subsets generated from mass cytometry. Schematic SPADE tree denotes subset names; subsets in red are those with high IgM and high BST2 expression. SPADE trees are from a representative healthy donor. **(C)** Scatterplots comparing BST2 median expression with IgM median expression across all nodes from the SPADE tree shown in panel B, from n=9 healthy donors and n=9 lupus nephritis patients. **(D)** Scatterplot comparing mean fluorescence intensity (MFI) of BST2 versus IgM in peripheral blood B cell subsets from n=8 healthy donors generated by flow cytometry.

Expression of IFITM1, MX1 and IRF7 across B cell subsets in the mass cytometry data was assessed in healthy donors. Similar to what was seen at the gene level (Figure 3.5, Chapter 3.3.3), it was found that transitional B cells had the highest significant median expression of IFITM1 in health, as shown in Figure 4.10A. IFITM1 expression was observed in T1 cells in healthy donor samples and it was found that T1 cells had significantly higher expression compared to naive, MZP, MZB2, CSM IgA+ and DN1 subsets ($p<0.05$). It was determined that the T2 population expressed IFITM1 significantly more than all other B cell populations, except T1 cells, shown in Figure 4.10A. In the healthy donor cohort, it was found that aside from transitional cells, there was no significant difference in median IFITM1 expression between all other B cell subsets, as demonstrated in Figure 4.10A.

Furthermore, expression of MX1 between early B cell subsets was variable. T1 cells had significantly higher expression of MX1 compared to naïve, MZP, MZB2, CSM IgA- and DN1 cells in healthy donors, as shown in Figure 4.10B. Naïve B cells were seen to have significantly lower median expression of MX1 in health compared to transitional, aNAV, MZB1 and DN2 cells, at a similar level to memory B cell subsets, as displayed in Figure 4.10B. DN2 cells from healthy donors had the highest median MX1 expression.

Median expression of interferon regulator IRF7 in cells from healthy donors was found to be significantly lower in the naïve subset compared to all other B cell subsets except MZP and CSM IgA- cells, as displayed in Figure 4.10C. Similar to what was seen with regard to MX1 expression, the DN2 subset expressed highest IRF7 in healthy donors. Overall, it was found that MX1 expression was expressed at the highest level compared to IFITM1 and IRF7.

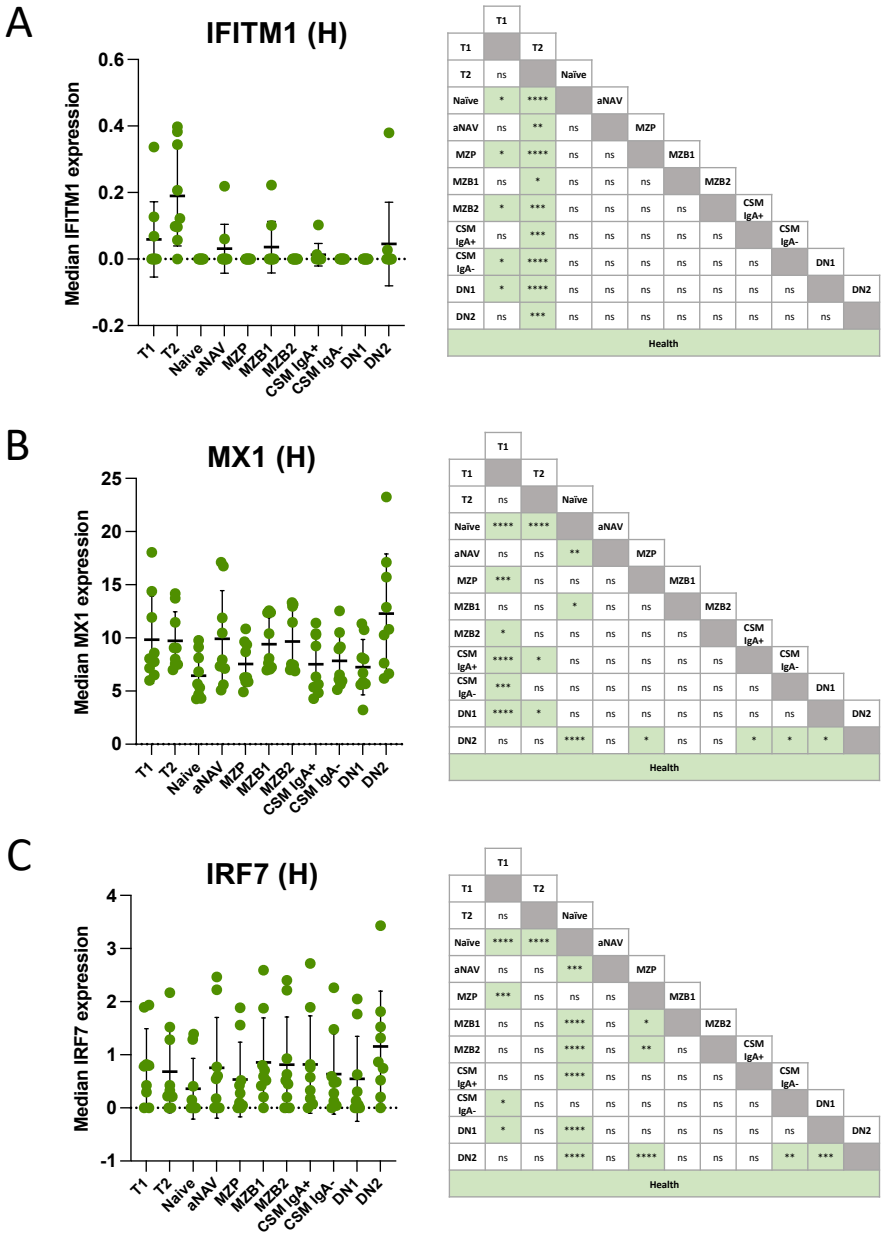

Figure 4.10: Expression of interferon-stimulatory and interferon-regulatory protein markers in healthy donors. Median expression of protein markers IFITM1 **(A)**, MX1 **(B)** and IRF7 **(C)**, in CD19+ peripheral blood B cell subsets in n=9 healthy donors. On graphs, horizontal bars represent mean and error bars denote ±SD. Tables show significant differences between median protein expression between B cell subsets. Significance was calculated by 2-way ANVOA with Tukey's multiple comparisons test. Significant differences between subsets are highlighted in green. Significant was deemed as $p<0.05$.

Expression of IFITM1, MX1 and IRF7 was then evaluated across B cell subsets from lupus nephritis patients. As in health, transitional cells from lupus nephritis patients were found to have the highest expression of IFITM1 compared to all other peripheral B cell subsets. T2 cells from lupus nephritis patients were found to have significantly greater median expression of IFITM1 compared to all B cell subsets except T1 and MZB1, demonstrated in Figure 4.11A. T1 cells showed significantly greater median expression of IFITM1 compared to naïve, MZP, MZB2, CSM IgA- and DN1 cells. Both double negative subsets and CSM IgA- cells were found to have the lowest expression of IFITM1.

T1 cells were found to have the highest median expression of MX1 in lupus nephritis patients, as shown in Figure 4.11B. Naïve B cells were found to have the lowest median expression of MX1, in comparison to transitional, aNAV, CSM IgA+ and DN1 subsets. Similarly, the naïve B cell subset in lupus nephritis patients had significantly lower median IRF7 expression compared to all subsets, apart from aNAV, CSM IgA- and DN1, demonstrated in Figure 4.11C and T1 cells were found to have the highest median expression of IRF7. T2 cells from lupus nephritis patients had significantly higher expression of IRF7 than several all CD27-IgD+CD10- subsets (naïve, aNAV and MZP). Overall, MX1 expression was the greatest across B cell subsets compared to IFITM1 and IRF7 in lupus nephritis as it was in the healthy donor cohort.

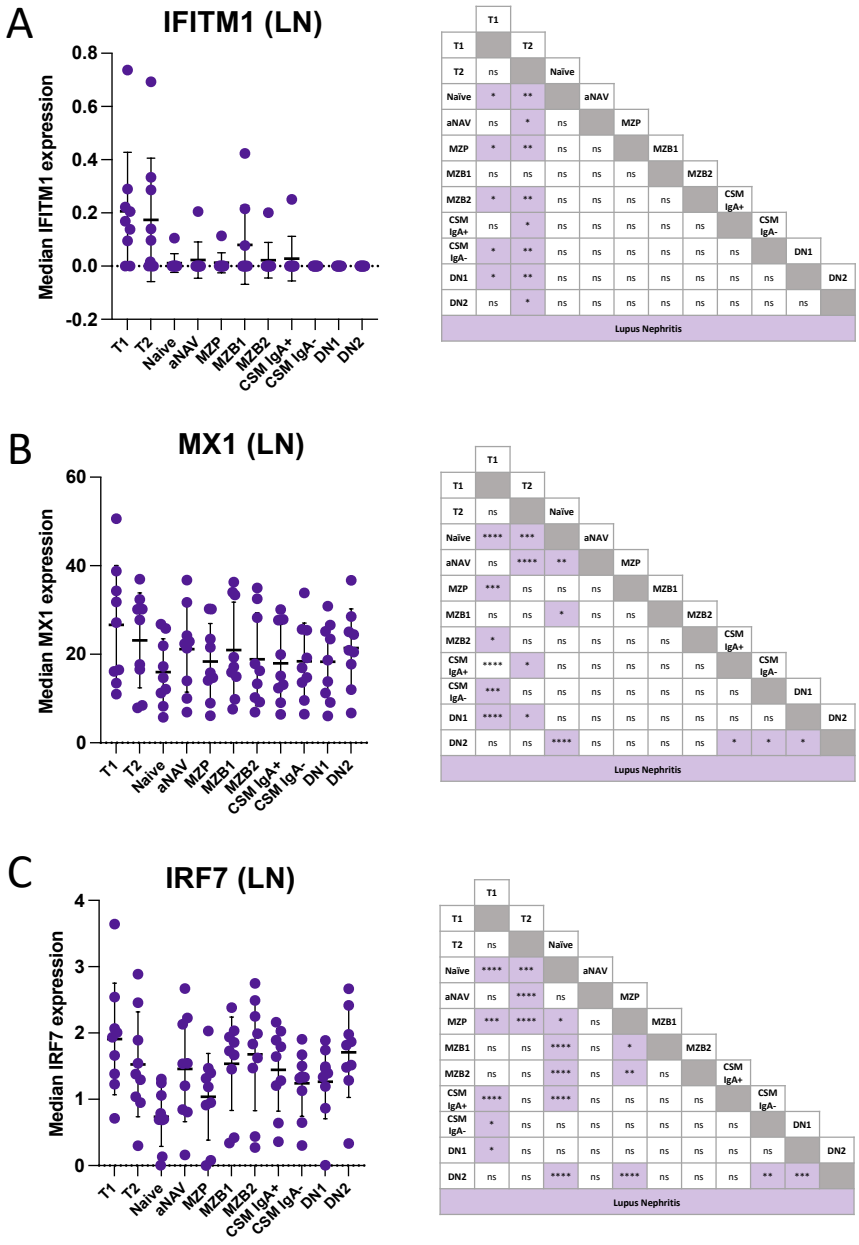

Figure 4.11: Expression of interferon-stimulatory and interferon-regulatory protein markers in lupus nephritis patients. Median expression of protein markers IFITM1 **(A)**, MX1 **(B)** and IRF7 **(C)**, in CD19+ peripheral blood B cell subsets in n=9 lupus nephritis patients. On graphs, horizontal bars represent mean and error bars denote ±SD. Tables show significant differences between median protein expression between B cell subsets. Significance was calculated by 2-way ANVOA with Tukey's multiple comparisons test. Significant differences between subsets are highlighted in purple. Significant was deemed as $p<0.05$.

The results of the ANOVA, displayed in Table 4.1, revealed that expression of all three markers of interest were significantly different between B cell subsets ($p<0.0001$), across all B cells. IFITM1 expression did not significantly different between health and lupus nephritis. As shown in Figure 4.12A, median expression of IFITM1 was relatively similar between health and lupus across all B cell subsets. On the other hand, MX1 and IRF7 expression were found to be significantly different between health and lupus nephritis ($p=0.0135$ and $p=0.0144$, respectively). This difference in expression was found to be greater in lupus nephritis compared to health, as shown in Figure 4.12B and 4.12C.

Table 4.1: 2-Way ANOVA results comparing expression of IFITM1, MX1 and IRF7 between B cell subsets (T1, T2, Naïve, aNAV, MZP, MZB1, MZB2, CSM IgA+, CSM IgA-, DN1 and DN2) and between the entire peripheral B cell pool in healthy donor versus lupus nephritis patient samples (disease status). Significance was deemed as $p<0.05$, indicated by *. Non-significant comparisons are denoted by 'ns'.

Marker	Variable	p-value	Significance
IFITM1	B Cell Subset	p<0.0001	****
	Disease Status	p=0.3402	ns
MX1	B Cell Subset	p<0.0001	****
	Disease Status	p=0.0135	*
IRF7	B Cell Subset	p<0.0001	****
	Disease Status	p=0.0144	*

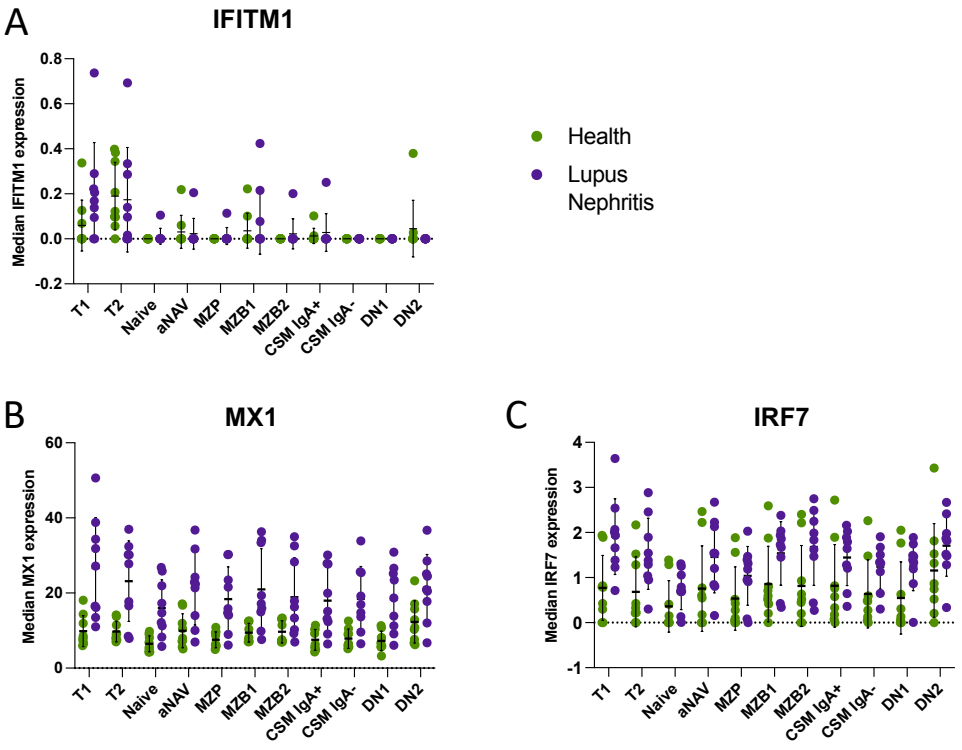

Figure 4.12: Median IFITM1, MX1 and IRF7 expression in B cells in health versus lupus nephritis. Plots showing median expression of IFITM1 **(A)**, MX1 **(B)** and IRF7 **(C)** generated by mass cytometry of peripheral blood B cell subsets from healthy donors (n=9) and lupus nephritis patients (n=9). Data from healthy donors is shown in green and data from lupus nephritis patients is shown in purple. Horizontal bars indicate mean and error bars represent ±SD.

This analysis revealed some differences in the patterns of expression in proteins that has been previously identified as markers of transitional and naïve B cells that have an interferon gene signature. It was found that IFITM1 protein expression is a feature of transitional B cells similarly to how it was found to be feature of this subset at the gene level in the previous chapter. Furthermore, expression of MX1 and IRF7 are significantly increased in all B cells in lupus nephritis compared to health and are a feature of all peripheral B cell subsets, not just early B cell subsets.

4.3.4 Investigation of interferon-associated transitional and naïve B cells

This study so far has shown that IFITM1 is expressed predominantly by transitional B cells in both health and lupus nephritis and was a marker for transitional B cells with an interferon gene signature. It was deemed important to understand whether transitional B cells with an interferon gene signature were a distinct subset of transitional cells or whether they were a group of cells within the known transitional B cell subsets. To investigate this, transitional B cell nodes from the T1 and T2 subsets shown in the SPADE tree in Figure 4.6 were exported and re-analysed, which allowed for a better resolution for in-depth analysis of the cells belonging to these subsets. After exporting nodes, a new viSNE was generated using transitional-associated markers CD10, CD38, CD24, CD21 and IgM. The viSNE coordinates were used to generate a new SPADE tree comprising only transitional B cells. CD38 and CD21 expression was used to classify nodes as either T1, which had higher in CD38 and lower CD21 expression, or T2, which had lower CD38 and higher CD21 expression, displayed in Figure 4.13A.

Post-classification, IFITM1 expression was overlaid onto the transitional SPADE tree to visualise whether a group of nodes could be identified as an IFITM1+ subset. Since IFITM1 was not used in the viSNE clustering it did not influence the distribution of the nodes. As shown in Figure 4.13B, across health and lupus nephritis samples it was evident that cells with high IFITM1 expression were spread across both T1 and T2 subsets and were not consistently expressed within the same nodes between samples. This suggested that IFITM1 was not associated with a phenotypically defined group of cells.

The lack of association between expression of IFITM1 and a phenotypically defined subset of cells prompted a re-evaluation of the clustering of transitional B cells within the single-cell RNA-sequencing dataset, described in Chapter 3. The aim of this analysis was to determine if cells with an interferon gene signature were clustering together based on ISGs only and were not a discrete population of transitional cells. In other words, we considered the possibility that the ISGs themselves were driving the accumulation of cells that expressed those genes.

The same data analysis pipeline outlined in Chapter 3 was followed, but prior to clustering using the top 2000 differentially expressed genes, all ISGs were removed. This meant that no interferon-stimulated or -regulatory genes contributed to the new clustering. Cells that were originally from the “IFN” cluster were then overlaid back onto the UMAP and it was found that these cells were dispersed across the UMAP, predominantly within the T2 clusters, as demonstrated in Figure 4.13C. This was observed in both healthy donors and lupus nephritis patients.

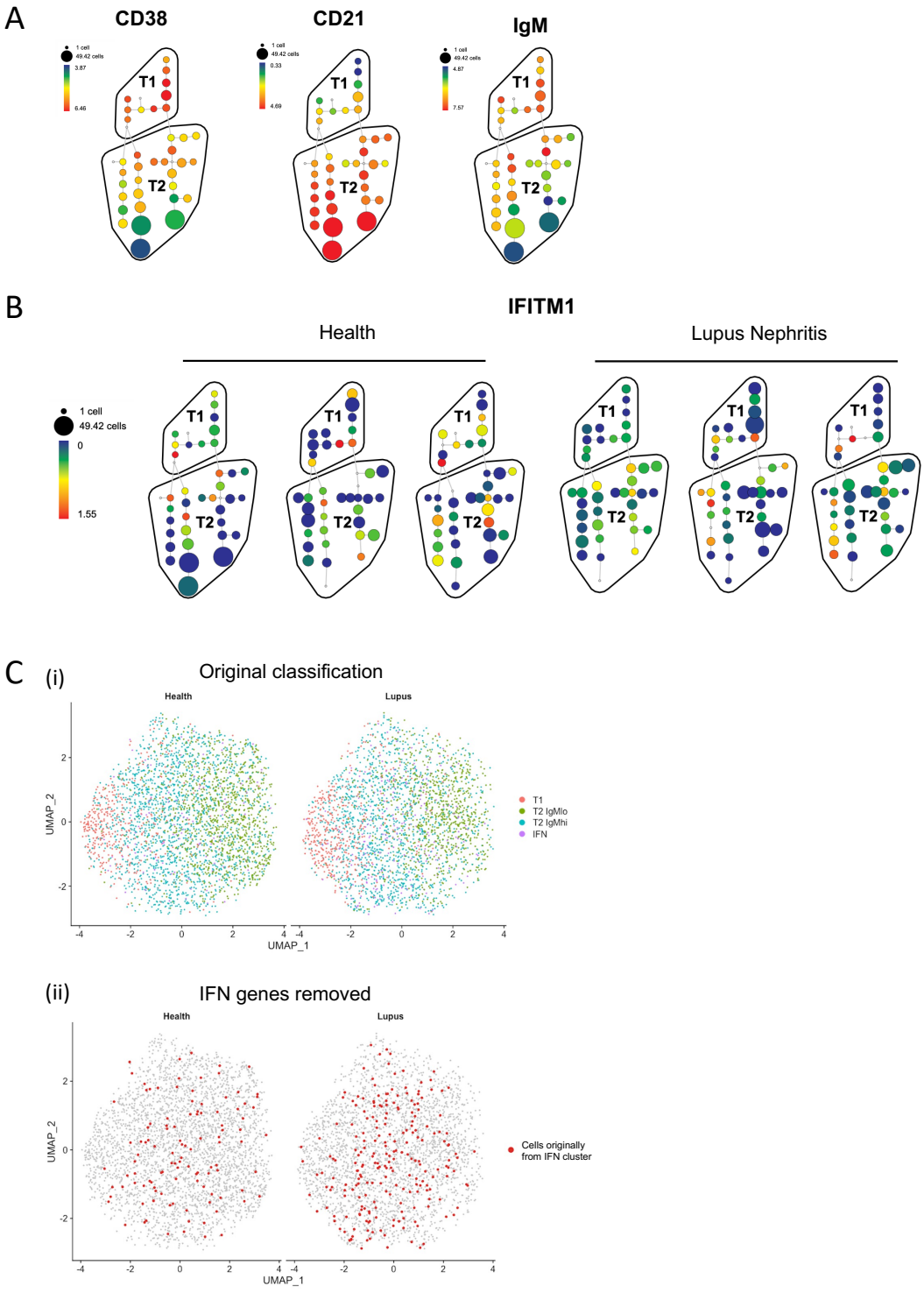

Figure 4.13: Transitional B cells with an interferon gene signature are not a distinct subset of cells. (A) SPADE tree of classified transitional B cells generated from mass cytometry of PBMCs from healthy donors (n=9) and lupus nephritis patients (n=9). Size of nodes denote number of cells within node. Colour scale indicates level of expression. T1 nodes are CD38+++CD21+ and T2 nodes are CD38++/+CD21+++. T1 nodes are IgM+++ and T2 nodes are a mix of IgMhi and IgMlo. SPADE trees are from a healthy donor representative. **(B)** SPADE

trees from panel A overlaid with IFITM1 expression. SPADE trees are from n=3 healthy donors and n=3 lupus nephritis patients. **(C)** (i) UMAP plots showing four clusters of transitional B cells from n=3 healthy donors and n=3 lupus nephritis patients, generated from 2000 differentially expressed genes, excluding ISGs. (ii) UMAP plot from panel C(i) showing cells belonging to IFN cluster, highlighted in red.

The same observation was made regarding the cluster of naïve B cells with an interferon gene signature, shown previously in Figure 3.12 in 3.3.7. ISGs were removed from the clustering process and then cells originally belonging to the interferon naïve cluster were overlaid onto the UMAP of CD19+ B cells, shown in Figure 4.14A. As seen in Figure 4.14B, the majority of cells from the interferon cluster mapped back onto the naïve (*TCL1A*-) region of the UMAP in both health and lupus nephritis but did not remain clustered in one distinct group.

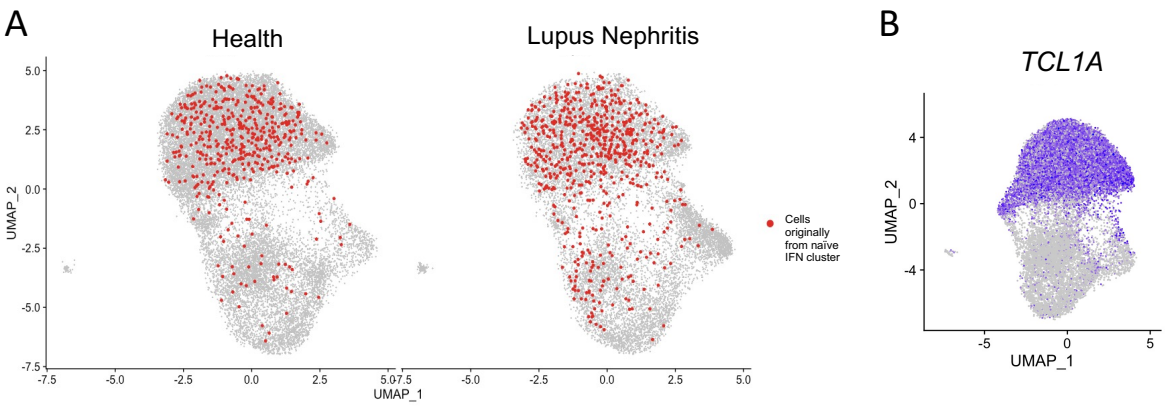

Figure 4.14: Naïve B cells with an interferon gene signature do not represent a distinct subset of naïve cells. (A) UMAP plots displaying CD19+ B cells from n=3 healthy donors and n=3 lupus nephritis patients. UMAPs were generated from 2000 differentially expressed genes, excluding ISGs. Red cells indicate naïve B cells which have an interferon gene signature. **(B)** UMAP plot of CD19+ B cells overlaid with *TCL1A* gene expression.

It was concluded that early B cells with an interferon gene signature are not a discrete subset but are groups of cells that are present within the transitional and naïve subsets. Therefore, it was important to investigate whether these cells are linked to a particular developmental trajectory.

Tull et al. (2021) have previously described a bifurcation in peripheral B cell development at the T1 stage which gives rise to two populations of T2 B cells which can be distinguished based on surface expression of IgM. As the group of transitional B cells with an interferon gene signature are not a separate subset, it was important to understand if these cells were associated with the IgMhi or IgMlo trajectory. Therefore, the exported T2 B cell nodes, shown previously in Figure 4.13A, were sub-divided into IgMhi and IgMlo populations, as shown in Figure 4.15, and it was investigated whether interferon markers were expressed differently between these two populations.

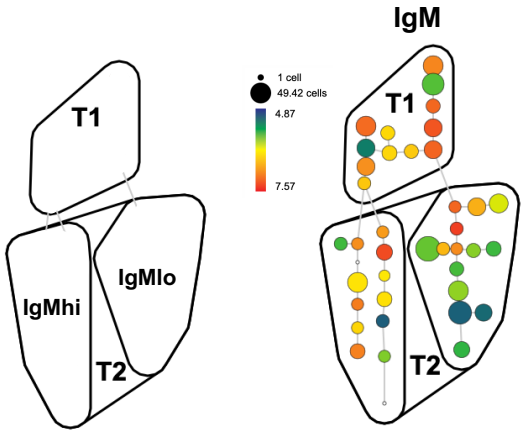

Figure 4.15: Classification of IgMhi and IgMlo T2 B cells. SPADE tree nodes from T2 B cells divided into IgMhi and IgMlo populations based on median IgM expression. Size of nodes denote number of cells within node. Colour scale indicates level of expression. SPADE tree shown in from a representative healthy donor.

Classification of nodes into respective T2 IgMhi and T2 IgMlo subsets was confirmed by assessing median expression of IgM, integrin β_7 and CD1c across all health and lupus nephritis samples. It was confirmed that nodes classified as IgMhi expressed significantly higher IgM, integrin β_7 and CD1c, as demonstrated in Figure 4.16A and 4.16C. MX1 and IRF7 median expression was not significantly different between T2 IgMhi and IgMlo subsets, as shown in Figure 4.16B and 4.16D. Whilst the difference in median IFITM1 expression between T2 IgMhi and T2 IgMlo cells was not statistically significantly different in health or lupus nephritis, in both cohorts there was a trend towards greater expression of IFITM1 in IgMhi T2 nodes, as shown in Figure 4.16B and 4.16D.

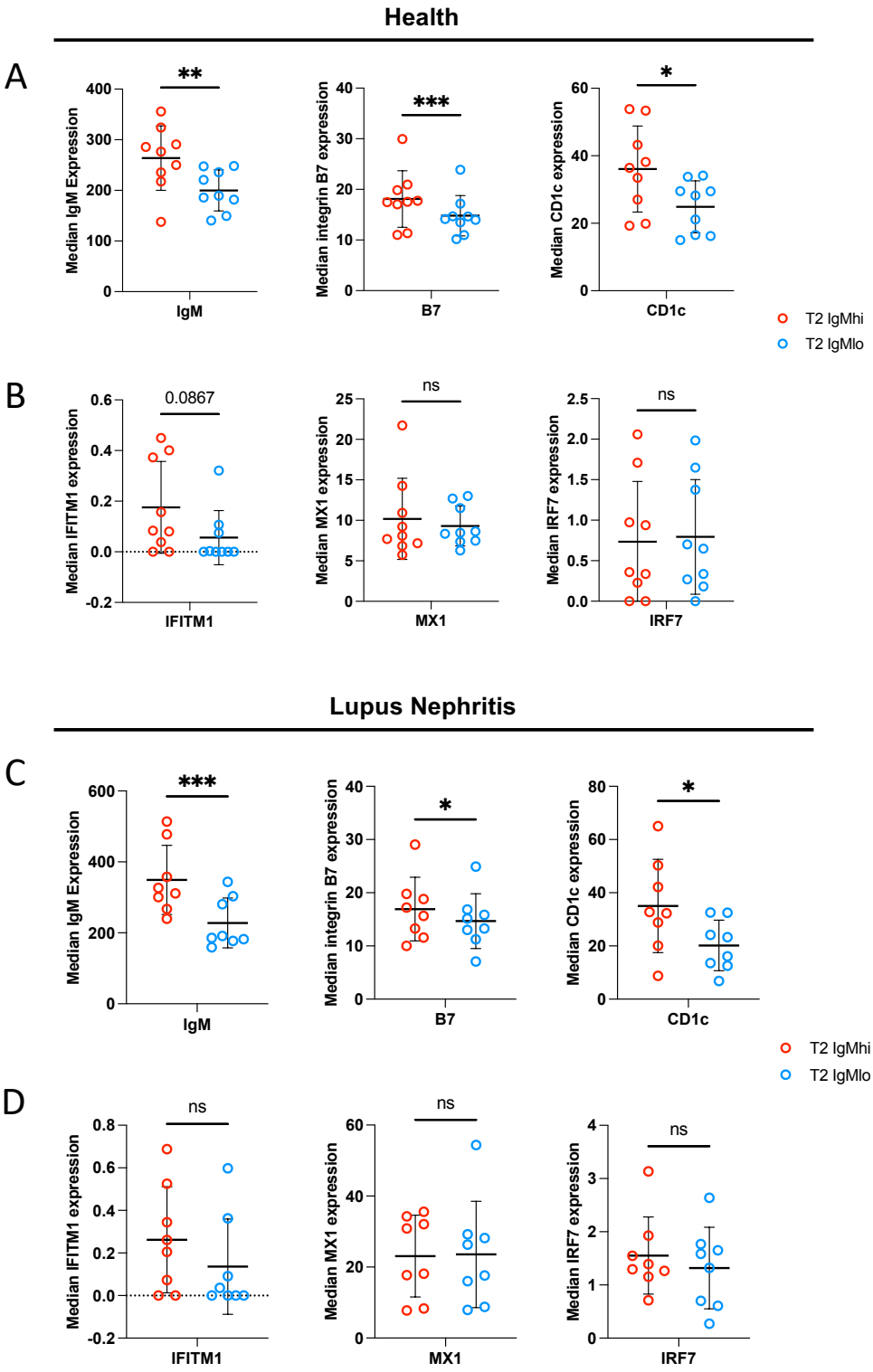

Figure 4.16: Comparison of protein marker expression in T2 IgMhi B cells versus T2 IgMlo B cells. (A) Comparison of median IgM, integrin β_7 (B7) and CD1c expression in T2 IgMhi and T2 IgMlo cells in healthy donors. **(B)** Comparison of median IFITM1, MX1 and IRF7 expression in T2 IgMhi and T2 IgMlo cells in healthy donors. **(C)** Comparison of median IgM, integrin β_7 (B7) and CD1c expression in T2 IgMhi and T2 IgMlo cells in lupus nephritis patients. **(D)** Comparison

of median IFITM1, MX1 and IRF7 expression in T2 IgMhi and T2 IgMlo cells in lupus nephritis patients. Statistical significance was determined by paired t-tests and significance was deemed as $p<0.05$.

As previously shown in Table 4.1 and Figure 4.12A in 4.4.3, it was found that there was no significant difference in IFITM1 expression across all B cell subsets between health and lupus nephritis. After classifying T2 nodes into IgMhi and IgMlo, a similar observation was made whereby it was found that there was no significant difference in IFITM1 expression between health and lupus nephritis in sub-classified T2 subsets, T2 IgMhi and T2 IgMlo, shown in Figure 4.17. It was also noted that there was no significant difference in IFITM1 expression in T1 B cells between health and lupus nephritis, demonstrated in Figure 4.17.

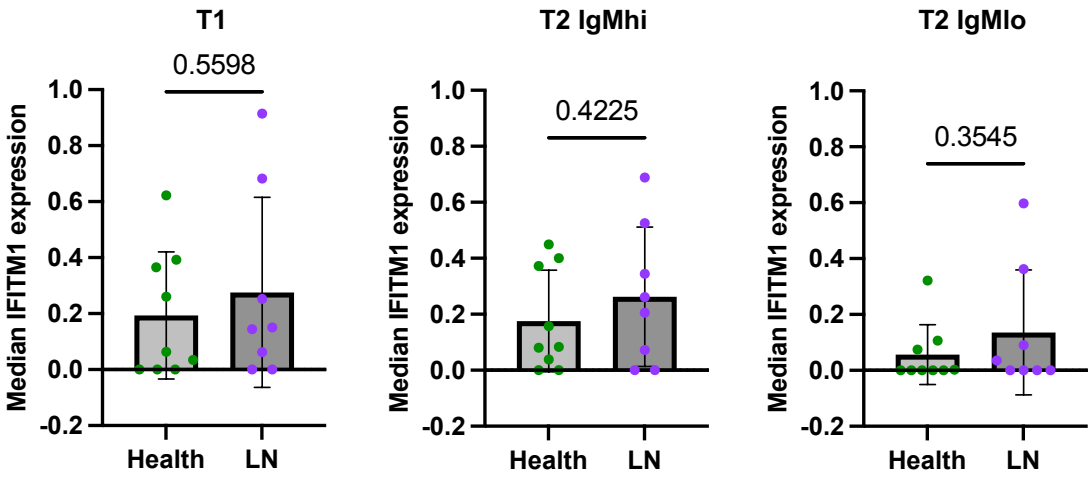

Figure 4.17: Comparison of IFITM1 expression in transitional B cell subsets between health and lupus nephritis. Median IFITM1 expression of transitional B cell subsets, T1, T2 IgMhi and T2 IgMlo from healthy donors and lupus nephritis patients. Data were generated by exporting median IFITM1 expression values (from Cytobank software) from classified nodes shown in the SPADE tree in Figure 26. Comparisons were made using an un-paired t-test and statistical significance was deemed as $p<0.05$.

The mass cytometry data presented in this study suggest that whilst there is no difference in IFITM1 protein expression between health and lupus nephritis, there may be a variation in IFITM1 expression between IgMhi and IgMlo cells so further

investigation into the association between IFITM1 and the features of IgMhi cells was warranted.

CITE-seq antibody staining data from the single-cell RNA-sequencing dataset, shown in Figure 3.3G from Chapter 3.3.3, demonstrated that the cluster of transitional B cells with an interferon gene signature (cluster 5) was found to express high levels of surface integrin β_7. It is known that integrin β_7 is associated with B cell homing to the gut and is expressed by gut-homing T2 IgMhi cells (Tull et al., 2021; Vossenkämper et al., 2013; Kraal et al., 1995). Thus, the relationship between markers of interferon-associated transitional cells and integrin β_7 was investigated. Using the mass cytometry data set, median protein marker expression from all CD19+ B cell nodes (200 nodes per sample) were extracted from the Cytobank software and plotted to determine any correlations between markers.

It was found that in both health and lupus nephritis samples, IFITM1 protein expression significantly correlated with integrin β_7 expression ($p<0.0001$), as displayed in Figure 4.18A. Conversely, MX1 expression did not correlate with integrin β_7 expression in either sample cohort, demonstrated in Figure 4.18B. It is known that IgMhi B cells express high levels of integrin β_7 (Tull et al., 2021); an observation that was also seen in this data set (Figure 4.18C). These observations in conjunction with the trend in higher IFITM1 expression in T2 IgMhi lead us to ask whether IFITM1 correlates with IgM integrin β_7 expression and could perhaps be associated with gut-homing peripheral blood B cells.

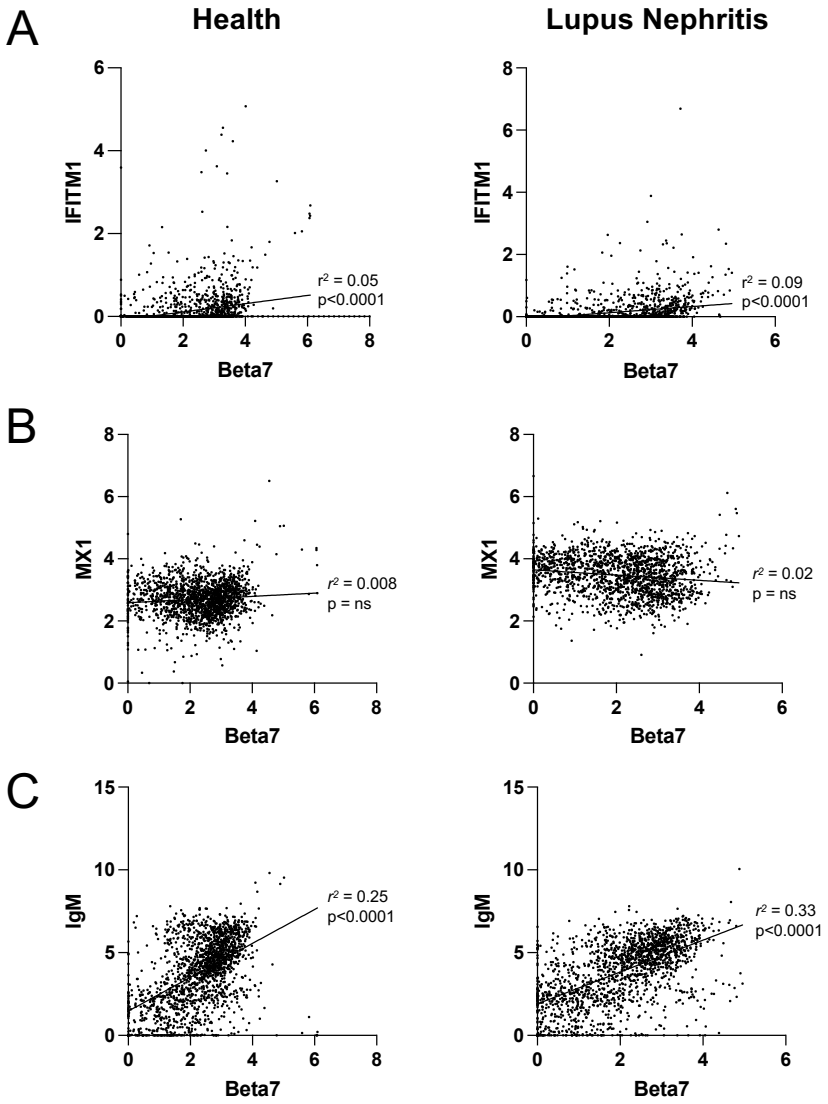

Figure 4.18: Relationship between integrin β_7 and IFITM1, MX1 and IgM in CD19+ B cells. Expression values are from mass cytometry data of CD19+ B cells from n=9 healthy donors and n=9 lupus nephritis patients. Lines on all scatterplots represent simple linear regression. The r^2 values denote the squared correlation coefficient. The p values denote if the slope is significantly different from zero. Significance was defined as p<0.05. Scatterplots show the relationship between expression of and integrin β_7 versus **(A)** IFITM1, **(B)** MX1 and **(C)** IgM.

Flow cytometry was used to consider the relationship between integrin β_7 and IgM with IFITM1. PBMCs from healthy donors (n=10) and lupus nephritis patients (n=10) were stained and data was recorded on a BD Fortessa™. Analysis was performed using FlowJo software. Transitional B cells, identified as CD27-IgD+CD10+, and naïve B cells, identified as CD27-IgD+CD10-, were split into IFITM1+ and IFITM1- groups. Integrin β_7

mean fluorescence intensity (MFI) was calculated using the FlowJo software. As shown in Figure 4.19A, IFITM1+ transitional cells had significantly greater integrin β_7 MFI compared to IFITM1- cells in both health and lupus nephritis. However, there was no significant difference in integrin β_7 MFI between IFITM1+ and IFITM1- naïve B cells. To determine if a relationship between IFITM1 and IgM was apparent in early B subsets, transitional and naïve cells were separated into IgMhi and IgMlo subsets, then IFITM1 MFI was compared between these groups of cells. It was found that in both transitional and naïve subsets, in health and lupus nephritis, IgMhi cells had significantly greater IFITM1 MFI, as demonstrated in Figure 4.19B. To confirm IgMhi and IgMlo gates were correctly placed, integrin β_7 MFI was determined and IgMhi cells were confirmed as having greater integrin β_7 expression, as shown in Figure 4.19C.

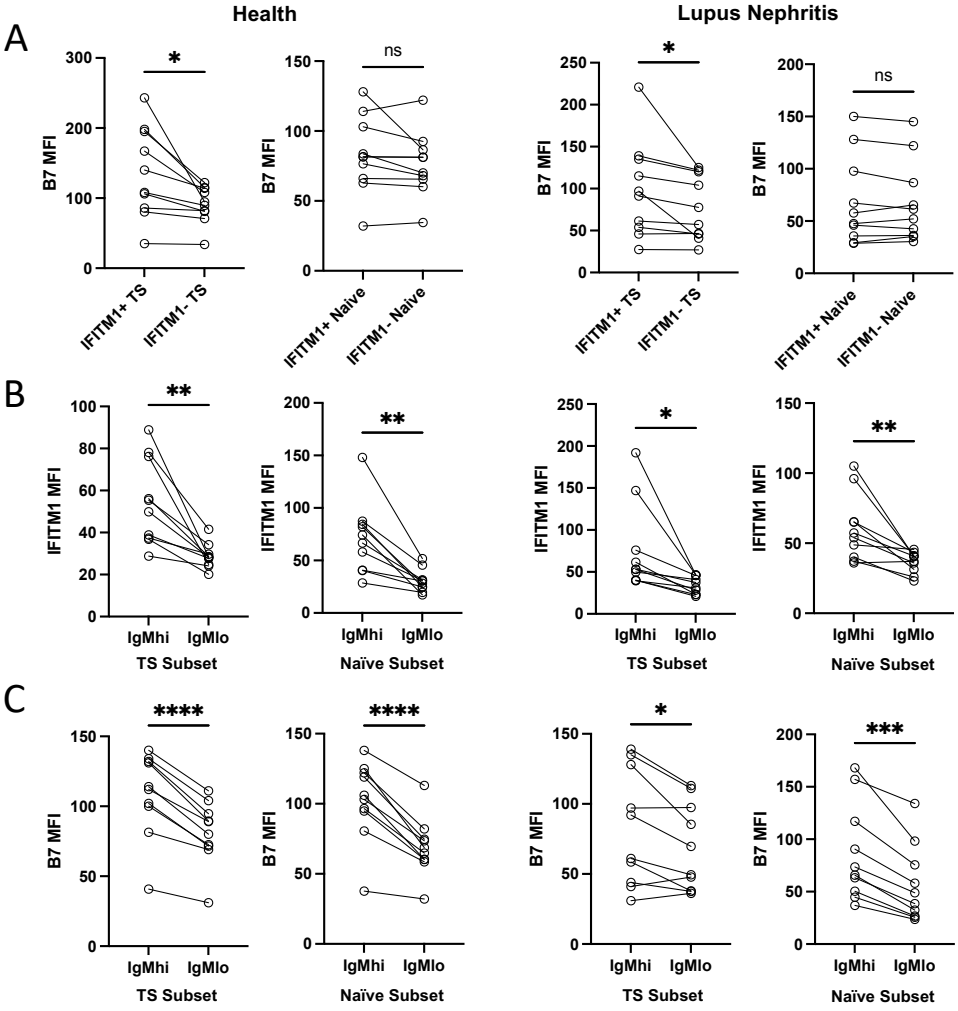

Figure 4.19: Expression of IFITM1 and integrin β_7 in transitional and naïve B cells. (A) Plots showing integrin β_7 mean fluorescence intensity (MFI) in IFITM1+ and IFITM1- transitional

(TS) and naïve cells in healthy donors (n=10) and lupus nephritis patients (n=10). **(B)** Plots showing IFITM1 MFI in IgMhi and IgMlo transitional and naïve B cells in healthy donors and lupus nephritis patients. **(C)** Plots showing integrin β_7 MFI in IgMhi and IgMlo transitional and naïve subsets in healthy donors and lupus nephritis patients. For all plots paired data points are joined together by a solid black line. Asterisks indicate statistical significance as calculated by paired t-test. Significant was deemed as $p<0.05$. ns; not significant.

Thus far, this study has shown that at the gene level *IFITM1* expression in transitional and naïve B cells is greater in lupus nephritis compared to health (shown in Figures 3.11 and 3.12D in 3.3.6) through analysis of single-cell RNA-sequencing data. The mass cytometry data presented in this chapter has shown that at the protein level IFITM1 expression across all B cell subsets (shown in Table 4.1 and Figure 4.12A in 4.4.3) and in classified transitional B cell subsets (shown in Figure 4.17 in 4.3.4) does not significantly differ between health and lupus nephritis.

Flow cytometry has also been used in this study to investigate IFITM1 expression at the protein level. A comparison of IFITM1 expression between health and lupus nephritis using flow cytometry was conducted to determine if the observations noted in the mass cytometry dataset could be seen using another method. As shown in Figure 4.20A, when using flow cytometry, there was no significant difference in IFITM1 MFI between health and lupus nephritis in both IgMhi and IgMlo transitional B cells. In addition, it was found that there was no significant difference in IFITM1 MFI between health and lupus nephritis in both IgMhi and IgMlo naïve B cells, as displayed in Figure 4.20B. The observations regarding the similar expression of IFITM1 at the protein level in health and lupus nephritis initially observed using mass cytometry were also seen when using flow cytometry.

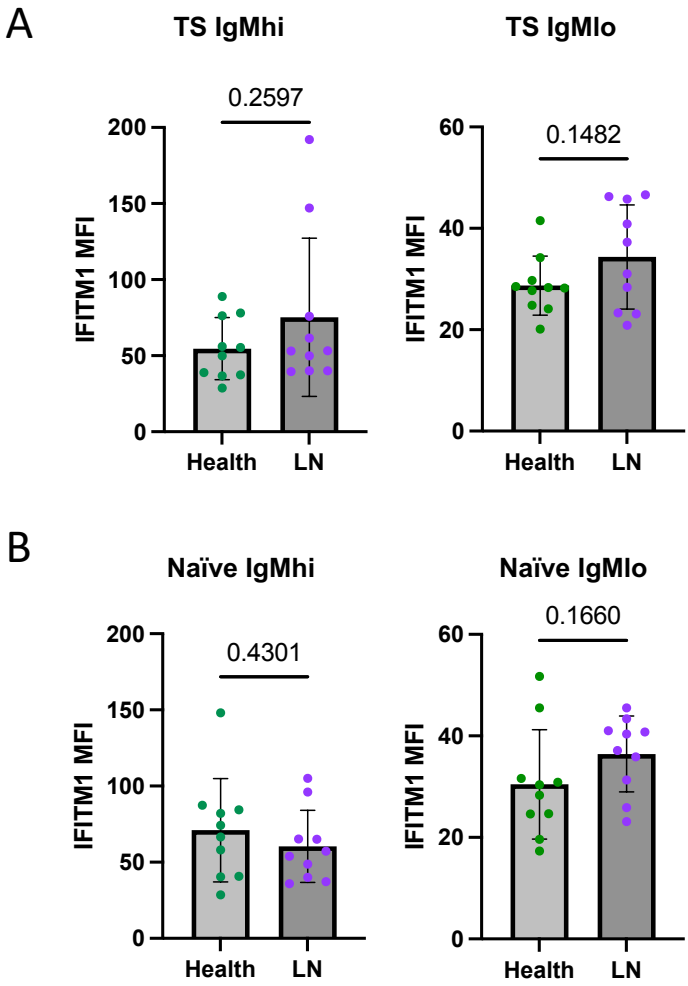

Figure 4.20: Comparison of IFITM1 expression in transitional and naïve B cells between health and lupus nephritis. IFITM1 mean fluorescence intensity (MFI) of IgMhi and IgMlo transitional (TS) **(A)** and naïve **(B)** B cells from healthy donors (n=10) and lupus nephritis patients (n=10). Comparisons were made using an un-paired t-test and statistical significance was deemed as $p<0.05$.

The data from this study show that IFITM1 expression is a feature of transitional B cells and can be used a marker for a group of early B cells with an interferon gene signature. It was previously identified that the groups of transitional and naïve B cells with an interferon gene signature accounted for a greater proportion of B cells in lupus nephritis than in health. Flow cytometry was used to ask whether that the IFITM1+ cells were more abundant in transitional and naïve cells from lupus nephritis patients compared to healthy donors and lupus patients without renal involvement. As shown

in Figure 4.21A, it was determined that there were significantly more IFITM1+ transitional and naïve B cells in lupus nephritis compared to healthy donors and non-nephritis lupus patients. There was no significant difference in IFITM1+ transitional cells between health and non-nephritis lupus and were significantly more naïve IFITM1+ cells in health compared to non-nephritis lupus. Additionally, it was found that in all patient cohorts there was a significantly greater percentage of IFITM1+ transitional B cells compared to IFITM1+ naïve B cells, as demonstrated in Figure 4.21B.

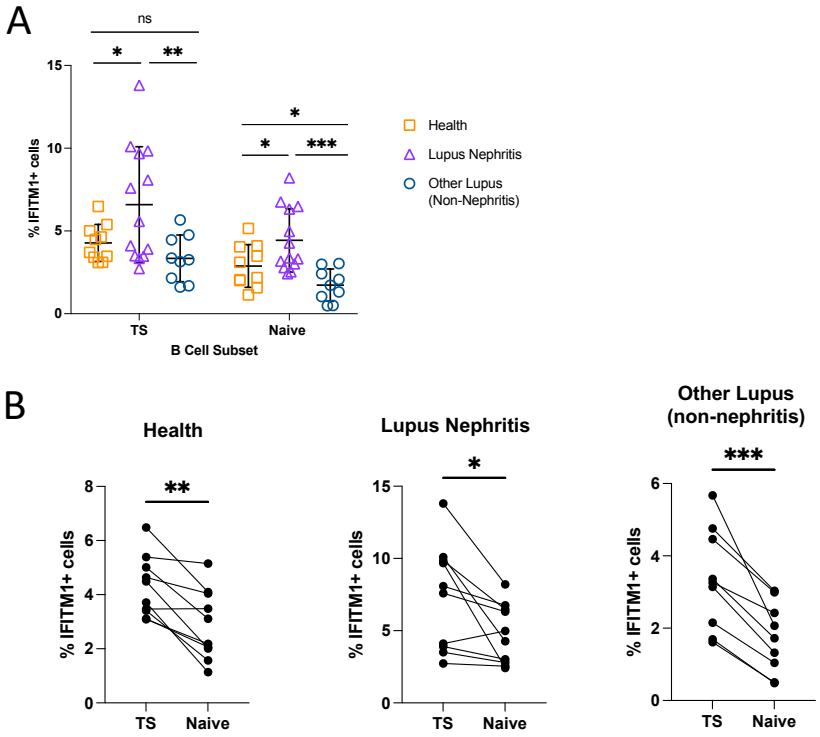

Figure 4.21: IFITM1+ cells in health and lupus. (A) Plot showing differences in percentage of IFITM1+ transitional (TS) and naïve B cells in healthy donors, lupus nephritis patients and lupus patients with no nephritis. Asterisks indicate statistical significance as calculated by paired t-test. Significant was deemed as $p<0.05$. ns; not significant. **(B)** Plots showing percentage of IFITM1+ cells in transitional B cells versus naïve B cells in various patient cohorts. For all plots paired data points are joined together by a solid black line. Asterisks indicate statistical significance as calculated by paired t-test. Significant was deemed as $p<0.05$. ns; not significant.

4.3.5 Investigation of protein expression of differentially expressed markers of early B cells with an interferon gene signature

In the previous chapter (3.3.6), it was found that the groups of transitional and naïve B cells with an interferon gene signature differentially expressed genes such as chemokine *CXCR4* and genes associated with activation such as *CD83* and *CD69* in healthy donors compared to lupus nephritis patients. This observation was made at the gene level and so the mass cytometry dataset was used to compare expression of CXCR4, CD83 and CD69 in B cell subsets in health versus lupus nephritis at the protein level. A 2-way ANOVA was run to determine if expression of CXCR4, CD83 and CD69 significantly varied across all B cell subsets in general between health and lupus nephritis. It was found that expression of these markers of interest was significantly different between B cell subsets ($p<0.0001$) as expected, shown in Table 4.2. However, in contrast to what was previously seen in chapter 3 at the gene level, there was no significant difference in expression between health and lupus nephritis.

Table 4.2: 2-Way ANOVA results comparing expression of CD69, CD83 and CXCR4 between B cell subsets (T1, T2, Naïve, aNAV, MZP, MZB1, MZB2, CSM IgA+, CSM IgA-, DN1 and DN2) and between the entire peripheral B cell pool in healthy donor versus lupus nephritis patient samples (disease status). Significance was deemed as $p<0.05$, indicated by *. Non-significant comparisons are denoted by 'ns'.

Marker	Variable	p-value	Significance
CD69	B Cell Subset	p<0.0001	****
	Disease Status	p=0.1305	ns
CD83	B Cell Subset	p<0.0001	****
	Disease Status	p=0.9044	ns
CXCR4	B Cell Subset	p<0.0001	****
	Disease Status	p=0.9375	ns

It was established that median CXCR4 expression was significantly greater in early B cell subsets, transitional and naïve, compared to MZB2 and both memory and double-negative subsets in healthy donor samples, demonstrated in 4.22A. The DN2 subset had the lowest CXCR4 expression. CD83 median expression was found to be highest in T2 and MZB1 cells in

healthy donors and naïve, aNAV, CSM IgA- and both double negative subsets were found to have significantly lower expression of CD83 compared to transitional and marginal zone subsets, shown in Figure 4.22B. CD69 median expression was highest in T2 cells compared to all subsets, except T1 and MZB1, and was lowest in DN1 cells, shown in Figure 4.22C.

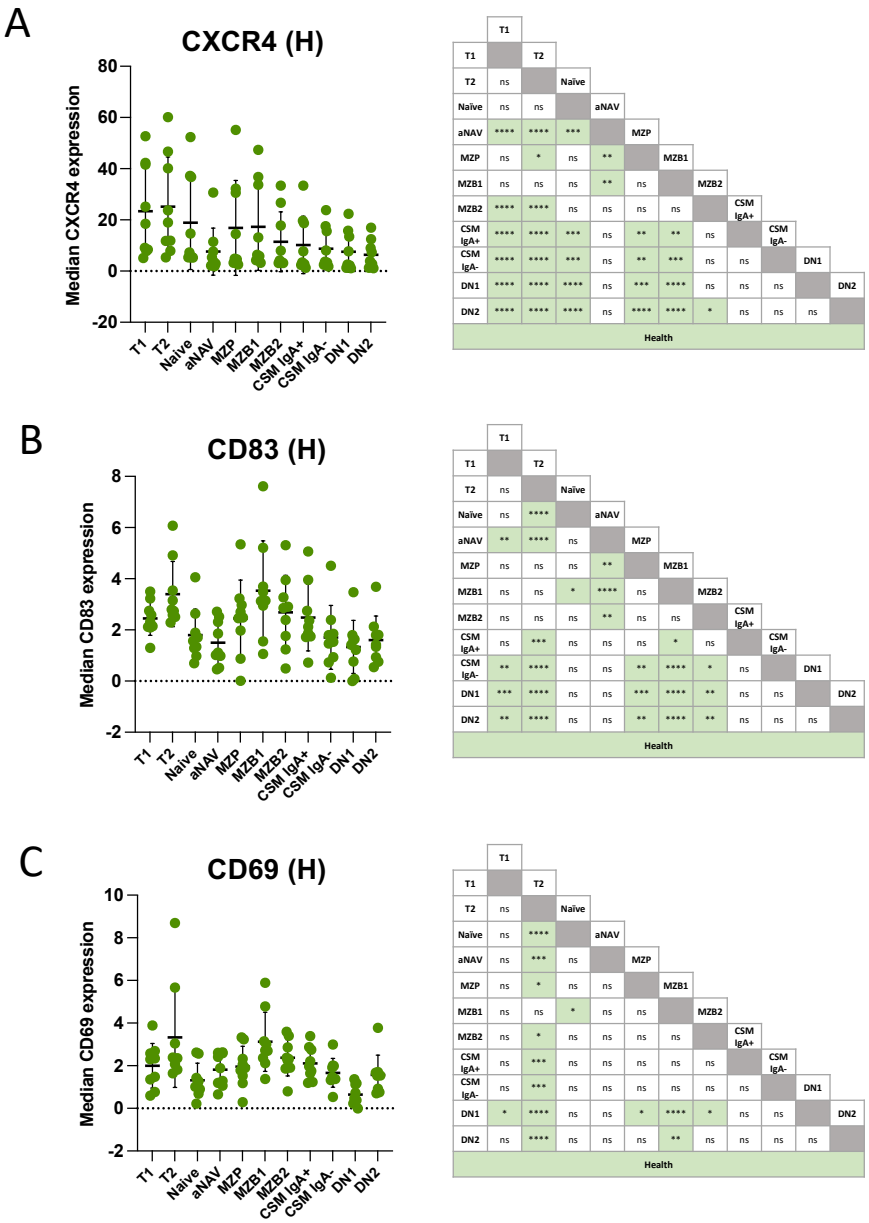

Figure 4.22: Expression of CXCR4, CD83 and CD69 in B cell subsets in healthy donors. Median expression of protein markers CXCR4 **(A)**, CD83 **(B)** and CD69 **(C)**, in CD19+ peripheral blood B cell subsets in n=9 healthy donor samples. On graphs, horizontal bars represent mean and error bars denote ±SD. Tables show significant differences between median protein expression between B cell subsets. Significance was calculated by 2-way ANVOA with Tukey's

multiple comparisons test. Significant differences between subsets are highlighted in green. Significant was deemed as $p<0.05$.

Transitional B cells were found to have the greatest median expression of CXCR4 in lupus nephritis patients compared to aNAV and most CD27+ subsets, except MZB1, as shown in Figure 4.23A. It was noted that B cells from three patients expressed CXCR4 far higher than the rest of the cohort, highlighting the heterogeneity of B cells in lupus nephritis. T2 cells were found to have the highest CD83 expression and overall transitional and marginal zone subsets expressed higher CD83 levels than CSM and double negative subsets, as demonstrated in Figure 4.23B. T2 B cells were also found the greatest expression of CD69 compared to all other subsets except T1 and MZB1 subsets, as shown in Figure 4.23C. Overall it was evident that transitional B cells expressed these markers of interest at significantly higher levels compared to antigen-experienced subsets. However, this data show that at the protein level, expression of these markers in early B cells do not differ between health and lupus nephritis.

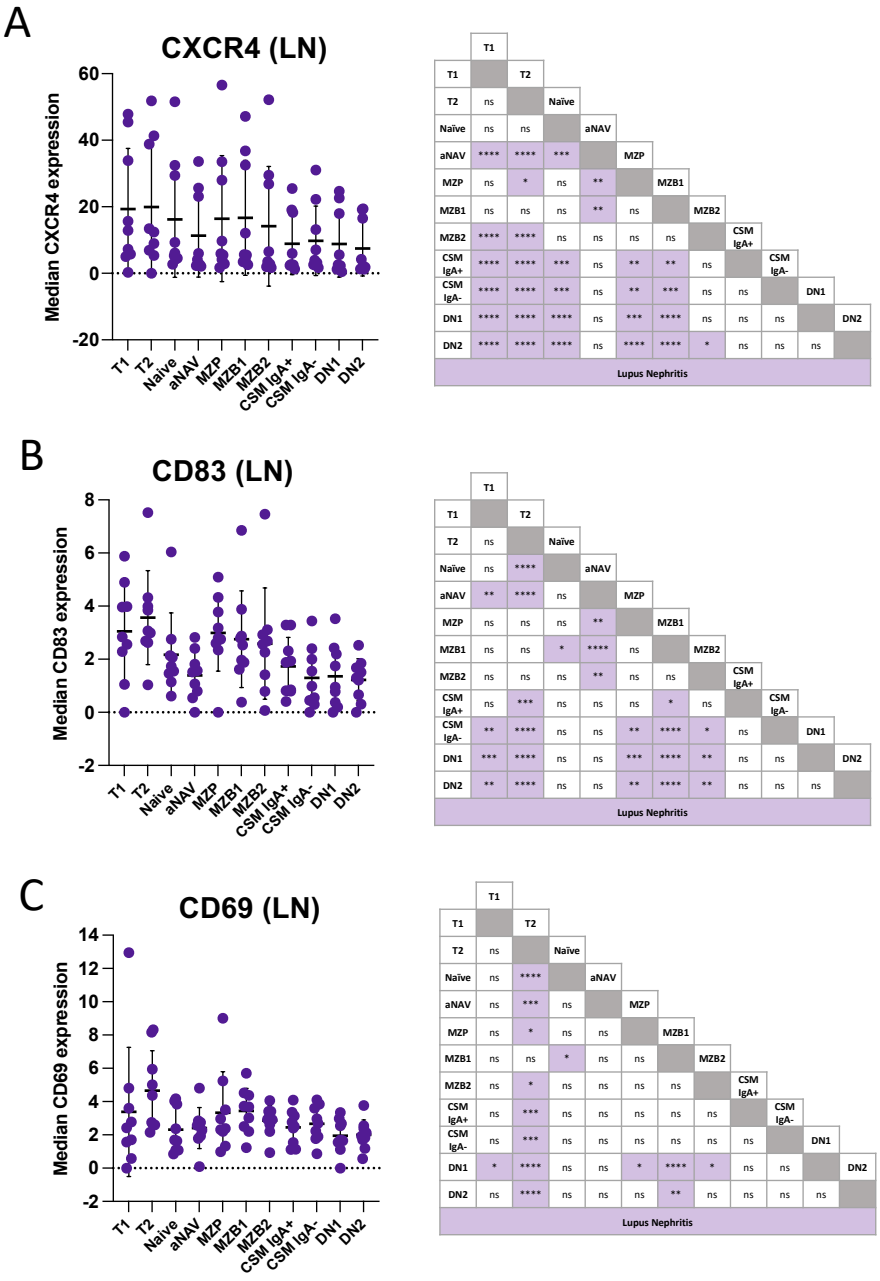

Figure 4.23: Expression of CXCR4, CD83 and CD69 in B cell subsets in lupus nephritis patients. Median expression of protein markers CXCR4 **(A)**, CD83 **(B)** and CD69 **(C)**, in CD19+ peripheral blood B cell subsets in n=9 lupus nephritis patient samples. On graphs, horizontal bars represent mean and error bars denote ±SD. Tables show significant differences between median protein expression between B cell subsets. Significance was calculated by 2-way ANVOA with Tukey's multiple comparisons test. Significant differences between subsets are highlighted in green. Significant was deemed as $p<0.05$.

4.4 Chapter 4 Summary

The data presented in Chapter 4 have demonstrated that expression patterns of ISG markers in transitional B cells, previously identified by single-cell RNA-sequencing (Chapter 3), are varied and are not always more prevalent in lupus nephritis B cells compared to health. A key finding from this dataset identified that expression of the protein IFITM1 is significantly greater in transitional B cells compared to all other peripheral B cell subsets and the level of expression is the same in health and lupus nephritis. Moreover, it was realized that the IgMhi subsets of transitional and naïve B cells expressed IFITM1 greater than their IgMlo equivalent subsets, as shown in summary Figure 4.24. IFITM1 expression was found to correlate with integrin β_7 expression.

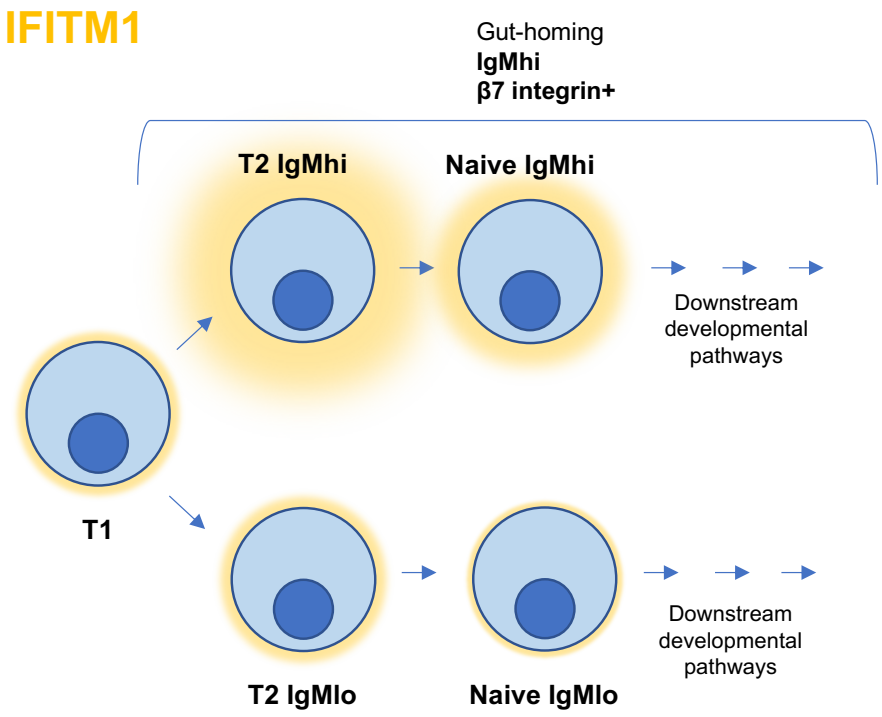

Figure 4.24: Summary of Chapter 4. Schematic diagram showing the subsets of peripheral blood B cells that express protein IFITM1. Yellow glow indicates level of expression relative to subsets shown on schematic diagram. T2 IgMhi B cells have the highest expression and naïve IgMlo have the lowest expression. Expression pattern shown is apparent for B cells from both healthy donors and lupus nephritis patients.

4.5 Discussion

This study has used mass cytometry to highlight differential expression of protein markers associated with interferon across peripheral blood B cell subsets in health and lupus nephritis. Two contrasting patterns in expression were observed, Whilst IFITM1 expression varied between subsets, these subset variations were consistent between health and lupus nephritis. In contrast MX1 and IRF7 were variable between subsets, but expression was significantly enhanced in across subsets in lupus nephritis.

As evidenced in 4.3.3, it was found that IFITM1 was predominantly expressed by transitional B cells, with T2 B cells having the highest IFITM1 expression across all B cell subsets in both healthy donors and lupus nephritis patients. The role of IFITM1 in healthy B cells is not well described, however there is evidence to suggest that IFITM1 has anti-proliferative properties (Evans et al., 1990; Yang et al., 2007). Therefore, it could be hypothesised that IFITM1 is expressed in transitional B cells and acts to regulate proliferation of the earliest peripheral B cell subset. IFITM1 is primarily known for its anti-viral properties whereby it restricts entry of several viruses including influenza A and SARS coronavirus (Huang et al., 2011). Wu et al. (2018) have described the expression of IFITM1, along with multiple other anti-viral genes, in healthy human embryonic stem cells and the potential for these genes to give protection to these cells at the earliest stages of development. This could suggest that the somewhat preferential expression of IFITM1 in the early, immature transitional B cells identified in this study could be a similar protective mechanism for these cells to allow successful B cell development in the periphery.

Whilst IFITM1 expression did not significantly differ between health and lupus nephritis, expression of both MX1 and IRF7 was found to be significantly higher in the lupus nephritis cohort compared to health. This observation is consistent with the literature that states interferon-inducible markers are more highly expressed in SLE compared to health (Baechler et al., 2003). However, as IFITM1 expression was comparable between cohorts it suggests that IFITM1 may have a role in healthy B cells.

Expression of MX1 and IRF7 between B cell subsets was found to be different in health versus lupus nephritis. The subset with the highest expression of both MX1 and IRF7 was the DN2 subset in healthy donors. Expression of MX1 and other ISGs in the DN2 subset has been previously described in both health and SLE (Jenks et al., 2018; Tull et al., 2021). Conversely, the subset with the greatest MX1 and IRF7 expression in lupus nephritis was found to be T1 cells. This supports the finding that groups of early B cells express interferon-stimulated markers and suggests that potentially type I interferon regulation in lupus nephritis is greater in early stages of peripheral B cell development as opposed to later in development at the DN2 stage.

This mass cytometry analysis combined with single-cell RNA-sequencing analysis, previously highlighted in Chapter 3, showed that the groups of transitional and naïve B cells with an interferon gene signature are not a distinct subset. By removing ISGs from the single-cell RNA-sequencing clustering pipeline, it was found that the groups of cells with an interferon signature previously clustered together solely based on their expression of ISGs, without ISGs contributing to the clustering these cells clustered with respective T1, T2 or naïve subsets. This suggests that groups of early B cell subsets are possibly encountering an interferon-rich environment and subsequently upregulate the expression of ISGs, or they may express ISGs as part of an intrinsic protection against viruses (Wu et al., 2018).

IFITM1 expression across all B cell subsets was found to correlate with integrin β_7 expression, however this was not the case with MX1 expression, which did not correlate with β_7. This suggests that different interferon markers do not necessarily correlate with the same trajectories or the same subsets of cells. For instance, Wu et al. (2018) previously identified the association of IFITM1 with an interferon gene signature in stem cells but found MX1 to be negatively expressed in those cells.

Flow cytometry analysis revealed a link between IFITM1, integrin β_7 and IgM. It was found that IFITM1+ transitional and naïve B cells had higher integrin β_7 MFI compared to IFITM1- transitional and naïve B cells in both healthy donors and lupus nephritis patients. Additionally, it was found that IgMhi transitional and naïve B cells have

higher IFITM1 MFI compared to IgMlo transitional and naïve B cells in both health and lupus nephritis samples. There is a known association between integrin β_7 and the IgMhi B cell developmental trajectory which leads to the development of marginal zone B cells (Tull et al., 2021). The data presented in this study suggests that IFITM1 may be another potential marker of the IgMhi branch of B cell development.

Previously described in Chapter 3, the groups of transitional and naïve cells with an interferon signature were twice as abundant in lupus nephritis compared to health. Flow cytometry was used to determine if this was a feature of all types of lupus or if it was a feature of lupus nephritis specifically. It was found that IFITM1+ transitional and naïve B cells were significantly more abundant in lupus nephritis patients compared to other, non-nephritis lupus patients and healthy donors. This suggests that early B cells expressing interferon markers are a feature of nephritis and therefore may be significant in nephritis pathology.

It was determined that there are significantly more IFITM1+ cells in the transitional subset compared to the naïve subset in healthy donors, lupus nephritis patients and non-nephritis lupus patients. This observation was consistent with a finding reported by Liu et al. (2019) which stated that transitional B cells had a greater responsiveness to type I interferon receptor and subsequently expressed ISGs more than naïve B cells in SLE. The expression of ISGs was found to promote survival in transitional B cells in in SLE (Liu et al., 2019). Therefore, it is possible that the presence of IFITM1+ transitional cells may contribute to cell survival.

Both the percentage of IFITM1+ cells and IFITM1 MFI were measured for the flow cytometry analysis. The percentage of IFITM1+ cells was used to assess protein of interest expression in any cells that expressed IFITM1, regardless of the level of expression. The IFITM1 MFI was used to measure which groups of cells expressed IFITM1 at the greatest level. The percentage of IFITM1+ cells was found to be greater in lupus nephritis compared to health. In other words, there were more cells within the transitional and naïve populations that expressed IFITM1 in lupus compared to

health. But the level of expression of IFITM1 protein, inferred by IFITM1 MFI, did not differ between health and lupus on those cells that expressed the protein.

CXCR4 expression was previously found to be greater in lupus nephritis compared to health at the gene level in naïve B cells with an interferon gene signature, described in Chapter 3, and has been seen to be overexpression collectively in all B cells at the protein level in SLE (Zhao et al., 2017). In contrast, in this study no significant difference in CXCR4 protein expression between health and lupus nephritis was observed, but it was noted that CXCR4 expression was a feature of transitional B cells in lupus nephritis and health. Furthermore, expression of CD83 and CD69 was found to be significantly higher in transitional subsets but no different between health and lupus nephritis. This suggests that early B cells in lupus nephritis are not more activated than those in health according to protein expression. The discrepancy between the expression of the markers at RNA and protein levels is not clear.

Overall, this study has shown that expression of proteins of ISGs are differentially expressed across B cell subsets. Additionally, IFITM1 expression is predominantly a feature of transitional B cells and correlates with integrin β_7 and IgM expression, suggesting a possible link to the IgMhi branch of peripheral blood B cell developmental.

5 Changes in B cell subset proportions in lupus nephritis at different disease severities

5.1 Introduction

Changes in the frequencies of peripheral B cell subsets in lupus nephritis have often been reported in the literature (Landolt-Marticorena et al., 2011; Simon et al., 2016; Tipton et al., 2015; Tull et al., 2021; Zhu et al., 2018). It has been found that changes in the proportions of B cell subsets occur at all stages of peripheral B cell development in the blood from the earliest subsets, the transitional cells, through to the terminally differentiated subsets, such as marginal zone B cells. It has been reported that there is an increase in CD24hiCD38hi B cells in SLE compared to health (Simon et al., 2016). Additionally, it has been found that there is a reduction in the percentage of T2 IgMhi cells in SLE compared to health (Tull et al., 2021). Other B cell subsets that make up the IgMhi developmental trajectory including marginal zone B cells and their precursors have also been found to be reduced in patients with lupus nephritis compared to healthy donors (Tull et al., 2021; Zhu et al., 2018). In addition, it has been established that populations of B cells belonging to the extrafollicular pathway, such as aNAV and DN2 cells, are expanded in lupus nephritis (Jenks et al., 2018; Tipton et al., 2015).

Whilst several of these changes in have been observed in lupus nephritis, it is not fully understood whether these changes are correlated with disease flares or if they are a permanent feature of the peripheral B cell compartment in individuals with SLE regardless of whether they are flaring or not.

For this study, flow cytometry was used to compare the proportions of peripheral blood B cell subsets in lupus nephritis at different disease severities compared to health. This study used paired blood samples from lupus nephritis patients (n=7), which were taken at two different timepoints. One sample was from a period in which the patient was flaring and the other was from a period where the patient's disease was stable. In the clinic prior to experimental protocols, the "flare" samples were defined as those where the patient had a high SLEDAI score (>11), and "stable"

samples were those where the patient had a lower SLEDAI score of 5 or less. Additionally, urine protein levels, dsDNA titres and complement level were also assessed to assist with categorising the samples as either “flare” or “stable”. Urine protein was inferred by protein:creatinine ratio. “Flare” samples were those with higher urine protein and dsDNA titres, and lower complement levels. “Stable” samples had lower urine protein and dsDNA titres and usually had normal complement levels.

There were a few limitations to this dataset. It was not possible to have an equal length of time between when flare and stable samples were taken due to the heterogeneity of the disease course itself, the different treatment regimens patients were on and the differences in the responses to treatment. The mean time between flare and stable samples was 24.7 months. Whilst all patients included in this study had had nephritis confirmed via a kidney biopsy, the periods after diagnosis in which they were flaring differed simply because patterns of flares are not the same from patient to patient. It was ensured that all samples included were from patients who were not on any biologic treatment, but due to the heterogeneity of lupus, even individuals on the exact same medication may respond to treatment differently thus may go for longer periods of time without experiencing any flares. Additionally, the time in which the paired samples were taken were limited to when the patients visited the clinic, it cannot be guaranteed that all patients had an appointment at the exact same time during a flare or the exact same time after a flare when they clinically improved.

5.2 Aims

- Investigate the changes in B cell subset proportions in lupus nephritis patients at different stages of disease activity

5.3 Results

5.3.1 Investigating changes in proportions of transitional B cells

In this study, flow cytometry was used to compare the proportions of all peripheral B cell subsets from healthy donors (n=8) and lupus nephritis patients (n=7). This dataset included paired samples from each of the lupus nephritis patients, which were taken at different timepoints at different disease severities. One sample was taken when a patient was in a period of disease flare and the other was taken when their disease was stable. Peripheral B cell subsets were gated in the FlowJo software using the gating strategy displayed in Figure 2.1 in 2.5.5. in Materials and Methods.

The earliest subset of B cells found in the peripheral blood are the transitional B cells, which were identified as CD27-IgD+CD10+ B cells. It has previously been reported in the literature that in individuals with severe SLE, there are an increase in CD24hiCD38hi B cells compared to health (Simon et al., 2016). Data from this study did not reveal this same significant increase in T1 B cells in lupus nephritis, however, as shown in Figure 5.1A, the mean percentage of T1 cells in stable lupus nephritis is greater than that of health, albeit not significantly different. As displayed in Figure 5.1A, the mean percentage of T1 B cells from healthy donors and lupus nephritis patients during periods of flare were comparable. Furthermore, when comparing the proportion of T1 cells at different disease severities in lupus nephritis, it was found that there was a significantly greater percentage of T1 cells in stable disease compared to flare, demonstrated in Figure 5.1A.

A reduction in T2 IgMhi B cells in the peripheral blood of patients with lupus nephritis has previously been described by Tull et al. (2021). As shown in Figure 5.1B, the mean percentage of T2 IgMhi cells in lupus nephritis patients during periods of flare was slightly lower compared to the mean percentage of T2 IgMhi cells in health, however

this was not a statistically significantly difference. It was found that the proportions of T2 IgMhi cells in health and stable lupus nephritis samples were not significantly different, suggesting that levels of T2 IgMhi cells in stable lupus nephritis are comparable to that of health. When comparing data from the paired lupus nephritis samples, it was noted that there was a trend towards an increase in the percentage of T2 IgMhi cells when lupus nephritis patients have stable disease compared to when they are flaring, as displayed in Figure 5.1B. However, this was not the case for all paired lupus samples thus this trend was not significant ($p=0.0899$).

Changes in the proportions of T2 IgMlo B cells in lupus nephritis and any links to disease severity have not been reported in the literature thus far. Data presented in Figure 5.1C show that there is a lower mean percentage of T2 IgMlo cells in lupus nephritis flare samples compared to health, but this difference did not meet the $p<0.05$ threshold for significance ($p=0.07$). Additionally, there was no difference in the percentage of T2 IgMlo cells between health and stable lupus nephritis. Moreover, it was found that there was a significantly smaller proportion of T2 IgMlo cells during disease flare compared to stable disease, shown in Figure 5.1C. The proportion of T2 IgMlo cells in stable lupus samples was over twice as much as the proportion of these cells in flare lupus samples.

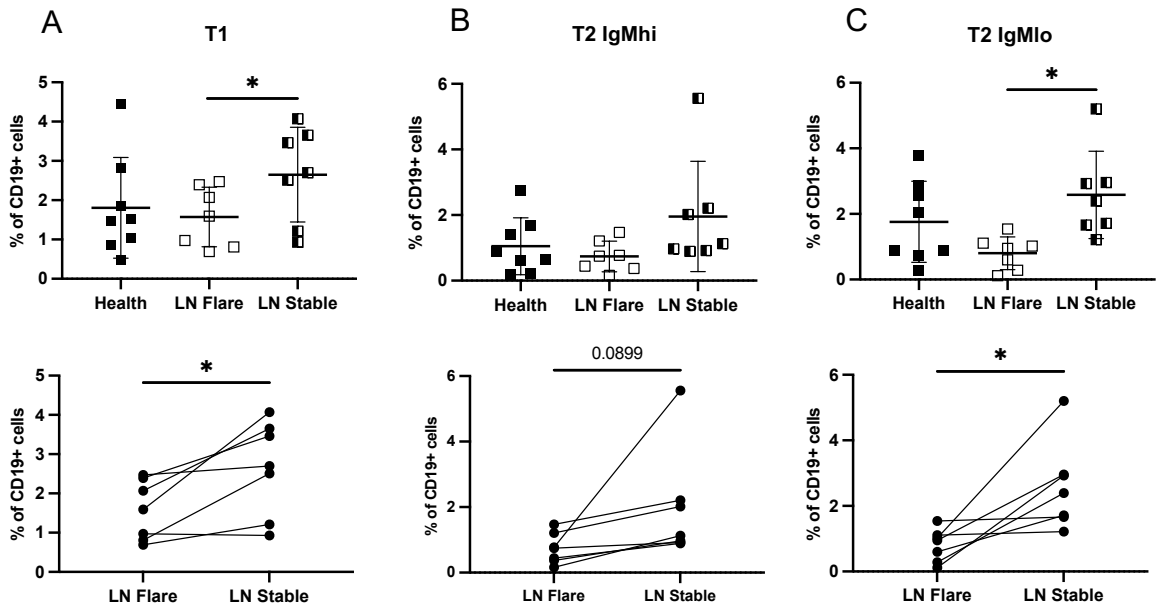

Figure 5.1: Proportions of T1 and T2 B cells from peripheral blood in health and lupus nephritis at different disease severities. Top panel shows proportions of transitional B cell subsets as a percentage of total CD19+ B cells in healthy donors (n=8) and lupus nephritis patients (n=7). Samples from lupus nephritis patients are paired samples taken at periods of disease flare (LN Flare) and stable disease (LN Stable). Bottom panel shows comparison of the proportion of transitional B cell subsets from n=7 lupus nephritis patients during different disease severities. Paired samples are connected by a solid black line. Asterisks denote statistical significance ($p<0.05$). Comparisons between health and lupus were conducted by an unpaired t-test and comparisons between LN flare and LN stable were conducted by a paired t-test. **(A)** T1. **(B)** T2 IgMhi. **(C)** T2 IgMlo.

T2 B cells have been found to give rise to a population of CD10- transitional B cells known as T3 B cells (Palanichamy et al., 2009), these cells can be distinguished from CD10- naïve B cells based on their inability to extrude rhodamine or MitoTracker^{R} green dyes due to the T3 population's lack of expression of the ABCB1 transporter (Wirths & Lanzavecchia, 2005). T3 B cells have a CD27-IgD+CD10-ABCB1- surface phenotype. In mice, it has been proposed that T3 B cells may resemble anergic B cells (Merrell et al., 2006) as well as that they are the precursors of naïve B cells (Allman et al., 2001). However, it is not entirely evident what the role of these T3 B cells is in humans. It has been reported that two groups of T3 B cells exist and can be

distinguished based on their expression of CD45RB into T3 CD45RBhi and T3 CD45RBlo. Additionally, surface IgM expression correlates with CD45RB expression on these cells and so CD45RBhi T3 cells are also IgMhi and CD45RBlo T3 cells are IgMlo (Tull et al., 2021).

In this study, there was a trend towards the mean percentage of T3 CD45RBhi cells in both flaring and stable lupus nephritis being reduced in comparison to healthy donors, shown in Figure 5.2A. This observation concurs with a previous observation made by Tull et al. (2021) whereby it was found that T3 CD45RBhi cells were significantly reduced in lupus nephritis regardless of disease severity. Furthermore, there was no significant difference between the mean percentage of T3 CD45RBhi cells in flare versus stable lupus nephritis. In contrast, the proportions of the T3 CD45RBlo subset appeared to be greater in lupus nephritis compared to health. As shown in Figure 5.2B, the proportion of T3 CD45RBlo cells was significantly greater in lupus nephritis flare samples compared to healthy donors. The same observation was made when comparing stable lupus nephritis with health, however this was not statistically significant. Similar to what was seen in CD45RBhi T3 cells, the proportion of CD45RBlo T3 cells was not different between flare and stable disease, demonstrated in Figure 5.2B.

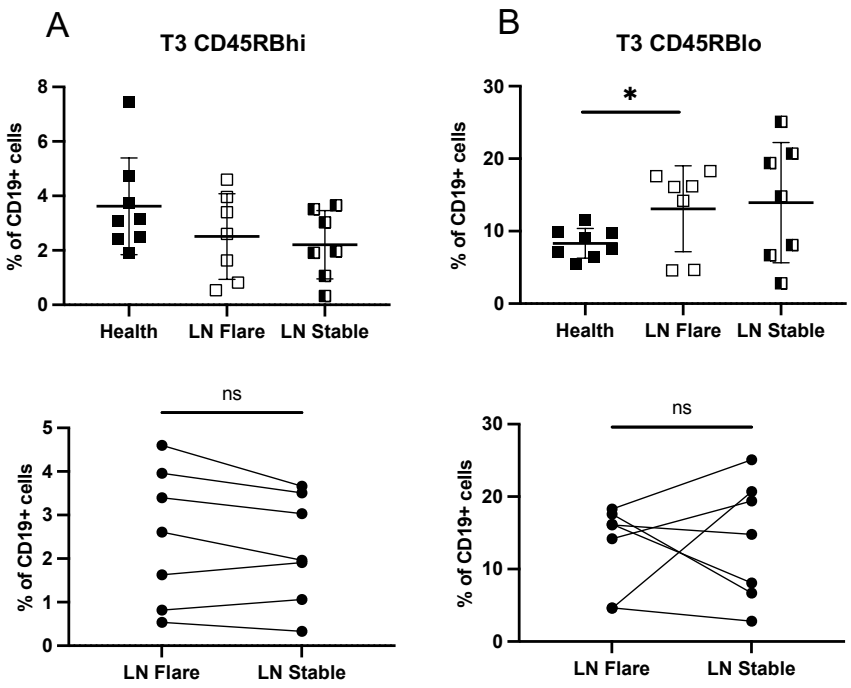

Figure 5.2: Proportions of T3 B cells from peripheral blood in health and lupus nephritis at different disease severities. Top panel shows proportions of T3 B cell subsets as a percentage of CD19+ B cells in healthy donors (n=8) and paired lupus nephritis patients (n=7 taken at periods of disease flare (LN Flare) and stable disease (LN Stable). Bottom panel shows comparison of the proportion of T3 B cell subsets from lupus nephritis patients during different flare and stable disease. Paired samples are connected by a solid black line. Asterisks denote statistical significance ($p<0.05$). Comparisons between health and lupus were conducted by an unpaired t-test and comparisons between LN flare and LN stable were conducted by a paired t-test. **(A)** T3 CD45RBhi. **(B)** T3 CD45RBlo.

5.3.2 Investigating changes in proportions of naïve B cells

Naïve B cells are the largest subset of B cells making up approximately 60% of all CD19+ B cells in peripheral blood (Morbach et al., 2010). In this study, naïve B cells were classified as CD27-IgD+CD10-CD45RB-RH123-. Changes to the proportion of the naïve B cell compartment in lupus nephritis at varying disease severities have not been well described. Flow cytometry data from Tull et al. (2021) established that the entire naïve B cell population is significantly reduced in both lupus nephritis and other non-nephritis forms of lupus compared to healthy donors. This study has investigated the changes in the proportions of sub-classified naïve B cells (naïve IgMhi and naïve IgMlo cells) to determine whether the reduction in naïve B cells in SLE previously identified by Tull et al. (2021) is a feature of a specific sub-population of naïve B cells or of all naïve B cells in general. In addition, Tull et al. (2021) also highlighted the reduction in the proportion of multiple B cell subsets belonging to the IgMhi developmental pathway in lupus nephritis and so it was hypothesised that naïve IgMhi cells would also be reduced in lupus nephritis compared to health.

In agreement with the hypothesis, data from this study showed that the mean percentage of naïve IgMhi B cells was significantly lower in samples from lupus nephritis patients during periods of flare compared to the mean percentage of naïve IgMhi cells in healthy donors, as shown in figure 5.3A. In contrast, it was found that the proportion of naïve IgMhi cells from lupus nephritis patients at periods of stable disease was significantly greater than the proportion of naïve IgMhi cells in health. When comparing the proportion of naïve IgMhi cells in lupus nephritis at different disease severities, it was determined that this subset of naïve B cells was significantly reduced in samples taken when patients where flaring compared to when their disease was stable, as demonstrated in Figure 5.3A. These observations indicate that the reduction in naïve IgMhi cells in lupus nephritis occurs when disease activity is highest, during periods of flare.

A similar observation to what was found regarding the naïve IgMhi subset was found in the naïve IgMlo subset. Data presented in Figure 5.3B showed that there was a significantly smaller proportion of naïve IgMlo B cells in lupus nephritis flare samples

compared to health. However, there was no significant difference between the proportion of naïve IgMlo cells between stable lupus nephritis and health. Additionally, when comparing the percentage of naïve IgMlo B cells between the paired lupus nephritis samples it was found that there was a significantly smaller percentage of naïve IgMlo cells in flare samples compared to stable disease samples, as demonstrated in Figure 5.3B.

It has been reported that there is an increase in activated naïve (aNAV) B cells in SLE compared to health (Tipton et al., 2015). aNAV cells have previously been described as the precursors to DN2 B cells (Jenks et al., 2018). As demonstrated in Figure 5.3C, the mean percentage of aNAV cells was greater in lupus nephritis flare samples compared to health, although this was not statistically significant. There was no significant difference between the proportion of aNAV cells between health and samples from lupus nephritis patients where their disease was stable. Furthermore, there was a trend towards the proportion of aNAV cells from stable lupus nephritis samples to be reduced more than the proportion of these cells from flaring disease, as shown in Figure 5.3C, however this was not deemed as statistically significant.

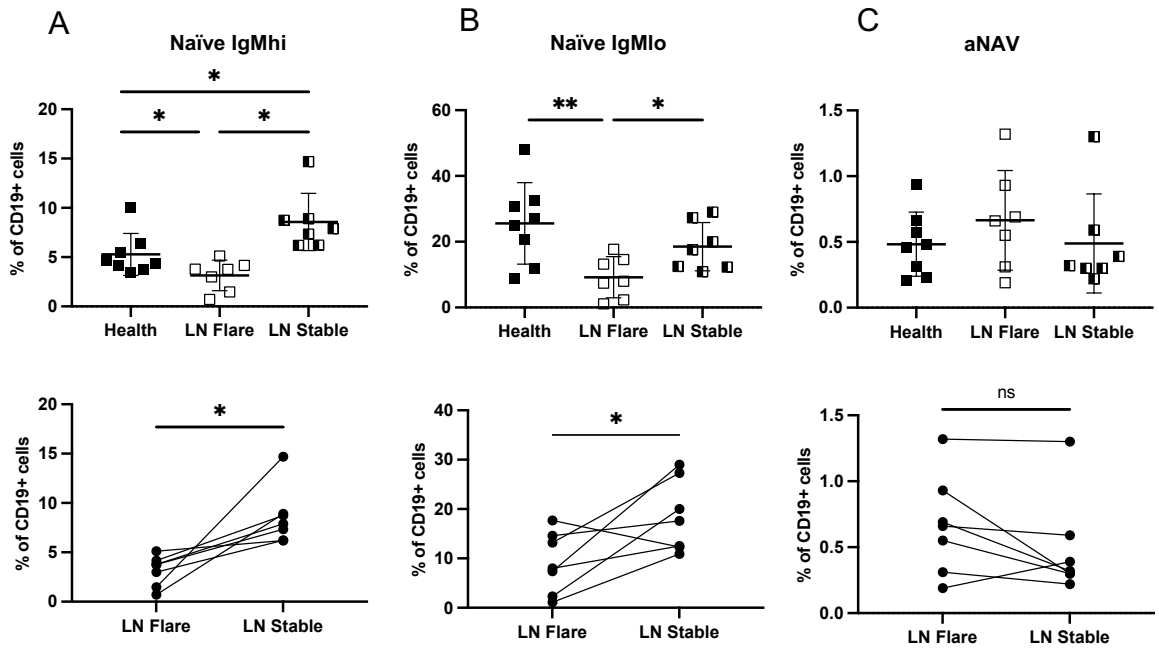

Figure 5.3: Proportions of naïve and activated naïve B cells from peripheral blood in health and lupus nephritis at different disease severities. Top panel shows proportions of naïve and activated naïve B cell subsets as a percentage of CD19+ B cells in healthy donors (n=8) and lupus nephritis patients (n=7). Lupus nephritis samples are paired samples and were taken at periods of disease flare (LN Flare) and stable disease (LN Stable). Bottom panel shows comparison of the proportion of naïve and activated naïve B cell subsets from lupus nephritis patients during different flare and stable disease. Paired samples are connected by a solid black line. Asterisks denote statistical significance ($p<0.05$). Comparisons between health and lupus were conducted by an unpaired t-test and comparisons between LN flare and LN stable were conducted by a paired t-test. **(A)** Naïve IgMhi. **(B)** Naïve IgMlo. **(C)** aNAV (activated naïve).

5.3.3 Investigating changes in proportions of marginal zone B cells and their precursors

Altered frequencies of marginal zone B cells and their precursors in SLE have been reported in the literature and it has been established that marginal zone B cells are significantly reduced in lupus nephritis compared to health in peripheral blood (Siu et al., 2022; Tull et al., 2021; Zhu et al., 2018). However, it is not known whether the reduction in the proportion of marginal zone B cells is a feature of lupus nephritis at any disease severity, or whether it is only evident during disease flares. In this study, marginal zone B cells were gated as CD27+IgD+IgM+CD1c+ B cells, as shown in the flow cytometry gating strategy in Figure 2.1 in 2.5.5. in Materials and Methods.

As displayed in Figure 5.4A, MZP cells as a percentage of all CD19+ cells were significantly reduced in lupus nephritis flares compared to health. It was noted that there was no significant difference between the proportion of MZP between health and samples during stable lupus nephritis. Furthermore, the data presented in Figure 5.4A suggested that the mean percentage of MZP cells increased upon disease stability in lupus nephritis after a period of flare, however this was not statistically significant.

It was found that the mean percentage of marginal zone B cells in health, which was approximately 7%, was significantly greater than the mean percentages of marginal zone cells in both flare and stable lupus nephritis samples, which were 2.25% and 2.02%, respectively, shown in Figure 5.4B. It was determined that there was no significant difference between the proportion of marginal zone B cells in lupus nephritis flare compared to when patients were stable. The data presented in Figure 5.4 suggest that marginal zone B cells are significantly reduced in lupus nephritis compared to health regardless of whether a patient is flaring or not.

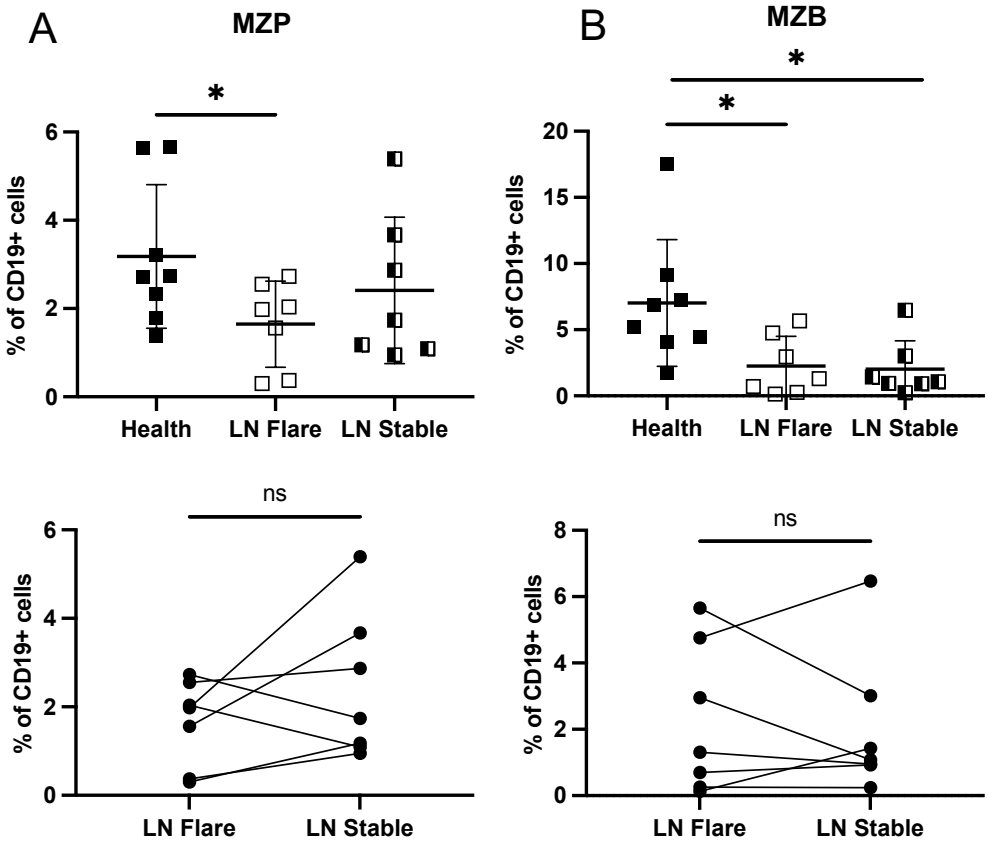

Figure 5.4: Proportions of marginal zone precursors and marginal zone B cells from peripheral blood in health and lupus nephritis at different disease severities. Top panel shows proportions of marginal zone precursors (MZP) and marginal zone B (MZB) cells as a percentage of CD19+ B cells in healthy donors (n=8) and lupus nephritis patients (n=7). Lupus nephritis samples are paired samples and were taken at periods of disease flare (LN Flare) and stable disease (LN Stable). Bottom panel shows comparison of the proportion of MZP and MZB subsets from lupus nephritis patients during different flare and stable disease. Paired samples are connected by a solid black line. Asterisks denote statistical significance ($p<0.05$). Comparisons between health and lupus were conducted by an unpaired t-test and comparisons between LN flare and LN stable were conducted by a paired t-test. **(A)** MZP. **(B)** MZB.

5.3.4 Investigating changes in proportions of memory B cells

Alterations in the frequency of memory B cells in lupus nephritis is not well understood. For the purposes of this study, class-switched memory B cells were identified as CD27+IgD-IgM- cells. A previous study identified a reduction in the proportion of class-switched memory B cells in newly diagnosed SLE patients compared to SLE patients on treatment and healthy donors (Peng et al., 2020). All lupus nephritis patients in this study were on active treatment and so it was of interest to investigate whether the proportion of class-switched memory B cells varied between different disease activity levels.

The data displayed in Figure 5.5A indicate that there is a trend towards the mean percentage of class-switched memory B cells is increased in four out of seven of the lupus nephritis patient samples during flares compared to health, but this was not the case for all lupus nephritis samples and so it was not found to be statistically significant. There was no significant difference between the proportion of class-switched memory B cells in stable lupus nephritis compared to health, shown in Figure 5.5A. The proportion of the class-switched memory subset appeared to be greater in lupus flares compared to stable lupus, but the data did not meet the $p<0.05$ threshold for significance ($p=0.089$).

IgM-only B cells are thought to be a group of pre-switched memory B cells that are yet to undergo class-switched recombination. They have a surface phenotype of CD27+IgD-IgM+. Changes in the abundance of IgM-only memory B cells in lupus nephritis has not previously been reported in the literature. In this study, it was found that there was a significant decrease in the proportion of the IgM-only subset in stable lupus nephritis compared to health, as demonstrated in Figure 5.5B. Moreover, there was no significant difference between the proportion of IgM-only cells in lupus nephritis flare compared to health. As shown in Figure 5.5B, there appeared to be a increase in the frequency of IgM-only cells in lupus flare samples compared to stable lupus samples, however this was difference was not statistically significant ($p=0.0753$).

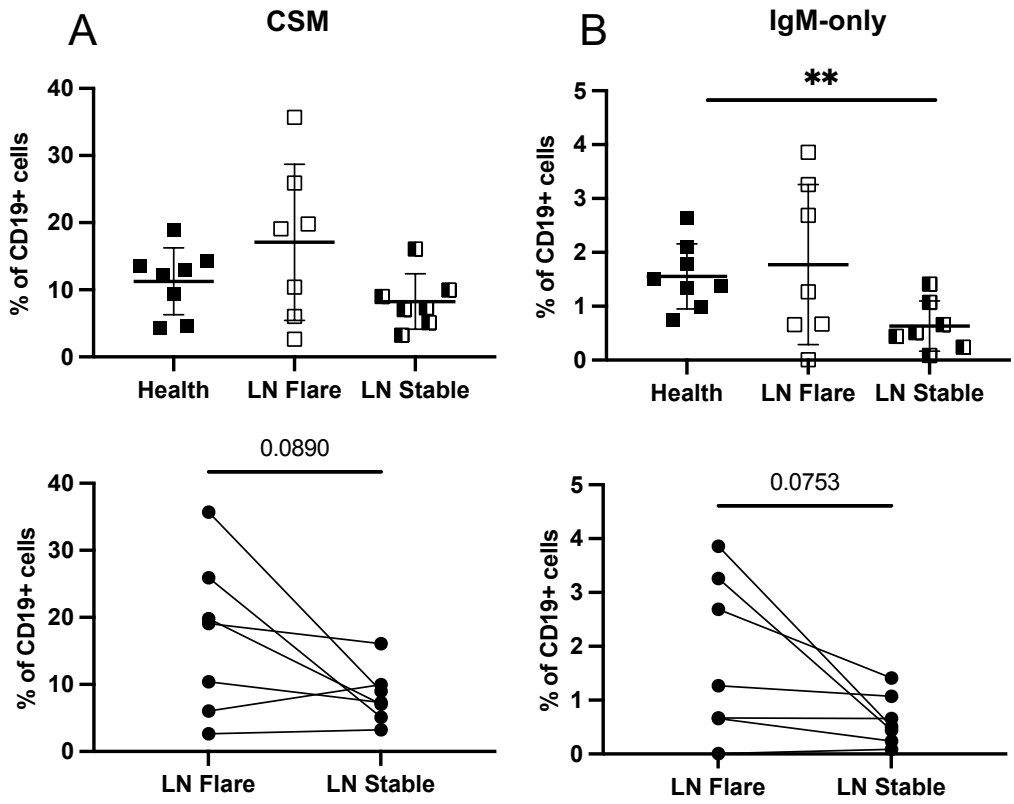

Figure 5.5: Proportions of class-switched and IgM-only memory B cells from peripheral blood in health and lupus nephritis at different disease severities. Top panel shows proportions of class-switched memory (CSM) and IgM-only B cell subsets as a percentage of total CD19+ B cells in healthy donors (n=8) and lupus nephritis patients (n=7). Samples from lupus nephritis patients are paired samples taken at periods of disease flare (LN Flare) and stable disease (LN Stable). Bottom panel shows comparison of the proportion of CSM and IgM-only B cell subsets from n=7 lupus nephritis patients during different disease severities. Paired samples are connected by a solid black line. Asterisks denote statistical significance ($p<0.05$). Comparisons between health and lupus were conducted by an unpaired t-test and comparisons between LN flare and LN stable were conducted by a paired t-test. **(A)** Class-switched memory (CSM). **(B)** IgM-only.

5.3.5 Investigating changes in proportions of double negative B cells

Double negative B cells, particularly the DN2 subset, are the B cell subset most associated with SLE. This subset of cells, sometimes referred to as atypical memory cells, are known to be CD27-IgD-. Several markers such as CD11c, CD21, CD24 and CXCR5 are commonly used to distinguish DN1 and DN2 cells. For this study, DN1 cells were defined as CD27-IgD-CD21+CD24+ and DN2 cells were defined as CD27-IgD-CD21-CD24-. DN1 are known to represent the greatest proportion of double negative B cells in health, whereas DN2 B cells are the largest double negative subset in SLE (Jenks et al., 2018).

In this study, it was found that there was no significant difference in the proportion of DN1 cells in both flare and stable lupus nephritis compared to health, as displayed in Figure 5.6A. In several of the paired lupus samples there was a greater proportion of DN1 cells in lupus flares compared to stable lupus, however a paired t-test determined this observation and not significant.

The DN2 B cell subset is known to be greatly expanded in peripheral blood in patients with SLE (Jenks et al., 2018; Wei et al., 2007). DN2 B cells are derived from aNAV B cells and have been proposed as the precursors to autoreactive plasmablasts (Jenks et al., 2018; Tipton et al., 2015). The observations made in this study about the differences in the proportions of DN2 B cells in SLE agreed with what has been published in the literature. It was noted that the mean percentage of DN2 B cells was significantly greater in both lupus nephritis flare and stable lupus nephritis samples compared to health, as shown in Figure 5.6B. The proportion of DN2 cells in lupus flares was over ten times greater than the proportion of DN2 B cells in health. Furthermore, it was found that the mean percentage of DN2 cells in stable lupus was smaller than the mean percentage of DN2 cells in lupus nephritis flares, as displayed in Figure 5.6B. This observation did not meet the $p<0.05$ threshold for significance ($p=0.0837$) but the data suggest that when SLE disease activity is lowered after a flare, the proportion of DN2 cells goes down.

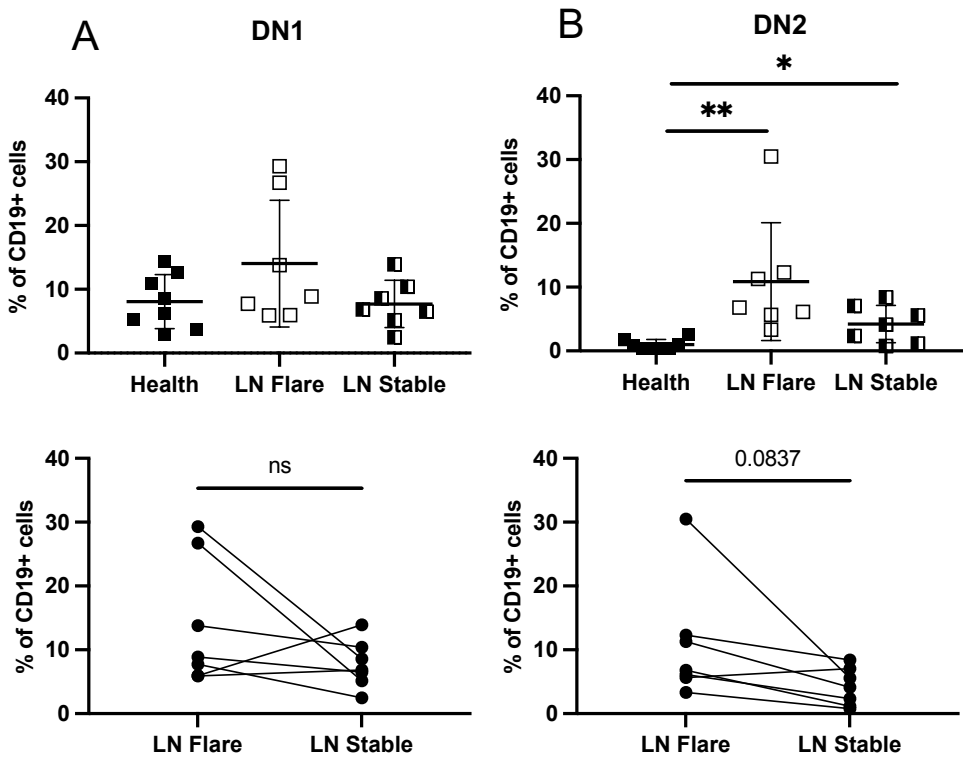

Figure 5.6: Proportions of double negative B cells from peripheral blood in health and lupus nephritis at different disease severities. Top panel shows proportions of DN1 and DN2 B cell subsets as a percentage of total CD19+ B cells in healthy donors (n=8) and lupus nephritis patients (n=7). Samples from lupus nephritis patients are paired samples taken at periods of disease flare (LN Flare) and stable disease (LN Stable). Bottom panel shows comparison of the proportion of DN1 and DN2 B cell subsets from n=7 lupus nephritis patients during different disease severities. Paired samples are connected by a solid black line. Asterisks denote statistical significance ($p<0.05$). Comparisons between health and lupus were conducted by an unpaired t-test and comparisons between LN flare and LN stable were conducted by a paired t-test. **(A)** DN1. **(B)** DN2.

5.4 Chapter 5 Summary

The data presented in Chapter 5 reveals changes in the abundance of peripheral blood B cell subsets in lupus nephritis at different disease severities. Whilst the sample size for this experiment is small, some interesting trends were noted. Subsets along the IgMhi developmental trajectory were notably decreased during lupus flares and subsets belonging to the extrafollicular pathway, namely aNAV and DN2, were increased during lupus flares. A schematic diagram summarising the changes observed in this study is presented in Figure 5.7.

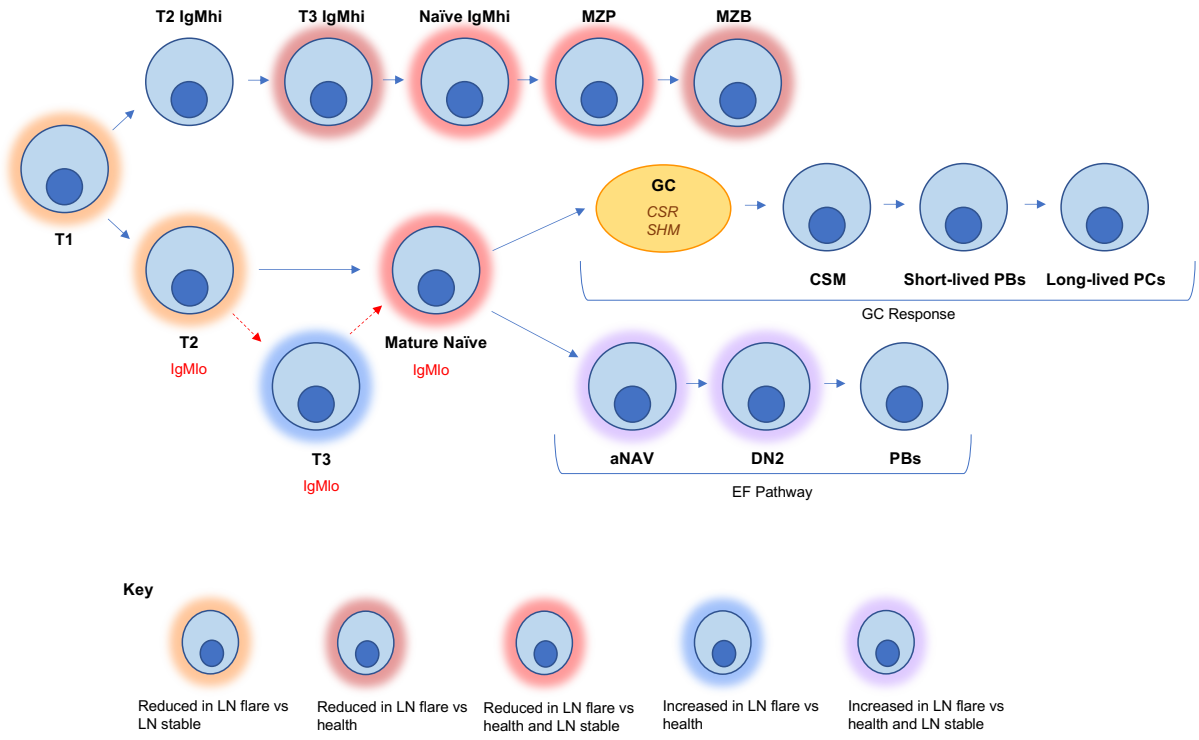

Figure 5.7: Summary of Chapter 5. Schematic diagram of peripheral B cell development colour-coded to indicate changes in subset abundance in lupus nephritis flares compared to stable lupus nephritis and health. Coloured glow indicates change in lupus nephritis flares (shown in key).

5.5 Discussion

This study has used flow cytometry to compare the proportions of peripheral B cell subsets in lupus nephritis patients during periods of disease flare compared to when their disease is stable and in comparison, to frequencies in healthy donors. It was observed that some of the changes in B cell subsets often associated with SLE appear to be a features of disease flare, whereas others seem to be features of lupus nephritis regardless of disease severity.

Data from this study suggests that the depletion of some stages in the IgMhi B cell developmental trajectory identified by Tull et al. (2021) are partly recovered during periods where lupus nephritis patients experience stable disease. For example, the T2 IgMhi, naïve IgMhi and MZP were reduced in lupus nephritis flare samples compared to the lupus nephritis samples from the same patients when their disease activity was lower, and they were stable. It was found that the proportions of these IgMhi subsets from stable lupus nephritis samples was often comparable to the proportion of these subsets in health. This suggests that the loss of the IgMhi B cell development branch is a feature of lupus nephritis flares, and this loss is somewhat restored when patients regain disease stability.

In contrast, the marginal zone subset was found to be significantly reduced in both flare and stable lupus nephritis samples compared to health; the increase in the percentage of this subset was not seen when patients were stable as it was seen in the other IgMhi subsets, which are all precursors to marginal zone B cells. This could suggest that either the reduction in marginal zone B cells in the peripheral blood is a feature of lupus nephritis regardless of disease activity or it may be possible that the restoration of marginal zone B cells in the blood after a period of flaring takes a long time and the samples used in this dataset were not collected over a long enough period to identify this change.

Changes in the IgMlo population of naïve B cells in lupus nephritis have not previously been described. This study has demonstrated that there is a significant reduction in

the naïve IgMlo population of B cells during lupus nephritis flares compared to health and compared to stable lupus nephritis, respectively. It is not fully understood which peripheral blood B cell subsets IgMlo naïve cells give rise to. As it is known that aNAV cells are predominantly IgMlo (Sanz et al., 2019), it could be hypothesised that naïve IgMlo cells mature into aNAV, which are known to be precursors of DN2 B cells. The reduction in the naïve IgMlo B cell compartment identified in this study may be a result of rapid maturation into aNAV cells and subsequent development and marked expansion of the DN2 B cell subset, therefore it could be hypothesised that B cells on this developmental path do not remain naïve for a long period of time.

Data from this study suggest that subsets of B cells belonging to the extrafollicular pathway, aNAV and DN2 cells, are expanded during periods of flare and this increase is reduced when disease activity lowers and patients become stable. Albeit not statistically significant, it was found that there was a trend towards an increase in aNAV B cells in lupus nephritis flare samples compared to samples from the same lupus nephritis patients when their disease was stable. A positive correlation between proportion of aNAV B cells and SLEDAI score has recently been reported (Wangriatisak et al., 2021), this suggests that the expansion of aNAV cells is exacerbated when disease activity is highest, and proportions of this subset can reduce back to proportions more comparable to that of health when disease activity is lowered.

A similar observation was noted regarding the DN2 B cell subset. In this study, it was found that the proportion of DN2 B cells in flare lupus samples was greater than the proportion of DN2 cells in stable lupus samples, although DN2 B cells were found to be significantly increased in both flare and stable lupus nephritis samples compared to health. This suggests that the extrafollicular pathway is enhanced during periods of flare in lupus nephritis compared to when disease is stable. Jenks et al. (2018) have previously described how periods of flare are characterised by greater how periods of flare are characterised by greater anti-dsDNA antibody titres due to an increase in pathogenic antibody-secreting cells, which are derived from DN2 B cells.

Overall, this dataset demonstrated the plasticity of the B cells compartment and how proportions of B cell subsets are fluid and has highlighted how the frequencies of the subsets making up the peripheral B cell pool in lupus nephritis can change depending on disease activity. Interestingly, there are several changes in the peripheral blood B cell compartment in lupus nephritis flares that have not yet been associated with pathogenic or autoimmune processes and so it would be of interest in future studies to investigate if some of these subset changes are causing a disease phenotype or if they are a result of disease activity.

6 Two subsets of marginal zone B cells and how they are impacted in lupus nephritis

6.1 Introduction

Marginal zone B cells are CD27+IgD+IgM+CD1c+ B cells that develop over the first two years of life in humans (Weller et al., 2003). This subset of B cells in peripheral blood have been termed “marginal zone” B cells due to their shared surface phenotype with B cells that reside in the marginal zone of the spleen (Cerutti et al., 2013; Weller et al., 2004). Marginal zone B cells are innate-like lymphocytes that play a role in immunity against encapsulated bacteria (Kruetzmann et al., 2003; Weller et al., 2004). Previous work from our lab has shown that marginal zone B cells develop from a subset of transitional B cells that are IgMhi and express higher levels of α4β7, that mediates homing of lymphocytes into the gut, than IgMlo transitional B cells. Marginal zone B cells, along with several other peripheral blood B cell subsets that are on the IgMhi developmental trajectory have previously been found to be significantly reduced in severe SLE (Tull et al., 2021; Zhu et al., 2018).

Data presented in this thesis chapter contributed to a study that is now published (Siu et al., 2022). A single-cell RNA-sequencing dataset that incorporated CITE-seq antibody labelling had been generated from B cells in tissues sampled from three sites from three cadaver donors: gut-associated lymphoid tissue in appendix, spleen, and mesenteric lymph node. Analysis of the transcriptomes of B cells isolated from the tissues suggested the existence of two distinct clusters of B cells, each with a CD27+IgD+IgM+ marginal zone B cell surface phenotype. One cluster had higher expression of *CCR7* and integrin β7 expression compared to the other cluster of marginal zone B cells. These subsets were referred to as MZB1 and MZB2, respectively. It was noted that in all three tissues MZB1 cells accounted for a greater proportion of the total B cell pool (5-25%) compared to MZB2 cells, which made up less than 10% of the total CD19+ population. This data was supported by findings using mass cytometry (Siu et al., 2022). Single-cell RNA-sequencing also identified the two clusters of marginal zone B cells in the peripheral blood of a small set of samples from cohorts of healthy donors (n=3) and lupus nephritis patients (n=3).

It was considered surprising that marginal zone B cells appeared heterogeneous and therefore a key step in the validation process was to design a panel of antibodies for flow cytometry to see if the two subsets could be resolved by this method. In the single-cell RNA-sequencing dataset from peripheral blood, it was inferred that the MZB1 subset were reduced in SLE but the MZB2 subset was not. It was also considered important to validate this finding on further samples from lupus nephritis patients, should the existence of MZB1 and MZB2 be confirmed by flow cytometry.

6.2 Aims

- To develop a flow cytometry gating strategy to test the hypothesis that two populations of marginal zone B cells are present in peripheral blood that can be discriminated by their expression of integrin β7 and CCR7
- To compare any differences in marginal zone B cells in peripheral blood in healthy blood donors with those in blood from lupus nephritis patients

6.3 Results

6.3.1 Gating for two subsets of marginal zone B cells

In this study, flow cytometry was used to develop a gating strategy to investigate the existence of two subsets of marginal zone B cells, MZB1 and MZB2, in the peripheral blood of healthy donors and lupus nephritis patients. First, cryopreserved PBMC from healthy donors (n=10) and lupus nephritis patients (n=10) were thawed and stained according to the protocols outlined in 2.5.1 and 2.5.5 in Materials and Methods. PBMC were stained with a panel of surface antibodies that included known marginal B cell markers, such as CD19, CD27, IgD, IgM and CD1c, in addition to markers such as CCR7 and integrin β7, which were identified as distinguishing markers of MZB1 and MZB2. In tissues, MZB1 had been found to express higher levels of CCR7 and integrin β7 compared to MZB2 (Siu et al., 2022).

The gating strategy, shown in Figure 6.1, was conducted using FlowJo software. Healthy donor samples were gated first, after which the gating strategy was implemented for the lupus nephritis patient samples. Live, singlet lymphocytes were selected from all events. B cells, which were identified as events positive for CD19, were selected. It is well-established that marginal zone B cells have a CD27+IgD+IgM+CD1c+ surface phenotype (Weller et al., 2003). In this study, CD27+IgD+ B cells were gated for first then within the CD27+IgD+ population IgM+CD1c+ cells were selected, as demonstrated in Figure 6.1. It is often assumed that all CD27+IgD+ cells represent the marginal zone B cell subset, however the additional IgM/CD1c gate allowed for a more dependable identification of true human marginal zone B cells. Within the marginal zone gate, CCR7+ and CCR7- gates were placed. The

CCR7- gate was placed using an isotype control, which facilitated the division of positive and negative CCR7 staining. B cells belonging to the MZB1 subset were classed as CCR7+ and cells that were CCR7- were classed as MZB2. In order to validate the single-cell RNA-sequencing dataset, the expression of integrin β7 within the CCR7+ and CCR7- gates was measured, as demonstrated in Figure 6.1. It was found that cells within the CCR7+ gate had higher integrin β7 expression than cells within the CCR7- gate, thus confirming the identification of CCR7+β7+ (MZB1) and CCR7-β7lo (MZB2) groups of marginal zone B cells.

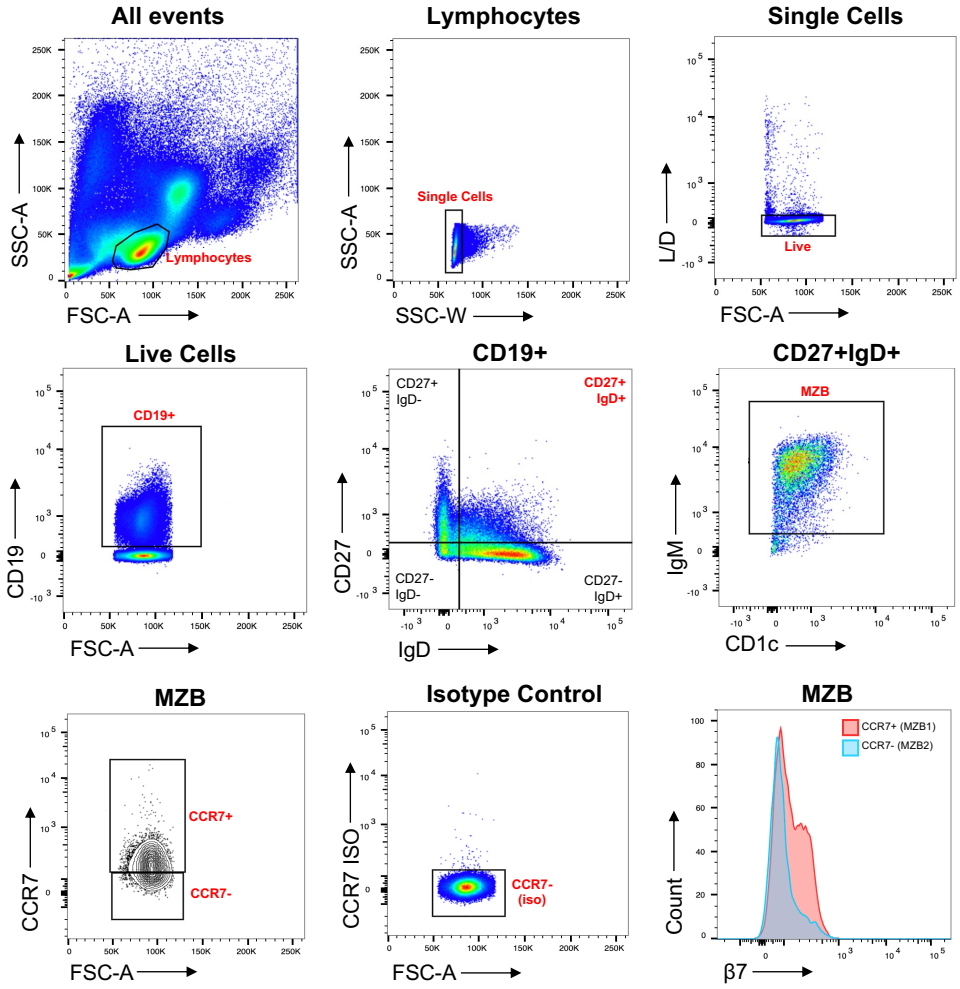

Figure 6.1: Flow cytometry gating strategy for the identification of two subsets of marginal zone B cells in health. Dot plots generated from flow cytometry of peripheral blood CD19+ B cells from a representative healthy donor. Lymphocytes are identified according to forward scatter area (FSC-A) and side scatter area (SSC-A). Single cells are gated for using SSC area and width. Live cells are selected as events negative for DAPI staining. B cells are gated as CD19+

cells. Marginal zone B cells are classed as CD27+IgD+IgM+CD1c events. Within the marginal zone B cell gate, cells are classed as either CCR7+ or CCR7-. The CCR7- negative gate is determined using an isotype control, which allows for the identification of non-specific binding. Integrin β7 expression is used to confirm gate placement. CCR7+ cells have higher integrin β7 expression and are classed as MZB1. CCR7- cells have lower integrin β7 expression and are classed as MZB2.

After the gating strategy had been used to identify MZB1 and MZB2 subsets in healthy donors, it was used to identify these populations in samples from a cohort of lupus nephritis patients, as shown in Figure 6.2.

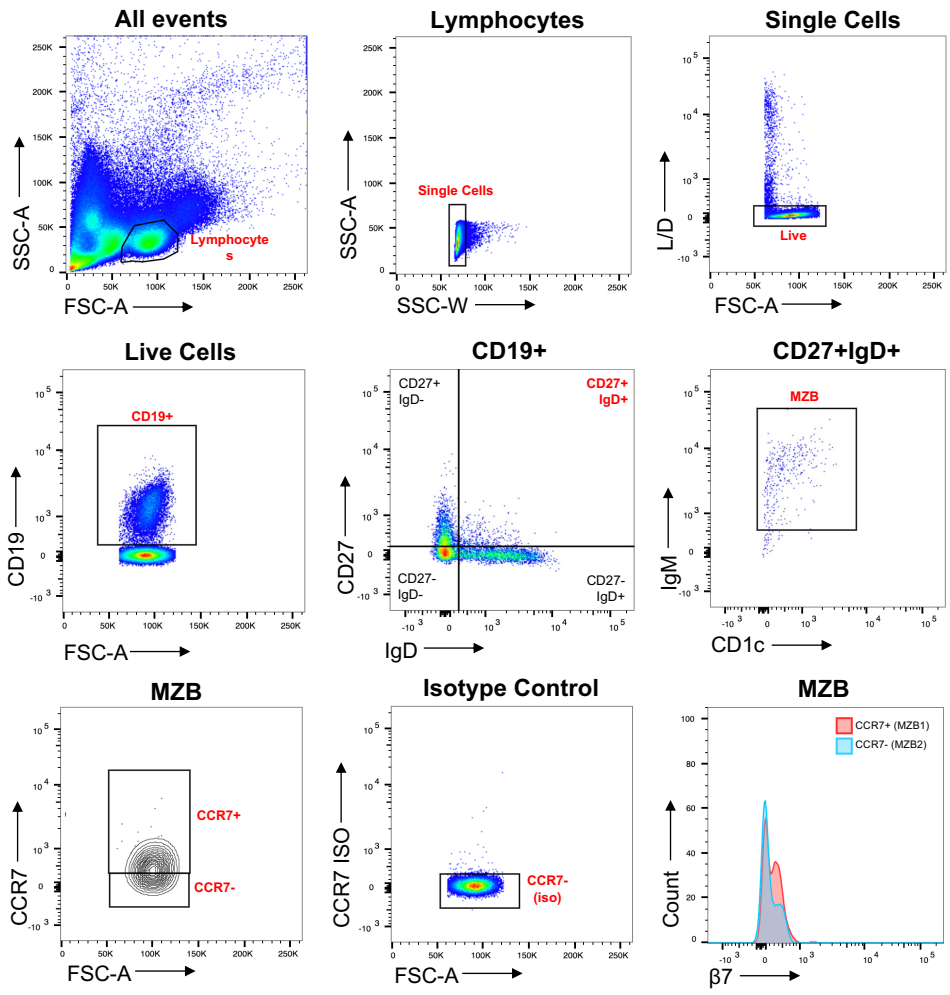

Figure 6.2: Flow cytometry gating strategy for the identification of two subsets of marginal zone B cells in lupus nephritis. Dot plots generated from flow cytometry of peripheral blood CD19+ B cells from a representative lupus nephritis patient. B cells are gated as CD19+ cells. Marginal zone B cells are classed as CD27+IgD+IgM+CD1c. Within the marginal zone B cell

gate, cells are classed as either CCR7+ or CCR7-. The CCR7- negative gate is determined using an isotype control, which allows for the identification of non-specific binding. Integrin β7 expression is used to confirm gate placement. CCR7+ cells have higher integrin β7 expression and are classed as MZB1. CCR7- cells have lower integrin β7 expression and are classed as MZB2.

There were noticeably far fewer cells in the CD27+IgD+IgM+CD1c+ gate in the lupus nephritis patient samples compared to that of the healthy donor samples, as is expected given that this has previously been reported in the literature. However, it was important to determine whether this reduction in marginal zone B cells in lupus nephritis was specific to one subset of marginal zone B cells or if both subsets were reduced.

6.3.2 Changes in the proportions of marginal zone B cell subsets in lupus nephritis

The reduction of marginal zone B cells in the peripheral blood in patients with severe SLE has been reported in the literature (Tull et al., 2021; Zhu et al., 2018). In this study, it was deemed important to understand how the two new novel subsets of marginal zone B cells are altered in lupus nephritis.

The frequency of each marginal zone B cell subset was calculated in both the health (n=10) and lupus nephritis (n=10) cohorts. As demonstrated in Figure 6.3A, it was found that MZB1 cells, as a percentage of total CD19+ B cells, were significantly reduced in lupus nephritis compared to health. On the other hand, there was no significant difference in the proportion of MZB2 cells in lupus nephritis compared to health, as shown in Figure 6.3A. Overall, the two marginal zone B cell subsets in health each accounted for approximately 3-10% of all peripheral blood B cells. It was determined that there was no significant difference in the proportion of MZB1 cells compared to MZB2 cells in healthy donors. The marginal zone subsets accounted for a far smaller proportion of the total peripheral blood B cell compartment in lupus nephritis, with each subset making up approximately 2% of all CD19+ B cells. It was found that there was no significant difference in the proportion of MZB1 cells compared to MZB2 cells in lupus nephritis, shown in Figure 6.3A, this was also observed within the healthy donor cohort, albeit the proportion of marginal zone B cells overall was far lower in lupus.

In order to further validate the gating strategy used to identify MZB1 and MZB2 using flow cytometry, the mean fluorescence intensity (MFI) of integrin β7 was measured. As seen in Figure 6.3B, in both samples from healthy donors and lupus nephritis patients, MZB1 cells had significantly higher integrin β7 MFI compared to MZB2 cells, confirming appropriate gate placement. It was found that there was no significant difference between integrin β7 MFI between health and lupus nephritis in both MZB1 and MZB2 subsets, as displayed in Figure 6.3B, suggesting that the gating strategy used was suitable for gating the same populations in both health and lupus nephritis.

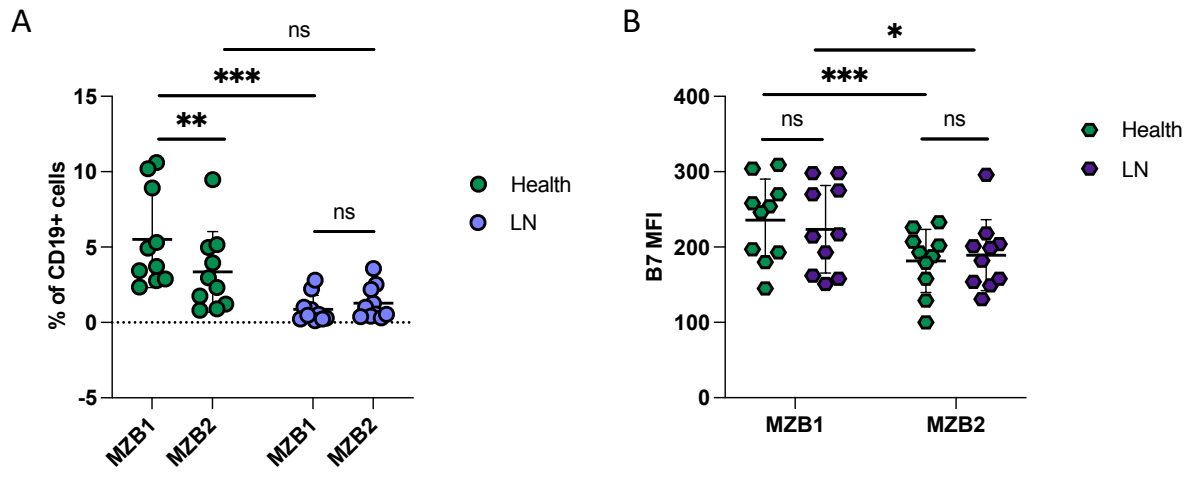

Figure 6.3: Proportions of MZB1 and MZB2 B cells from peripheral blood in healthy donors and lupus nephritis patients. (A) Proportions of MZB1 and MZB2 B cell subsets as a percentage of total CD19+ B cells in peripheral blood from healthy donors (n=10) and lupus nephritis patients (n=10) measured by flow cytometry. **(B)** Mean fluorescence intensity (MFI) of integrin β7 in MZB1 and MZB2 B cell subsets in healthy donors (n=10) and lupus nephritis patients (n=10). Data points from healthy donors are shown in green and data points from lupus nephritis patients (LN) are shown in purple. Asterisks denote statistical significance, which was deemed as $p<0.05$. Statistical significance was determined using an unpaired t-test when comparing health and lupus and a paired t-test when comparing factors within the same patient cohort.

6.3.3 Comparing protein expression in two groups of marginal zone B cells

The flow cytometry gating strategy developed in this study demonstrated the use of CCR7 and integrin β7 as markers for identification of two subsets of marginal zone B cells, one of which is reduced in lupus nephritis. As this gating strategy was based on surface protein marker expression, it was anticipated that MZB1 and MZB2 could also be identifiable in blood using mass cytometry. The differences in protein expression between MZB1 and MZB2 were not fully investigated in blood when using flow cytometry given the limited panel size available for this technique. Mass cytometry allows for a much more extensive panel of proteins to be analysed and so the mass cytometry dataset described in Chapter 4 was used to investigate differences between the two subsets of marginal zone B cells in blood from healthy donors and patients with lupus nephritis. The mass cytometry data were pre-processed and the viSNE plots and SPADE trees were generated as described in 4.3.1 and 4.3.2. Marginal zone B cell nodes were classified as CD27+IgD+IgM+CD1c+, as shown in the SPADE tree in Figure 4.6 in 4.3.2 and MZB1 and MZB2 were distinguished based on CCR7 and integrin β7.

For in-depth analysis, the marginal zone B cell nodes were exported from the original SPADE tree, shown in Figure 6.4A, and a new viSNE and subsequent SPADE tree were generated comprising only marginal zone B cell nodes, shown in Figure 6.4B. Nodes were separated into MZB1 and MZB2; nodes with higher expression of CCR7 and integrin β7 were classed as MZB1 and those with lower expression of these two markers were classed as MZB2, as shown in the representative SPADE tree in Figure 6.4B. Expression of CCR7 and integrin β7 was quantified to confirm classification of nodes. As shown in Figure 6.4C, in both health (n=9) and lupus nephritis (n=9) cohorts, MZB1 had significantly higher expression of both CCR7 and integrin β7 compared to MZB2. Additionally, the median expression of CD1c and IgM was quantified to confirm that both subsets were marginal zone B cells. There was no significant difference in CD1c or IgM expression between MZB1 and MZB2 in both health and lupus nephritis, shown in Figure 6.4D. It was deemed that marginal zone B cell nodes had been accurately classified and so differences in expression of proteins of interest was investigated.

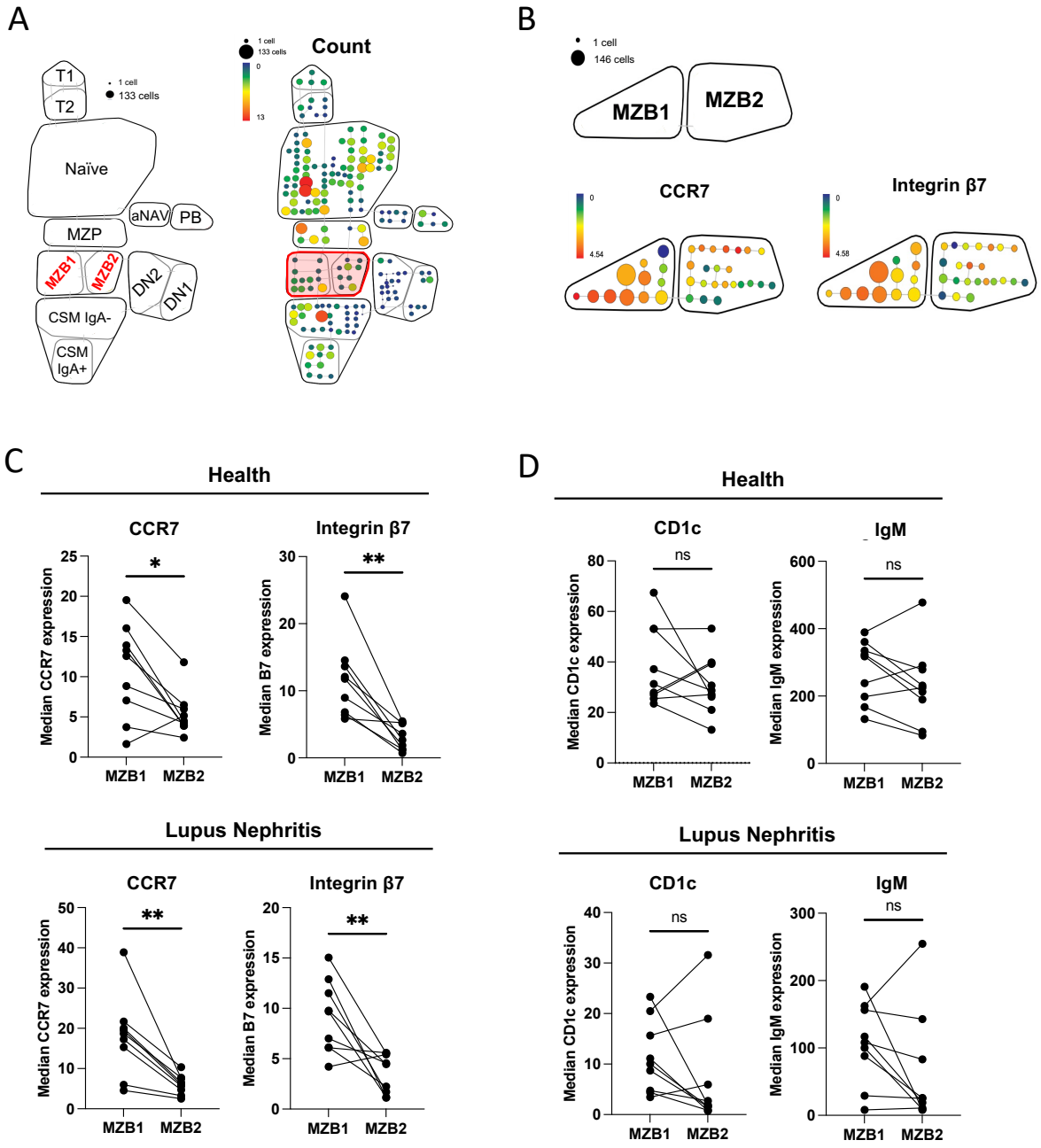

Figure 6.4: Two subsets of marginal zone B cells defined by CCR7 and integrin β7. (A) Mass cytometry data displayed as a SPADE tree generated from viSNE shown in Figure 4.3 in 4.3.2. Colour of nodes indicate cell count; the greatest cell count is represented by red nodes and the lowest cell count is represented by blue nodes. The size of the nodes also denotes cell count. The bigger the node, the greater the cell count. SPADE tree is from a representative healthy donor. Schematic tree shows names of classified B cell subsets. Nodes from the marginal zone B cell subsets, MZB1 and MZB2, that were exported for downstream analysis are highlighted in red. **(B)** SPADE trees generated by exporting marginal zone B cell nodes,

shown in red in panel A, and re-running analysis pipeline to plot a SPADE tree comprising only marginal zone B cells. Schematic tree shows classification of marginal zone B cell subsets. SPADE trees show expression of CCR7 and integrin β7. Level of expression is indicated by the colour scale. Nodes with the highest protein marker expression are shown in red and nodes with the lowest expression are shown in blue. The size of the nodes represent cell count whereby the bigger the node, the greater the cell count. SPADE trees are from a representative healthy donor. **(C)** Quantification of expression of CCR7 and integrin β7 in MZB1 compared to MZB2 in healthy donors (n=9) and lupus nephritis patients (n=9). Asterisks denote statistical significance which was deemed as $p<0.05$. A paired t-test was used to calculate significance. **(D)** Quantification of expression of CD1c and IgM in MZB1 compared to MZB2 in healthy donors (n=9) and lupus nephritis patients (n=9). A paired t-test was used to calculate significance, which was deemed as $p<0.05$. 'ns' denotes non-significant p-values.

Using the panel of markers, shown in Table 2.2 in Materials and Methods, the differences in expression of selected proteins of interest between MZB1 and MZB2 were studied. For this exploratory analysis, protein markers from three broad categories were investigated; these included proteins associated with B cell activation, chemokine signalling and interferon. The aim of this analysis was two-fold; first to determine whether there were any differences in protein marker expression between MZB1 and MZB2, second to understand whether the patterns in protein expression were comparable between health and lupus nephritis.

Firstly, expression of protein markers associated with B cell activation were compared between the two subsets of marginal zone B cells in both health and lupus nephritis. As shown in Figure 6.5A, it was found that expression of CD69 and CD40 were significantly higher in MZB1 compared to MZB2 in health. There was a trend towards CD83 expression also being higher in MZB1 compared to MZB2 in health, however this did not meet the $p<0.05$ statistical significance threshold ($p=0.0620$). It was found that median CD21 expression was significantly greater in MZB1 compared to MZB2 in health, as demonstrated in Figure 6.5A. Expression of the same protein markers associated with B cell activation was then compared in lupus nephritis. In contrast to healthy donors, median expression of CD69, CD83 and CD40 did not significantly differ

between MZB1 and MZB2 in lupus nephritis patients, as displayed in Figure 6.5B. But the pattern of CD21 expression was similar to what was observed in health whereby median CD21 expression was significantly greater in MZB1 compared to MZB2 in lupus nephritis, as shown in Figure 6.5B. The data presented in Figure 6.5 suggest that MZB1 cells express markers of activation at a greater level than MZB2 cells in health, but this difference in activation marker expression is not evident in lupus nephritis.

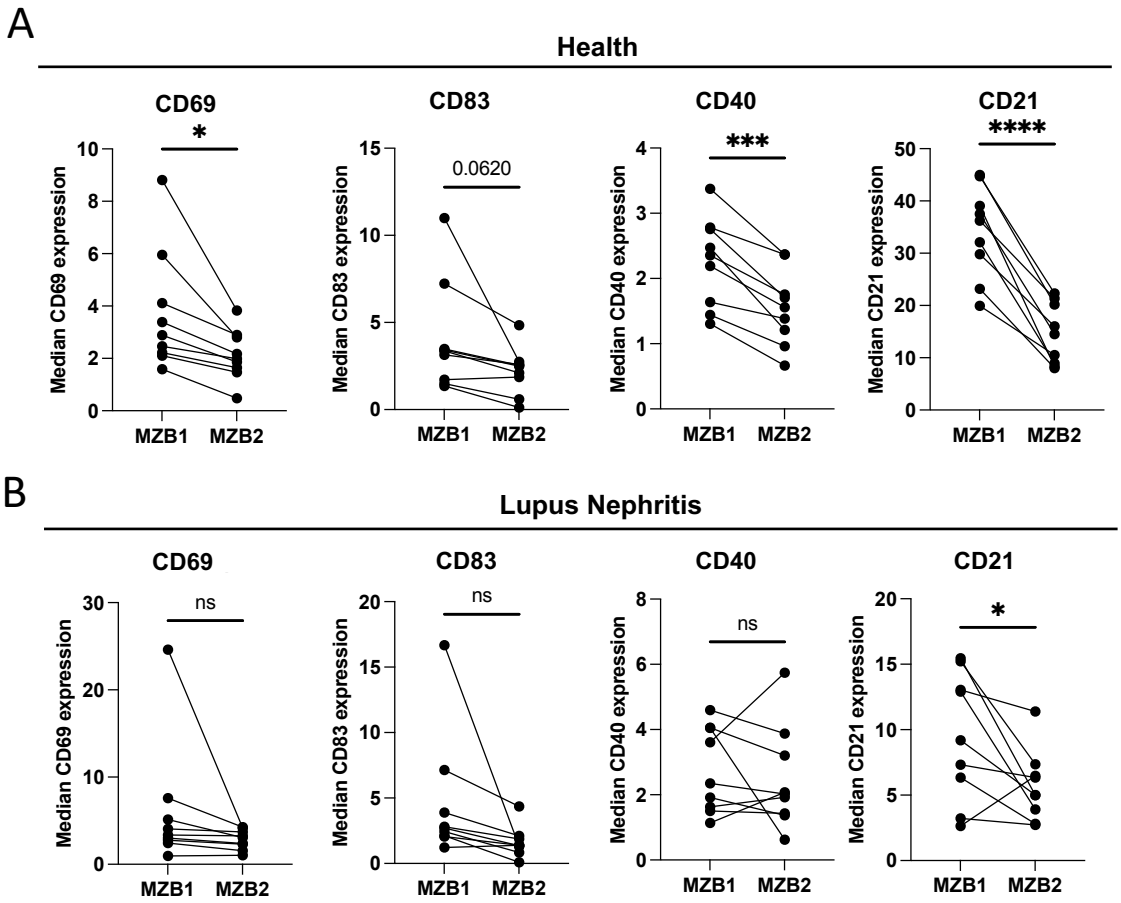

Figure 6.5: Expression of protein markers associated with B cell activation in marginal zone B cell subsets in health and lupus nephritis. Comparison of median expression of CD69, CD83, CD40 and CD21 between MZB1 and MZB2 in **(A)** healthy donors (n=9) and **(B)** lupus nephritis patients (n=9). Data is exported from SPADE tress shown in Figure 6.4B generated from mass cytometry data. Asterisks denote statistical significance which was deemed as $p<0.05$. Paired t-tests were used to calculate significance. 'ns' denotes non-significant p-values.

Chemokines CXCR5 and CXCR4 were the next group of markers investigated to understand whether there are any potential differences in the migration of marginal zone B cell subsets. It was found that in health, CXCR5 expression was significantly greater in MZB1 cells compared to MZB2 and there was a trend towards CXCR4 expression being higher in MZB1 cells as well, however this observation was not statistically significant (p=0.0605), as shown in Figure 6.6A. The same pattern of expression between marginal zone B cell subsets was observed in lupus nephritis, shown in Figure 6.6B, whereby median CXCR5 expression was significantly higher in MZB1 cells compared to MZB2 and there was a trend towards higher CXCR4 expression in MZB1, but this was not statistically significant (p=0.0683).

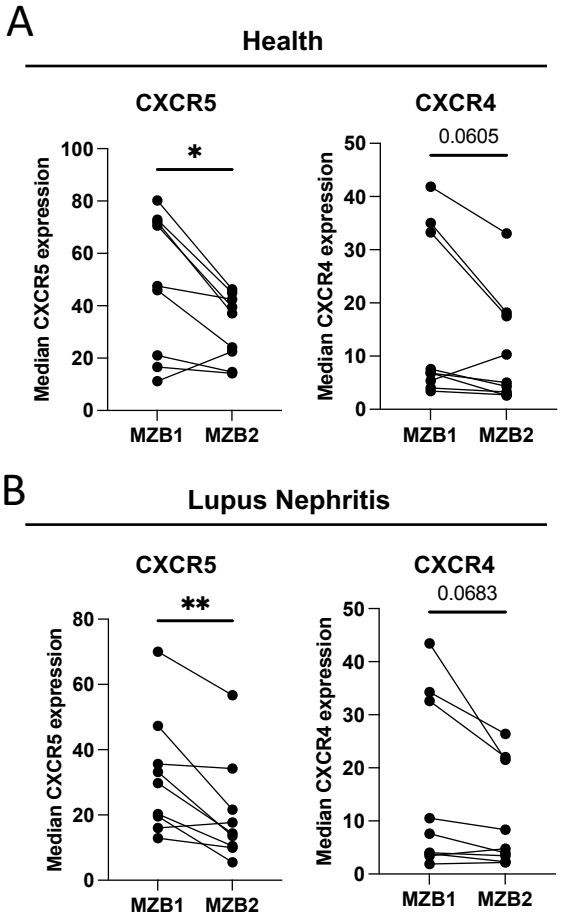

Figure 6.6: Expression of chemokine protein markers in marginal zone B cell subsets in health and lupus nephritis. Comparison of median expression of CXCR5 and CXCR4 between MZB1 and MZB2 in **(A)** healthy donors (n=9) and **(B)** lupus nephritis patients (n=9). Data is exported from SPADE tress shown in Figure 6.4B generated from mass cytometry data.

Asterisks denote statistical significance which was deemed as $p<0.05$. Non-significant p-values are shown in place of asterisks. Paired t-tests were used to calculate statistical significance.

The mass cytometry panel used for this analysis was originally designed to explore expression of proteins of ISGs. Previous data in this study shown in Figures 4.18 and 4.19 in 4.3.4 suggest that IFITM1 expression correlates with high IgM expression, whereas MX1 expression does not. Marginal zone B cells are known to be IgMhi (Tull et al., 2021; Weller et al., 2003). The expression of MX1, IRF7 and IFITM1 in MZB1 was compared to expression in MZB2 in both health and lupus nephritis. It was found that there was no significant difference in expression of all three markers between MZB1 and MZB2 in healthy donors, shown in Figure 6.7A. When investigating protein expression in samples from lupus nephritis patients, it was found that there was no significant difference in MX1 and IRF7 expression between MZB1 and MZB2, as shown in Figure 6.8B. However, it was found that median expression of IFITM1 was significantly greater in MZB1 compared to MZB2 in lupus nephritis, as depicted in Figure 6.7B.

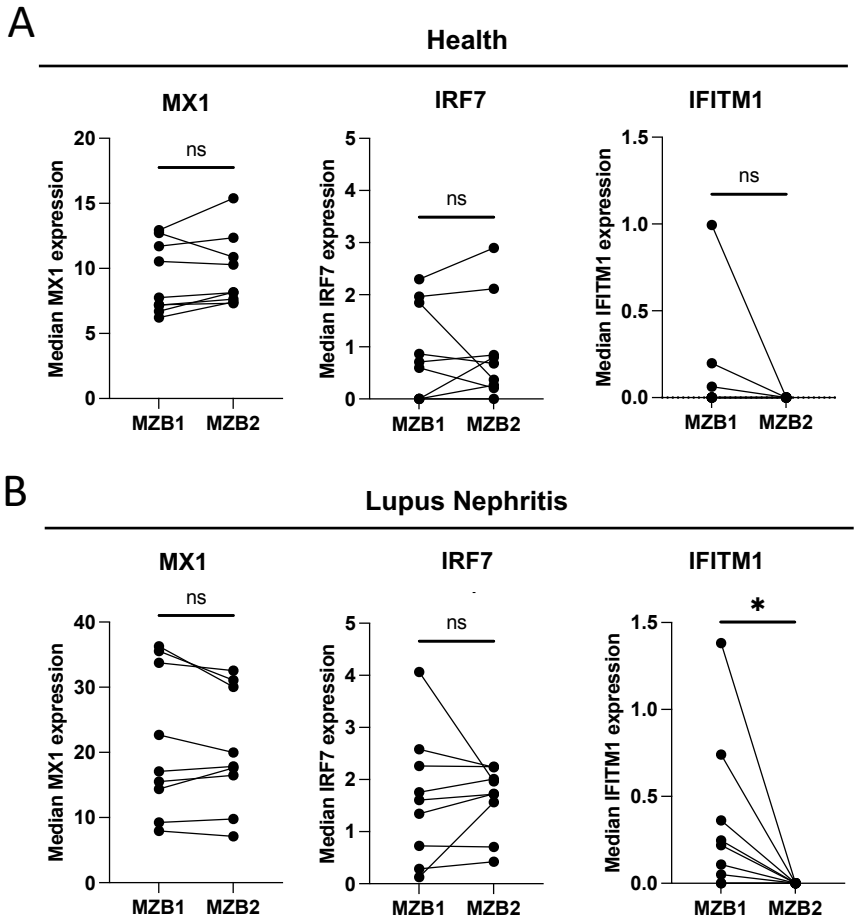

Figure 6.7: Expression of protein markers associated with interferon-stimulated genes in marginal zone B cell subsets in health and lupus nephritis. Comparison of median expression of MX1, IRF7 and IFITM1 between MZB1 and MZB2 in **(A)** healthy donors (n=9) and **(B)** lupus nephritis patients (n=9). Data is exported from SPADE tress shown in Figure 6.4B generated from mass cytometry data. Asterisks denote statistical significance which was deemed as $p<0.05$. Paired t-tests were used to calculate statistical significance. 'ns' denotes non-significant p-values.

Overall, this analysis has highlighted some differences in protein expression between MZB1 and MZB2, which could be explored further in future studies to determine whether these two subsets of marginal zone B cells have different functions in peripheral blood and whether these functions are altered in lupus nephritis.

6.4 Chapter 6 Summary

Data presented in Chapter 6 of this study focused on the notion that there are two groups of marginal zone B cells one of which, MZB1, is depleted in lupus nephritis. The two subsets of marginal zone B cells were gated for using a flow cytometry gating strategy developed in this study. Mass cytometry data analysis revealed that in health, MZB1 and MZB2 differ in terms of expression of groups of proteins associated with different cells. A schematic diagram summarising the findings of Chapter 6 is displayed in Figure 6.8.

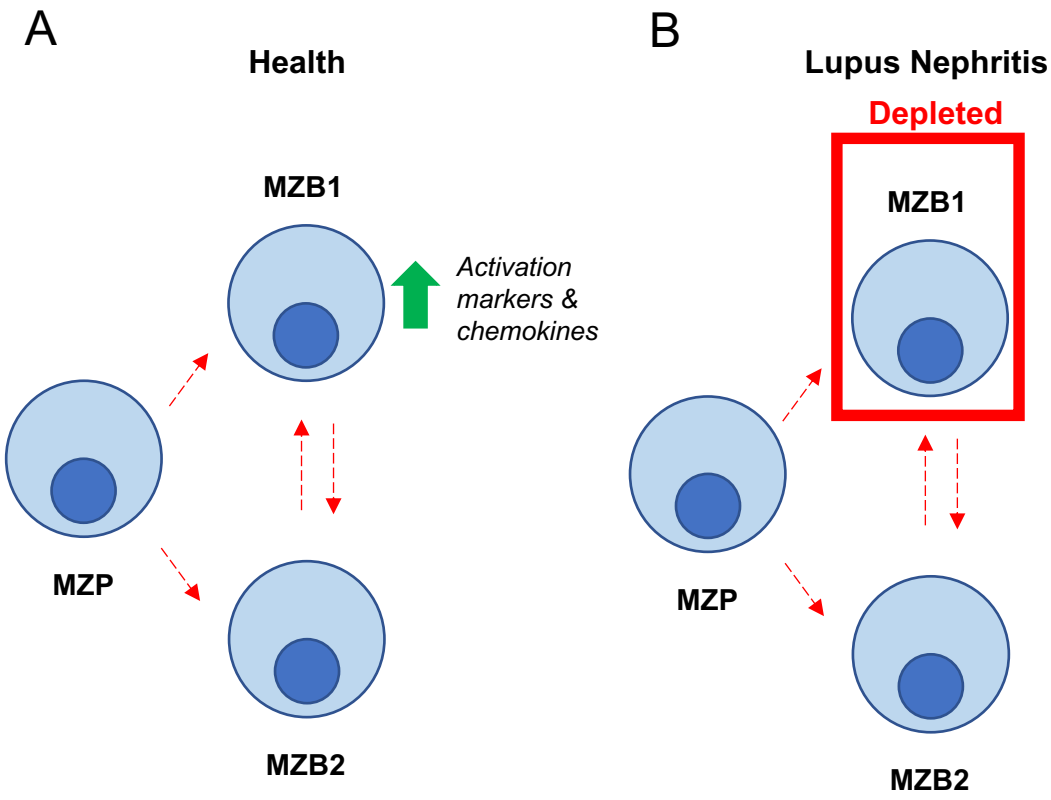

Figure 6.8: Summary of Chapter 6. (A) Schematic diagram showing two populations of marginal zone B cells (MZB1 and MZB2) in health. Red dotted arrows indicate possible developmental pathways not yet confirmed. Green arrow demonstrates the greater expression of activation markers and chemokine proteins in MZB1 compared to MZB2. **(B)** Schematic diagram showing two populations of marginal zone B cells (MZB1 and MZB2) in lupus nephritis. Red dotted arrows indicate possible developmental pathways not yet confirmed. MZB1 cells are significantly depleted in lupus nephritis compared to health, but MZB2 are not.

6.5 Discussion

This study has developed a flow cytometry gating strategy to effectively gate for two subsets of marginal zone B cells in peripheral blood, thus validating their existence. Antibodies for surface protein markers CCR7 and integrin β7 can be used to gate for MZB1 and MZB2 within the marginal zone B cell (CD27+IgD+IgM+CD1c+) gate. When this gating strategy was implemented, it was found that there was a significant reduction in the proportion of MZB1 cells in lupus nephritis compared to health. Conversely, there was no significant difference in the proportion of MZB2 cells in lupus nephritis compared to health. It is known that the peripheral blood marginal zone B cell population is reduced in severe SLE (Tull et al., 2021; Zhu et al., 2018), however the data from this study suggests that a specific group of marginal zone B cells are depleted, whilst some marginal zone cells are still present within the peripheral blood of individuals with SLE at the same proportion at which they are present in health.

The two populations of marginal zone B cells were also identified in a mass cytometry dataset comprising blood samples from healthy donors and lupus nephritis patients using the same markers used in the flow cytometry gating strategy. The mass cytometry data were generated as described in 4.3.1 and 4.3.2. It was found that MZB1 cells in health have higher median expression of protein markers associated with B cell activation, namely CD69, CD83, CD40 and CD21 compared to MZB2 cells. Early stages of B cell activation include the upregulation of several proteins including CD69 and CD40 (Kaminski et al., 2012). Although CD83 is primarily associated with dendritic cells, increased expression of CD83 in activated B cells has also been reported in the literature (Krzyzak et al., 2016; Prazma & Tedder, 2008). CD21 is known to form a co-receptor to the B cell receptor with CD19 and CD81 to lower the threshold for B cell activation via the B cell receptor (Matsumoto et al., 1991). This observation suggests that in health the MZB1 subset of marginal zone B cells are more activated than MZB2 cells.

In contrast, in samples from lupus nephritis patients, there was no significant difference in expression of CD69, CD40 and CD83 between the two subsets of marginal

zone B cells. This suggests that marginal zone B cells in lupus nephritis do not have differential activation markers, thus may not be differentially activated. MZB1 cells had significantly more CD21 than MZB2, however this difference was not as marked as it was in health. It is important to note that the MZB1 subset in lupus nephritis is depleted and so when investigating protein expression patterns in this subset, any observations made are regarding the small proportion of MZB1 cells that are present.

Analysis from the mass cytometry dataset also showed that median expression of CXCR5 was higher in MZB1 compared to MZB2 in both health and lupus nephritis. It was also noted that there was a trend towards greater median expression of CXCR4 in MZB1 compared to MZB2 in both cohorts of samples, however this did not meet the $p<0.05$ threshold to be deemed statistically significant in health ($p=0.0605$) or lupus nephritis ($p=0.0683$). These findings suggest that MZB1 cells may home to the follicles of secondary lymphoid tissues due to higher expression of CXCR5 (Förster et al., 1996; Legler et al., 1998) more so than MZB2 cells. Data from Siu et al. (2022) show that MZB1 cells are more abundant than MZB2 cells in the tissues of secondary lymphoid organs from healthy donor cadavers.

When investigating the expression of protein markers of ISGs, it was found that whilst overall expression was low, there was higher median expression of IFITM1 in MZB1 cells compared to MZB2 cells in lupus nephritis. This suggests that potentially MZB1 B cells are exposed to more interferon than MZB2 cells in lupus nephritis. The trend towards higher IFITM1 expression in MZB1 cells was also seen in a small number of healthy donor samples, however expression levels were negligible and so this was not a statistically significant finding. These findings together with data from Siu et al. (2022) that link MZB1 to the gut-homing developmental trajectory described by Tull et al. (2021), possibly suggest that IFITM1 expression is linked to this developmental pathway.

Overall, this study has demonstrated an effective gating strategy to identify two populations of marginal zone B cells and only one of these populations is depleted in lupus nephritis. Several differences in protein expression patterns between MZB1 and

MZB2 have been highlighted and in future studies, it would be important to investigate the functional relevance the differential protein expression has on these subsets of marginal zone B cells.

7 Conclusions and future directions

The data presented in this thesis have highlighted some interesting features of peripheral B cell subsets in both health and lupus nephritis and therefore have presented questions that could be answered in future studies. Typically, transitional B cells are sub-divided into T1 and T2 (Simon et al., 2016; Suryani et al., 2010) and recently Tull et al. (2021) further sub-categorised T2 B cells based on their surface expression of IgM into T2 IgMhi and T2 IgMlo. Single-cell RNA-sequencing data from this study, outlined in Chapter 3, demonstrated the heterogeneity of transitional B cells from peripheral blood in health and suggested that cells belonging to T2 IgMhi and T2 IgMlo subsets, respectively, segregate based on expression of genes associated with an immature B cell genotype, such as *VPREB1* and *IGLL5*. In future studies, trajectory analysis tools could potentially be used to characterise the changes in gene expression across cells belonging to a single subset to identify early-stage and late-stage CD10+ transitional B cells in health. This could then be compared to transitional B cells from lupus nephritis samples where alterations in transitional B cells have already been characterised (Landolt-Marticorena et al., 2011; Tull et al., 2021) to determine any differences in transitional B cell maturation that could possibly lead to altered downstream development.

The data shown in Chapter 3 also investigates the presence of transitional and naïve B cells with an interferon gene signature from both healthy donors and lupus nephritis patients. B cells with interferon signatures have been found using single-cell RNA-sequencing in other studies (Nehar-Belaid et al., 2020; Zheng et al., 2022), however these were often identified on a broad scale across all CD19+ B cells and were often found to be plasmablasts. In this study, groups of cells with an interferon gene signature within specific antigen-inexperienced subsets have been identified. Whilst it initially appears as though these cells with an interferon gene signature belong to a distinct group of transitional or naïve B cells, this study demonstrates how these cells belong to known B cell subsets (T1, T2 IgMhi and T2 IgMlo). This observation presents the question as to why newly emerged and antigen-inexperienced cells harbour an interferon gene signature. To build upon the findings presented in Chapter 3, a future

single-cell RNA-sequencing experiment could comprise a larger cohort of lupus nephritis patient and healthy donor samples and additional markers in the CITE-seq antibody panel to allow for the classification of additional B cell subsets based on their surface marker expression. For example, the inclusion of CITE-seq antibodies for CD11c, which would allow for the identification of DN2 B cells, and CD1c, which would identify marginal zone precursors as well as marginal zone B cells, all of which are key cells in the pathogenesis of lupus nephritis.

Future studies could look to investigate whether early B cell subsets are encountering interferon in the periphery or whether these cells harbour this interferon signature much earlier in development, and if so when and how. In addition, it was found that the populations of transitional and naïve B cells with an interferon gene signature were twice as abundant in lupus nephritis patients compared to health. It is currently unknown what the importance of these cells is in health and why they are more abundant in lupus and whether this has any impact on subsequent peripheral B cell development. Characterising genotype and surface phenotype of transitional B cells from cord blood and bone marrow using single-cell RNA-sequencing and mass cytometry would help to begin to answer these questions.

The mass cytometry data in Chapter 4 revealed an interesting protein marker expressed on transitional B cells, IFITM1. As previously stated, interferon signatures are well-characterised in SLE (Baechler et al., 2003; El-Sherbiny et al., 2018), but interestingly no difference in expression of IFITM1 was found between health and lupus nephritis, unlike the other interferon inducible markers MX1 and IRF7. Upon further investigation, IFITM1 expression was found to correlate with integrin β7 expression and that IgMhi transitional and naïve subsets had higher IFITM1 expression than their IgMlo respective populations. This data suggests that IFITM1 may be linked to the IgMhi, integrin β7+ gut-homing developmental trajectory. The observations made about IFITM1 were evident in both healthy donors and lupus nephritis patients, suggesting that if IFITM1 does have a link to a particular developmental trajectory it does so in the healthy immune system. Future experiments could investigate the

function significance of IFITM1 in B cell development, possibly by antagonising IFITM1 and stimulating the B cell receptor, then observing functional changes.

Data presented in Chapter 5 demonstrated the plasticity of the peripheral B cell compartment during different periods of disease activity in lupus nephritis. For instance, changes in the proportions of some of the B cell subsets during disease flares, such as a decrease in naïve IgMhi and MZP cells and an increase in aNAV cells, were not seen when patients were stable, and the proportions of these subsets was similar to that of health. This suggests that the abundance of certain peripheral B cell subsets is more characteristic of lupus flares. Given the precious nature of paired lupus samples, it was not possible to have samples taken at the exact same timepoints and so in future studies it would be beneficial to use samples from patients taken within a similar time frame as well as using multiple samples over a longer time frame to determine if any changes in the peripheral B cell compartment occur after a long period of disease stability. Furthermore, it would also be beneficial to increase the sample size of this dataset to allow for the identification of more prominent trends and patterns in changes in B cell subset abundances.

The data presented in the final chapter of this thesis, Chapter 6, used flow cytometry to validate the presence of two groups of marginal zone B cells in peripheral blood and showed that it is the MZB1 population that is depleted in lupus nephritis. MZB1 were distinguished from MZB2 by higher expression of CCR7 and integrin β7. In this study, expression of various surface marker proteins between the two marginal zone subsets was compared using mass cytometry. It was found that MZB1 cells in health expressed markers of activation, such as CD69 and CD40, more than MZB2 in health, but this was not seen regarding the lupus nephritis cohort, suggesting that MZB1 may not be in a more activate state than MZB2 cells in lupus nephritis. In addition, there was a trend towards MZB1 expressing higher levels of IFITM1 compared to MZB2 in health and the same significant difference was observed in lupus nephritis. Siu et al. (2022) showed that both MZB1 and MZB2 express IgM but is the MZB1 subset that is related to IgMhi trajectory populations. This data provided another suggestion that IFITM1 may be linked to the gut-homing IgMhi developmental trajectory that is lost in

lupus nephritis and future studies investigating this link could be of importance. In addition, it would be of interest in future studies to investigate if there are any functional differences in the two newly identified MZB populations. This information could then provide an insight into which functions are lost in lupus nephritis upon the loss of MZB1 cells.

8 References

Agematsu, K., Hokibara, S., Nagumo, H., & Komiyama, A. (2000). CD27: a memory B-cell marker. *Immunology Today*, *21*(5), 204–206. https://doi.org/10.1016/S0167-5699(00)01605-4

Agrawal, S., Smith, S. A. B. C., Tangye, S. G., & Sewell, W. A. (2013). Transitional B cell subsets in human bone marrow. *Clinical and Experimental Immunology*, *174*(1), 53–59. https://doi.org/10.1111/cei.12149

Akkaya, M., Kwak, K., & Pierce, S. K. (2020). B cell memory: building two walls of protection against pathogens. In *Nature Reviews Immunology* (Vol. 20, Issue 4, pp. 229–238). Nature Research. https://doi.org/10.1038/s41577-019-0244-2

Allan, L. L., Stax, A. M., Zheng, D.-J., Chung, B. K., Kozak, F. K., Tan, R., & van den Elzen, P. (2011). CD1d and CD1c Expression in Human B Cells Is Regulated by Activation and Retinoic Acid Receptor Signaling. *The Journal of Immunology*, *186*(9), 5261–5272. https://doi.org/10.4049/jimmunol.1003615

Allen, C. D. C., Ansel, K. M., Low, C., Lesley, R., Tamamura, H., Fujii, N., & Cyster, J. G. (2004). Germinal center dark and light zone organization is mediated by CXCR4 and CXCR5. *Nature Immunology*, *5*(9), 943–952. https://doi.org/10.1038/ni1100

Allman, D., Lindsley, R. C., DeMuth, W., Rudd, K., Shinton, S. A., & Hardy, R. R. (2001). Resolution of Three Nonproliferative Immature Splenic B Cell Subsets Reveals Multiple Selection Points During Peripheral B Cell Maturation. *The Journal of Immunology*, *167*(12), 6834–6840. https://doi.org/10.4049/jimmunol.167.12.6834

Alrumaihi, F. (2022). The Multi-Functional Roles of CCR7 in Human Immunology and as a Promising Therapeutic Target for Cancer Therapeutics. In *Frontiers in Molecular Biosciences* (Vol. 9). Frontiers Media S.A. https://doi.org/10.3389/fmolb.2022.834149

Amir, E. A. D., Davis, K. L., Tadmor, M. D., Simonds, E. F., Levine, J. H., Bendall, S. C., Shenfeld, D. K., Krishnaswamy, S., Nolan, G. P., & Pe'Er, D. (2013). ViSNE enables visualization of high dimensional single-cell data and reveals phenotypic heterogeneity of leukemia. *Nature Biotechnology*, *31*(6), 545–552. https://doi.org/10.1038/nbt.2594

An, J., Woodward, J. J., Lai, W., Minie, M., Sun, X., Tanaka, L., Snyder, J. M., Sasaki, T., & Elkon, K. B. (2018). Inhibition of Cyclic GMP-AMP Synthase Using a Novel Antimalarial Drug Derivative in *Trex1* -Deficient Mice. *Arthritis & Rheumatology*, *70*(11), 1807–1819. https://doi.org/10.1002/art.40559

Anderson, S. M., Khalil, A., Uduman, M., Hershberg, U., Louzoun, Y., Haberman, A. M., Kleinstein, S. H., & Shlomchik, M. J. (2009). Taking Advantage: High-Affinity B Cells in the Germinal Center Have Lower Death Rates, but Similar Rates of Division, Compared to Low-Affinity Cells. *The Journal of Immunology*, *183*(11), 7314–7325. https://doi.org/10.4049/jimmunol.0902452

Arbuckle, M. R., McClain, M. T., Rubertone, M. v., Scofield, R. H., Dennis, G. J., James, J. A., & Harley, J. B. (2003). Development of Autoantibodies before the Clinical Onset of Systemic Lupus Erythematosus. *New England Journal of Medicine*, *349*(16), 1526–1533. https://doi.org/10.1056/NEJMoa021933

Au, W. C., Moore, P. A., LaFleur, D. W., Tombal, B., & Pitha, P. M. (1998). Characterization of the interferon regulatory factor-7 and its potential role in the transcription activation of interferon A genes. *Journal of Biological Chemistry*, *273*(44), 29210–29217. https://doi.org/10.1074/jbc.273.44.29210

Baechler, E. C., Batliwalla, F. M., Karypis, G., Gaffney, P. M., Ortmann, W. A., Espe, K. J., Shark, K. B., Grande, W. J., Hughes, K. M., Kapur, V., Gregersen, P. K., & Behrens, T. W. (2003).

Interferon-inducible gene expression signature in peripheral blood cells of patients with severe lupus. *Proceedings of the National Academy of Sciences*, *100*(5), 2610–2615. https://doi.org/10.1073/pnas.0337679100

Baker, K. P., Edwards, B. M., Main, S. H., Choi, G. H., Wager, R. E., Halpern, W. G., Lappin, P. B., Riccobene, T., Abramian, D., Sekut, L., Sturm, B., Poortman, C., Minter, R. R., Dobson, C. L., Williams, E., Carmen, S., Smith, R., Roschke, V., Hilbert, D. M., … Albert, V. R. (2003). Generation and characterization of LymphoStat-B, a human monoclonal antibody that antagonizes the bioactivities of B lymphocyte stimulator. *Arthritis & Rheumatism*, *48*(11), 3253–3265. https://doi.org/10.1002/art.11299

Battaglia, M., & Garrett-Sinha, L. A. (2021). Bacterial infections in lupus: Roles in promoting immune activation and in pathogenesis of the disease. *Journal of Translational Autoimmunity*, *4*, 100078. https://doi.org/10.1016/j.jtauto.2020.100078

Båve, U., Magnusson, M., Eloranta, M.-L., Perers, A., Alm, G. v., & Rönnblom, L. (2003). FcγRIIa Is Expressed on Natural IFN-α-Producing Cells (Plasmacytoid Dendritic Cells) and Is Required for the IFN-α Production Induced by Apoptotic Cells Combined with Lupus IgG. *The Journal of Immunology*, *171*(6), 3296–3302. https://doi.org/10.4049/jimmunol.171.6.3296

Bemark, M. (2015). Translating transitions - How to decipher peripheral human B cell development. In *Journal of Biomedical Research* (Vol. 29, Issue 4, pp. 264–284). Nanjing Medical University. https://doi.org/10.7555/JBR.29.20150035

Bendall, S. C., Davis, K. L., Amir, E. A. D., Tadmor, M. D., Simonds, E. F., Chen, T. J., Shenfeld, D. K., Nolan, G. P., & Pe'Er, D. (2014). Single-cell trajectory detection uncovers progression and regulatory coordination in human b cell development. *Cell*, *157*(3), 714–725. https://doi.org/10.1016/j.cell.2014.04.005

Bennett, L., Palucka, A. K., Arce, E., Cantrell, V., Borvak, J., Banchereau, J., & Pascual, V. (2003). Interferon and granulopoiesis signatures in systemic lupus erythematosus blood. *Journal of Experimental Medicine*, *197*(6), 711–723. https://doi.org/10.1084/jem.20021553

Berkowska, M. A., Driessen, G. J. A., Bikos, V., Grosserichter-Wagener, C., Stamatopoulos, K., Cerutti, A., He, B., Biermann, K., Lange, J. F., van der Burg, M., van Dongen, J. J. M., & van Zelm, M. C. (2011). Human memory B cells originate from three distinct germinal center-dependent and -independent maturation pathways. *Blood*, *118*(8), 2150–2158. https://doi.org/10.1182/blood-2011-04-345579

Blair, P. A., Noreña, L. Y., Flores-Borja, F., Rawlings, D. J., Isenberg, D. A., Ehrenstein, M. R., & Mauri, C. (2010). CD19+CD24hiCD38hi B Cells Exhibit Regulatory Capacity in Healthy Individuals but Are Functionally Impaired in Systemic Lupus Erythematosus Patients. *Immunity*, *32*(1), 129–140. https://doi.org/10.1016/j.immuni.2009.11.009

Bombardier, C., Gladman, D. D., Urowitz, M. B., Caron, D., Chang, C. H., Austin, A., Bell, A., Bloch, D. A., Corey, P. N., Decker, J. L., Esdaile, J., Fries, J. F., Ginzler, E. M., Goldsmith, C. H., Hochberg, M. C., Jones, J. v., Riche, N. G. H. le, Liang, M. H., Lockshin, M. D., … Schur, P. H. (1992). Derivation of the SLEDAI. A disease activity index for lupus patients. *Arthritis & Rheumatism*, *35*(6), 630–640. https://doi.org/10.1002/art.1780350606

Brinas, F., Danger, R., & Brouard, S. (2021). Tcl1a, b cell regulation and tolerance in renal transplantation. In *Cells* (Vol. 10, Issue 6). MDPI. https://doi.org/10.3390/cells10061367

Brink, R., Goodnow, C. C., Crosbie, J., Adams, E., Eris, J., Mason, D. Y., Hartley, S. B., & Basten, A. (1992). Immunoglobulin M and D antigen receptors are both capable of mediating B lymphocyte activation, deletion, or anergy after interaction with specific antigen. *Journal of Experimental Medicine*, *176*(4), 991–1005. https://doi.org/10.1084/jem.176.4.991

Brinkmann, V., & Zychlinsky, A. (2007). Beneficial suicide: why neutrophils die to make NETs. *Nature Reviews Microbiology*, *5*(8), 577–582. https://doi.org/10.1038/nrmicro1710

Brown, G. J., Cañete, P. F., Wang, H., Medhavy, A., Bones, J., Roco, J. A., He, Y., Qin, Y., Cappello, J., Ellyard, J. I., Bassett, K., Shen, Q., Burgio, G., Zhang, Y., Turnbull, C., Meng, X., Wu, P., Cho, E., Miosge, L. A., … Vinuesa, C. G. (2022). TLR7 gain-of-function genetic variation causes human lupus. *Nature*, *605*(7909), 349–356. https://doi.org/10.1038/s41586-022-04642-z

Casamayor-Palleja, M., Feuillard, J., Ball, J., Drew, M., & MacLennan, I. C. M. (1996). Centrocytes rapidly adopt a memory B cell phenotype on co-culture with autologous germinal centre T cell-enriched preparations. *International Immunology*, *8*(5), 737–744. https://doi.org/10.1093/intimm/8.5.737

Castellano, G., Cafiero, C., Divella, C., Sallustio, F., Gigante, M., Pontrelli, P., de Palma, G., Rossini, M., Grandaliano, G., & Gesualdo, L. (2015). Local synthesis of interferon-alpha in lupus nephritis is associated with type I interferons signature and LMP7 induction in renal tubular epithelial cells. *Arthritis Research and Therapy*, *17*(1). https://doi.org/10.1186/s13075-015-0588-3

Ceppellini, R., Polli, E., & Celada, F. (1957). A DNA-Reacting Factor in Serum of a Patient with Lupus Erythematosus Diffusus. *Experimental Biology and Medicine*, *96*(3), 572–574. https://doi.org/10.3181/00379727-96-23544

Cerutti, A., Cols, M., & Puga, I. (2013). Marginal zone B cells: Virtues of innate-like antibody-producing lymphocytes. In *Nature Reviews Immunology* (Vol. 13, Issue 2, pp. 118–132). https://doi.org/10.1038/nri3383

Cervera, R., Khamashta, M. A., Font, J., Sebastiani, G. D., Gil, A., Lavilla, P., Mejía, J. C., Aydintug, A. O., Chwalinska-Sadowska, H., de Ramón, E., Fernández-Nebro, A., Galeazzi, M., Valen, M., Mathieu, A., Houssiau, F., Caro, N., Alba, P., Ramos-Casals, M., Ingelmo, M., & Hughes, G. R. V. (2003). Morbidity and Mortality in Systemic Lupus Erythematosus During a 10-Year Period. *Medicine*, *82*(5), 299–308. https://doi.org/10.1097/01.md.0000091181.93122.55

Chaudhuri, J., Tian, M., Khuong, C., Chua, K., Pinaud, E., & Alt, F. W. (2003). Transcription-targeted DNA deamination by the AID antibody diversification enzyme. *Nature*, *422*(6933), 726–730. https://doi.org/10.1038/nature01574

Cherukuri, A., Cheng, P. C., Sohn, H. W., & Pierce, S. K. (2001). The CD19/CD21 Complex Functions to Prolong B Cell Antigen Receptor Signaling from Lipid Rafts strated to regulate the function of the Src family kinase Lyn by a novel mechanism that involves the amplification of Lyn activation (Fujimoto et al., 2000). The importance of CD19 as a coreceptor for the BCR in vivo has been demonstrated by the phenotype of mice that lack. In *Immunity* (Vol. 14).

Christian, S. L. (2022). CD24 as a Potential Therapeutic Target in Patients with B-Cell Leukemia and Lymphoma: Current Insights. In *OncoTargets and Therapy* (Vol. 15, pp. 1391–1402). Dove Medical Press Ltd. https://doi.org/10.2147/OTT.S366625

Cuss, A. K., Avery, D. T., Cannons, J. L., Yu, L. J., Nichols, K. E., Shaw, P. J., & Tangye, S. G. (2006). Expansion of Functionally Immature Transitional B Cells Is Associated with Human-Immunodeficient States Characterized by Impaired Humoral Immunity. *The Journal of Immunology*, *176*(3), 1506–1516. https://doi.org/10.4049/jimmunol.176.3.1506

Danza, A., & Ruiz-Irastorza, G. (2013). Infection risk in systemic lupus erythematosus patients: susceptibility factors and preventive strategies. *Lupus*, *22*(12), 1286–1294. https://doi.org/10.1177/0961203313493032

Darnell, J. E., Kerr, Ian M., & Stark, G. R. (1994). Jak-STAT Pathways and Transcriptional Activation in Response to IFNs and Other Extracellular Signaling Proteins. *Science*, *264*(5164), 1415–1421. https://doi.org/10.1126/science.8197455

D'cruz, D. P., Khamashta, A., & Hughes, G. R. v. (2007). Systemic lupus erythematosus. In *www.thelancet.com* (Vol. 369). www.thelancet.com

Deane, J. A., Pisitkun, P., Barrett, R. S., Feigenbaum, L., Town, T., Ward, J. M., Flavell, R. A., & Bolland, S. (2007). Control of Toll-like Receptor 7 Expression Is Essential to Restrict Autoimmunity and Dendritic Cell Proliferation. *Immunity*, *27*(5), 801–810. https://doi.org/10.1016/j.immuni.2007.09.009

Der, S. D., Zhou, A., Williams, B. R. G., & Silverman, R. H. (1998). Identification of genes differentially regulated by interferon, or using oligonucleotide arrays. In *Medical Sciences Communicated by George R. Stark, Cleveland Clinic Foundation* (Vol. 95). www.pnas.org.

Descatoire, M., Weller, S., Irtan, S., Feuillard, J., Storck, S., Guiochon-Mantel, A., Bouligand, J., Morali, A., Cohen, J., Jacquemin, E., Iascone, M., Bole-Feysot, C., Cagnard, N., Weill, J. C., & Reynaud, C. A. (2014). Identification of a human splenic marginal zone B cell precursor with NOTCH2-dependent differentiation properties. *Journal of Experimental Medicine*, *211*(5), 987–1000. https://doi.org/10.1084/jem.20132203

di Noia, J., & Neuberger, M. S. (2002). *Altering the pathway of immunoglobulin hypermutation by inhibiting uracil-DNA glycosylase*. http://chick.umist.ac.uk

Dickerson, S. K., Market, E., Besmer, E., & Papavasiliou, F. N. (2003). AID mediates hypermutation by deaminating single stranded DNA. *Journal of Experimental Medicine*, *197*(10), 1291–1296. https://doi.org/10.1084/jem.20030481

Dieudonné, Y., Gies, V., Guffroy, A., Keime, C., Bird, A. K., Liesveld, J., Barnas, J. L., Poindron, V., Douiri, N., Soulas-Sprauel, P., Martin, T., Meffre, E., Anolik, J. H., & Korganow, A. S. (2019). Transitional B cells in quiescent SLE: An early checkpoint imprinted by IFN. *Journal of Autoimmunity*, *102*, 150–158. https://doi.org/10.1016/j.jaut.2019.05.002

Dima, A., Jurcut, C., Chasset, F., Felten, R., & Arnaud, L. (2022). Hydroxychloroquine in systemic lupus erythematosus: overview of current knowledge. *Therapeutic Advances in Musculoskeletal Disease*, *14*, 1759720X2110730. https://doi.org/10.1177/1759720X211073001

dos Santos, B., Valverde, J., Rohr, P., Monticielo, O., Brenol, J., Xavier, R., & Chies, J. (2012). TLR7/8/9 polymorphisms and their associations in systemic lupus erythematosus patients from Southern Brazil. *Lupus*, *21*(3), 302–309. https://doi.org/10.1177/0961203311425522

Dunnick, W., Hertz, G. Z., Scappino, L., & Gritzmacher, C. (1993). DNA sequences at immunoglobulin switch region recombination sites. In *Nucleic Acids Research* (Vol. 21, Issue 3). https://academic.oup.com/nar/article/21/3/365/2386279

Duty, J. A., Szodoray, P., Zheng, N.-Y., Koelsch, K. A., Zhang, Q., Swiatkowski, M., Mathias, M., Garman, L., Helms, C., Nakken, B., Smith, K., Farris, A. D., & Wilson, P. C. (2009). Functional anergy in a subpopulation of naive B cells from healthy humans that express autoreactive immunoglobulin receptors. *Journal of Experimental Medicine*, *206*(1), 139–151. https://doi.org/10.1084/jem.20080611

Edberg, J. C., Wu, J., Langefeld, C. D., Brown, E. E., Marion, M. C., McGwin, G., Petri, M., Ramsey-Goldman, R., Reveille, J. D., Frank, S. G., Kaufman, K. M., Harley, J. B., Alarcón, G. S., & Kimberly, R. P. (2008). Genetic variation in the CRP promoter: association with systemic lupus erythematosus. *Human Molecular Genetics*, *17*(8), 1147–1155. https://doi.org/10.1093/hmg/ddn004

Elgueta, R., Benson, M. J., de Vries, V. C., Wasiuk, A., Guo, Y., & Noelle, R. J. (2009). Molecular mechanism and function of CD40/CD40L engagement in the immune system. In *Immunological Reviews* (Vol. 229, Issue 1, pp. 152–172). https://doi.org/10.1111/j.1600-065X.2009.00782.x

Elkon, K., & Casali, P. (2008). Nature and functions of autoantibodies. *Nature Clinical Practice Rheumatology*, *4*(9), 491–498. https://doi.org/10.1038/ncprheum0895

El-Sherbiny, Y. M., Md Yusof, M. Y., Psarras, A., Hensor, E. M. A., Kabba, K. Z., Dutton, K., Mohamed, A. A. A., Elewaut, D., McGonagle, D., Tooze, R., Doody, G., Wittmann, M., Emery, P., & Vital, E. M. (2020). B Cell Tetherin: A Flow Cytometric Cell-Specific Assay for Response to Type I Interferon Predicts Clinical Features and Flares in Systemic Lupus Erythematosus. *Arthritis and Rheumatology*, *72*(5), 769–779. https://doi.org/10.1002/art.41187

El-Sherbiny, Y. M., Psarras, A., Yusof, M. Y. M., Hensor, E. M. A., Tooze, R., Doody, G., Mohamed, A. A. A., McGonagle, D., Wittmann, M., Emery, P., & Vital, E. M. (2018). A novel two-score system for interferon status segregates autoimmune diseases and correlates with clinical features. *Scientific Reports*, *8*(1). https://doi.org/10.1038/s41598-018-24198-1

Evans, S., Lee, D., Han, T., Tomasi, T., & Evans, R. (1990). Monoclonal antibody to the interferon-inducible protein Leu-13 triggers aggregation and inhibits proliferation of leukemic B cells. *Blood*, *76*(12), 2583–2593. https://doi.org/10.1182/blood.V76.12.2583.2583

Facchetti, F., Appiani, C., Salvi, L., Levy, J., & Notarangelo, L. D. (1995). Immunohistologic analysis of ineffective CD40-CD40 ligand interaction in lymphoid tissues from patients with X-linked immunodeficiency with hyper-IgM. Abortive germinal center cell reaction and severe depletion of follicular dendritic cells. *Journal of Immunology (Baltimore, Md. : 1950)*, *154*(12), 6624–6633.

Fairhurst, A., Hwang, S., Wang, A., Tian, X., Boudreaux, C., Zhou, X. J., Casco, J., Li, Q., Connolly, J. E., & Wakeland, E. K. (2008). Yaa autoimmune phenotypes are conferred by overexpression of TLR7. *European Journal of Immunology*, *38*(7), 1971–1978. https://doi.org/10.1002/eji.200838138

Fearon, D. T., & Carter, R. H. (1995). The CD19/CR2/TAPA-1 Complex of B Lymphocytes: Linking Natural to Acquired Immunity. *Annual Review of Immunology*, *13*(1), 127–149. https://doi.org/10.1146/annurev.iy.13.040195.001015

Feng, D., Stone, R. C., Eloranta, M.-L., Sangster-Guity, N., Nordmark, G., Sigurdsson, S., Wang, C., Alm, G., SyvÃ¤nen, A.-C., RÃ¶nnblom, L., & Barnes, B. J. (2010). Genetic variants and disease-associated factors contribute to enhanced IRF-5 expression in blood cells of systemic lupus erythematosus patients. *Arthritis & Rheumatism*, NA-NA. https://doi.org/10.1002/art.27223

Fienberg, H. G., Simonds, E. F., Fantl, W. J., Nolan, G. P., & Bodenmiller, B. (2012). A platinum-based covalent viability reagent for single-cell mass cytometry. *Cytometry Part A*, *81A*(6), 467–475. https://doi.org/10.1002/cyto.a.22067

Flores-Mendoza, G., Sansón, S. P., Rodríguez-Castro, S., Crispín, J. C., & Rosetti, F. (2018). Mechanisms of Tissue Injury in Lupus Nephritis. In *Trends in Molecular Medicine* (Vol. 24, Issue 4, pp. 364–378). Elsevier Ltd. https://doi.org/10.1016/j.molmed.2018.02.003

Font, J., Pizcueta, P., Ramos-Casals, M., Cervera, R., García-Carrasco, M., Navarro, M., Ingelmo, M., & Engel, P. (2002). Increased serum levels of soluble l-selectin (CD62L) in patients with active systemic lupus erythematosus (SLE). *Clinical and Experimental Immunology*, *119*(1), 169–174. https://doi.org/10.1046/j.1365-2249.2000.01082.x

Förster, R., Davalos-Misslitz, A. C., & Rot, A. (2008). CCR7 and its ligands: Balancing immunity and tolerance. In *Nature Reviews Immunology* (Vol. 8, Issue 5, pp. 362–371). https://doi.org/10.1038/nri2297

Förster, R., Emrich, T., Kremmer, E., & Lipp, M. (1994). Expression of the G-protein--coupled receptor BLR1 defines mature, recirculating B cells and a subset of T-helper memory cells. *Blood*, *84*(3), 830–840. https://doi.org/10.1182/blood.V84.3.830.830

Förster, R., Mattis, A. E., Kremmer, E., Wolf, E., Brem, G., & Lipp, M. (1996). A Putative Chemokine Receptor, BLR1, Directs B Cell Migration to Defined Lymphoid Organs and Specific Anatomic Compartments of the Spleen. *Cell*, *87*(6), 1037–1047. https://doi.org/10.1016/S0092-8674(00)81798-5

Förster, R., Schubel, A., Breitfeld, D., Kremmer, E., Renner-Müller, I., Wolf, E., & Lipp, M. (1999). CCR7 Coordinates the Primary Immune Response by Establishing Functional Microenvironments in Secondary Lymphoid Organs. *Cell*, *99*(1), 23–33. https://doi.org/10.1016/S0092-8674(00)80059-8

Friedman, R. L., Manly, S. P., McMahon, M., Kerr, I. M., & Stark, G. R. (1984). Transcriptional and posttranscriptional regulation of interferon-induced gene expression in human cells. *Cell*, *38*(3), 745–755. https://doi.org/10.1016/0092-8674(84)90270-8

Fu, Q., Zhao, J., Qian, X., Wong, J. L. H., Kaufman, K. M., Yu, C. Y., Mok, M. Y., Harley, J. B., Guthridge, J. M., Song, Y. W., Cho, S.-K., Bae, S.-C., Grossman, J. M., Hahn, B. H., Arnett, F. C., Shen, N., & Tsao, B. P. (2011). Association of a functional IRF7 variant with systemic lupus erythematosus. *Arthritis & Rheumatism*, *63*(3), 749–754. https://doi.org/10.1002/art.30193

Gallatin, W. M., Weissman, I. L., & Butcher, E. C. (1983). A cell-surface molecule involved in organ-specific homing of lymphocytes. *Nature*, *304*(5921), 30–34. https://doi.org/10.1038/304030a0

Galy, A., Travis, M., Cen, D., & Chen, B. (1995). Human T, B, Natural Killer, and Dendritic Cells Arise from a Common Bone Marrow Progenitor Cell Subset. In *Immunity* (Vol. 3).

Garcia-Romo, G. S., Caielli, S., Vega, B., Connolly, J., Allantaz, F., Xu, Z., Punaro, M., Baisch, J., Guiducci, C., Coffman, R. L., Barrat, F. J., Banchereau, J., & Pascual, V. (2011). Netting Neutrophils Are Major Inducers of Type I IFN Production in Pediatric Systemic Lupus Erythematosus. *Science Translational Medicine*, *3*(73). https://doi.org/10.1126/scitranslmed.3001201

Garside, P., Ingulli, E., Merica, R. R., Johnson, J. G., Noelle, R. J., & Jenkins, M. K. (1998). Visualization of Specific B and T Lymphocyte Interactions in the Lymph Node. *Science*, *281*(5373), 96–99. https://doi.org/10.1126/science.281.5373.96

Gateva, V., Sandling, J. K., Hom, G., Taylor, K. E., Chung, S. A., Sun, X., Ortmann, W., Kosoy, R., Ferreira, R. C., Nordmark, G., Gunnarsson, I., Svenungsson, E., Padyukov, L., Sturfelt, G., Jönsen, A., Bengtsson, A. A., Rantapää-Dahlqvist, S., Baechler, E. C., Brown, E. E., … Graham, R. R. (2009). A large-scale replication study identifies TNIP1, PRDM1, JAZF1,

UHRF1BP1 and IL10 as risk loci for systemic lupus erythematosus. *Nature Genetics*, *41*(11), 1228–1233. https://doi.org/10.1038/ng.468

Gathings, W. E., Lawton, A. R., & Cooper, M. D. (1977). Immunofluorescent studies of the development of pre-B cells, B lymphocytes and immunoglobulin isotype diversity in humans. *European Journal of Immunology*, *7*(11), 804–810. https://doi.org/10.1002/eji.1830071112

Gay, D., Saunders, T., Camper, S., & Weigert, M. (1993). Receptor editing: an approach by autoreactive B cells to escape tolerance. *Journal of Experimental Medicine*, *177*(4), 999–1008. https://doi.org/10.1084/jem.177.4.999

Geha, R. S., Jabara, H. H., & Brodeur, S. R. (2003). The regulation of immunoglobulin E class-switch recombination. In *Nature Reviews Immunology* (Vol. 3, Issue 9, pp. 721–732). https://doi.org/10.1038/nri1181

Gladman, D. D., Ibañez, D., & Urowitz, M. B. (2002). Systemic lupus erythematosus disease activity index 2000. *The Journal of Rheumatology*, *29*(2), 288–291.

Golinski, M. L., Demeules, M., Derambure, C., Riou, G., Maho-Vaillant, M., Boyer, O., Joly, P., & Calbo, S. (2020). CD11c+ B Cells Are Mainly Memory Cells, Precursors of Antibody Secreting Cells in Healthy Donors. *Frontiers in Immunology*, *11*. https://doi.org/10.3389/fimmu.2020.00032

Gorfu, G., Rivera-Nieves, J., & Ley, K. (2009). *Role of β 7 integrins in intestinal lymphocyte homing and retention*.

Gracia-Tello, B., Ezeonyeji, A., & Isenberg, D. (2017). The use of rituximab in newly diagnosed patients with systemic lupus erythematosus: long-term steroid saving capacity and clinical effectiveness. *Lupus Science & Medicine*, *4*(1), e000182. https://doi.org/10.1136/lupus-2016-000182

Graham, R. R., Kozyrev, S. v., Baechler, E. C., Reddy, M. V. P. L., Plenge, R. M., Bauer, J. W., Ortmann, W. A., Koeuth, T., Escribano, M. F. G., Pons-Estel, B., Petri, M., Daly, M., Gregersen, P. K., Martín, J., Altshuler, D., Behrens, T. W., & Alarcón-Riquelme, M. E. (2006). A common haplotype of interferon regulatory factor 5 (IRF5) regulates splicing and expression and is associated with increased risk of systemic lupus erythematosus. *Nature Genetics*, *38*(5), 550–555. https://doi.org/10.1038/ng1782

Guerrier, T., Youinou, P., Pers, J.-O., & Jamin, C. (2012). TLR9 drives the development of transitional B cells towards the marginal zone pathway and promotes autoimmunity. *Journal of Autoimmunity*, *39*(3), 173–179. https://doi.org/10.1016/j.jaut.2012.05.012

Han, J. W., Zheng, H. F., Cui, Y., Sun, L. D., Ye, D. Q., Hu, Z., Xu, J. H., Cai, Z. M., Huang, W., Zhao, G. P., Xie, H. F., Fang, H., Lu, Q. J., Xu, J. H., Li, X. P., Pan, Y. F., Deng, D. Q., Zeng, F. Q., Ye, Z. Z., … Zhang, X. J. (2009). Genome-wide association study in a Chinese Han population identifies nine new susceptibility loci for systemic lupus erythematosus. *Nature Genetics*, *41*(11), 1234–1237. https://doi.org/10.1038/ng.472

Hanly, J. G., O'Keeffe, A. G., Su, L., Urowitz, M. B., Romero-Diaz, J., Gordon, C., Bae, S. C., Bernatsky, S., Clarke, A. E., Wallace, D. J., Merrill, J. T., Isenberg, D. A., Rahman, A., Ginzler, E. M., Fortin, P., Gladman, D. D., Sanchez-Guerrero, J., Petri, M., Bruce, I. N., … Farewell, V. (2015). The frequency and outcome of lupus nephritis: Results from an international inception cohort study. *Rheumatology (United Kingdom)*, *55*(2), 252–262. https://doi.org/10.1093/rheumatology/kev311

Hannan, P. J. (2016). The Structure-Function Relationships of Complement Receptor Type 2 (CR2; CD21). *Current Protein & Peptide Science*, *17*(5), 463–487. https://doi.org/10.2174/1389203717666151201192124

Harley, J. B., Alarcón-Riquelme, M. E., Criswell, L. A., Jacob, C. O., Kimberly, R. P., Moser, K. L., Tsao, B. P., Vyse, T. J., Langefeld, C. D., Nath, S. K., Guthridge, J. M., Cobb, B. L., Mirel, D. B., Marion, M. C., Williams, A. H., Divers, J., Wang, W., Frank, S. G., Namjou, B., … Kelly, J. A. (2008). Genome-wide association scan in women with systemic lupus erythematosus identifies susceptibility variants in ITGAM, PXK, KIAA1542 and other loci. *Nature Genetics*, *40*(2), 204–210. https://doi.org/10.1038/ng.81

Henneken, M., Dörner, T., Burmester, G.-R., & Berek, C. (2005). Differential expression of chemokine receptors on peripheral blood B cells from patients with rheumatoid arthritis and systemic lupus erythematosus. *Arthritis Research & Therapy*, *7*(5), R1001. https://doi.org/10.1186/ar1776

Hertz, M., & Nemazee, D. (1997). BCR Ligation Induces Receptor Editing in IgM+IgD− Bone Marrow B Cells In Vitro. *Immunity*, *6*(4), 429–436. https://doi.org/10.1016/S1074-7613(00)80286-1

Hjelm, F., Carlsson, F., Getahun, A., & Heyman, B. (2006). Antibody-Mediated Regulation of the Immune Response. *Scandinavian Journal of Immunology*, *64*(3), 177–184. https://doi.org/10.1111/j.1365-3083.2006.01818.x

Honczarenko, M., Glodek, A. M., Swierkowski, M., Na, I. K., & Silberstein, L. E. (2006). Developmental stage-specific shift in responsiveness to chemokines during human B-cell development. *Experimental Hematology*, *34*(8), 1093–1100. https://doi.org/10.1016/j.exphem.2006.05.013

Honda, K., & Taniguchi, T. (2006). IRFs: Master regulators of signalling by Toll-like receptors and cytosolic pattern-recognition receptors. In *Nature Reviews Immunology* (Vol. 6, Issue 9, pp. 644–658). https://doi.org/10.1038/nri1900

Honda, K., Yanai, H., Negishi, H., Asagiri, M., Sato, M., Mizutani, T., Shimada, N., Ohba, Y., Takaoka, A., Yoshida, N., & Taniguchi, T. (2005). IRF-7 is the master regulator of type-I interferon-dependent immune responses. *Nature*, *434*(7034), 772–777. https://doi.org/10.1038/nature03464

Houssiau, F. A., D'Cruz, D., Sangle, S., Remy, P., Vasconcelos, C., Petrovic, R., Fiehn, C., de Ramon Garrido, E., Gilboe, I.-M., Tektonidou, M., Blockmans, D., Ravelingien, I., le Guern, V., Depresseux, G., Guillevin, L., & Cervera, R. (2010). Azathioprine versus mycophenolate mofetil for long-term immunosuppression in lupus nephritis: results from the MAINTAIN Nephritis Trial. *Annals of the Rheumatic Diseases*, *69*(12), 2083–2089. https://doi.org/10.1136/ard.2010.131995

Huang, I. C., Bailey, C. C., Weyer, J. L., Radoshitzky, S. R., Becker, M. M., Chiang, J. J., Brass, A. L., Ahmed, A. A., Chi, X., Dong, L., Longobardi, L. E., Boltz, D., Kuhn, J. H., Elledge, S. J., Bavari, S., Denison, M. R., Choe, H., & Farzan, M. (2011). Distinct patterns of IFITM-mediated restriction of filoviruses, SARS coronavirus, and influenza A virus. *PLoS Pathogens*, *7*(1). https://doi.org/10.1371/journal.ppat.1001258

Iwamoto, T., Dorschner, J. M., Selvaraj, S., Mezzano, V., Jensen, M. A., Vsetecka, D., Amin, S., Makol, A., Osborn, T., Moder, K., Chowdhary, V. R., Izmirly, P., Belmont, H. M., Clancy, R. M., Buyon, J. P., Wu, M., Loomis, C. A., & Niewold, T. B. (2022). High Systemic Type I Interferon Activity Is Associated With Active Class III/IV Lupus Nephritis. *The Journal of Rheumatology*, *49*(4), 388–397. https://doi.org/10.3899/jrheum.210391

Izmirly, P. M., Parton, H., Wang, L., McCune, W. J., Lim, S. S., Drenkard, C., Ferucci, E. D., Dall'Era, M., Gordon, C., Helmick, C. G., & Somers, E. C. (2021). Prevalence of Systemic Lupus Erythematosus in the United States: Estimates From a Meta-Analysis of the

Centers for Disease Control and Prevention National Lupus Registries. *Arthritis and Rheumatology*, *73*(6), 991–996. https://doi.org/10.1002/art.41632

Izui, S., Merino, R., Fossati, L., & Iwamoto, M. (1994). The Role of the Yaa Gene in Lupus Syndrome. *International Reviews of Immunology*, *11*(3), 211–230. https://doi.org/10.3109/08830189409061728

Jenks, S. A., Cashman, K. S., Woodruff, M. C., Lee, F. E., & Sanz, I. (2019). Extrafollicular responses in humans and SLE. *Immunological Reviews*, *288*(1), 136–148. https://doi.org/10.1111/imr.12741

Jenks, S. A., Cashman, K. S., Zumaquero, E., Marigorta, U. M., Patel, A. v., Wang, X., Tomar, D., Woodruff, M. C., Simon, Z., Bugrovsky, R., Blalock, E. L., Scharer, C. D., Tipton, C. M., Wei, C., Lim, S. S., Petri, M., Niewold, T. B., Anolik, J. H., Gibson, G., … Sanz, I. (2018). Distinct Effector B Cells Induced by Unregulated Toll-like Receptor 7 Contribute to Pathogenic Responses in Systemic Lupus Erythematosus. *Immunity*, *49*(4), 725-739.e6. https://doi.org/10.1016/j.immuni.2018.08.015

Kaminski, D. A., Wei, C., Qian, Y., Rosenberg, A. F., & Sanz, I. (2012). Advances in human B cell phenotypic profiling. In *Frontiers in Immunology* (Vol. 3, Issue OCT). https://doi.org/10.3389/fimmu.2012.00302

Katze, M. G., He, Y., & Gale, M. (2002). Viruses and interferon: A fight for supremacy. In *Nature Reviews Immunology* (Vol. 2, Issue 9, pp. 675–687). https://doi.org/10.1038/nri888

Kaul, A., Gordon, C., Crow, M. K., Touma, Z., Urowitz, M. B., van Vollenhoven, R., Ruiz-Irastorza, G., & Hughes, G. (2016). Systemic lupus erythematosus. *Nature Reviews Disease Primers*, *2*. https://doi.org/10.1038/nrdp.2016.39

Kay, A. W., Strauss-Albee, D. M., & Blish, C. A. (2016). Application of mass cytometry (CyTOF) for functional and phenotypic analysis of natural killer cells. In *Methods in Molecular Biology* (Vol. 1441, pp. 13–26). Humana Press Inc. https://doi.org/10.1007/978-1-4939-3684-7_2

Kerr, W. G., Cooper, M. D., Feng, L., Burrows, P. D., & Hendershot, L. M. (1989). Mu heavy chains can associate with a pseudo-light chain complex (ψL) in human pre-B cell lines. *International Immunology*, *1*(4), 355–361. https://doi.org/10.1093/intimm/1.4.355

Klein, U., Küppers, R., & Rajewsky, K. (1997). Evidence for a Large Compartment of IgM-Expressing Memory B Cells in Humans. *Blood*, *89*(4), 1288–1298. https://doi.org/10.1182/blood.V89.4.1288

Klein, U., Rajewsky, K., & Küppers, R. (1998). Human Immunoglobulin (Ig)M IgD Peripheral Blood B Cells Expressing the CD27 Cell Surface Antigen Carry Somatically Mutated Variable Region Genes: CD27 as a General Marker for Somatically Mutated (Memory) B Cells. In *J. Exp. Med* (Vol. 188, Issue 9). http://www.jem.org

Kohn, L. A., Hao, Q. L., Sasidharan, R., Parekh, C., Ge, S., Zhu, Y., Mikkola, H. K. A., & Crooks, G. M. (2012). Lymphoid priming in human bone marrow begins before expression of CD10 with upregulation of L-selectin. *Nature Immunology*, *13*(10), 963–971. https://doi.org/10.1038/ni.2405

Korsmeyer, S. J., Hieter, P. A., Sharrow, S. O., Goldman, C. K., Leder, P., & Waldmann, T. A. (1982). Normal human B cells display ordered light chain gene rearrangements and deletions. In *Journal of Experimental Medicine* • (Vol. 156). http://rupress.org/jem/article-pdf/156/4/975/1092838/975.pdf

Kotenko, S. v., Gallagher, G., Baurin, V. v., Lewis-Antes, A., Shen, M., Shah, N. K., Langer, J. A., Sheikh, F., Dickensheets, H., & Donnelly, R. P. (2003). IFN-λs mediate antiviral protection

through a distinct class II cytokine receptor complex. In *Nature Immunology* (Vol. 4, Issue 1, pp. 69–77). https://doi.org/10.1038/ni875

Kraal, G., Schornagel, K., Streeter, P. R., Holzmann, B., & Butcher, E. C. (1995). Expression of the Mucosal Vascular Addressin, MAdCAM-1, on Sinus-Lining Cells in the Spleen. In *American Journal ofPathology* (Vol. 147, Issue 3).

Kruetzmann, S., Rosado, M. M., Weber, H., Germing, U., Tournilhac, O., Peter, H. H., Berner, R., Peters, A., Boehm, T., Plebani, A., Quinti, I., & Carsetti, R. (2003). Human immunoglobulin M memory B cells controlling Streptococcus pneumoniae infections are generated in the spleen. *Journal of Experimental Medicine*, *197*(7), 939–945. https://doi.org/10.1084/jem.20022020

Krzyzak, L., Seitz, C., Urbat, A., Hutzler, S., Ostalecki, C., Gläsner, J., Hiergeist, A., Gessner, A., Winkler, T. H., Steinkasserer, A., & Nitschke, L. (2016). CD83 Modulates B Cell Activation and Germinal Center Responses. *The Journal of Immunology*, *196*(9), 3581–3594. https://doi.org/10.4049/jimmunol.1502163

Kumar, K., Chambers, S., & Gordon, C. (2009). Challenges of ethnicity in SLE. In *Best Practice and Research: Clinical Rheumatology* (Vol. 23, Issue 4, pp. 549–561). https://doi.org/10.1016/j.berh.2009.04.005

Kužnik, A., Benčina, M., Švajger, U., Jeras, M., Rozman, B., & Jerala, R. (2011). Mechanism of Endosomal TLR Inhibition by Antimalarial Drugs and Imidazoquinolines. *The Journal of Immunology*, *186*(8), 4794–4804. https://doi.org/10.4049/jimmunol.1000702

Kyogoku, C., Ortmann, W. A., Lee, A., Selby, S., Carlton, V. E. H., Chang, M., Ramos, P., Baechler, E. C., Batliwalla, F. M., Novitzke, J., Williams, A. H., Gillett, C., Rodine, P., Graham, R. R., Ardlie, K. G., Gaffney, P. M., Moser, K. L., Petri, M., Begovich, A. B., … Behrens, T. W. (2004). Genetic Association of the R620W Polymorphism of Protein Tyrosine Phosphatase PTPN22 with Human SLE. *The American Journal of Human Genetics*, *75*(3), 504–507. https://doi.org/10.1086/423790

Lafouresse, F., Bellard, E., Laurent, C., Moussion, C., Fournié, J.-J., Ysebaert, L., & Girard, J.-P. (2015). L-selectin controls trafficking of chronic lymphocytic leukemia cells in lymph node high endothelial venules in vivo. *Blood*, *126*(11), 1336–1345. https://doi.org/10.1182/blood-2015-02-626291

Lamphier, M., Zheng, W., Latz, E., Spyvee, M., Hansen, H., Rose, J., Genest, M., Yang, H., Shaffer, C., Zhao, Y., Shen, Y., Liu, C., Liu, D., Mempel, T. R., Rowbottom, C., Chow, J., Twine, N. C., Yu, M., Gusovsky, F., & Ishizaka, S. T. (2014). Novel Small Molecule Inhibitors of TLR7 and TLR9: Mechanism of Action and Efficacy In Vivo. *Molecular Pharmacology*, *85*(3), 429–440. https://doi.org/10.1124/mol.113.089821

Lande, R., Ganguly, D., Facchinetti, V., Frasca, L., Conrad, C., Gregorio, J., Meller, S., Chamilos, G., Sebasigari, R., Riccieri, V., Bassett, R., Amuro, H., Fukuhara, S., Ito, T., Liu, Y.-J., & Gilliet, M. (2011). Neutrophils Activate Plasmacytoid Dendritic Cells by Releasing Self-DNA–Peptide Complexes in Systemic Lupus Erythematosus. *Science Translational Medicine*, *3*(73). https://doi.org/10.1126/scitranslmed.3001180

Landolt-Marticorena, C., Wither, R., Reich, H., Herzenberg, A., Scholey, J., Gladman, D. D., Urowitz, M. B., Fortin, P. R., & Wither, J. (2011). Increased expression of B cell activation factor supports the abnormal expansion of transitional B Cells in systemic lupus erythematosus. *Journal of Rheumatology*, *38*(4), 642–651. https://doi.org/10.3899/jrheum.100214

Lanzavecchia, A. (1985). Antigen-specific interaction between T and B cells. *Nature*, *314*(6011), 537–539. https://doi.org/10.1038/314537a0

Legler, D. F., Loetscher, M., Roos, R. S., Clark-Lewis, I., Baggiolini, M., & Moser, B. (1998). B Cell-attracting Chemokine 1, a Human CXC Chemokine Expressed in Lymphoid Tissues, Selectively Attracts B Lymphocytes via BLR1/CXCR5. In *J. Exp. Med* (Vol. 187, Issue 4). http://www.jem.org

Levinsky, R. J., Cameron, J. S., & Soothill, J. F. (1977). Serum immune complexes and disease activity in lupus nephritis. *The Lancet*, *309*(8011), 564–567. https://doi.org/10.1016/S0140-6736(77)91998-5

Li, F. J., Schreeder, D. M., Li, R., Wu, J., & Davis, R. S. (2013). FCRL3 promotes TLR9-induced B-cell activation and suppresses plasma cell differentiation. *European Journal of Immunology*, *43*(11), 2980–2992. https://doi.org/10.1002/eji.201243068

Liu, M., Guo, Q., Wu, C., Sterlin, D., Goswami, S., Zhang, Y., Li, T., Bao, C., Shen, N., Fu, Q., & Zhang, X. (2019). Type I interferons promote the survival and proinflammatory properties of transitional B cells in systemic lupus erythematosus patients. *Cellular and Molecular Immunology*, *16*(4), 367–379. https://doi.org/10.1038/s41423-018-0010-6

Lodwig, E. M., Hosie, A. H. F., Bourdès, A., Findlay, K., Allaway, D., Karunakaran, R., Downie, J. A., & Poole, P. S. (2003). Amino-acid cycling drives nitrogen fixation in the legume-Rhizobium symbiosis. *Nature*, *422*(6933), 722–726. https://doi.org/10.1038/nature01527

Ma, Q., Jones, D., & Springer, T. A. (1999). The Chemokine Receptor CXCR4 Is Required for the Retention of B Lineage and Granulocytic Precursors within the Bone Marrow Microenvironment. In *Immunity* (Vol. 10). Berliner.

Mai, L., Asaduzzaman, A., Noamani, B., Fortin, P. R., Gladman, D. D., Touma, Z., Urowitz, M. B., & Wither, J. (2021). The baseline interferon signature predicts disease severity over the subsequent 5 years in systemic lupus erythematosus. *Arthritis Research and Therapy*, *23*(1). https://doi.org/10.1186/s13075-021-02414-0

Maria, N. I., & Davidson, A. (2020). Protecting the kidney in systemic lupus erythematosus: from diagnosis to therapy. In *Nature Reviews Rheumatology* (Vol. 16, Issue 5, pp. 255–267). Nature Research. https://doi.org/10.1038/s41584-020-0401-9

Marie-Cardine, A., Divay, F., Dutot, I., Green, A., Perdrix, A., Boyer, O., Contentin, N., Tilly, H., Tron, F., Vannier, J. P., & Jacquot, S. (2008). Transitional B cells in humans: Characterization and insight from B lymphocyte reconstitution after hematopoietic stem cell transplantation. *Clinical Immunology*, *127*(1), 14–25. https://doi.org/10.1016/j.clim.2007.11.013

Maroz, N., & Segal, M. S. (2013). Lupus Nephritis and End-stage Kidney Disease. *The American Journal of the Medical Sciences*, *346*(4), 319–323. https://doi.org/10.1097/MAJ.0b013e31827f4ee3

Martin-Gutierrez, L., Peng, J., Thompson, N. L., Robinson, G. A., Naja, M., Peckham, H., Wu, W., J'bari, H., Ahwireng, N., Waddington, K. E., Bradford, C. M., Varnier, G., Gandhi, A., Radmore, R., Gupta, V., Isenberg, D. A., Jury, E. C., & Ciurtin, C. (2021). Stratification of Patients With Sjögren's Syndrome and Patients With Systemic Lupus Erythematosus According to Two Shared Immune Cell Signatures, With Potential Therapeutic Implications. *Arthritis & Rheumatology*, *73*(9), 1626–1637. https://doi.org/10.1002/art.41708

Matsumoto, A. K., Kopicky-Burd, J., Carter, R. H., Tuveson, D. A., Tedder, T. F., & Fearon, D. T. (1991). Intersection of the complement and immune systems: a signal transduction complex of the B lymphocyte-containing complement receptor type 2 and CD19. *Journal of Experimental Medicine*, *173*(1), 55–64. https://doi.org/10.1084/jem.173.1.55

McNab, F., Mayer-Barber, K., Sher, A., Wack, A., & O'Garra, A. (2015). Type I interferons in infectious disease. In *Nature Reviews Immunology* (Vol. 15, Issue 2, pp. 87–103). Nature Publishing Group. https://doi.org/10.1038/nri3787

Merrell, K. T., Benschop, R. J., Gauld, S. B., Aviszus, K., Decote-Ricardo, D., Wysocki, L. J., & Cambier, J. C. (2006). Identification of Anergic B Cells within a Wild-Type Repertoire. *Immunity*, *25*(6), 953–962. https://doi.org/10.1016/j.immuni.2006.10.017

Mishra, D., Singh, S., & Narayan, G. (2016). Role of B Cell Development Marker CD10 in Cancer Progression and Prognosis. *Molecular Biology International*, *2016*, 1–9. https://doi.org/10.1155/2016/4328697

Miyamoto, M., Fujita, T., Kimura, Y., Maruyama, M., Harada, H., Sudo, Y., Miyata, T., & Taniguchi, T. (1988). Regulated expression of a gene encoding a nuclear factor, IRF-1, that specifically binds to IFN-β gene regulatory elements. *Cell*, *54*(6), 903–913. https://doi.org/10.1016/S0092-8674(88)91307-4

Morbach, H., Eichhorn, E. M., Liese, J. G., & Girschick, H. J. (2010). Reference values for B cell subpopulations from infancy to adulthood. *Clinical and Experimental Immunology*, *162*(2), 271–279. https://doi.org/10.1111/j.1365-2249.2010.04206.x

Morris, D. L., Roberts, A. L., Witherden, A. S., Tarzi, R., Barros, P., Whittaker, J. C., Cook, T. H., Aitman, T. J., & Vyse, T. J. (2010). Evidence for both copy number and allelic (NA1/NA2) risk at the FCGR3B locus in systemic lupus erythematosus. *European Journal of Human Genetics*, *18*(9), 1027–1031. https://doi.org/10.1038/ejhg.2010.56

Muramatsu, M., Kinoshita, K., Fagarasan, S., Yamada, S., Shinkai, Y., & Honjo, T. (2000). Class Switch Recombination and Hypermutation Require Activation-Induced Cytidine Deaminase (AID), a Potential RNA Editing Enzyme. In *Cell* (Vol. 102).

Muramatsu, M., Sankaranand, V. S., Anant, S., Sugai, M., Kinoshita, K., Davidson, N. O., & Honjo, T. (1999). Specific Expression of Activation-induced Cytidine Deaminase (AID), a Novel Member of the RNA-editing Deaminase Family in Germinal Center B Cells. *Journal of Biological Chemistry*, *274*(26), 18470–18476. https://doi.org/10.1074/jbc.274.26.18470

Naradikian, M. S., Myles, A., Beiting, D. P., Roberts, K. J., Dawson, L., Herati, R. S., Bengsch, B., Linderman, S. L., Stelekati, E., Spolski, R., Wherry, E. J., Hunter, C., Hensley, S. E., Leonard, W. J., & Cancro, M. P. (2016). Cutting Edge: IL-4, IL-21, and IFN-γ Interact To Govern T-bet and CD11c Expression in TLR-Activated B Cells. *The Journal of Immunology*, *197*(4), 1023–1028. https://doi.org/10.4049/jimmunol.1600522

Navarra, S. v, Guzmán, R. M., Gallacher, A. E., Hall, S., Levy, R. A., Jimenez, R. E., Li, E. K.-M., Thomas, M., Kim, H.-Y., León, M. G., Tanasescu, C., Nasonov, E., Lan, J.-L., Pineda, L., Zhong, Z. J., Freimuth, W., & Petri, M. A. (2011). Efficacy and safety of belimumab in patients with active systemic lupus erythematosus: a randomised, placebo-controlled, phase 3 trial. *The Lancet*, *377*(9767), 721–731. https://doi.org/10.1016/S0140-6736(10)61354-2

Nehar-Belaid, D., Hong, S., Marches, R., Chen, G., Bolisetty, M., Baisch, J., Walters, L., Punaro, M., Rossi, R. J., Chung, C. H., Huynh, R. P., Singh, P., Flynn, W. F., Tabanor-Gayle, J. A., Kuchipudi, N., Mejias, A., Collet, M. A., Lucido, A. L., Palucka, K., … Banchereau, J. F. (2020). Mapping systemic lupus erythematosus heterogeneity at the single-cell level. *Nature Immunology*, *21*(9), 1094–1106. https://doi.org/10.1038/s41590-020-0743-0

Neil, S. J. D., Zang, T., & Bieniasz, P. D. (2008). Tetherin inhibits retrovirus release and is antagonized by HIV-1 Vpu. *Nature*, *451*(7177), 425–430. https://doi.org/10.1038/nature06553

Nemazee, D. (2017). Mechanisms of central tolerance for B cells. In *Nature Reviews Immunology* (Vol. 17, Issue 5, pp. 281–294). Nature Publishing Group. https://doi.org/10.1038/nri.2017.19

Nemazee, D. A., & Bürki, K. (1989). Clonal deletion of B lymphocytes in a transgenic mouse bearing anti-MHC class I antibody genes. *Nature*, *337*(6207), 562–566. https://doi.org/10.1038/337562a0

Nemazee, D., & Buerki, K. (1989). Clonal deletion of autoreactive B lymphocytes in bone marrow chimeras. *Proceedings of the National Academy of Sciences*, *86*(20), 8039–8043. https://doi.org/10.1073/pnas.86.20.8039

Nie, Y., Han, Y. C., & Zou, Y. R. (2008). CXCR4 is required for the quiescence of primitive hematopoietic cells. *Journal of Experimental Medicine*, *205*(4), 777–783. https://doi.org/10.1084/jem.20072513

Nie, Y., Waite, J., Brewer, F., Sunshine, M. J., Littman, D. R., & Zou, Y. R. (2004). The role of CXCR4 in maintaining peripheral B cell compartments and humoral immunity. *Journal of Experimental Medicine*, *200*(9), 1145–1156. https://doi.org/10.1084/jem.20041185

Nishimoto, N., Kubagawa, H., Ohno, T., Gartland, G. L., Stankovic, A. K., & Cooper, M. D. (1991). Normal pre-B cells express a receptor complex of mu heavy chains and surrogate light-chain proteins. *Proceedings of the National Academy of Sciences*, *88*(14), 6284–6288. https://doi.org/10.1073/pnas.88.14.6284

Novick, D., Cohen, B., & Rubinstein, M. (1994). The Human Interferon a/p Receptor: Characterization and Molecular Cloning. In *Cell* (Vol. 77).

Okada, T., Miller, M. J., Parker, I., Krummel, M. F., Neighbors, M., Hartley, S. B., O'Garra, A., Cahalan, M. D., & Cyster, J. G. (2005). Antigen-Engaged B Cells Undergo Chemotaxis toward the T Zone and Form Motile Conjugates with Helper T Cells. *PLoS Biology*, *3*(6), e150. https://doi.org/10.1371/journal.pbio.0030150

Otero, D. C., Anzelon, A. N., & Rickert, R. C. (2003). CD19 Function in Early and Late B Cell Development: I. Maintenance of Follicular and Marginal Zone B Cells Requires CD19-Dependent Survival Signals. *The Journal of Immunology*, *170*(1), 73–83. https://doi.org/10.4049/jimmunol.170.1.73

Palanichamy, A., Barnard, J., Zheng, B., Owen, T., Quach, T., Wei, C., Looney, R. J., Sanz, I., & Anolik, J. H. (2009). Novel Human Transitional B Cell Populations Revealed by B Cell Depletion Therapy. *The Journal of Immunology*, *182*(10), 5982–5993. https://doi.org/10.4049/jimmunol.0801859

Paus, D., Tri, G. P., Chan, T. D., Gardam, S., Basten, A., & Brink, R. (2006). Antigen recognition strength regulates the choice between extrafollicular plasma cell and germinal center B cell differentiation. *Journal of Experimental Medicine*, *203*(4), 1081–1091. https://doi.org/10.1084/jem.20060087

Peng, Y., Guo, F., Liao, S., Liao, H., Xiao, H., Yang, L., Liu, H. feng, & Pan, Q. (2020). Altered frequency of peripheral B-cell subsets and their correlation with disease activity in patients with systemic lupus erythematosus: A comprehensive analysis. *Journal of Cellular and Molecular Medicine*, *24*(20), 12044–12053. https://doi.org/10.1111/jcmm.15836

Pestka, S., Krause, C. D., & Walter, M. R. (2004). Interferons, interferon-like cytokines, and their receptors. *Immunological Reviews*, *202*(1), 8–32. https://doi.org/10.1111/j.0105-2896.2004.00204.x

Piedra-Quintero, Z. L., Wilson, Z., Nava, P., & Guerau-de-Arellano, M. (2020). CD38: An Immunomodulatory Molecule in Inflammation and Autoimmunity. In *Frontiers in*

Immunology (Vol. 11). Frontiers Media S.A. https://doi.org/10.3389/fimmu.2020.597959

Pisitkun, P., Deane, J. A., Difilippantonio, M. J., Tarasenko, T., Satterthwaite, A. B., & Bolland, S. (2006). Autoreactive B Cell Responses to RNA-Related Antigens Due to TLR7 Gene Duplication. *Science*, *312*(5780), 1669–1672. https://doi.org/10.1126/science.1124978

Poe, J. C., Fujimoto, M., Jansen, P. J., Miller, A. S., & Tedder, T. F. (2000). CD22 Forms a Quaternary Complex with SHIP, Grb2, and Shc. *Journal of Biological Chemistry*, *275*(23), 17420–17427. https://doi.org/10.1074/jbc.M001892200

Ponticelli, C., & Moroni, G. (2017). Hydroxychloroquine in systemic lupus erythematosus (SLE). *Expert Opinion on Drug Safety*, *16*(3), 411–419. https://doi.org/10.1080/14740338.2017.1269168

Prazma, C. M., & Tedder, T. F. (2008). Dendritic cell CD83: A therapeutic target or innocent bystander? In *Immunology Letters* (Vol. 115, Issue 1, pp. 1–8). https://doi.org/10.1016/j.imlet.2007.10.001

Prelli Bozzo, C., Nchioua, R., Volcic, M., Koepke, L., Krüger, J., Schütz, D., Heller, S., Stürzel, C. M., Kmiec, D., Conzelmann, C., Müller, J., Zech, F., Braun, E., Groß, R., Wettstein, L., Weil, T., Weiß, J., Diofano, F., Rodríguez Alfonso, A. A., … Kirchhoff, F. (2021). IFITM proteins promote SARS-CoV-2 infection and are targets for virus inhibition in vitro. *Nature Communications*, *12*(1). https://doi.org/10.1038/s41467-021-24817-y

Provost, T. T., Levin, L. S., Watson, R. M., Mayo, M., & Ratrie, H. (1991). Detection of anti-Ro(SSA) antibodies by gel double diffusion and a 'sandwich' ELISA in systemic and subacute cutaneous lupus erythematosus and Sjögren's syndrome. *Journal of Autoimmunity*, *4*(1), 87–96. https://doi.org/10.1016/0896-8411(91)90009-2

Psarras, A., Emery, P., & Vital, E. M. (2017). Type I interferon–mediated autoimmune diseases: pathogenesis, diagnosis and targeted therapy. *Rheumatology*, kew431. https://doi.org/10.1093/rheumatology/kew431

Qiu, P., Simonds, E. F., Bendall, S. C., Gibbs, K. D., Bruggner, R. v., Linderman, M. D., Sachs, K., Nolan, G. P., & Plevritis, S. K. (2011). Extracting a cellular hierarchy from high-dimensional cytometry data with SPADE. *Nature Biotechnology*, *29*(10), 886–893. https://doi.org/10.1038/nbt.1991

Quách, T. D., Manjarrez-Orduño, N., Adlowitz, D. G., Silver, L., Yang, H., Wei, C., Milner, E. C. B., & Sanz, I. (2011). Anergic Responses Characterize a Large Fraction of Human Autoreactive Naive B Cells Expressing Low Levels of Surface IgM. *The Journal of Immunology*, *186*(8), 4640–4648. https://doi.org/10.4049/jimmunol.1001946

Rada, C., di Noia, J. M., & Neuberger, M. S. (2004). Mismatch Recognition and Uracil Excision Provide Complementary Paths to Both Ig Switching and the A/T-Focused Phase of Somatic Mutation. *Molecular Cell*, *16*(2), 163–171. https://doi.org/10.1016/j.molcel.2004.10.011

Ricker, E., Manni, M., Flores-Castro, D., Jenkins, D., Gupta, S., Rivera-Correa, J., Meng, W., Rosenfeld, A. M., Pannellini, T., Bachu, M., Chinenov, Y., Sculco, P. K., Jessberger, R., Prak, E. T. L., & Pernis, A. B. (2021). Altered function and differentiation of age-associated B cells contribute to the female bias in lupus mice. *Nature Communications*, *12*(1). https://doi.org/10.1038/s41467-021-25102-8

Rock, K. L., Benacerraf, B., & Abbas, A. K. (1984). Antigen presentation by hapten-specific B lymphocytes. I. Role of surface immunoglobulin receptors. *Journal of Experimental Medicine*, *160*(4), 1102–1113. https://doi.org/10.1084/jem.160.4.1102

Rodziewicz, M., Dyball, S., Lunt, M., McDonald, S., Sutton, E., Parker, B., Bruce, I. N., Abernethy, R., Ahmad, Y., Akil, M., Bartram, S., Batley, M., Bharadwaj, A., Bruce, I., Carlucci, F., Chan, A., Dasgupta, B., D'Cruz, D., de Lord, D., … Zoma, A. (2023). Early infection risk in patients with systemic lupus erythematosus treated with rituximab or belimumab from the British Isles Lupus Assessment Group Biologics Register (BILAG-BR): a prospective longitudinal study. *The Lancet Rheumatology*, *5*(5), e284–e292. https://doi.org/10.1016/S2665-9913(23)00091-7

Rönnblom, L., & Alm, G. v. (2001). An etiopathogenic role for the type I IFN system in SLE. *Trends in Immunology*, *22*(8), 427–431. https://doi.org/10.1016/S1471-4906(01)01955-X

Sanz, I., Wei, C., Jenks, S. A., Cashman, K. S., Tipton, C., Woodruff, M. C., Hom, J., & Lee, F. E. H. (2019). Challenges and opportunities for consistent classification of human b cell and plasma cell populations. In *Frontiers in Immunology* (Vol. 10, Issue OCT). Frontiers Media S.A. https://doi.org/10.3389/fimmu.2019.02458

Sanz, I., Wei, C., Lee, F. E. H., & Anolik, J. (2008). Phenotypic and functional heterogeneity of human memory B cells. In *Seminars in Immunology* (Vol. 20, Issue 1, pp. 67–82). https://doi.org/10.1016/j.smim.2007.12.006

Saunders, S. P., Ma, E. G. M., Aranda, C. J., & Curotto de Lafaille, M. A. (2019). Non-classical B Cell Memory of Allergic IgE Responses. In *Frontiers in immunology* (Vol. 10, p. 715). NLM (Medline). https://doi.org/10.3389/fimmu.2019.00715

Schoggins, J. W., & Rice, C. M. (2011). Interferon-stimulated genes and their antiviral effector functions. In *Current Opinion in Virology* (Vol. 1, Issue 6, pp. 519–525). Elsevier B.V. https://doi.org/10.1016/j.coviro.2011.10.008

See, P., Lum, J., Chen, J., & Ginhoux, F. (2018). A Single-Cell Sequencing Guide for Immunologists. *Frontiers in Immunology*, *9*. https://doi.org/10.3389/fimmu.2018.02425

Shemesh, M., Lochte, S., Piehler, J., & Schreiber, G. (2021). IFNAR1 and IFNAR2 play distinct roles in initiating type I interferon–induced JAK-STAT signaling and activating STATs. *Science Signaling*, *14*(710). https://doi.org/10.1126/scisignal.abe4627

Shen, N., Fu, Q., Deng, Y., Qian, X., Zhao, J., Kaufman, K. M., Wu, Y. L., Yu, C. Y., Tang, Y., Chen, J.-Y., Yang, W., Wong, M., Kawasaki, A., Tsuchiya, N., Sumida, T., Kawaguchi, Y., Howe, H. S., Mok, M. Y., Bang, S.-Y., … Tsao, B. P. (2010). Sex-specific association of X-linked Toll-like receptor 7 (TLR7) with male systemic lupus erythematosus. *Proceedings of the National Academy of Sciences*, *107*(36), 15838–15843. https://doi.org/10.1073/pnas.1001337107

Siegal, F. P., Kadowaki, N., Shodell, M., Fitzgerald-Bocarsly, P. A., Shah, K., Ho, S., Antonenko, S., & Liu, Y.-J. (1999). The Nature of the Principal Type 1 Interferon-Producing Cells in Human Blood. *Science*, *284*(5421), 1835–1837. https://doi.org/10.1126/science.284.5421.1835

Sieger, N., Fleischer, S. J., Mei, H. E., Reiter, K., Shock, A., Burmester, G. R., Daridon, C., & Dörner, T. (2013). CD22 ligation inhibits downstream B cell receptor signaling and Ca $^{2+}$ flux upon activation. *Arthritis & Rheumatism*, *65*(3), 770–779. https://doi.org/10.1002/art.37818

Simon, Q., Pers, J. O., Cornec, D., le Pottier, L., Mageed, R. A., & Hillion, S. (2016). In-depth characterization of CD24highCD38high transitional human B cells reveals different regulatory profiles. *Journal of Allergy and Clinical Immunology*, *137*(5), 1577-1584.e10. https://doi.org/10.1016/j.jaci.2015.09.014

Sims, G. P., Ettinger, R., Shirota, Y., Yarboro, C. H., Illei, G. G., & Lipsky, P. E. (2005). *Identification and characterization of circulating human transitional B cells*. https://doi.org/10.1182/blood-2004-11

Siu, J. H., Pitcher, M. J., Tull, T. J., Velounias, R. L., Guesdon, W., Montorsi, L., Mahbubani, K. T., Ellis, R., Dhami, P., Todd, K., Kadolsky, U. D., Kleeman, M., D, D. P., Saeb-Parsy, K., Bemark, M., Pettigrew, G. J., & Spencer, J. (2022). Two subsets of human marginal zone B cells resolved by global analysis of lymphoid tissues and blood. In *Sci. Immunol* (Vol. 7). https://www.science.org

Smith, C. K., & Kaplan, M. J. (2015). The role of neutrophils in the pathogenesis of systemic lupus erythematosus. *Current Opinion in Rheumatology*, *27*(5), 448–453. https://doi.org/10.1097/BOR.0000000000000197

Sosa-Hernández, V. A., Torres-Ruíz, J., Cervantes-Díaz, R., Romero-Ramírez, S., Páez-Franco, J. C., Meza-Sánchez, D. E., Juárez-Vega, G., Pérez-Fragoso, A., Ortiz-Navarrete, V., Ponce-de-León, A., Llorente, L., Berrón-Ruiz, L., Mejía-Domínguez, N. R., Gómez-Martín, D., & Maravillas-Montero, J. L. (2020). B Cell Subsets as Severity-Associated Signatures in COVID-19 Patients. *Frontiers in Immunology*, *11*. https://doi.org/10.3389/fimmu.2020.611004

Stoeckius, M., Hafemeister, C., Stephenson, W., Houck-Loomis, B., Chattopadhyay, P. K., Swerdlow, H., Satija, R., & Smibert, P. (2017). Simultaneous epitope and transcriptome measurement in single cells. *Nature Methods*, *14*(9), 865–868. https://doi.org/10.1038/nmeth.4380

Stuart, T., Butler, A., Hoffman, P., Hafemeister, C., Papalexi, E., Mauck, W. M., Hao, Y., Stoeckius, M., Smibert, P., & Satija, R. (2019). Comprehensive Integration of Single-Cell Data. *Cell*, *177*(7), 1888-1902.e21. https://doi.org/10.1016/j.cell.2019.05.031

Subramanian, S., Tus, K., Li, Q.-Z., Wang, A., Tian, X.-H., Zhou, J., Liang, C., Bartov, G., McDaniel, L. D., Zhou, X. J., Schultz, R. A., & Wakeland, E. K. (2006). A Tlr7 translocation accelerates systemic autoimmunity in murine lupus. *Proceedings of the National Academy of Sciences*, *103*(26), 9970–9975. https://doi.org/10.1073/pnas.0603912103

Suryani, S., Fulcher, D. A., Santner-Nanan, B., Nanan, R., Wong, M., Shaw, P. J., Gibson, J., Williams, A., & Tangye, S. G. (2010). Differential expression of CD21 identifies developmentally and functionally distinct subsets of human transitional B cells. *Blood*, *115*(3), 519–529. https://doi.org/10.1182/blood-2009-07-234799

Suzuki, K., Grigorova, I., Phan, T. G., Kelly, L. M., & Cyster, J. G. (2009). Visualizing B cell capture of cognate antigen from follicular dendritic cells. *Journal of Experimental Medicine*, *206*(7), 1485–1493. https://doi.org/10.1084/jem.20090209

Suzuki, T., Kiyokawa, N., Taguchi, T., Sekino, T., Katagiri, Y. U., & Fujimoto, J. (2001). CD24 Induces Apoptosis in Human B Cells Via the Glycolipid-Enriched Membrane Domains/Rafts-Mediated Signaling System. *The Journal of Immunology*, *166*(9), 5567–5577. https://doi.org/10.4049/jimmunol.166.9.5567

Takahashi, Y., Dutta, P. R., Cerasoli, D. M., & Kelsoe, G. (1998). In Situ Studies of the Primary Immune Response to (4-Hydroxy-3-Nitrophenyl)Acetyl. V. Affinity Maturation Develops in Two Stages of Clonal Selection. *Journal of Experimental Medicine*, *187*(6), 885–895. https://doi.org/10.1084/jem.187.6.885

Tan, E. M., & Kunkel, H. G. (1966). Characteristics of a soluble nuclear antigen precipitating with sera of patients with systemic lupus erythematosus. *The Journal of Immunology*, *96*(3). http://journals.aai.org/jimmunol/article-pdf/96/3/464/1480621/ji0960030464.pdf

Taniguchi, T., Ogasawara, K., Takaoka, A., & Tanaka, N. (2001). IRF Family of Transcription Factors as Regulators of Host Defense. *Annual Review of Immunology*, *19*(1), 623–655. https://doi.org/10.1146/annurev.immunol.19.1.623

Terao, C., Ohmura, K., Kawaguchi, Y., Nishimoto, T., Kawasaki, A., Takehara, K., Furukawa, H., Kochi, Y., Ota, Y., Ikari, K., Sato, S., Tohma, S., Yamada, R., Yamamoto, K., Kubo, M., Yamanaka, H., Kuwana, M., Tsuchiya, N., Matsuda, F., & Mimori, T. (2013). PLD4 as a novel susceptibility gene for systemic sclerosis in a Japanese population. *Arthritis & Rheumatism*, *65*(2), 472–480. https://doi.org/10.1002/art.37777

Tew, J. G., Kosco, M. H., Burton, G. F., & Szakal, A. K. (1990). Follicular Dendritic Cells as Accessory Cells. *Immunological Reviews*, *117*(1), 185–211. https://doi.org/10.1111/j.1600-065X.1990.tb00573.x

Tiegs, S. L., Russell, D. M., & Nemazee, D. (1993). Receptor editing in self-reactive bone marrow B cells. *Journal of Experimental Medicine*, *177*(4), 1009–1020. https://doi.org/10.1084/jem.177.4.1009

Tipton, C. M., Fucile, C. F., Darce, J., Chida, A., Ichikawa, T., Gregoretti, I., Schieferl, S., Hom, J., Jenks, S., Feldman, R. J., Mehr, R., Wei, C., Lee, F. E. H., Cheung, W. C., Rosenberg, A. F., & Sanz, I. (2015). Diversity, cellular origin and autoreactivity of antibody-secreting cell population expansions in acute systemic lupus erythematosus. *Nature Immunology*, *16*(7), 755–765. https://doi.org/10.1038/ni.3175

Tonegawa, S. (1983). Somatic generation of antibody diversity. *Nature*, *302*(5909), 575–581. https://doi.org/10.1038/302575a0

Tull, T. J., Pitcher, M. J., Guesdon, W., Siu, J. H. Y., Lebrero-Fernández, C., Zhao, Y., Petrov, N., Heck, S., Ellis, R., Dhami, P., Kadolsky, U. D., Kleeman, M., Kamra, Y., Fear, D. J., John, S., Jassem, W., Groves, R. W., Sanderson, J. D., Robson, M. D., … Spencer, J. (2021). Human marginal zone B cell development from early T2 progenitors. *Journal of Experimental Medicine*, *218*(4). https://doi.org/10.1084/JEM.20202001

van den Berge, K., Roux de Bézieux, H., Street, K., Saelens, W., Cannoodt, R., Saeys, Y., Dudoit, S., & Clement, L. (2020). Trajectory-based differential expression analysis for single-cell sequencing data. *Nature Communications*, *11*(1). https://doi.org/10.1038/s41467-020-14766-3

Vossenkämper, A., Blair, P. A., Safinia, N., Fraser, L. D., Das, L., Sanders, T. J., Stagg, A. J., Sanderson, J. D., Taylor, K., Chang, F., Choong, L. M., D'Cruz, D. P., MacDonald, T. T., Lombardi, G., & Spencer, J. (2013). A role for gut-associated lymphoid tissue in shaping the human b cell repertoire. *Journal of Experimental Medicine*, *210*(9), 1665–1674. https://doi.org/10.1084/jem.20122465

Wang, C. M., Chang, S. W., Wu, Y. J. J., Lin, J. C., Ho, H. H., Chou, T. C., Yang, B., Wu, J., & Chen, J. Y. (2014). Genetic variations in Toll-like receptors (TLRs 3/7/8) are associated with systemic lupus erythematosus in a Taiwanese population. *Scientific Reports*, *4*. https://doi.org/10.1038/srep03792

Wang, K., Wei, G., & Liu, D. (2012). CD19: a biomarker for B cell development, lymphoma diagnosis and therapy. *Experimental Hematology & Oncology*, *1*(1). https://doi.org/10.1186/2162-3619-1-36

Wangriatisak, K., Thanadetsuntorn, C., Krittayapoositpot, T., Leepiyasakulchai, C., Suangtamai, T., Ngamjanyaporn, P., Khowawisetsut, L., Khaenam, P., Setthaudom, C., Pisitkun, P., & Chootong, P. (2021). The expansion of activated naive DNA autoreactive B cells and its association with disease activity in systemic lupus erythematosus patients. *Arthritis Research and Therapy*, *23*(1). https://doi.org/10.1186/s13075-021-02557-0

Wardemann, H., Yurasov, S., Schaefer, A., Young, J. W., Meffre, E., & Nussenzweig, M. C. (2003). Predominant Autoantibody Production by Early Human B Cell Precursors. *Science*, *301*(5638), 1374–1377. https://doi.org/10.1126/science.1086907

Wei, C., Anolik, J., Cappione, A., Zheng, B., Pugh-Bernard, A., Brooks, J., Lee, E.-H., Milner, E. C. B., & Sanz, I. (2007). A New Population of Cells Lacking Expression of CD27 Represents a Notable Component of the B Cell Memory Compartment in Systemic Lupus Erythematosus. *The Journal of Immunology*, *178*(10), 6624–6633. https://doi.org/10.4049/jimmunol.178.10.6624

Weller, S., Braun, M. C., Tan, B. K., Rosenwald, A., Cordier, C., Conley, M. E., Plebani, A., Kumararatne, D. S., Bonnet, D., Tournilhac, O., Tchernia, G., Steiniger, B., Staudt, L. M., Casanova, J. L., Reynaud, C. A., & Weill, J. C. (2004). Human blood IgM "memory" B cells are circulating splenic marginal zone B cells harboring a prediversified immunoglobulin repertoire. *Blood*, *104*(12), 3647–3654. https://doi.org/10.1182/blood-2004-01-0346

Weller, S., Faili, A., Aoufouchi, S., Guéranger, Q., Braun, M., Reynaud, C. A., & Weill, J. C. (2003). Hypermutation in human B cells in Vivo and in Vitro. *Annals of the New York Academy of Sciences*, *987*, 158–165. https://doi.org/10.1111/j.1749-6632.2003.tb06044.x

Weller, S., Faili, A., Garcia, C., Braun, M. C., le Deist, F., de Saint Basile, G., Hermine, O., Fischer, A., Reynaud, C.-A., & Weill, J.-C. (2001). CD40-CD40L independent Ig gene hypermutation suggests a second B cell diversification pathway in humans. *Proceedings of the National Academy of Sciences*, *98*(3), 1166–1170. https://doi.org/10.1073/pnas.98.3.1166

Wirths, S., & Lanzavecchia, A. (2005). ABCB1 transporter discriminates human resting naive B cells from cycling transitional and memory B cells. *European Journal of Immunology*, *35*(12), 3433–3441. https://doi.org/10.1002/eji.200535364

Woodruff, M. C., Ramonell, R. P., Nguyen, D. C., Cashman, K. S., Saini, A. S., Haddad, N. S., Ley, A. M., Kyu, S., Howell, J. C., Ozturk, T., Lee, S., Suryadevara, N., Case, J. B., Bugrovsky, R., Chen, W., Estrada, J., Morrison-Porter, A., Derrico, A., Anam, F. A., … Sanz, I. (2020). Extrafollicular B cell responses correlate with neutralizing antibodies and morbidity in COVID-19. *Nature Immunology*, *21*(12), 1506–1516. https://doi.org/10.1038/s41590-020-00814-z

Wu, X., Dao Thi, V. L., Huang, Y., Billerbeck, E., Saha, D., Hoffmann, H. H., Wang, Y., Silva, L. A. V., Sarbanes, S., Sun, T., Andrus, L., Yu, Y., Quirk, C., Li, M., MacDonald, M. R., Schneider, W. M., An, X., Rosenberg, B. R., & Rice, C. M. (2018). Intrinsic Immunity Shapes Viral Resistance of Stem Cells. *Cell*, *172*(3), 423-438.e25. https://doi.org/10.1016/j.cell.2017.11.018

Xiao, Z. X., Miller, J. S., & Zheng, S. G. (2021). An updated advance of autoantibodies in autoimmune diseases. *Autoimmunity Reviews*, *20*(2), 102743. https://doi.org/10.1016/j.autrev.2020.102743

Xu, W. D., Zhang, Y. J., Xu, K., Zhai, Y., Li, B. Z., Pan, H. F., & Ye, D. Q. (2012). IRF7, a functional factor associates with systemic lupus erythematosus. In *Cytokine* (Vol. 58, Issue 3, pp. 317–320). https://doi.org/10.1016/j.cyto.2012.03.003

Yang, G., Xu, Y., Chen, X., & Hu, G. (2007). IFITM1 plays an essential role in the antiproliferative action of interferon-γ. *Oncogene*, *26*(4), 594–603. https://doi.org/10.1038/sj.onc.1209807

Yaniv, G., Twig, G., Shor, D. B. A., Furer, A., Sherer, Y., Mozes, O., Komisar, O., Slonimsky, E., Klang, E., Lotan, E., Welt, M., Marai, I., Shina, A., Amital, H., & Shoenfeld, Y. (2015). A volcanic explosion of autoantibodies in systemic lupus erythematosus: A diversity of 180

different antibodies found in SLE patients. In *Autoimmunity Reviews* (Vol. 14, Issue 1, pp. 75–79). Elsevier. https://doi.org/10.1016/j.autrev.2014.10.003

Yao, Y., Liu, R., Shin, M. S., Trentalange, M., Allore, H., Nassar, A., Kang, I., Pober, J. S., & Montgomery, R. R. (2014). CyTOF supports efficient detection of immune cell subsets from small samples. *Journal of Immunological Methods*, *415*, 1–5. https://doi.org/10.1016/j.jim.2014.10.010

Yurasov, S., Wardemann, H., Hammersen, J., Tsuiji, M., Meffre, E., Pascual, V., & Nussenzweig, M. C. (2005). Defective B cell tolerance checkpoints in systemic lupus erythematosus. *Journal of Experimental Medicine*, *201*(5), 703–711. https://doi.org/10.1084/jem.20042251

Zhang, L., & Pagano, J. S. (1997). IRF-7, a New Interferon Regulatory Factor Associated with Epstein-Barr Virus Latency. In *MOLECULAR AND CELLULAR BIOLOGY* (Vol. 17, Issue 10).

Zhao, L., Liang, D., Wu, X., Li, Y., Niu, J., Zhou, C., Wang, L., Chen, H., Zheng, W., Fei, Y., Tang, F., Li, Y., Zhang, F., He, W., Cao, X., & Zhang, X. (2017). Contribution and underlying mechanisms of CXCR4 overexpression in patients with systemic lupus erythematosus. *Cellular & Molecular Immunology*, *14*(10), 842–849. https://doi.org/10.1038/cmi.2016.47

Zhao, Y., Uduman, M., Siu, J. H. Y., Tull, T. J., Sanderson, J. D., Wu, Y. C. B., Zhou, J. Q., Petrov, N., Ellis, R., Todd, K., Chavele, K. M., Guesdon, W., Vossenkamper, A., Jassem, W., D'Cruz, D. P., Fear, D. J., John, S., Scheel-Toellner, D., Hopkins, C., … Spencer, J. (2018). Spatiotemporal segregation of human marginal zone and memory B cell populations in lymphoid tissue. *Nature Communications*, *9*(1). https://doi.org/10.1038/s41467-018-06089-1

Zheng, M., Hu, Z., Mei, X., Ouyang, L., Song, Y., Zhou, W., Kong, Y., Wu, R., Rao, S., Long, H., Shi, W., Jing, H., Lu, S., Wu, H., Jia, S., Lu, Q., & Zhao, M. (2022). Single-cell sequencing shows cellular heterogeneity of cutaneous lesions in lupus erythematosus. *Nature Communications*, *13*(1), 7489. https://doi.org/10.1038/s41467-022-35209-1

Zhu, L., Yin, Z., Ju, B., Zhang, J., Wang, Y., Lv, X., Hao, Z., & He, L. (2018). Altered frequencies of memory B cells in new-onset systemic lupus erythematosus patients. *Clinical Rheumatology*, *37*(1), 205–212. https://doi.org/10.1007/s10067-017-3877-1

Zikherman, J., Doan, K., Parameswaran, R., Raschke, W., & Weiss, A. (2012). Quantitative differences in CD45 expression unmask functions for CD45 in B-cell development, tolerance, and survival. *Proceedings of the National Academy of Sciences of the United States of America*, *109*(1). https://doi.org/10.1073/pnas.1117374108